DISSERTATION

THE ROLE OF MICROGLIAL SYNAPTIC PRUNING IN MURINE MODELS OF PSYCHIATRIC SYMPTOMS

DIE ROLLE VON SYNAPTIC PRUNING DURCH MIKROGLIA IN EXPERIMENTELLEN MODELLEN VON PSYCHIATRISCHEN SYMPTOMEN

zur Erlangung des akademischen Grades
Doctor of Philosophy (PhD)

vorgelegt der Medizinischen Fakultät
Charité – Universitätsmedizin Berlin

von

BILGE UGURSU

Erstbetreuer*in: Prof. Dr. Helmut Kettenmann
Datum der Promotion: 30.06.2024

Table of Contents

List of Tables

List of Figures

List of Abbreviations

AChE-like	Acetylcholine esterase-like
ACSF	Artificial cerebral spinal fluid
ADAM10	A disintegrine and metalloproteinase 10
ADAM17	A disintegrine and metalloproteinase 17
AMPAR	α-amino-3-hydroxy-5-methyl-4-isoxazolepropionic acid receptor
AP5	2-Amino-5-Phosphonovalerate
ApoE	Apolipoprotein E
ASD	Autism spectrum disorder
Au	Arbitrary unit
avg_log2FC	Average log2-fold change
BAM	Border-associated macrophages
BCA	Bicinchoninic acid
BM	Bone marrow
C1qb	Complement component 1, q subcomponent, B chain.
C4A	Complement component 4 protein
CA-1	Cornu Ammonis -1
CA-3	Cornu Ammonis -3
CaMKII	Calmodulin-dependent protein kinase II
CDC	Centers for Disease Control and Prevention
CNS	Central nervous system
COVID-19	Coronavirus Disease 2019
CR3	Complement receptor 3
CSF	Cerebrospinal fluid
CSF-1R	colony-stimulating factor 1 receptor
DAP10	DNAX activating protein-10
DAP12	DNAX activating protein-12
DPBS	Dulbecco's phosphate-buffered saline
ELISA	Enzyme-linked immunosorbent assay
EPM	Elevated plus maze
EPSP	Excitatory postsynaptic potential
FACS	Fluorescence-activated single cell sorting
fMRI	Functional Magnetic Resonance Imaging
GABA	γ-aminobutyric acid
GABAA	γ-Aminobutyric acid type A
GC content	Guanine-Cytosine content
GFP	Green fluorescent protein
GluR	Glutamate receptor
GWAS	Genome-wide association studies
HAB	Mice with high anxiety behavior
IBA-1	Ionized calcium-binding adaptor molecule 1

IFN-α	Interferon alpha
IFN-resp I-III	Interferon-responsive microglia I to III
IL-1β	Interleukin-1-beta
IL-6	IL-6
IL33-R	Interleukin 33 receptor
IPSP	inhibitory postsynaptic potentials
LD	Light-dark test
LNS	Laminin G/Neurexin/Sex Hormone Binding Globulin
LPS	Lipopolysaccharide
LTP	Long term potentiation
MI; MV	Microglia-I to Microglia-V
MAPK	Mitogen-activated protein kinase
MDD	Major depressive disorder
MDGA1	MAM glycosylphosphatidylinositol anchor 1
MDGA2	MAM glycosylphosphatidylinositol anchor 2
MFI	Mean fluorescence intensity
MIA	Maternal immune activation
mPFC	Medial prefrontal cortex
MRI	Magnetic resonance imaging
MWM	Morris Water Maze
NAB	Mice with normal anxiety behavior
NL4	Neuroligin 4
NL4 -/-	Neuroligin 4 knockout
NMDA	N-methyl-D-aspartic acid
NMDAR	The N-methyl-D-aspartate receptor
NNT	Nicotinamide nucleotide transhydrogenase
Nrxn	Neurexin
p_val_adj	Adjusted p value
P15	Postnatal day 15
P90	Postnatal day 90
PAR	Pseudoautosomal region
PBS	Phosphate buffered saline
pct.1	The percentage of cells where the feature is detected in the first group
pct.2	The percentage of cells where the feature is detected in the second group
PET	Positron emission tomography
poly(I:C)	Polyinosinic:polycytidylic acid
PS	Phosphatidylserine
PSD	Post synaptic density
PSD-95	Postsynaptic density protein of 95 kDa
SAM	Synaptic cell adhesion molecules
scRNA-seq	Single cell RNA Sequencing

SEM	Standard error of the mean
SIRPα	Signal-regulatory protein alpha
sTREM2	soluble TREM2
t-SNE	t-distributed stochastic neighbor embedding
TLR	Toll-like receptor
TMT	Tandem mass tag
TNF-α	Tumour Necrosis Factor alpha
TREM2	Triggering Receptor Expressed On Myeloid Cells 2
TSPO	Translocator protein
TyroBP	Tyrosine kinase binding protein
UDP	Uridine diphosphate
VGLUT	Vesicular glutamate transporter
WDFY1	WD repeat and FYVE domain-containing protein-1

ABSTRACT

Microglia are first responders to disruptions in homeostasis and key modulators of synaptic refinement in the central nervous system (CNS). Alterations in microglia phenotype have been implicated in psychiatric disorders including autism spectrum disorder (ASD), innate high anxiety and depression, with little attention given to the interplay of microglia and synapses. Therefore, I investigated the microglial engulfment of synapses, along with the main pathways regulating this function, by using two mouse models for symptoms of psychiatric disorders: mice with innate high anxiety-related behavior (HAB) and the *Neuroligin-4* knockout (*Nlgn4*-KO) mouse model of ASD.

In the first project (**A**), I focused on the ASD model and found reduced engulfment of synapses by microglia in the *Nlgn4*-KO hippocampus, which appeared stronger in males compared to females. In addition to demonstrating deficits in synaptic engulfment, I reported significant dysregulations in the TREM2 signaling pathway, including reduced surface expression of TREM2 on microglia, elevated levels of soluble TREM2, and decreased levels of APOE in the *Nlgn4*-KO hippocampus at postnatal day 90 (P90). I also demonstrated that neither the synaptic engulfment deficits nor the dysregulations in the TREM2 pathway were present at an earlier developmental time point (P15), suggesting that they occur later in development and contribute to an abnormal microglial response at the adult stage in the *Nlgn4*-KO hippocampus. I also addressed the changes in the synaptosome proteome, as well as in behavior; and reported impaired spatial learning and memory in the *Nlgn4*-KO male mice; whereas found no major changes in the synaptosome proteome in the *Nlgn4*-KO hippocampus.

In the second project (**B**), I focused on the innate high anxiety and depression model (HAB). I analyzed microglial heterogeneity in both sexes of HABs using single-cell RNA sequencing, which revealed ten distinct clusters varied by their frequency and gene expression status. I found striking sex-related differences, including a higher proportion of microglia clusters associated with phagocytosis in the HAB female compared to the HAB male. Furthermore, I reported that these clusters primarily upregulate the genes related to synaptic engulfment such as *Trem2* in females. I functionally validated these findings by showing that a greater number of synapses were engulfed by the female HAB microglia compared to the male HAB in the hippocampus. I also investigated the effect of minocycline, which significantly reduced the engulfment of synapses by microglia in females, suggesting a sexually dimorphic recovery in response to the treatment.

Overall, herein I have identified sex-dependent dysregulations in the microglial engulfment of synapses and TREM2 signaling in both models for symptoms of psychiatric disorders. I propose these sex-specific dysregulations as potential avenues to target microglia in a broader context of psychiatric disorders.

ZUSAMMENFASSUNG

Mikroglia sind die ersten Zellen des zentralen Nervensystems, die auf Störungen der Homöostase reagieren und sie kontrollieren auch die Anzahl der Synapsen. Veränderungen des Mikroglia-Phänotyps wurden bei psychiatrischen Störungen wie Autismus-Spektrum-Störungen (ASD) und Angststörungen sowohl in Tiermodellen als auch bis zu einem gewissen Grad bei Patienten nachgewiesen. Dem Zusammenspiel zwischen Mikroglia und Synapsen wurde jedoch bisher wenig Aufmerksamkeit geschenkt. Daher konzentriere ich mich in der vorliegenden Arbeit auf das "synaptische Pruning" anhand von zwei verschiedenen Mausmodellen mit psychiatrischer Symptomatik: Mäuse mit angeborenem hohem Angstverhalten (HAB) und das Neuroligin-4-Knockout-Mausmodell (*Nlgn4*-KO) für ASD.

Im ersten Projekt (A) konzentriere ich mich auf das Modell für ASD und zeige ein reduziertes "synaptisches Pruning" durch Mikroglia im *Nlgn4*-KO-Hippocampus. Darüber hinaus berichte ich über signifikante Dysregulationen im TREM2-Signalweg, z. B. eine geringere Oberflächenexpression von TREM2 auf *Nlgn4*-KO-Mikroglia zusammen mit höheren Spiegeln von löslichem TREM2 und geringeren APOE-Werten im *Nlgn4*-KO-Hippocampus bei P90. Im Vergleich dazu zeigte ich bei P15 keine Defizite bei der synaptischen Aufnahme, was darauf hindeutet, dass Dysregulationen bei der TREM2-Signalübertragung und eine damit verbundene mikrogliale Reaktion erst im *Nlgn4*-KO-Hippocampus im Erwachsenenalter nachweisbar sind. Darüber hinaus habe ich bei männlichen *Nlgn4*-KO-Mäusen eine Beeinträchtigung des räumlichen Lernens und Gedächtnisses festgestellt, während es im Synaptosom-Proteom des *Nlgn4*-KO-Hippocampus keine größeren Veränderungen gab.

Im zweiten Projekt (B) konzentriere ich mich auf die mikrogliale Dysfunktion im Zusammenhang mit angeborener Angststörung und Depression. Ich habe die mikrogliale Heterogenität in beiden Geschlechtern von HABs mittels Einzelzell-RNA-Sequenzierung analysiert. Ich fand geschlechtsspezifische Unterschiede, einschließlich eines höheren Anteils an phagozytose-assoziierten Mikroglia-Clustern bei weiblichen HABs im Vergleich zu männlichen. Darüber hinaus konnte ich zeigen, dass diese Cluster in erster Linie Gene hochregulieren, die bei weiblichen Mäusen mit dem synaptischen "Pruning" in Verbindung gebracht werden, wie z. B. Trem2, was ich funktionell bestätigte, indem ich zeigte, dass weibliche HAB-Mikroglia im Vergleich zu männlichen HAB-Mikroglia eine größere Menge an Synapsen phagozytierten. Außerdem konnte ich nachweisen, dass Minocyclin die Aufnahme von Synapsen durch Mikroglia bei weiblichen Tieren deutlich verringert.

Insgesamt habe ich hier geschlechtsabhängige Dysregulationen bei der mikroglialen Aufnahme von Synapsen und der TREM2-Signalgebung in beiden Modellen für Symptome psychiatrischer Störungen festgestellt. Ich schlage diese geschlechtsspezifischen Dysregulationen als potenzielle Wege vor, um Mikroglia in einem breiteren Kontext psychiatrischer Störungen zu beeinflussen.

1. INTRODUCTION

1.1 Autism Spectrum Disorder

1.1.1 History and Prevalence of Autism

In 1943, Leo Kanner introduced "classical autism" as an unique disease concept. He reported eight boys and three girls, ages from two to eight, who lacked the ability to communicate through words, exhibited monotonous repetitions of vocalizations, and obsession with items. In addition, these repetitive routines were extensively resistant to change (Kanner, 1943). A year later, in 1944, Hans Asperger described a group of children who had no verbal impairment associated with the classic autism, but they used their speech skills for monologues about their own unique and restricted interests. These children were near to being categorized as normal or exceptionally intelligent, but they were unable to integrate into their social environment, frequently displayed difficulties with learning particular tasks, and exhibited stereotyped behaviors (Asperger, 1944). Because of their overlapping symptoms, these two kinds of autism definition were merged into the same group of neurodevelopmental disorders roughly thirty years later. Today, the descriptions of Kanner and Asperger have been extensively refined, and autism is regarded as a broad spectrum of behavioral manifestations with varying degrees of severity. Autism spectrum disorder (ASD) is a complex neurodevelopmental disorder with a spectrum of heterogeneous clinical symptoms and striking inter-individual differences (Guang et al., 2018). It shows three core behavioral manifestations: (1) an impairment in social interaction skills, (2) a lack of proper language and communication skills, and (3) repetitive and restricted behaviors (Guang et al.,

2018). In addition to the different severity levels of these core symptoms, autism also displays a range of comorbidities such as intellectual impairment, anxiety, sleep disturbance, gastrointestinal, and immune dysfunction (Careaga et al., 2010; Doshi-Velez et al., 2014). ASD affects 1 in 44 children in the United States, and is four times more prevalent in males than in females, according to the CDC's Autism and Related Disorders Monitoring Network, 2018 (Maenner et al., 2021). Such sex-related differences may be due to the interaction between the sex steroid system with neurodevelopment (Simantov et al., 2022), as well as due to the phenotype of female autism, which generates a bias due to misdiagnosis and/or even due to the overlooking of females given that they are more likely to conceal their social impairments (Hodges et al., 2020).

1.1.2 Pathology and Genetics of Autism

ASD is a complex disorder, and genetic as well as environmental factors play a role in the multifactorial disease etiology (Lipkin, Bresnahan & Susser, 2023). Previous clinical and preclinical research has advanced our understanding of the disease's origin, indicating a great complexity with no unifying underlying mechanism. Several clinical studies have reported abnormalities such as increased brain volume in children with ASD (Nickl-Jockschat et al., 2012; Haar et al., 2016). They also revealed variations in the cerebellar connections, changes in the frontal and temporal lobes, as well as limbic system abnormalities (Johnson & Myers, 2007; Stoodley et al., 2017). Increase in neural density (Casanova et al., 2002; Casanova et al., 2006) , region-specific delay of neural growth and dysplasia have also been reported in the brains of individuals with ASD (Wegiel et al., 2010). These findings, along with cortical, hippocampal, and cerebral dysplasia, which reflect abnormal neural immaturity, migration,

and cellular organization (Wegiel et al., 2010), are among the most common forms of neurodevelopmental changes found in the brains of autistic subjects. Such changes have the potential to modify local connectivity and signal transduction in the reported brain regions, including the hippocampus and medial prefrontal cortex (mPFC) (Amaral et al., 2008; Nicolson et al., 2006; Richards et al., 2020). However, considering inter-personal heterogeneity, these findings mostly are not generalized but rather refer to a subset of patients. Given the behavioral phenotype, complexity, and heterogeneity of ASD, it is indeed unlikely that a single anatomical alteration or neuropathological hallmark underlies the origin of the disease (Masi et al., 2017). However, these findings still significantly contribute to our understanding of autism, especially concerning subgroups of individuals with such specific alterations. Recent findings point to two major hypotheses emerging as common etiological factors in autism. The first refers to the imbalance between excitation and inhibition in neural circuits, which might be due to alterations in the neuronal density and functionality of synaptic cell adhesion molecules (Wass, 2011; Gao & Penzes, 2015). The second theory proposes overconnectivity in specific brain regions, which has also been supported by fMRI studies (Wass, 2011; Gao & Penzes, 2015). Brain region-specificity of such alterations still contributes to the degree of heterogeneity in the autistic brains (Gao & Penzes, 2015).

Autism also has a strong genetic component, with an estimated heritability ranging from 40% to 90%, according to several twin and family studies (Cross-Disorder Group of the Psychiatric Genomics Consortium et al., 2013; Gaugler et al., 2014). Recent advances in genome-wide association studies (GWAS) and whole exome sequencing techniques have advanced our knowledge of ASD susceptibility genes. Intriguingly, genes associated with ASD tend to cluster in specific pathways, which are predominantly associated with neural processes, such as

synaptogenesis and synaptic function (Gilbert & Man, 2017; Guang et al., 2018; Pinto et al., 2014; Yuen et al., 2017) and have shown various copy number variations and point mutations in genes such as *NRXN, NLGN,* and *SHANK*, which converge at the synaptic function and specification (Wang et al., 2016, Stessman et al., 2017; Grove et al., 2019; Lim et al., 2022). These findings suggest that at least a part of the pathogenesis of ASD may be attributable to synaptic dysfunction, which can result in cognitive impairments. Other candidate genes linked to ASD are related to WNT signaling, MAPK signaling, as well as regulation of translational processes (Kumar et al., 2019).

1.2 Anxiety and Depression

1.2.1 History, Prevalence and Pathology

Anxiety and depression are among the most common mental disorders in the world. They tend to emerge around adolescence to middle adulthood and share up to 80% comorbidity rate (Kalin, 2020; Klenk et al., 2011; Strand et al., 2021). Kessler et al. (2015) reported that 45.7% of patients with a lifetime history of major depression also had a history of anxiety disorder. Given the effect of the COVID-19 pandemic, the recent prevalence of depression and anxiety symptoms was reported as 25.2% and 20.5%, respectively, higher than that recorded in previous years (Racine et al., 2021).

Anxiety is originally defined as the anticipation of a future threat. It is a typical, adaptive feeling from an evolutionary standpoint, since it improves survival by causing individuals to avoid dangerous situations (Kalin, 2020). Prior to the 19th century; anxiety, depression, or even schizophrenia, were not widely acknowledged as 'real' diseases. However, since the 20th

century, anxiety has been classified as a psychiatric disorder (Crocq, 2015; Kalin, 2020) that is characterized by strong, uncontrollable feelings of worry and unfounded distress (Dieleman et al., 2016). The dividing line between ordinary adaptive anxiety and severe pathological anxiety is subject to clinical judgement. Depressive symptoms similarly include distress, lack of interest and pleasure in activities, as well as disruptions to physiological functions such as sleep (American Psychiatric Association, 2013). Extensive literature analysis has shown a higher prevalence of anxiety and depression in females compared to males (Kessler et al., 2012; Strand et al., 2021; McLean et al., 2011; Bailey & Crawley, 2009; Moser et al., 2016). The male-to-female prevalence ratios for anxiety-related disorders are 1:1.7 for generalized anxiety, 1:1.5 for major depression, 1:2 for panic, and 1:2.7 for post-traumatic stress disorder (McLean et al., 2011; Yanguas-Casás, 2020).

Early childhood stress such as trauma or neglect, as well as present stress exposure, are common nongenetic risk factors related to anxiety and comorbid depression (Weger & Sandi, 2018; Kalin, 2020). Deficits in activation and connectivity of the ventral anterior cingulate and amygdala were observed both in anxiety and depression patients (Etkin & Schatzberg, 2011). In addition, altered brain connectivity has been reported in early trait anxiety (Kalin et al., 2017), and studies indicate a link between synaptic pruning and anxiety-related behavior (Socodato et al., 2020; Bolton et al., 2022). The majority of clinical evidence, which is primarily limited to peripheral cytokine levels, suggests that immune dysregulation is also associated with the pathophysiology of anxiety and depression (Passos et al., 2015; Rao et al., 2015; Fontenelle et al., 2012; Hou et al., 2017).

1.3 Synaptic Transmission

1.3.1 Synaptogenesis and Synapse Maturation

Synapses are specialized, asymmetrical intercellular junctions that mediate the rapid transmission of electrical or chemical signals between neurons. Functionality of these specialized junctions is essential for neural processing and higher cognitive functions (Nichols & Newsome, 1999). Synapse formation requires the assembly of highly organized protein complexes involving receptors, synaptic cell adhesion molecules, soluble signaling molecules (released either by neurons or glia) and scaffolding proteins (Li & Sheng, 2003; Waites et al., 2005). Chemical synapses consist of a pre-synaptic terminal that is specialized for the release of neurotransmitters triggered by Ca^{+2}, and a post-synaptic terminal that is specialized for the reception of neurotransmitters (Südhof, 2021). Pre-synaptic specializations are majorly formed by axons, and post-synaptic specializations are most commonly formed on dendritic spines or dendritic shafts (for excitatory or inhibitory synapses, respectively) (Südhof, 2021). During the initial phase of synapse formation, pre- and post-synaptic membranes are aligned and initial contact is established through the interaction of synaptic cell adhesion molecules. The site of synaptic vesicle fusion and neurotransmitter release at the pre-synaptic terminal is called as the active zone (Südhof, 2012). Following depolarization of the presynaptic terminal, Ca^{+2} influx initiates vesicle fusion with the pre-synaptic membrane and neurotransmitter molecules diffuse across the synaptic cleft to bind neurotransmitter receptors on the post-synaptic membrane (Südhof, 2012; 2013). Excitatory neurotransmitters enhance the likelihood that a post-synaptic neuron will depolarize and generate an action potential, whereas inhibitory neurotransmitters decrease this likelihood (Südhof, 2018). On the post-synaptic membrane, neurotransmitters bind to ionotropic (ion channels) and

metabotropic (G-protein coupled) receptors, which undergo confirmational changes upon this binding and allow ion influx across the post-synaptic neural membrane (Purves, Augustine & Fitzpatrick et al. 2001). Excitatory neurotransmitters generate excitatory post-synaptic potential (EPSP), which increase the likelihood of a post-synaptic action potential generation. They render the membrane potential more positive, which brings it closer to the action potential threshold. However, it is important to note that many neurons integrate inhibitory and excitatory inputs, and result in a computed signal to the next neuron without generating a post-synaptic action potential (Purves, Augustine & Fitzpatrick et al., 2001). In contrast, inhibitory post-synaptic potentials (IPSP) are induced by inhibitory neurotransmitters and decrease the likelihood of a post-synaptic action potential by generating a hyperpolarizing current, which takes the post-synaptic membrane potential away from the action potential threshold (Purves, Augustine & Fitzpatrick et al., 2001). The brain displays an astonishing diversity of synaptic connections in terms post-synaptic receptor composition, pre-synaptic and post-synaptic cell adhesion molecules, release probability, neurotransmitter type, and location of the synapses (Südhof, 2021). Four main neurotransmitter receptor families exist, which are tetrameric glutamate receptors (NMDAR, AMPAR, kainate receptors), pentameric cys-loop receptors (GABAA receptors, glycine receptors, nicotine receptors), trimeric receptors (ATP receptors) and G protein-coupled receptors (Südhof, 2021). Individual synapses are specialized to contain one type of receptor to define their response at the post-synaptic terminals (Südhof, 2018; 2021). The formation of new synapses occurs throughout an organism's lifetime, but is most prominent during the early phases of nervous system development (Südhof, 2018).

1.3.2 Excitatory and Inhibitory Synaptic Architecture

Excitatory synapses are mostly formed on dendritic spines, whereas inhibitory synapses are formed at the shaft of dendrites, on cell bodies, and on axon initial segments (Bourne & Harris, 2008). On the post-synaptic side, excitatory synapses differ from inhibitory synapses in terms of their neurotransmitter receptors, morphology, molecular composition, and organization (Scheefhals & MacGillavry, 2018). Excitatory synapses display a distinctive morphological and functional specialization at the post-synaptic membrane: "the post-synaptic density (PSD)", which is located at the apex of the dendritic spines (Sheng & Kim, 2011). Abundant PSD proteins include the CaMKII family (CaMKIIα + CaMKIIβ), PSD-95 family (PSD-95, PSD-93, SAP97), Shank/ ProSAP family (Shank1, Shank2, Shank3), Homer Family (Homer1, Homer2, Homer3), glutamate receptors (AMPA -*GluR1, GluR2, GluR*- ; NMDA -*NR1,NR2A*-), N-Cadherin, and β-Catenin (Sheng & Kim, 2011). PSD-95 is a scaffolding protein that is enriched at glutamatergic synapses and modulates the clustering of various neurotransmitter receptors to keep them in close proximity at postsynaptic terminals (Keith and El-Husseini, 2008). Homer and Shank as well are master scaffold proteins in the PSD that form a mesh-like matrix assembly structure to cluster other PSD proteins (Hayashi et al., 2009). Components of the excitatory synaptic architecture is summarized in the **Figure 1.1**. Given the crucial role of PSD proteins in synapse development, structure, function, and specification, it is not surprising that the majority of PSD gene mutations are associated with psychiatric diseases, including ASD, with the majority of mutations reported in the *SHANK3*, *NLGN-1*, *NLGN-3*, *NLGN-4X*, and *NRXN-1* genes (Südhof, 2008).

Inhibitory synapses are primarily formed on the shaft of dendrites or surrounding the neural cell body (Südhof, 2018). On the contrary to the case of excitatory synapses, there is only a slight electron-density associated with the post-synaptic membrane (Gray, 1959). Gephyrin, a post-synaptic scaffold protein, directly interacts with neurotransmitter receptors at inhibitory synapses such as the GABAA and glycine receptors. While gephyrin is critical for glycine receptor clustering at the inhibitory post-synapse, it is less crucial for GABAA receptor clustering (Kneussel et al., 2001; Lévi et al., 2004). GABAA receptors can also be clustered by mechanisms independent of gephyrin but can as well recruit gephyrin to drive inhibitory postsynaptic differentiation (Lévi et al., 2004; Sheng & Kim, 2011). Components of the inhibitory synaptic architecture is visualized in the **Figure 1.1.** In the view of current findings, protein components of the excitatory PSD have been intensively studied, whereas the composition and function of inhibitory post-synaptic specializations have lagged behind and are yet to be studied in detail (Südhof, 2018). Thus, additional research is required to further decipher inhibitory post-synaptic specifications, particularly considering that inhibitory synapses are highly dynamic to assure a precise transmission of information in the brain (Villa et al., 2016).

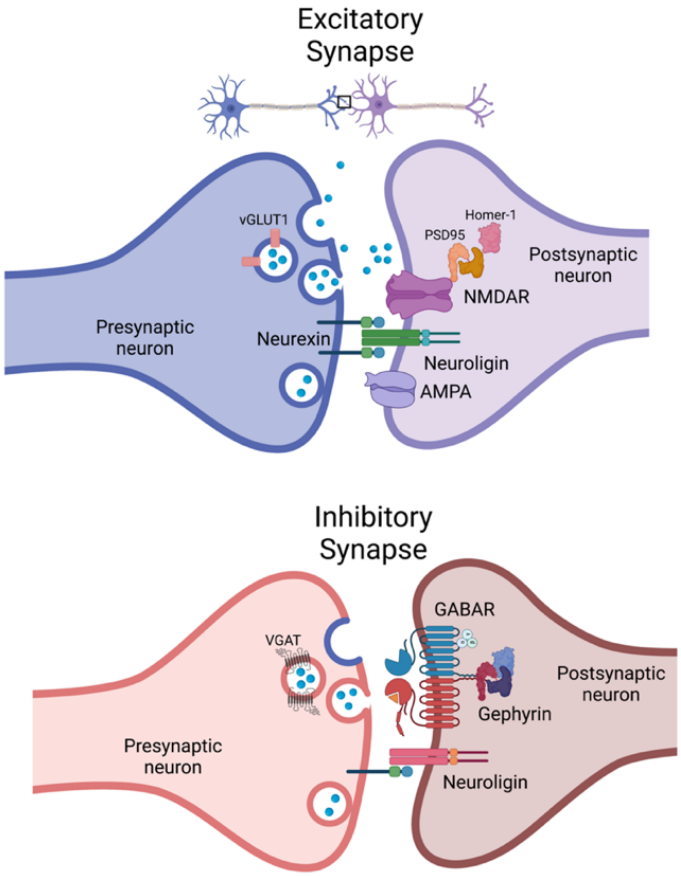

Figure 1.1 *Schematic representation of the excitatory and inhibitory synaptic architecture (created by using biorender.com).*

1.3.3 Neuroligin-Neurexin Interactions and Synaptic Function

Synaptic cell adhesion molecules (SAM) form transcellular assemblies between pre- and post-synaptic cell surfaces to mediate synaptic alignment and contact. During this initial contact of axons and dendrites, the interaction of pre- and post-synaptic cell adhesion molecules determines synaptic formation, specificity as well as maturation (Südhof, 2017; 2018; Yuzaki, 2018). The interaction between pre-synaptic neurexins and post-synaptic neuroligins, which act as calcium-dependent cell adhesion molecules, is the most thoroughly reported trans-synaptic interaction implicated in synaptogenesis and neural transmission (Südhof, 2008).

Neurexins, the key pre-synaptic SAMs, interact with multiple pre-synaptic and post-synaptic ligands to play a key role in neural circuit assembly (Südhof, 2017). They bind to pre-synaptic scaffold molecules through their PDZ domain interactions that couple neurexin signaling to synaptic vesicle exocytosis and bring out changes in the actin cytoskeleton (Hata et al., 1996; Butz et al., 1998). Neurexins also have a network of interaction partners on post-synaptic membranes, including at least seven post-synaptic protein families, as well as adaptor proteins, and their interaction depends on the alternative splicing of *Nrxn* genes (Südhof, 2008). There are three mammalian neurexin genes (*Nrxn1-3*), each of which encodes three splice variants: α-, β-, and γ-neurexin. These proteins share identical intracellular domains, but α-neurexin has a larger extracellular domain which might indicate its possible role in distinct extracellular interactions (Missler & Südhof, 1998). *Nrxn1-3* genes show similar expression levels in the brain; however, α-neurexins are much more abundant than the β-neurexins (Aoto et al., 2013; Schreiner et al., 2014; Anderson et al., 2015). Alternative splicing results in over a thousand neurexin isoforms, each with the potential to determine the specificity and function of synaptic connections (Ushkaryov & Sudhof, 1993; Ullrich, Ushkaryov & Südhof, 1995; Missler & Südhof, 1998). Neurexins are primarily expressed by neurons (Ushkaryov et al., 1992) and astrocytes (Zhang et al., 2014; Gokce et al., 2016; Tan & Eroglu, 2021). Considering their great potential with a variety of ligands and splice variants, they mediate highly complex interaction networks in the CNS (Dalva, McClelland & Kayser, 2007; Südhof, 2008). Studies using triple *Nrxn1-3* knockout mice have shown that the neurexin isoforms are not essential for synapse formation but are fundamental regulators of synaptic function (Chen et al., 2017).

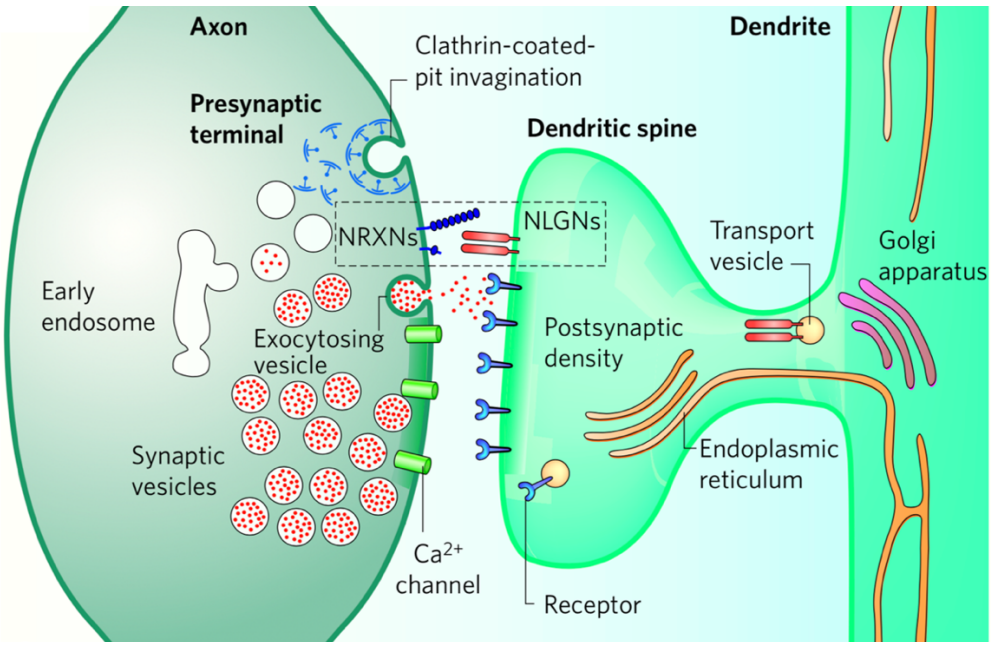

Figure 1. 2 *Interaction of presynaptic Neurexins and postsynaptic Neuroligins (Adapted from Südhof, 2008).*

Neuroligins (NL) are type-1 membrane proteins with a single large extracellular domain composed of an enzymatically inactive esterase-homology domain, a transmembrane region, and a short cytoplasmic tail. They are post-synaptic cell adhesion molecules that are localized at different synapses, and they modulate synaptic function, transduction, and specificity (Südhof, 2008; Liu et al., 2022). NLs, through their acetylcholine esterase-like (AChE-like) domain, bind to the Laminin G/Neurexin/Sex Hormone Binding Globulin (LNS) domain of neurexins (Südhof, 2008). The synaptogenic activity of neuroligins depends on the cis-clustering of neuroligin molecules, and this multimerized complex then interacts with neurexins and clusters them (Dean et al., 2003). On the post-synaptic side, neuroligins bind to the post-synaptic scaffold proteins, which in turn clusters other post-synaptic proteins that play a role in the recruitment of the pre-synaptic machinery (Friedman et al., 2000; Gerrow et al., 2006; Dalva, McClelland & Kayser, 2007).

The ligand network of neuroligins and neurexins is highly complex considering their localization at different synapses, their splice variants, interaction partners as well as dimerization partners. For instance, the *Nlgn-1*-SSB+ splice variant can only bind to NRXN1-β but not NRXN1-α (Comoletti et al., 2006). Although the current data is limited to certain isoforms and subtypes of neuroligins, it can already highlight the degree of complexity by revealing numerous possibilities of synaptic assemblies mediated by the interaction of neuroligin and neurexins (Südhof, 2008). Neurexin-neuroligin interactions modulate the specificity and function of inhibitory or excitatory synapses based on their subtypes, splice variants, and different combinations with transsynaptic adhesion molecules (Dalva, McClelland & Kayser, 2007; Sheng & Kim, 2011).

There are four neuroligin genes, *Nlgn1* to *Nlgn4*, expressed in mice; and five in humans, including the *NLGN4X* and *NLGNY* (Ichtchenko et al., 1995; 1996; Bolliger et al., 2008). They are expressed by neurons, astrocytes, and oligodendrocytes (Sakers & Eroglu, 2019). Genetic perturbation of neuroligins results in impaired synaptic function with consequent changes in the functionality of neuronal networks (Südhof, 2008). Constitutive *Nlgn1-2-3* triple-KO mice died at birth due to respiratory failure that resulted from impaired glutamatergic and GABAergic neurotransmission with no significant reduction in the synapse numbers (Varoqueaux et al., 2006). These mice displayed majorly impaired synaptic transmission, impaired synapse maturation, reduced neurotransmission, and a shift of excitatory to inhibitory balance (E/I) without an effect on the quantity of either excitatory or inhibitory synaptic contacts (Varoqueaux et al. 2006). This study indicates the fundamental role of neuroligins in synaptic function and transmission, rather than in the formation of synapses. Mice with conditional *Nlgn1-2-3* triple-KO in a subset of neurons similarly revealed impaired synaptic transmission with no change in synapse numbers (Chanda et al., 2017).

Neuroligin-1 (NL1) predominantly localizes to glutamatergic excitatory post-synapses (Song et al., 1999). *Nlgn1* overexpression induced accumulation of glutamatergic pre-and post-synaptic molecules *in vitro* (Song et al., 1999; Budreck & Scheiffele, 2007) and enhanced the excitatory post-synaptic currents (EPSCs) and E/I ratio in cultured hippocampal neurons, as well as in acute hippocampal slices (Prange et al., 2004; Dahlhaus et al., 2010). Deletion of *Nlgn1*, on the other hand, resulted in decreased excitatory synaptic response in cultured neurons (Jiang et al., 2017). Moreover, *Nlgn1* KO mice showed a reduction in EPSCs and NMDAR-mediated long-term potentiation (LTP) (Budreck et al., 2013).

Neuroligin-2 (NL2) is localized to GABAergic inhibitory post-synapses (Varoqueaux et al., 2004). Overexpression of NL2 promotes the formation of functional GABAergic synapses in cultured neurons (Varoqueaux et al., 2004; Chih et al., 2005; Levinson et al., 2005; Chubykin et al., 2007). Deletion of *Nlgn2* in mice does not lead to the elimination of inhibitory synapses but results in impaired inhibitory synaptic transmission (Chubykin et al., 2007; Varoqueaux et al., 2006; Gibson et al., 2009; Zhang et al., 2015), indicating that NL2 itself is not essential for synaptic formation but crucial for the functional maturation of inhibitory synapses.

Neuroligin 3 (NL3) is localized both at excitatory and inhibitory post-synapses depending on the brain region (Budreck & Scheiffele, 2007). Interestingly, *Nlgn3* deletion showed no effect on excitatory synaptic transmission in the hippocampus (Etherton et al., 2011a), but resulted in selective inhibition of tonic endocannabinoid signaling in CCK-positive synapses (Földy et al., 2013). In the striatum, on the other hand, *Nlgn3* deletion selectively impaired inhibitory inputs onto nucleus accumbens' medium spiny neurons (Rothwell et al., 2014). These data

indicate that the effect of *Nlgn3* deletion is determined by the context, neural subtype and the brain region.

In summary, current data suggests that neuroligin-neurexin interaction is a crucial regulator of synaptic maturation and function. They affect the function of synapses at multiple levels, from recruiting pre-synaptic and post-synaptic scaffold proteins to modulating synaptic function and specificity (Dalva, McClelland & Kayser, 2007). Neuroligins mediate an intriguing diversity of synaptic functions in an isoform-specific manner via multiple mechanisms based on their splice variants, interaction partners, subcellular location, and the brain region, which in turn gives rise to a great degree of complexity (Südhof, 2008). Recent studies have also revealed the binding of MDGA1 and MDGA2 proteins to NLs, in competition with neurexins (Lee et al., 2013; Pettem et al., 2013; Connor et al., 2016; Kim et al., 2017; Gangwar et al., 2017). These findings add to the existing level of complexity by showing the presence of other possible interaction partners of NLs amongst many others yet to be discovered. How different NLs are assigned to different types of synapses and how the same NLs mediate distinct, sometimes opposing functions, in different brain regions remain to be elucidated (Südhof, 2008). *Nlgn* mutations have been linked to monogenic forms of ASD (Jamain et al., 2003; Laumonnier et al., 2004; Yan et al., 2005, Nakanishi et al., 2017), where shifts in the E/I balance have also been reported (Jamain et al., 2003; Chih et al., 2004; Laumonnier et al., 2004).

1.3.3.1 Neuroligin-4 Protein: Function and Association with ASD

Neuroligin-4 (NL4) belongs to the highly conserved neuroligin family of post-synaptic neural cell adhesion molecules, and plays a critical role in synaptic function and maturation (Krueger-Burg et al., 2017; Südhof, 2017). NL4 is expressed throughout the CNS (Jamain et al., 2008; Hoon et al., 2011), and at similar levels in all subregions of the adult hippocampus (Hammer et al., 2015). It is localized at both excitatory and inhibitory post-synapses, which depends on the brain region (Krueger et al., 2012; Hammer, 2012; Delattre et al., 2013; Unichenko et al., 2018), just as NL3, the evolutionary closest NL4 isoform (Bolliger et al., 2008). NL4 is localized to inhibitory glycinergic synapses in the retina, spinal cord, and brain stem (Hoon et al., 2011; Zhang et al., 2018); inhibitory GABAergic synapses in the hippocampal CA3 (Hammer et al., 2015), excitatory glutamatergic and inhibitory GABAergic synapses in the hippocampal CA1 (Hammer, 2012).

Nlgn4 overexpression in cultured hippocampal neurons resulted in reduced spontaneous mEPSCs with an increased synaptic density, indicating the formation of synapses, but this appears to interfere with synaptic transmission (Zhang et al., 2009; Chanda et al., 2017). On the other hand, expression of *Nlgn4* promoted an excitatory synaptic response in rat hippocampal organotypic brain slices (Bemben et al., 2015). More comprehensive data came from *in vivo* studies using the *Nlgn-4* KO mouse model. *Nlgn-4* KO mice showed deficits of glycinergic synaptic transmission in the retina (Hoon et al., 2011), a reduction of GABAergic synaptic transmission along with aberrant γ-oscillations in the hippocampal CA3 (Hammer et al., 2015), and a predominantly impaired intracortical synaptic transmission along with reduced pre-synaptic vesicle pool size both at the GABAergic and glutamatergic synapses in the barrel cortex (Unichenko et al., 2018). These mice also showed an overall decrease in the

E/I ratio in addition to a hypo-reactive network in the somatosensory cortex (Delattre et al., 2013). Excitatory to inhibitory ratio (E/I) is defined as the ratio of mean amplitude EPSCs to mean amplitude of the IPSCs. Reduced E/I was also reported in the *Nlgn4*-KO barrel cortex in addition to the somatosensory cortex (Unichenko et al., 2018; Delattre et al., 2013). Whereas Hammer et al. (2015) reported a slight increase, in which spontaneous(s) IPSCs were reduced with no change in the sEPSC in the hippocampal CA3. Interestingly, several clinical studies also suggest that the E/I balance is shifted towards excitation in ASD cases (Rubenstein & Merzenich 2003; Gogolla et al., 2009; Tang et al., 2014). Overall, knowing that neuroligins can regulate excitatory or inhibitory synapses depending on the brain subregions, their region-specific functional plasticity might be the molecular machinery used to maintain the E/I ratio in the brain, which is disrupted in many psychiatric disorders including ASD (Cline, 2005; Levinson and El-Husseini, 2005; Hines et al., 2008; Jamain et al., 2003; Chih et al., 2004; Laumonnier et al., 2004).

NLGN4 variants indeed comprise the most frequent ASD-linked variants, with more than 50 mutations identified in individuals with ASD with almost 100% penetrance (Südhof, 2008; Kleijer et al., 2014; Chocholska et al., 2006, Laumonnier et al., 2004, Lawson-Yuen et al., 2008, Macarov et al., 2007, Marshall et al., 2008). The majority of these mutations are loss of function mutations (Zhang et al., 2009), and in parallel to this, *Nlgn4*-KO mouse model exhibited ASD-associated behavioral phenotypes, including repetitive behavior, restricted interests and reduced social interaction (Jamain et al., 2008; El-Kordi et al., 2013; Ju et al., 2014). Such behavioral phenotypes were also reported in the *Nlgn1*-KO and *Nlgn3*-KO mouse models (Blundell et al., 2010, Shinoda et al., 2013). Magnetic resonance imaging (MRI) volumetry revealed reduced brain volume in *Nlgn4*-KO mice (Jamain et al., 2008). This data is

also parallel to human studies indicating reduced gray matter volume in adults with ASD (Sato et al., 2017). Moreover, reduced social behavior and ultrasonic vocalization were reported in males (Jamain et al., 2008) and females (El-Kordi et al., 2013) at P90, along with higher marble burying, indicating stereotyped and repetitive behavioral patterns in both sexes of the *Nlgn4*-KO mice (El-Kordi et al., 2013). Similarly, pup and juvenile *Nlgn4*-KO mice (P8-P20) showed a deficiency in ultrasonic vocalization, which was more prominent in females at this developmental stage (Ju et al., 2014). The relation of *Nlgn4* and social behavior was also marked by a very interesting study reporting that the *Nlgn4* gene in the golden hamster contains a premature stop codon, which presumably results in a NL4 loss of function (Maxeiner et al., 2020). This indeed is a fascinating observation given that these hamsters live quite a solitary life as opposed to other rodents having a highly social life style (Gattermann et al., 2001).

In humans, the most robust NL4 protein expression was found in the cortex and parts of the striatum, which are among the brain regions regulating higher cognitive functions such as language, social interaction, and emotions (Marro et al., 2019). In human neurons, the NL4 protein was shown to be preferentially localized to the excitatory synapses and only to a subset of inhibitory synapses (Marro et al., 2019).

Previous studies stated that the mouse *Nlgn4* gene is poorly conserved compared to the human ortholog (Bolliger et al., 2008; Marro et al., 2019). Mouse *Nlgn4* is localized to the telomeric pseudoautosomal region (PAR) of the sex chromosomes. Unlike *Nlgn-1,2,3*; the sequences of mouse (-m) and human (-h) *Nlgn4* indeed show a substantial difference, indicating a lack of evolutionary conversation (Bolliger et al., 2008). However, an intriguing study by Maxeiner et. al. (2020) revealed that the majority of this diversification was the result

of increased GC content accumulation as well as highly repetitive sequences in the distinct coding regions and introns of the m-*Nlgn4*. Interestingly, distinct parts of the coding region remained conserved in spite of the substantial evolutionary pressure, which is known to result in destruction of several PAR genes (Maxeiner et al., 2020). More importantly, they compared the human and mouse NL4 protein structure, and reported that the insertions seem to occur in parts of the protein, where additional amino acid loops can be tolerated without interfering with the physiological function and synaptic localization of the NL4 protein (Maxeiner et al., 2020). Therefore, discussions about the evolutionary conversation of the NL4 protein should be revisited considering the recent advances in the literature.

1.3.4 Post-translational Processing of Neuroligins and ADAM10

Synaptic activity can regulate the surface expression, cleavage, and phosphorylation of NLs, *in vitro* and *in vivo* (Hu, Luo & Xu, 2015), suggesting that it is a key factor in regulating NL functions (Heine et al., 2008; Shipman et al., 2011; Burton et al., 2012). For instance, chemically induced LTP has been shown to increase the surface levels of NL1, NL2, and NL3 in acute hippocampal slices and cultured neurons (Schapitz et al., 2010), indicating that the translocation and surface levels of these NLs are under the regulation of synaptic network activity. When this activity was chronically inhibited by AP5 or KN93 treatment; NL1-induced increases in EPSCs as well as NL2-induced elevation of IPSCs were found to be suppressed (Chubykin et al., 2007; Hu, Luo & Xu, 2015). In addition to these findings, network activity has also been shown to affect the ectodomain shedding of neuroligins. m-NL1 cleavage has been reported to be activity-dependent and can be induced by ligand (such as soluble Neurexin) binding both *in vitro* and *in vivo* in mice (Suzuki et al., 2012; Peixoto et al., 2012). Its ectodomain shedding is predominantly mediated by A disintegrine and metalloproteinase 10

(ADAM10) and subsequent activity of γ-secretase (Suzuki et al., 2012; Trotter et al., 2019). Similarly, m-NL3 ectodomain shedding is also regulated by neural activity in an ADAM10-dependent manner (Venkatesh et al., 2017).

ADAM10 is expressed in various tissues in mice, at high levels, particularly in the brain (Marcinkiewicz & Seidah, 2000) and plays a critical role during development by modulating the organization, maintenance, and function of synapses through ectodomain-shedding of cell adhesion molecules (Marcinkiewicz & Seidah, 2000). *Adam10*-KO mice died on E9.5, indicating its crucial role during development (Hartmann et al., 2002). Conditional *Adam10*-KO mice exhibited hippocampal neurons with fewer and abnormally shaped dendritic spines, impaired induction of LTP and hippocampal network activity, reduced NMDA receptor expression, as well as impaired spatial learning and memory, indicating the profound effect of ADAM10 on synaptic transduction and behavior (Prox et al., 2013). ADAM10 protein can be present both at pre- and post-synapses, where its exact location and proximity to the synaptic cleft are crucial for the targeting of neuroligins and neurexins (Prox et al., 2013). Its regulation is controlled at post-transcriptional, translational, and post-translational levels, and such regulatory steps at multiple levels allow for rapid adaptation of ADAM10 to changes in the microenvironment (Endres & Deller, 2017). ADAM10 can cleave synaptic adhesion molecules such as N-cadherin (Warren et al., 2012), E-cadherin, CX3CL1 (Hundhausen et al., 2003), neurexins (Borcel et al., 2016; Kuhn et al., 2016) and neuroligins (Suzuki et al., 2012; Kuhn et al., 2016; Venkatesh et al., 2017), including the NL4X (Yumoto et al., 2020).

Neurons and glial cells, microglia in particular, are interdependent to regulate synapse functions in cooperation; and ADAM10 can modulate network activities also through glial cells. For instance, microglial surface protein triggering receptor expressed on myeloid cells 2

(TREM2) has also been identified as an ADAM10 target (Kuhn et al., 2016; Endres & Deller, 2017), suggesting a crucial role of this protein in modulating functions of different neural and glial cell types in the brain. In a healthy state, there is a balance in the activity of ADAM10 and its processing of neural cell adhesion molecules at synapses (Endres & Deller, 2017). The levels and/or function of ADAM10 may be altered by changes in neuronal activity or pathological conditions, resulting in changes in the ectodomain shedding of the ADAM10 substrates. This suggests that interfering with ADAM10 activity could be an effective strategy for modulating synaptic function as well as behavior (Vezzoli et al., 2019).

1.3.5 Synaptic Pruning Theory

In 1979, Peter Huttenlocher systematically counted synapses in electron micrographs of post-mortem human brains, from a new-born to a 90-year-old, and revealed that synaptic density in the cerebral cortex increases rapidly after birth, peaks at 1 to 2 years of age, and drops by about 50% during adolescence (Huttenlocher, 1979). In 1982, psychiatrist Irwin Feinberg used the term “synaptic pruning” to describe this reduction in synaptic density over time (Feinberg, 1982). Later in time, these findings have been reproduced by several scientists, who stated the first ~2 years of life as a period of excessive synapse formation, which is followed by a ~20 years period of net synapse elimination that leads to the loss of 40-50% of synapses during adolescence (Markus & Petit, 1987; Bourgeois and Rakic, 1993; Petanjek et al., 2011). Technological advancements such as unbiased machine learning algorithms simulating neural networks have confirmed the previous findings; moreover, have revealed the reduced pruning rate over time, with a phase of rapid and aggressive removal at the beginning of the development that was followed by a period of slower removal in the somatosensory cortex

(Navlakha et al., 2015). Neurons exhibit up to 40% synapse loss per month depending on the age and type of the neuron; and synapses are continuously formed and pruned throughout life instead of being restricted to an early developmental stage (Qiao et al., 2016; Südhof, 2017). Four decades of research following Huttenlocher's first findings identified several mechanisms underlying synaptic elimination, and suggested a key role played by microglia and astrocytes.

1.4 Microglia: The Immune Cells of the CNS

In 1856, Rudolf Virchow identified and defined '*glia*' for the first time by underlining the importance of understanding neuroglial biology (Virchow, 1858; Kierdorf & Prinz, 2017). Later on, in 1913, Santiago Ramón y Cajal defined the 'third element' in the brain, which was distinct from neurons and astrocytes (Cajal, 1913). This distinct cell type was first comprehensively defined by Pío del Río-Hortega as microglia along with its mesodermal origin, distinct morphology, and phagocytic capacity (Río-Hortega 1919a-1919d; Sierra et al., 2016 for the English translation). Following Río-Hortega's findings; several neuropathologists virtually disputed the existence of microglia for years; until Blinzinger and Kreutzberg marked the revival of microglia research in the late 1960s (Blinzinger and Kreutzberg, 1968).

Microglia are the resident macrophages and professional phagocytes of the central nervous system (CNS). They are present throughout the brain and the spinal cord, and make up about 5-20% of the total glial cell population in the CNS (Lawson et al., 1990; Perry, 1998). They continuously survey their microenvironment in order to detect a variety of molecular cues or insults. Upon "activation", they can acquire highly versatile and adaptable responses either

to maintain CNS homeostasis or to provide an immune defense (Hannisch & Kettenmann, 2007) **(Figure 1.3)**. Notably, microglia activation is not a uniphasic process, but rather a context-dependent response modified by changes in the microenvironment (Hannisch & Kettenmann, 2007; Prinz & Priller, 2014. Wolf et al., 2017). The term "activation" can be deceptive since microglia are indeed far from being inactive prior to a challenge. Therefore, the term "microglia activation" has recently been revised as the "change in the functional phenotype in a context and stimulus-dependent manner" (Paolicelli et al., 2022).

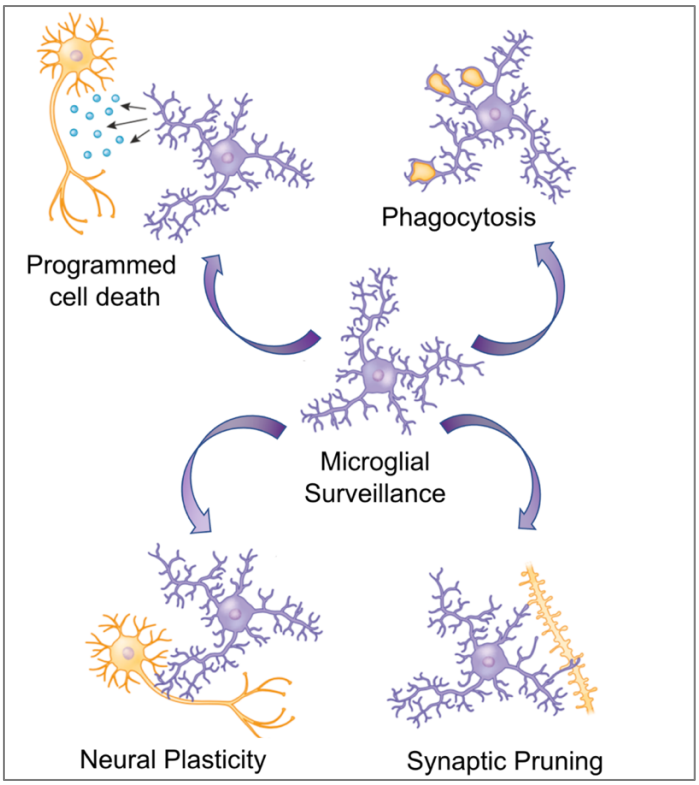

Figure 1.3 *Versatile functions of microglia under homeostasis (Adapted from Salter & Stevens, 2017).*

Microglia can actively modulate immune defense and inflammation but also promote tissue repair and remodeling, which is regulated by the molecular cues and signals that microglia are exposed to (Hannisch & Kettenmann, 2007; Wolf et al., 2017). In addition to their immune

function, microglial cells can recognize a wide variety of signals originating from homeostatic to pathological conditions, including the changes in the neural integrity. They sense pre-synaptic synaptic release by their various neurotransmitter receptors and modify their function (Färber & Kettenmann, 2008; Pocock & Kettenmann, 2007). Microglia control neurogenesis (Sierra et al., 2010), neural differentiation (Aarum et al., 2003), and affect the wiring of the developing embryonic brain (Squarzoni et al., 2014). They dynamically interact with synapses, and modulate synaptic elimination by engulfing synaptic structures (Tremblay et al., 2010; Stevens et al., 2007). In the prenatal brain, they regulate the growth of dopaminergic axons (Squarzoni et al., 2014) and in the postnatal brain, they are required for the remodeling of neural circuits as well as for maintaining the homeostasis (Paolicelli et al., 2011; Schafer et al., 2012). Microglia are distinct from perivascular, meningeal, and choroid plexus macrophages despite their large transcriptional overlap with perivascular macrophages, which is considerably more than between microglia and circulating monocytes (Goldmann et al., 2016).

Unlike macroglia and neurons emerging from neuroectoderm, microglia are of mesenchymal origin. They are derived from the embryonic yolk sac in mice (Ginhoux et al., 2010) and follow a step-wise maturation process before they infiltrate to the brain. $Runx1^{+}$/ $CD45^{-}$/ $c\text{-}kit^{+}$ erythromyeloid progenitor cells are the extraembryonic yolk sac-derived progenitors of microglia (Kierdorf et al., 2013a). They have the potential to give rise to microglia and macrophages, both *in vitro* and *in vivo*, under defined conditions (Kierdorf et al., 2013a). These progenitor cells develop into $CD45^{+}$/$c\text{-}kit^{low}$/$CX3CR1^{-}$ immature committed cells, which migrate to the developing brain through the blood stream from embryonic day (E) 8.5 in mice, before the blood-brain barrier (BBB) is firmly established (E13.5 to E14.5) (Ginhoux et al.,

2013; Matcovitch-Natan et al, 2016). In the developing brain, these cells mature into $CD45^{+}$/c-kit^{-}/$CX3CR1^{+}$ microglia with ramified morphology (Ginhoux et al., 2013; Matcovitch-Natan et al., 2016). Therefore, microglial cells already colonize the brain while other glial cells, such as astrocytes and oligodendrocytes, are not yet present at this early developmental stage (Squarzoni et al., 2014; Tay et al., 2017c; Matcovitch-Natan et al., 2016). After this voyage of microglia-progenitors to the brain is completed, and the BBB is fully constructed; the only source of microglia under homeostasis is self-renewal (Mildner et al., 2007; Ginhoux et al., 2013). As the CNS develops, microglia increasingly adapt to acquire diverse physiological functions, which are crucial for a normal brain development. Individual microglia are long-lived in healthy adults, with a turnover rate of 0.08% per day (Réu et al., 2017). Continued activation of the receptor for colony-stimulating factor 1 (CSF-1R), a crucial receptor for the development of microglia and macrophages, is required for the maintenance of microglia in the CNS (Ginhoux et al., 2010; Erblich et al., 2011; Salter & Stevens, 2017). New microglia are generated through self-renewal from local pools; therefore, microglia maintenance is independent of circulating monocytes (Sheng et al., 2015; Hashimoto et al., 2013; Bruttger et al., 2015). Nevertheless, it has also been reported that phagocytes with morphological resemblance to microglia can be derived from bone-marrow (BM) cells or circulating monocytes, which then contribute to the pathology under inflammatory conditions in case of a pathological insult (Mildner et al., 2007; Priller et al., 2001; Simard et al., 2006). Priller et al. (2001) were among the first to explore the long-term fate of myeloid cells in the mouse CNS following bone marrow (BM) transplantation using GFP-labelled hematopoietic cells. Similar to other groups, they were able to detect parenchymal microglia expressing GFP in the cerebellum, striatum, and hippocampus many weeks after the transplantation (Priller et al., 2001).

Microglia exhibit widely differing functions depending on the stage of life, the pathological insult at play, or the molecular cues received. Morphology, density, and gene expression of microglia have been reported to depend on age, brain region, sex, and context of homeostasis or disease (Masuda et al., 2019; Lenz et al., 2013; Butovsky et al., 2015; Hanamsagar et al., 2017; Guneykaya et al., 2018, Hammond et al., 2019). Different CNS regions contain 'adapted' microglia that display a context-dependent functional response, which is tuned to the molecular cues they receive in distinct brain regions and/or via contacts they establish with different cells of the CNS (Masuda et al., 2019). Local cues in the microenvironment or interactions with various neuronal subtypes and glial cells can explain this heterogeneity to a certain extent. Nevertheless, the possibility of microglial cells having intrinsic differences before infiltrating the CNS cannot be ruled out (Stratoulias et al., 2019). Thanks to recent advancements in single-cell technologies, microglia prove a remarkable heterogeneity also at the transcriptomic level (Hammond et al., 2019; Masuda et al., 2019). Although these findings are descriptive in terms of the state of microglia at a certain time and context, it is also questionable whether transcriptome and/or proteome heterogeneity translates to cellular heterogeneity (Okawa et al., 2018) or whether they just describe distinct molecular states within the same subpopulation. Defining a snapshot state of microglia by taking advantage of the recent transcriptomics technologies is indeed valuable; however, it is crucial to complement these findings with functional analyses of microglia to define varying subpopulations within the CNS.

1.4.1 Microglia and Synaptic Pruning

Mounting evidence indicates a fundamental role of microglia in normal brain development and wiring through modulating synaptic formation, maturation (Hoshiko et al., 2012; Ueno et al., 2013; Miyamoto et al., 2016), and regulation of synaptic pruning in physiological and pathological conditions (Stevens et al.,2007; Paolicelli et al., 2011; Schafer et al., 2012; Kim et al., 2017). *In vivo,* two-photon imaging studies of mice have revealed that GFP-labeled microglia continuously survey their local environment, and their fine processes continuously contact neurons, axons, and dendritic spines (Davalos et al., 2005; Nimmerjahn et al., 2005). It is anticipated that resident microglia can scan the entire brain volume within a matter of just few hours (Nimmerjahn et al., 2005). Microglial processes make direct and transient contacts with synaptic terminals; and several research groups have reported the presence of pre- and post-synaptic components inside microglial lysosomes, suggesting an active involvement of microglia in synaptic pruning (Tremblay et al., 2010; Paolicelli et al., 2011; Schafer et al., 2012; Filipello et al., 2018). For synaptic pruning and remodeling, microglia use their immune-phagocytic functions (Kettenmann, Kirchhoff & Verkhratsky, 2013). Phagocytosis is a complex process involving three primary steps: target recognition, engulfment, and digestion. Microglia sense “find me” signals before migrating toward the target, where they next detect “eat me” signals to initiate phagocytosis. The development of phagocytic cups is the initial step, which is followed by the engulfment and digestion of the target in lysosomes (Brown & Neher, 2014). Apart from phagocytosis, trogocytosis has also been reported in microglia, where they engulf only pre-synaptic material without forming the phagocytic cup in hippocampal organotypic brain slices (Weinhard et al., 2018). Contact of microglia with post-synaptic terminals, on the other hand, only resulted in the remodeling of

dendritic spines (Weinhard et al., 2018). Depletion of microglia at P19 or P30 revealed a significant decrease in synapse elimination and formation (Parkhurst et al., 2013). The neural activity appears critical to determine which synapses are to be preserved and which to be tagged for elimination. Since microglia have dynamic contacts with synapses, they sense the local synaptic release through their neurotransmitter receptors and engulf synapses that display lower activity (Schafer et al., 2013). However, neuronal activity is not the only factor that regulates microglia-mediated synaptic pruning, which also depends on the developmental stage, brain region, and the pathological insult (Paolicelli & Ferretti, 2017; Geloso et al., 2021; Mordelt and de Witte, 2023).

The most important and extensively studied pathways that mediate microglia-dependent synaptic engulfment are the complement pathway (Stevens et al., 2007), TREM2 pathway (Filipello et al., 2018), IL33-R signaling pathway (Vainchtein et al., 2018), SIRPα-mediated pathway (Ding et al., 2021; Lehrman et al., 2018), and Fractalkine pathway (Paolicelli et al., 2011).

First reported in the retinogeniculate system, complement signaling is one mechanism that microglia use together with astrocytes to identify and locate the unwanted synapses in the postnatal developmental. They recognize and engulf synapses tagged by complement cascade proteins, C1qb, and the downstream C3, through complement receptor 3 (CR3) in the visual thalamus (Stevens et al., 2007; Stephan, Barres & Stevens, 2012; Gomez-Arboledas, Acharya & Tenner, 2021).

In the hippocampus, different complement-independent mechanisms of synapse elimination have also been reported. During post-natal development, microglia eliminate excessive synapses via recognition of fractalkine (CX3CL1), which is secreted by neurons as a "find me/eat me" signal that can be recognized by the microglial CX3CR1. In parallel, *Cx3cr1*-KO mice display impairments in synaptic pruning and also in social behavior (Paolicelli et al., 2011; Zhan et al., 2014).

Another synaptic elimination mechanism is the TREM2-mediated phagocytosis of the synaptic components during periods of circuitry refinement in the hippocampus (Filipello et al., 2018). *Trem2*-KO mice show impaired synaptic engulfment and increased synaptic density in the hippocampus, along with reduced social interaction (Filipello et al., 2018). Another study reported that phosphatidylserine (PS) detection by microglia, especially through microglial TREM2, is another mechanism for the removal of synapses, which expose PS on their surface and signal microglia to engulf them in the hippocampus (Scott-Hewitt et al., 2020).

The IL-1 family cytokine Interleukin-33 (IL-33) is another molecular cue driving microglial engulfment of synapses. IL33 secreted by neurons (Nguyen et al., 2020) and by astrocytes represents a signal to microglia to engulf synapses in the thalamus, spinal cord, and hippocampus (Vainchtein et al., 2018; Nguyen et al., 2020).

SIRPα-mediated signaling also modulates microglia-synapse interaction through recognition of CD47, which is a "don't eat me" signal (Lehrman et al., 2018). In the retinogeniculate system, the interaction between CD47, which is expressed on the plasma membrane of neurons, and microglial SIRPα inhibit synaptic engulfment. This interaction might represent a

mechanism to "tag" and protect the necessary synapses from elimination (Lehrman et al., 2018; Ding et al., 2021).

Impairments in one or more of these mechanisms result in aberrant wiring of neural circuits or alter the homeostasis between excitatory and inhibitory synapses. Such dysregulations were discussed for the pathophysiology of neuropsychiatric disorders such as schizophrenia and autism spectrum disorder (Gupta et al., 2014, Sellgren et al., 2019), which supports the prominent role of microglia function in the context of “synaptopathies”.

Astrocytes also establish close contact at pre- and post-synaptic terminals, and form the "tripartite synapse". They are also involved in synaptic refinement during development and adulthood through mechanisms distinct from microglia. For instance, they can regulate the deposition of C1q on neurons, thereby activating microglial recognition of the synapses (Chung et al., 2015a; 2015b). In addition to astrocytes and pre- and post-synaptic neurons, microglia make up the “fourth component” of the “quad-partite synapse” (Paolicelli & Gross, 2011; Schafer et al., 2013) **(Figure 1.4)**.

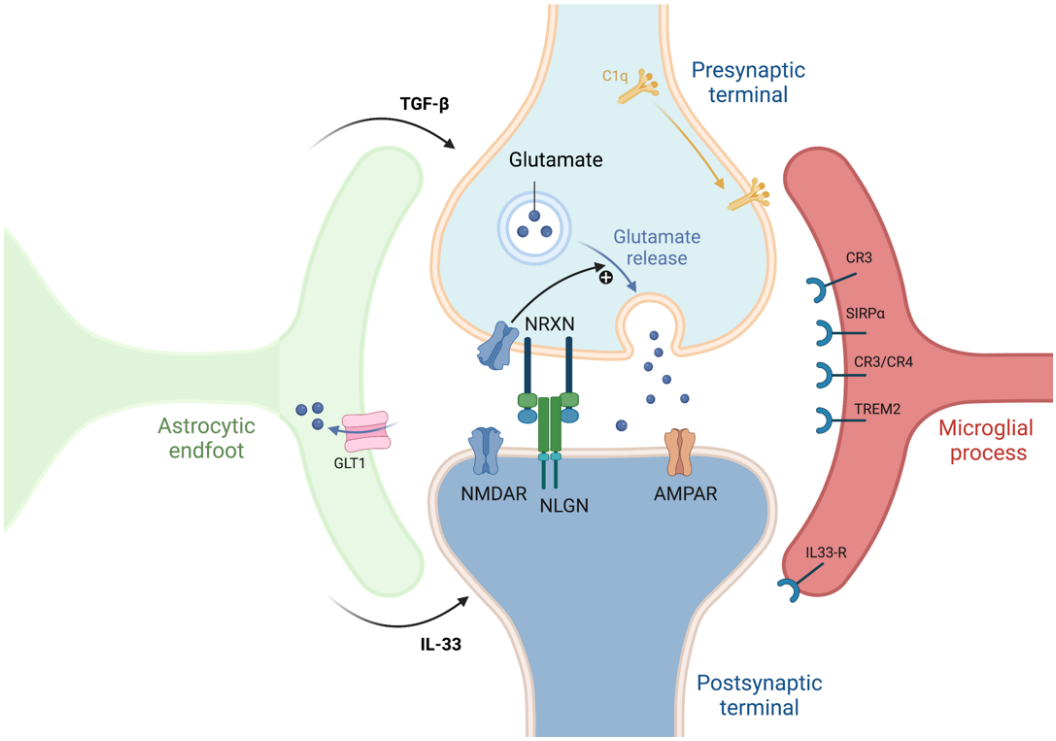

Figure 1.4 *Schematic representation of the quad-partite synapse (created by using biorender.com).*

1.4.1.1 Particular Emphasis on the Triggering Receptor Expressed on Myeloid Cells 2 (TREM2) Pathway

TREM2 is an innate immune receptor expressed by myeloid cells, such as macrophages, neutrophils, and also by microglia in the CNS. In the brain, TREM2 signaling induces a reactive microglia state and mediates several crucial microglial functions, such as survival, inflammation, phagocytosis, actin remodeling, cellular metabolism, and synaptic pruning (Brown & St. George-Hyslop, 2022; Filipello et al., 2022). TREM2 receptor-mediated signaling is induced by a ligand binding to the TREM2 ectodomain. Several classes of polyanionic molecules bind to the TREM2 ectodomain, such as bacterial components, anionic and zwitterionic lipids, myelin, apolipoprotein E (ApoE), and lipoprotein particles (Filipello et al., 2022). Upon ligand binding, TREM2 receptor signaling starts through association of the DAP12 (TYROBP) and DAP10 adaptor proteins with the intracellular C-terminus domain of surface

TREM2. The TREM2 cytoplasmic domain and DAP12 intracellular complex then activate multiple downstream signaling molecules that result in the activation of mitogen-activated protein kinase (MAPK)-mediated cascades among other pathways (Filipello et al., 2022). The plasma membrane levels of TREM2 are tightly regulated and show a rapid turnover. TREM2 undergoes ectodomain shedding by ADAM10 and ADAM17, which release soluble TREM2 (sTREM2) into the extracellular space, following which it becomes detectable in the cerebrospinal fluid (CSF) and peripheral blood (Piccio et al., 2008; Wunderlich et al., 2013). This proteolytic shedding of surface TREM2 can negatively regulate the TREM2 signaling (Filipello et al., 2022), and the residual TREM2 C-terminal fragment is degraded by γ-secretase (Wunderlich et al., 2013). ADAM17 is also involved in TREM2 ectodomain shedding in THP1 and CHO cell lines (Feuerbach et al., 2017), whereas ADAM10 plays a role in human macrophages, HEK293 cells, and murine microglia (Schlepckow et al., 2017; Thornton et al., 2017).

Another mechanism to generate sTREM2 is the translation of the alternative splicing product of the *Trem2* gene (TREM2$^{\Delta e2}$), which encodes for the soluble form of TREM2 instead of the surface-bound form (Del-Aguila et al., 2019; Filipello et al., 2022). Whether the ectodomain shedding and alternative splicing mechanisms work independently or in cooperation remains elusive. Notably, rapid turnover of TREM2 suggests either that TREM2 levels on the cell membrane must be tightly regulated or that sTREM2 has a certain cellular function and TREM2 might as well serve this function as a precursor of the functional sTREM2 (Brown & St George-Hyslop, 2022). sTREM2 has been shown to activate microglia (Zhong et al., 2017; 2019; Sheng et al., 2021), by an unknown mechanism, and it may also act as a decoy receptor, which can competitively bind to the TREM2 ligands and may negatively regulate TREM2

signaling (Filipello et al., 2022). Rare genetic variants of TREM2 are associated with an increased risk for Alzheimer's disease (Jonsson et al., 2013). On the other hand, the role and regulation of TREM2 signaling have not been addressed enough in the context of psychiatric disorders. Importantly, since TREM2 signaling results in an activated state of microglia (Zhong et al., 2017; 2019; Sheng et al., 2021), as well as is required for synapse elimination in a normal brain (Filipello et al., 2018), its role and regulation in various psychiatric disorders needs further investigation.

1.5 Inflammation and Psychiatric Disorders

Infections (Boksa, 2010) and stress (Merlot et al., 2008) , identified as triggers of acute and chronic inflammatory responses, have been linked to high susceptibility to mental disorders. Human epidemiological studies demonstrate associations between exposure to early-life stress and the increased likelihood of developing neuropsychiatric disorders later in life (MacMillan et al., 2001), including depression (Agid et al., 1999; St Clair et al., 2015) and ASD (Kinney et al., 2008). Similarly, prenatal infections that occur during the first and second trimesters of human pregnancy elevate the risk of schizophrenia (Brown et al., 2004; 2012) and ASD (Atladóttir et al., 2010; Di Marco et al., 2016; Brown et al., 2012).

There is a complex relationship between neuropsychiatric disorders and inflammation. Evolutionarily, there are a number of behaviors adapted to allocate energy resources to combat sickness and inflammatory response. These behaviors are called as "sickness behavior" in general; and include drowsiness, anhedonia, anxiety, diminished social engagement, lower locomotor activity, and reduced exploration in rodents (Dantzer et al.,

2008) and in humans (Harrison et al., 2009). The mechanism by which sickness behavior relates to neuro-immune interactions still remains poorly known. Yet, the existence of these sets of behaviors is a great evolutionary adaptation to preserve energy in favor of an effective immune response during an infectious disease and inflammation (Peters, 2006; Dantzer et al., 2008). Interestingly, several key characteristics of major depressive disorder, such as reduced social exploration and anhedonia, closely resemble to sickness behavior (Maes, 1993; Maes et al. 1993; Maes et al., 2012). This observation led to hypotheses that if inflammation has the potential to induce such short-term behavioral changes, then the chronicity of this inflammation could potentially induce a long-lasting phenotype of such behavioral alterations, which can be considered as a depressive phenotype. In particular, if the subjects are already genetically predisposed or have been exposed to a negative environment (Dantzer et al., 2008), inducing a depressive phenotype would even be more probable under inflammatory conditions. Observations of higher peripheral levels of proinflammatory cytokines in major depressive disorder (MDD) patients support this notion (Dowlati et al., 2010). Moreover, some treatment strategies, such as Interferon alpha (IFN-α) treatment for hepatitis C, are associated with the risk of severe depressive symptoms, supporting further the link between inflammatory phenotype and depressive behavior (Udina et al., 2012). PET studies have demonstrated an increase in TSPO ligand binding in the cortex of depressed patients (Richards et al., 2018). Moreover, multiple brain regions, primarily the cerebral cortex, amygdala, and hippocampus, have been reportedly showed higher TSPO ligand binding, indicating a response to inflammatory stimuli, in some individuals with ASD (Suzuki et al., 2013; Tay et al., 2018). These findings, therefore, suggest a proinflammatory profile in the brains of MDD and ASD patients. Several studies demonstrated persistent behavioral symptoms being associated with inflammatory response (Zheng et al., 2021; DiSabato et al.,

2016; Rosenblat et al., 2014; Shultz et al., 2012). Furthermore, anti-inflammatory agents, such as minocycline, demonstrated a promising potential to treat such behavioral symptoms (Chaudhry et al., 2012; Soczynska et al., 2017; Köhler et al., 2014; Nettis et al., 2021), suggesting that modulation of inflammation affects behavior. The COVID-19 pandemic has recently provided an additional evidence that even systemic inflammation and the accompanying cytokine storm can influence memory, cognition, and behavior, sometimes triggering or exacerbating mental disorders (Rogers et al., 2020; Xiong et al., 2020; Kempuraj et al., 2020).

Microglia are sentinels in the CNS and can induce a pro-inflammatory or anti-inflammatory response depending on the assault (Kettenmann & Hanisch, 2007). Given that the mounting evidence indicates a critical link between inflammation and psychiatric disorders, the role of microglia in neuroinflammation and thus the effect of inflammation on microglia became the focus of the psychoneuroimmunology research.

1.5.1 Microglia in Psychiatric Disorders

There is a limited understanding of the pathogenic mechanisms behind psychiatric disorders, which are evidently highly complex and heterogeneous. Genome-wide association studies (GWAS) have identified the association of immunological, neural, and synaptic pathways with a number of psychiatric disorders (The Network and Pathway Analysis Subgroup of the Psychiatric Genomics Consortium, 2015). Microglia have been the focus of several studies of psychiatric disorders, as they relate to all three of these pathways through their versatile functions in the CNS. Dysregulations in the microglia phenotype have been reported in both

preclinical and post-mortem human studies, including those on autism, anxiety and depression, Rett syndrome, obsessive-compulsive disorder, and schizophrenia (Mattei et al., 2017; Fillman et al., 2013; Dean et al., 2013; Frick et al., 2013; Steiner et al.,2008; Vargas et al., 2005; Morgan et al., 2010; Uranova et al., 2010; Bayer et al.,1999). Moreover, prenatal inflammation has been shown to shift the transcriptomic profile of early postnatal microglia towards adult signature, suggesting that many crucial microglia functions at those critical early stages of development can be affected in response to inflammation (Matcovitch-Natan et al., 2016). This study reports the impact of inflammation on microglia, which can have a variety of functional consequences that contribute to abnormal brain wiring and a proinflammatory response, both of which are linked to psychiatric disorders (Tay et al., 2017). Therefore, microglia are suggested to play a potential role in the start and/or progression of neuropsychiatric disorders via abnormal homeostasis maintenance, which in turn affects numerous brain functions (Salter & Stevens, 2017 ; Tay et al., 2017).

1.5.1.1 Microglial Dysregulation in Autism

Studies on post-mortem brains of individuals with autism have revealed altered expression of microglia-specific genes, including markers related to an inflammatory state (Voineagu et al., 2011; Gupta et al., 2014; Suzuki et al., 2013), as well as microglia with primed morphology (Morgan et al., 2010). In addition to human studies, impaired microglial function in mice has also been shown to induce behavioral abnormalities associated with the symptoms of schizophrenia, obsessive-compulsive disorder, and ASD (Chen et al., 2010; Derecki et al., 2012; Zhan et al., 2014). Maternal immune activation (MIA) is also associated with an elevated risk for autism (Tay et al., 2017) and various studies have reported microglial alterations in

the brains of offspring including changes in transcriptome, phagocytic capacity, motility, and morphology, in response to MIA (Sominsky et al., 2012; Mattei et al., 2017; Ozaki et al., 2020; Hayes et al., 2021). Notably, such microglial alterations can drive neuroinflammation but could also be a secondary, non-causal responses to neuroinflammation and neuronal death. Nevertheless; such alterations, whether caused directly or indirectly, impede microglia from carrying out their normal physiological functions, and this may have deleterious effects on neurogenesis, synaptogenesis, the wiring of brain circuits, and ultimately, behavior (Tay et al., 2017). Yet, it still is crucial to understand if the microglia are merely reacting to abnormal changes in the brain environment or if they play a causative role contributing to the underlying pathophysiology of autism.

1.5.1.2 Microglial Dysregulation in Anxiety and Depression

Many studies have shown abnormalities of peripheral cytokine levels in patients with depression, raising the question of whether there is a primary immunological reason underlying the pathology of MDD (Frick et al., 2013). Investigations using post-mortem brains of patients, who committed suicide have indicated elevated IBA-1-positive microglia density compared to the healthy controls (Steiner et al., 2008; Morgan et al., 2010; Torres-Platas et al., 2014). Stress-induced anxiety in rodents was also linked to increased microglia density, as well as altered morphology -toward ameboid- and elevated phagocytosis in the hippocampus, along with the secretion of proinflammatory cytokines such as IL-1β, IL-6, and TNF-α (Wohleb et al., 2018; Tynan et al., 2010). Neonatal exposure of rats to LPS was shown to induce increased anxiety-like behavior and microglial activation in adulthood (Sominsky et al., 2012), suggesting a link between inflammation, microglia phenotype and behavior. Mice with innate

high anxiety (HAB) also showed microglial dysregulations in the hippocampus such as the higher density and a higher CD68 immunoreactivity of microglia (Rooney et al., 2020). These studies, therefore, show that both stress-induced and innate high anxiety indicate an altered status of microglia along with dysregulations in the neuroimmune system. Overall, the current literature suggests a link between microglial dysregulation and high anxiety, as well as depression; however, it is not yet clear how these alterations contribute to the neuropathology of these psychiatric disorders.

1.6 Aim of the Present Study

In the light of recent reports highlighting the potential role of microglia in psychiatric disorders, the primary objective of the present study was to investigate how synaptic engulfment by microglia is regulated in mouse models of autism and innate high anxiety & depression, as well as what sort of dysregulations may drive an aberrant synaptic engulfment by microglia in these mouse models displaying psychiatric symptoms. The present dissertation consists of two independent projects, in which the contexts of autism (**A**) and anxiety & depression (**B**) were independently studied.

PROJECT (A)

A growing body of data implicates synaptopathy as an underlying reason for ASD; however, research on the interaction of microglia and synapses in ASD models is insufficient. We previously reported aberrant microglial function and phenotype in the *Nlgn4*-KO mouse, a model of ASD, along with significant sex-linked differences in microglia motility, morphology

and antigen presentation potential, which were profoundly altered in males in the hippocampus (Guneykaya et al., 2023). Taking into account the changes observed in microglial phenotype, as well as the role of microglia in synaptic refinement, herein I asked a major question of how microglia-synapse interaction is affected in the *Nlgn4*-KO model; and I mainly focused on microglial engulfment of synapses along with the investigation of main pathways involved in their cross-talk.

In the present study,

1. I investigated microglial engulfment of synapses in the *Nlgn4*-KO hippocampus using *in vitro* and *ex vivo* assays, both for vGLUT1^{+} excitatory synapses and for total synaptosomes.
2. I examined the TREM2, CX3CR1, IL33R, SIRPα, and complement signaling pathways to highlight potential targets underlying aberrant synaptic engulfment by microglia in the *Nlgn4*-KO hippocampus.
3. I reported (**1**) and (**2**) at two different developmental stages (P15 and P90) to present the effect of development on microglial engulfment of synapses along with the main pathways regulating this function in the *Nlgn4*-KO hippocampus.
4. I examined the effect of the absence of NL4 in the hippocampal synaptosome proteome.
5. I investigated the behavioral phenotype of *Nlgn4*-KO mice by particularly focusing on spatial learning and memory, considering its potential relevance to microglial pruning of synapses in the hippocampus.

2A Materials & Method

2A.1 Animals

All mice of both sexes used for the current study were on a C57BL/6N genetic background and were handled according to the governmental and internal regulations. *Nlgn4*-KO mice were generously provided to our group by Prof. Nils Brose (Max-Planck-Institute for Experimental Medicine, Göttingen). The mice were group-housed in ventilated cages under standard laboratory conditions with 12:12 light/dark cycle and with access to food and water.

2A.2 Ethics Statement

All animal-handling procedures were performed in accordance with the German Animal Protection Law and were approved by the Regional Office for Health and Social Services in Berlin (Landesamt für Gesundheit und Soziales, Berlin, Germany, G0434/17). Mice were sacrificed with an overdose of pentobarbital (Narcoren, Vetmedica GmbH, catalog no. 11336163) with intraperitoneal injection followed by decapitation.

2A.3 Flow Cytometry Analysis of Cell Surface Markers

Mice were intracardially perfused with 15ml ice-cold calcium- and magnesium-free Dulbecco's phosphate-buffered saline (DPBS). Hippocampi were dissected on a cooled, smooth glass platform and placed in ice-cold Hibernate-A medium (ThermoFisher Scientific, catalog no. A1247501). Mechanical dissociation protocol for cell isolation was adapted from Mattei et al., 2020 and carried out at 4°C using a Dounce homogenizer, with 30 gentle strokes using a loose pestle, until the hippocampi were completely homogenized in the Hibernate-A medium. The homogenates were then centrifuged at 400g for 10 minutes at 4°C, and the

pellet was dissolved in 1.5 ml DPBS. Myelin debris were removed via percoll gradient centrifugation by gently overlaying 2 ml PBS on the cell suspension including 22 % Percoll (GE Healthcare, catalog no.17-0891-01) in 2 ml final volume, and centrifuged for 10 minutes at 3000 g with full acceleration and no breaks. Myelin cloud and rest of the supernatant were gently removed. The pellets were washed once with 1 ml DPBS and centrifuged at 300g for 5 minutes at 4°C. The supernatant was discarded, and the total cell pellets were stained by using monoclonal anti-mouse antibodies: CD45 (BD, catalog no 559864, 1/100), CD11b (ThermoFisher Scientific, catalog no. 25-0112-82, 1/100), IL33R (ThermoFisher Scientific, catalog no. 12-9335-82, 1/100), TREM2 (R&D Systems, catalog no. FAB17291C, 1/200), CX3CR1 (BioLegend, catalog no. 149019, 1/100), SIRPα (ThermoFisher Scientific, catalog no. 12-1721-82, 1/100), CD16/CD32 (1/200, ThermoFisher Scientific, catalog no. 14-0161-82) for 30 min at 4°C. Cells were washed once at 300g 5 min at 4ºC, supernatant was discarded, and the pellet were resuspended in 250 µl FACS buffer (DPBS with 0.2% BSA). Data were immediately acquired on BD Fortessa flow cytometer and main fluorescence intensity (MFI) values were analyzed with FlowJo v10 (BD Bioscience).

2A.4 Microglial Engulfment of vGLUT1^{+} Synapses

Intracellular vGLUT1 staining protocol was adapted from Brioschi et al., 2020 with minor modifications provided below. The mechanical dissociation protocol (Mattei et al., 2020) for cell isolation, which is described above, was strictly followed. Upon percoll gradient centrifugation, total cell pellets were stained with fixable live/dead staining (ThermoFisher Scientific, catalog no. L34969, 1/1000 in DPBS) for 30 min at 4°C, and followingly stained for the microglial surface markers CD45 (BD, catalog no. 559864, 1/100), CD11b (ThermoFisher Scientific, catalog no. 25-0112-82, 1/100), Ly6C (BD, catalog no. 553104), and Ly6G (BD,

catalog no. 551460). Stained samples were fixed and permeabilized using the BD Cytofix/Cytoperm kit according to manufacturer's instructions (catalog no. 554714). Following fixation, intracellular staining for vGLUT1 Synaptic marker (Miltenyi Biotech, catalog no. 130-120-764, 1/200 in 1x BD Permeabilization Buffer) was performed for 1h at 4°C. Samples were acquired on FACS ARIA II (BD Bioscience) and microglia population was gated as $CD11b^{++}$/ $CD45^{+}$/ $Ly6C^{-}$/ $Ly6G^{-}$/ Viable cells. Spleen macrophages were used as negative control, which enabled us to quantify the percentage of vGLUT1 positive microglia residing above the spleen threshold gate. We also validated the specificity of our vGLUT1 antibody by using Vglut-IRES-Cre/ChR2-YFP mice, which were used as a positive control for the binding of the vGLUT1-FACS antibody. YFP is expressed by the glutamatergic neurons of these mice, indicating that the YFP positive population should also be vGLUT1 positive. We detected 98.7% of the YFP^{+} population as vGLUT1 positive by using our staining protocol, which validates the efficiency of our antibody **(Figure 2A.1)**. Detecting no positive events in spleen as a biological negative control, and using an isotype as a technical negative control, we confirmed that the vGLUT1 antibody used in the synaptic engulfment assay is specific. Gating strategy to define microglia is given in **Figure 2A.3**. Raw data were analyzed with FlowJo v10 (BD Bioscience). MFI of vGLUT1-PE was analyzed by gating on $CD11b^{++}$/ $CD45^{+}$/ $Ly6C^{-}$/ $Ly6G^{-}$/ Viable population to quantify the engulfment of $vGLUT1^{+}$ synapses by microglia.

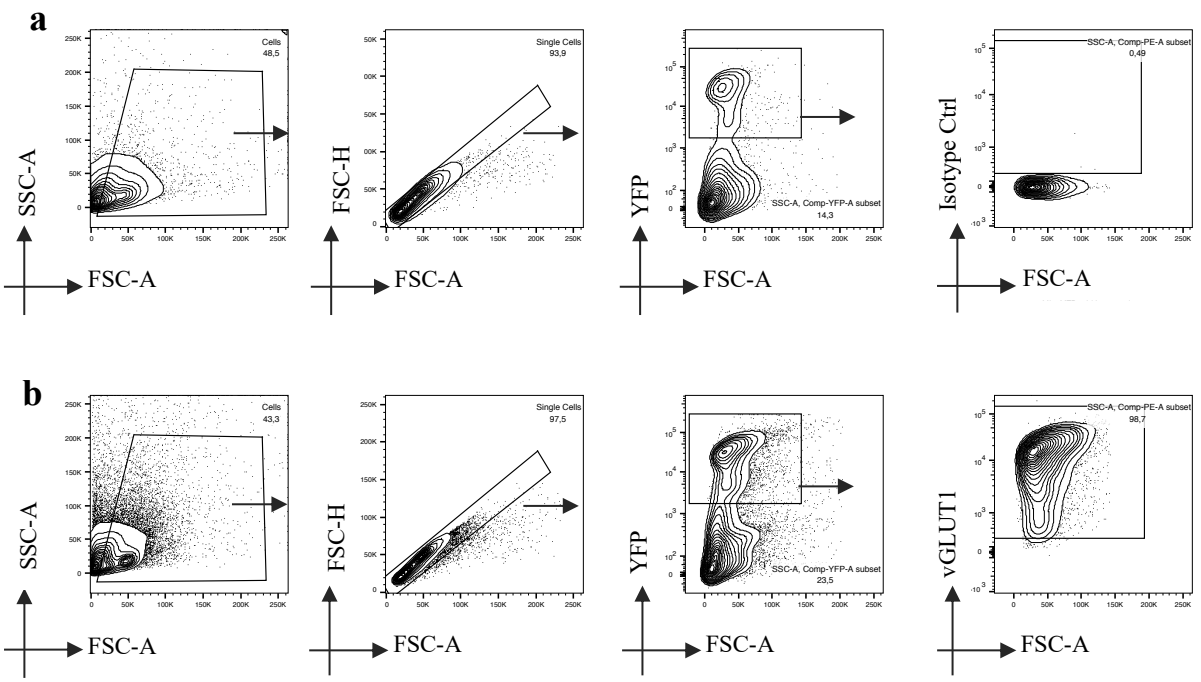

Figure 2A. 1 *Representative FACS plots demonstrating the gating strategy to test the specificity and efficiency of the vGLUT1 antibody.*

Gating strategy to define the YFP⁺ population from the hippocampus of Vglut-IRES-Cre//ChR2-YFP mice that were used as a positive control for testing the efficiency of the vGLUT1 FACS antibody. Compared to the Isotype control ***(a)****; 98.7% of YFP positive cell fraction is detected as vGLUT1 positive* ***(b)****.*

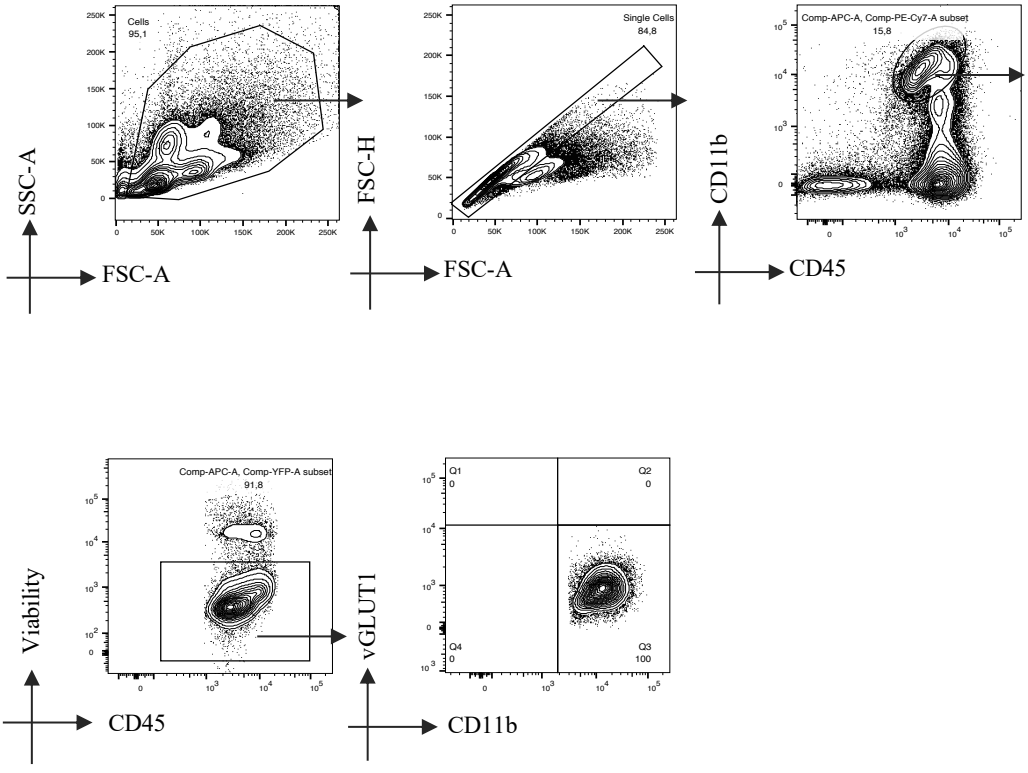

Figure 2A. 2 *Representative FACS plots demonstrating the gating strategy to define spleen macrophages.*

Spleen was used as a negative control in the experiments to test the microglial engulfment of synapses in the hippocampus, per experimental run. FACS plots given above define the spleen macrophages as CD11b^{++}/ CD45^{++}/ Viable population. This population was used to set a threshold gate to quantify vGLUT1^{+} microglia in the brain samples.

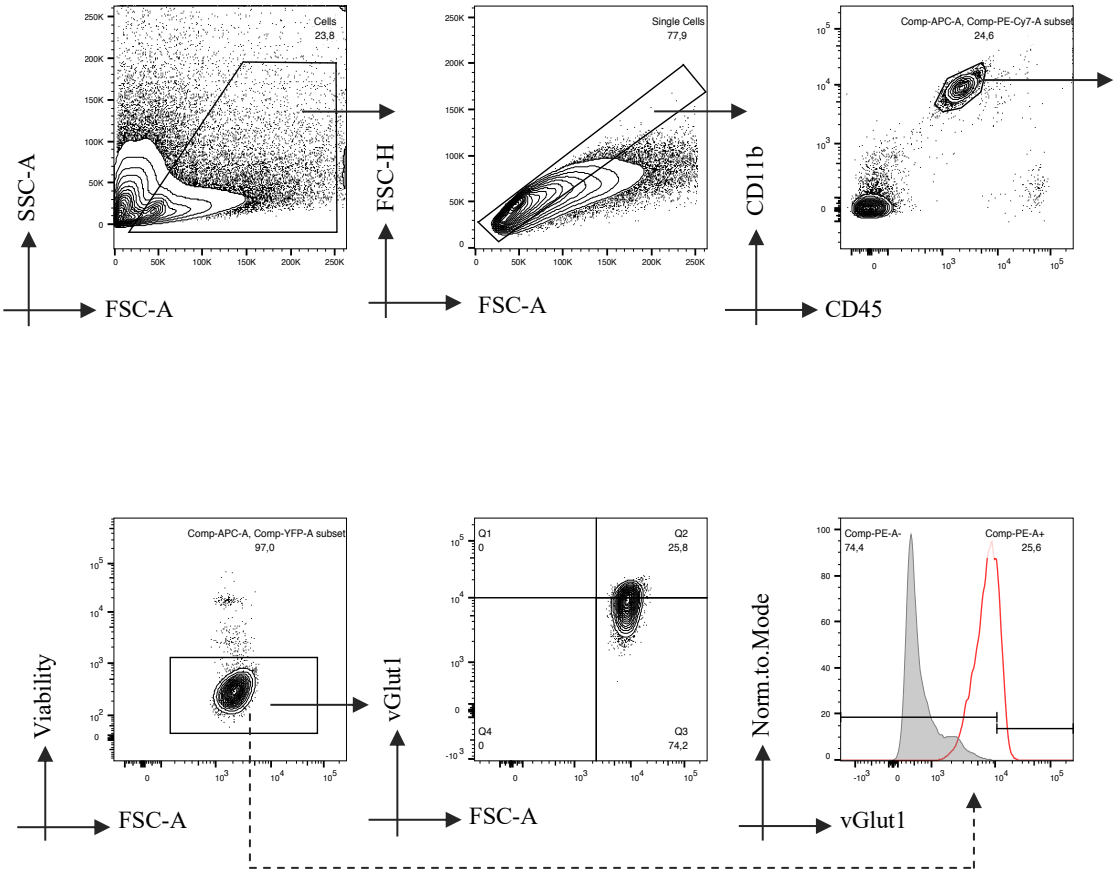

Figure 2A. 3 *Representative FACS plots indicating the gating strategy to define microglia as CD11b^{++}/ CD45^{+}/ Viable population.*

CD11b^{++}/ CD45^{+}/ Viable population was used to analyze vGLUT1-MFI as well as to quantify the percentage of vGLUT1^{+} microglia in the hippocampus based on the spleen threshold gate. Gray histogram defines the vGLUT1-MFI from the spleen macrophages and red histogram defines the vGLUT1-MFI from the hippocampal microglia. The gate indicated on the histogram starts at the level, where the vGLUT1-MFI from the spleen terminates (~10^{4}) and is used to analyze the vGLUT1 positive fraction in the brain samples.

2A.5 Total Synaptosome Isolation and pHrodo^{TM} Red Labeling

Hippocampal synaptic terminals were freshly isolated for each experiment, using Syn-PER Synaptic Protein Extraction Reagent (Thermo Fisher Scientific, catalog no. 87793) as recommended by the manufacturer. One tablet protease inhibitor was supplemented per 10 ml Syn-PER reagent (Roche, catalog no. 5892970001). Hippocampi from WT and *Nlgn4*-KO mice were dissected on ice-cold glass platform and homogenized by using a Dounce tissue grinder by ~30 gentle strokes. The homogenate was centrifuged at 1200g for 10 min, and the pellet was discarded. The supernatant was centrifuged at 15,000*g* for 20 min and the synaptosomal pellet was resuspended in 0.1M Na_2CO_3. 0.25 mM pHrodo^{TM}Red (ThermoFisher Scientific, catalog no. P36600) was used to label synaptosomes at room temperature for 1.5 h with gentle agitation. After seven times of washing with PBS to remove unbound excessive pHrodo^{TM}Red, synaptosomes were pelleted at full speed for 1 min and immediately snap frozen using liquid nitrogen.

For the tandem mass tag (TMT) mass spectrometry from synaptosomes, we used a different approach for the isolation of synaptosomes, since this approach has been proven to work better in mass spectrometry compared to the other isolation methods (Hoernberg et al., 2021; unpublished data). In this approach, we used Krebs buffer (118.5 mM NaCl, 2.5 mM $CaCl_2$, 1.18 mM KH_2PO_4,1.18 mM $MgSO_4$, 3.8 mM $MgCl_2$, 24.9 mM $NaHCO_3$, 212,7 mM glucose in distilled H_2O). One tablet protease inhibitor was supplemented per 10 ml Krebs buffer (Roche, catalog no. 5892970001). Hippocampi from WT and *Nlgn4*-KO mice were dissected on ice-cold glass platform and homogenized by using a Dounce tissue grinder by ~13 gentle strokes in ice-cold Krebs buffer. Homogenate were further processed by using a syringe with 18G needle, and filtered first through a special soft filter (Merck Millipore, catalog no. NY1H02500) with 100 µm pore size. The resulting filtrate was again filtered through another

special filter (Merck Millipore, catalog no. NY0502500) with 5 µm pore size; and the final filtrate was centrifuged for 10 min at 1,000 x g, 4°C. Neuro-synaptosome pellet were collected and resuspended in 500 µL Krebs buffer supplemented with protease inhibitor. Samples were centrifuged for another round for 10 min at 1,000 x g, 4°C and the pellet were collected and lysed in Krebs buffer supplemented with 25mM HEPES, 2% SDS, and protease inhibitor. Samples were then boiled at 95°C for 3 minutes, and cooled down to 4°C. They were next transferred to the proteomics core facility of the Max Delbrück Center for Molecular Medicine to perform the mass spectrometry experiments.

2A.6 Mass Spectrometry and Proteomics Data Analysis

Proteomes of neuro-synaptosomes were analyzed using TMT (ThermoFisher Scientific) isobaric labels combined with deep fractionation as described by Mertins et al., 2018. Pellets were lysed in SDS buffer (25mM HEPES, 2% SDS, protease and phosphatase inhibitors) and boiled at 95°C for 3 minutes. Peptides were cleaned-up and digested with trypsin using the SP3 protocol as previously described (Hughes et al., 2014). 100 µg of each peptide sample was subjected to TMT pro 18-plex (ThermoFisher Scientific) labelling with randomized channel assignments. Quantitation across two TMT plexes was achieved by including an internal reference derived from a mixture of all samples. Samples were fractionated into 24 fractions using an UltiMate 3000 Systems (ThermoFisher Scientific) and measured on an Exploris 480 orbitrap mass spectrometer connected to an EASY-nLC system 1200 system. Analysis was performed using MaxQuant version 2.1.4.0 (Cox et al., 2008) with MS2-based reporter ion quantitation. Carbamidomethylation was set as a fixed modification and acetylated N-termini as well as oxidized methionine as variable modifications. A PIF filter with a threshold value of 0.5 was applied, and a Uniprot mouse database (2022-03) plus common

contaminants were used for database search. Corrected log2-transformed reporter ion intensities were normalized to the internal reference samples and further normalized using median-MAD normalization before applying two-sample moderated t-tests (limma, Ritchie et al., 2015). P-values were adjusted using the Benjamini-Hochberg procedure.

2A.7 *In vitro* Synaptosome Engulfment Assay

Under deep anesthesia, 13 weeks old mice were transcardially perfused with DPBS. Hippocampi were dissected on a cooled glass platform, and placed in ice-cold Hibernate-A medium supplemented with B27 (ThermoFisher, catalog no. A1247501). Enzymatic dissociation was carried out using Worthington's papain dissociation kit (catalog no. LK003150) based on the manufacturer's instructions. Myelin debris were removed via percoll gradient centrifugation by overlaying 2 ml PBS on cell suspension including 500 ul, 22 % Percoll in 2 ml final volume and centrifuged for 10 minutes at 3000 g with full acceleration and no breaks. Myelin cloud and rest of the supernatant were removed, and the pellet were washed in ice-cold MACS-buffer (PBS, 2% bovine serum albumin) and stained with anti-mouse CD11b magnetic beads (1/20 , Miltenyi Biotech, catalog no. 130-049-601) at 4^{o}C for 20 minutes. Total cells were passed through MS MACS columns (Miltenyi Biotech, catalog no. 130-042-201). The flow through was discarded and the cells were flushed out of the column using a plunger into 1 ml Dulbecco's Modified Eagle Medium (DMEM, ThermoFisher, catalog no. 11965092) and pelleted down by centrifugation at 300g, 6 minutes. Resulted pellet were resuspended in DMEM complete (10% FBS and 0.1% Penicillin/Streptavidin), and seeded in 24-well culture plates at a density of 2.5 x 10^4 cells per well. After 1.5 h at 37^{o}C, medium was gentle taken out and cells were supplied with 500 µl fresh DMEM per well, supplemented with 1/50 synaptosomes per well, and incubated for 2h at 37^{o}C. For analyses, cells were

washed 3 times with DPBS, detached using 500 µl trypsin solution (ThermoFisher Scientific, catalog no. R001100), were stained with CD16/CD32 (1/200, ThermoFisher Scientific, catalog no. 14-0161-82) and kept for 10 minutes on ice. This step was followed by staining with 1/100 CD11b, 1/100 CD45 at 4°C for 20 minutes. After the incubation, data were acquired using BD Aria II, and were analyzed using FlowJo v10 (BD Bioscience).

We defined the microglia population as $CD11b^{++}/CD45^{+}$ subset **(Figure 2A.4),** and tested the efficiency of our protocol by using 100 µM UDP to simulate microglia for 3 hours to induce phagocytosis (Koizumi et al.2007). After 3 hours, we compared the engulfment of pHRodo™Red-labeled total synaptosomes by microglia in the presence and absence of UDP. By showing a higher microglial pHRodo™Red-MFI from the UDP condition, we preliminary validated that our protocol works efficiently to detect changes in the microglial phagocytosis of synaptic material **(Figure 2A.5)**.

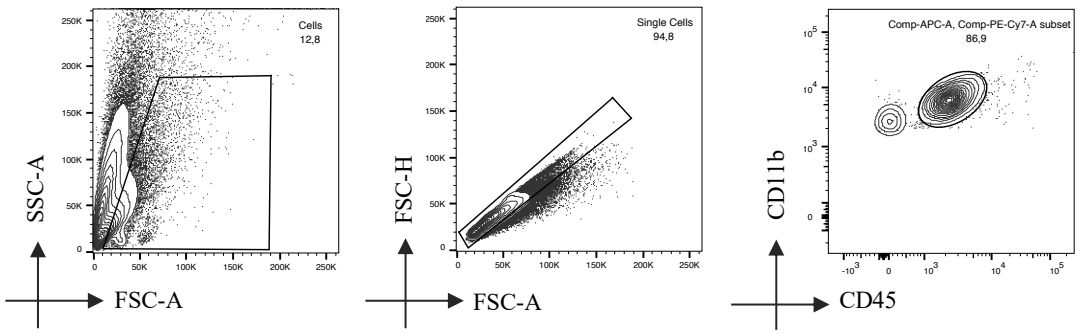

Figure 2A. 4 *Representative FACS plots demonstrating the gating strategy to define single/ $CD11b^{++}$/ $CD45^{+}$ microglia. $CD11b^{++}/CD45^{+}$* subpopulation was gated to analyze MFI of pHrodo™Red to quantify engulfment of pHrodo™Red-labeled synaptosomes by microglia. High number of events on the SSC-A axis indicates synaptosomes, which are located at SSC-A /FSC-A low axis.

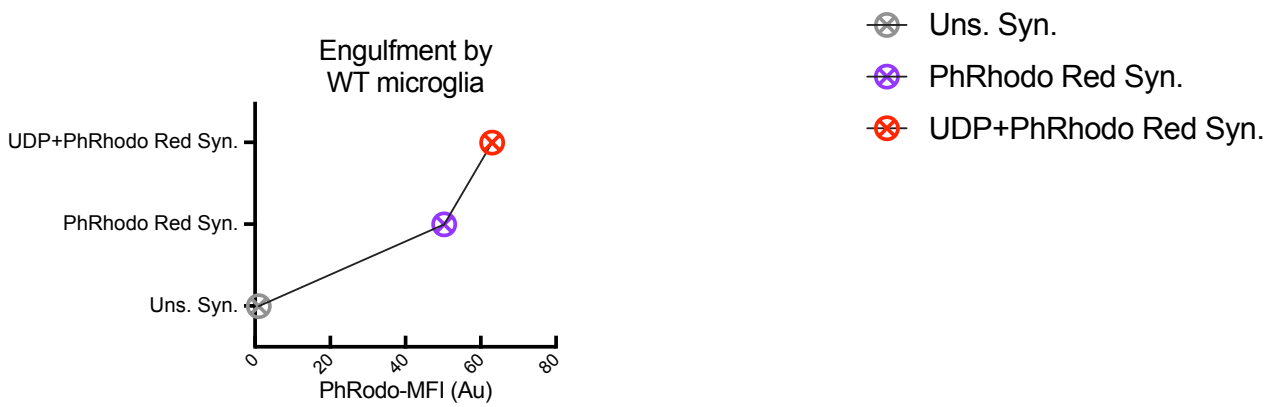

Figure 2A. 5 *Representative plot comparing the pHRodo™RED-MFI from different conditions.*

WT microglia fed with unstained WT synaptosomes showed the lowest pHRodo™RED-MFI (grey dot, normalized MFI=1), which gradually increase when the same microglia were fed with pHRodo™RED-labeled synaptosomes (purple dot, normalized MFI=50.32), then when stimulated with UDP and followingly fed with pHRodo™RED-labeled synaptosomes (red dot, normalized MFI=63.04). Each dot represents the same microglia at three different conditions (fed with unstained synaptosomes, fed with pHRodo™RED-labeled synaptosomes, stimulated with UDP and then fed with pHRodo™RED-labeled synaptosomes). pHRodo™RED MFI values detected in microglia were normalized to that of unstained synaptosomes prior to plotting.

2A.8 Protein Isolation and Enzyme-linked immunosorbent assay (ELISA)

Hippocampi were dissected from the WT and *Nlgn4*-KO mice, and hippocampal lysates were prepared in TRIS-HCl buffer (50 mM TRIS-HCl, 0.6M NaCl, 0.2% TritonX-100, 0.5% BSA, 1 tablet per 10 ml protease inhibitor Roche, catalog no. 5892970001) using FastPrep-24 classical instrument (MP Biomedicals). Hippocampal lysates were centrifuged at full speed (20815 g) for 30 minutes at 4ºC. Supernatant was collected and the total protein concentration was determined by using BCA assay (Pierce, ThermoFisher Scientific, catalog no. 23225). The enzyme-linked immunosorbent assay (ELISA; **Figure 2.5**) for complement component 3 (C3) (GenWay, catalog no. GWB-7555C7), for complement C1q subcomponent subunit B (C1QB) (Creative Biolabs, catalog no. CTK-031), fractalkine (CX3CL1) (R&D Systems, catalog no. MCX310), complement component 4A (C4A) (Assay Genie, catalog no. MODL00181),

Interleukin-33 (IL33) (ThermoFisher Scientific, catalog no. BMS6025), apolipoprotein E (APOE) (Assay Genie, catalog no. MOFI00648), TYRO protein tyrosine kinase-binding protein (TYROBP/ DAP12) (Assay Genie, catalog no. MOEB1092), soluble triggering receptor expressed on myeloid cells 2 (sTREM2) (MBS, catalog no. MBS7270015) were performed with 1⁄2 diluted hippocampal protein samples based on the manufacturers' instructions. A Disintegrin and metalloproteinase domain-containing protein 10 (ADAM10) enzyme activity assay (ANASpec, catalog no. AS-72226) was performed with the same hippocampal protein samples based on the manufacturer's instructions. Quantification of absorption and fluorescence values were detected using TECAN Infinite^{R}200 plate reader, and analyzed using a standard curve constructed by using the known concentrations versus absorption values of the respective targets.

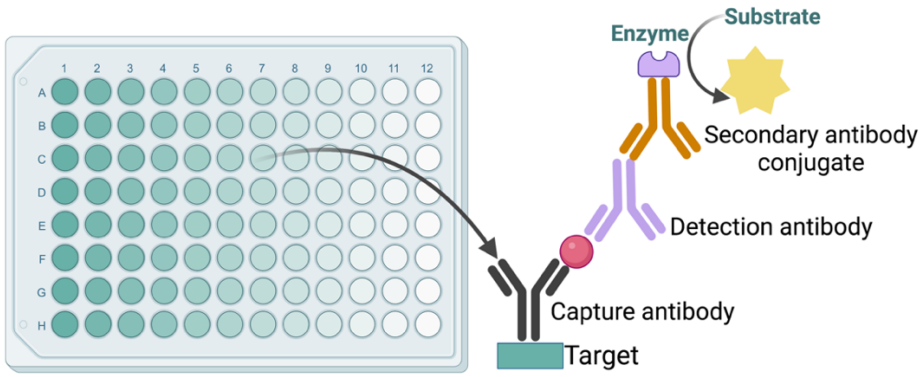

Figure 2A. 6 *Schematic representation of the enzyme-linked immunosorbent assay (ELISA) (created by using biorender.com).*

2A.9 Morris Water Maze

Nlgn4-KO and WT animals were subjected to Morris Water Maze (MWM) training, separated by 2 individual phases, which are acquisition (first 3 days) and reversal learning (last 2 days) to test for the cognitive flexibility. The commonly used protocol of six trials of training per day (Wolfer et al., 1997) was applied, and each trial lasted for 2 minutes. The pool, 112 cm in diameter, was sealed with non-toxic ecological paint and contained opaque water at the room temperature. Mice were subjected to the water maze containing a submerged escape platform that is 1 cm below the water surface. Latencies to reach the platform were compared between trials, and were recorded with an automatic video tracking system. The data was analyzed by ANY-maze video tracking program (Stoelting Co., Ireland).

2A.10 Statistical Analysis

Data analyses were performed with GraphPad Prism 8.0 software (GraphPad Software Inc., USA). A 95% confidence interval was used for statistical evaluation, and $P < 0.05$ was considered as statistically significant in all sampled groups. Data are presented as means ± standard error of the mean (S.E.M.). The respective statistical tests are mentioned in the figure legends.

3A RESULTS

3A.1 Lower percentage of vGLUT1⁺ microglia observed in the hippocampus of *Nlgn4*-KO males

We previously reported major dysregulations in the state and function of microglia in the *Nlgn4*-KO hippocampus (Guneykaya et al., 2023). In light of the reported status of microglia as well as that of synapses due to loss of NL4, we first examined engulfment of vGLUT1⁺ synapses by microglia and found lower engulfment in the *Nlgn4*-KO hippocampus, only in males **(Figure 3A.1).** Subsequently, we quantified the percentage of vGLUT1⁺ microglia in the *Nlgn4*-KO hippocampus and showed a significantly lower percentage only in males **(Figure 3A.1 e)**.

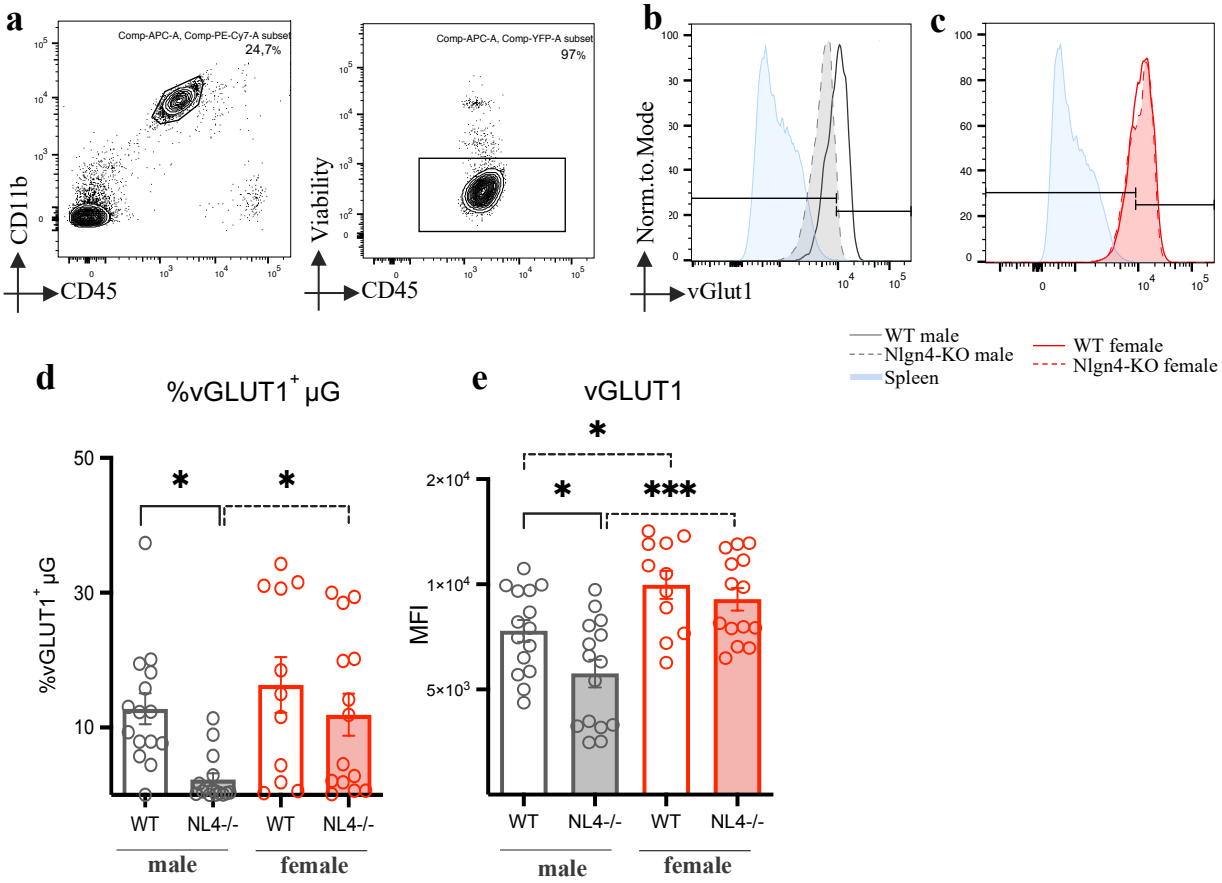

Figure 3A. 1 *Lower engulfment of vGLUT1^{+} synapses by microglia is detected in the NL4$^{-/-}$ male hippocampus.*

(a) *Gating strategy to define microglia as CD11b^{++}/CD45^{+}/ Viable subpopulation in the hippocampus.*
(b and c) *Representative histograms indicating vGLUT1 fluorescence signal from the hippocampal microglia of WT (line) and NL4$^{-/-}$ (dashes) male (grey) and female (red) mice. Spleen (light blue) is used as a negative control for each experiment, and at least 100k cells were recorded per sample.*
(d) *% vGLUT1^{+} microglia is found significantly less in NL4$^{-/-}$ hippocampus of males compared to WT (2-way ANOVA with Šídák's multiple comparisons test, male: n_{WT}=15 $n_{NL4-/-}$=15, p=0.0102; female: n_{WT}=11 $n_{NL4-/-}$=14, p=0.465; grey bar: WT male, grey-filled bar: NL4$^{-/-}$ male; red bar: WT female, red-filled bar: NL4$^{-/-}$ female). Data are represented as mean ± SEM, and each dot indicates 1 mouse. Significant sex differences are indicated with dashes between NL4$^{-/-}$ male and NL4$^{-/-}$ female ($p^{WTm/f}$ =0.599; $p^{NL4-/-\ m/f}$=0.022).*
(e) *Engulfment ability of NL4$^{-/-}$ and WT microglia was calculated by the vGLUT1-MFI signal of CD11b^{++}/CD45^{+}/Viable microglia in the hippocampus. NL4$^{-/-}$ male microglia show significantly lower vGLUT1^{+} MFI signal compared to WT. Data are represented as mean ± SEM, and each dot indicates 1 mouse. Significant sex differences are indicated with dashes between groups (2-way ANOVA with Šídák's multiple comparisons test, male: n_{WT}=15 $n_{NL4-/-}$=15, p=0.028; female: n_{WT}=11 $n_{NL4-/-}$=14, p=0.685, sex differences; $p^{WTm/f}$ =0.03, $p^{NL4-/-m/f}$ =0.0001 *P < 0.05; **P < 0.01; ***P < 0.001, NL4$^{-/-}$ indicates Nlgn4-KO on the presented plots).*

3A.2 Microglia from the *Nlgn4*-KO hippocampus phagocyte less synaptosomes

Since we observed a male-specific reduction in the synapse engulfment by microglia, as shown in **Figure 3A.1**, we next focused only on males and examined the engulfment of total synaptosomes instead of vGLUT1^{+} synapses in particular. For this purpose, we fed pHrodo^{TM}Red-labeled synaptosomes to freshly isolated microglia from the *Nlgn4*-KO and WT hippocampus. In order to compare the phagocytic function, we first supplied WT and *Nlgn4*-KO microglia with the same WT synaptosomes **(Figure 3A.2 a[d])** and detected impaired phagocytosis by *Nlgn4*-KO microglia **(Figure 3A.2 d)**. This data indicates that phagocytosis by

microglia towards synaptosomes is impaired in the *Nlgn4*-KO hippocampus. We also fed the same WT microglia either with WT or *Nlgn4*-KO synaptosomes **(Figure 3A.2 a[e])** to address the effect originated only by the synaptosomes. Our data indicate that *Nlgn4*-KO derived synaptosomes are less efficiently engulfed by WT microglia, indicating a poor cross-talk between them **(Figure 3A.2 e)**. This poor cross-talk indicated in the **Figure 3A.2 e** primarily is a result of synaptic composition of the *Nlgn4*-KO hippocampus, considering that phagocytosis by microglia towards WT synaptosomes is not hindered. We, therefore, report that both the engulfment of synaptosomes by microglia and the synapse-derived molecules signaling microglia to phagocyte are compromised in the *Nlgn4*-KO model. When *Nlgn4*-KO-derived synaptosomes were fed to WT and *Nlgn4*-KO microglia **(Figure 3A.2 a[f])**, as well as when synaptosomes of both origins were fed to *Nlgn4*-KO microglia **(Figure 3A.2a[g])**, we observed no significant difference in their engulfment **(Figures 3A.2 f and g)**.

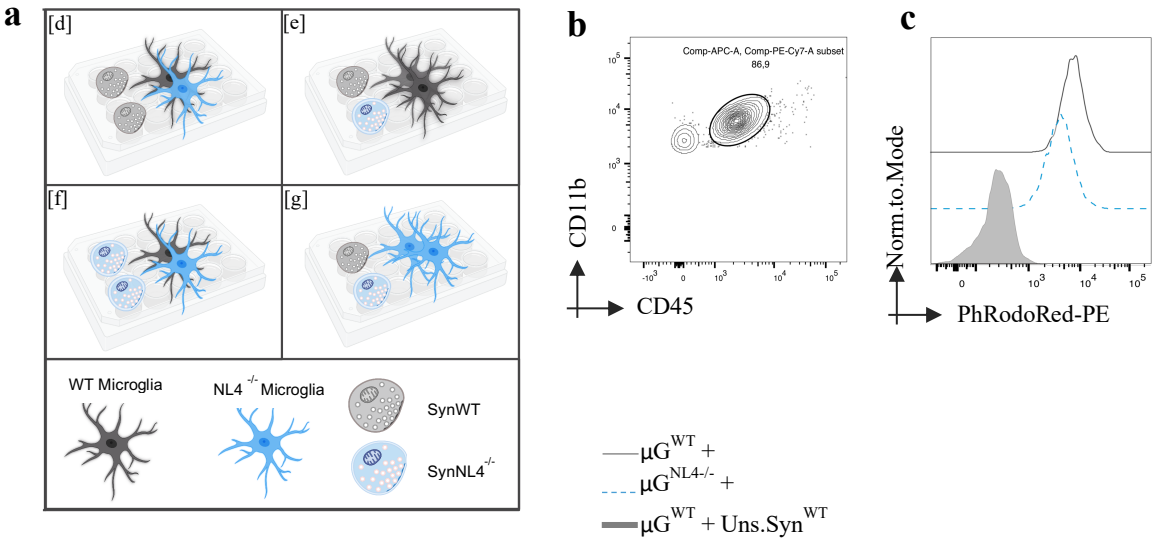

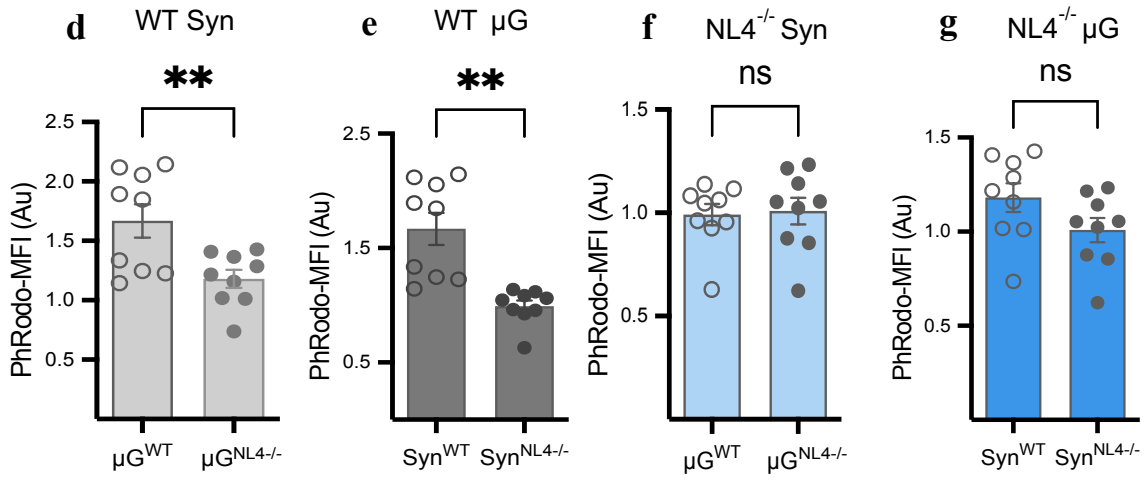

Figure 3A. 2 *NL4$^{-/-}$ microglia engulf synaptosomes less efficiently compared to WT microglia.*

(a)*Graphical illustration of four different experimental designs to detect engulfment of synaptosomes by microglia.* ***(a$^{[d]}$)****Freshly isolated microglia from WT and NL4$^{-/-}$ hippocampus are fed with the same WT synaptosomes.* ***(a$^{[e]}$)*** *Freshly isolated microglia from WT hippocampus are fed either with WT or NL4$^{-/-}$ synaptosomes****. (a$^{[f]}$)*** *Freshly isolated microglia from WT and NL4$^{-/-}$ hippocampus are fed with the same NL4$^{-/-}$ synaptosomes.* ***(a$^{[g]}$)*** *Freshly isolated microglia from NL4$^{-/-}$ hippocampus are fed either with WT or NL4$^{-/-}$ synaptosomes (WT microglia= grey, NL4$^{-/-}$ microglia= blue, WT synaptosomes= light grey, NL4$^{-/-}$ synaptosomes= light blue)****.***

(b) *Representative FACS plots indicating the gating strategy to define CD11b^{++}/CD45^{+} microglia population.*

(c) *Histogram comparing pHrodo^{TM}Red fluorescence intensity of WT (grey line), NL4$^{-/-}$ (light blue dashed-line) microglia fed with the pHrodo^{TM}Red-stained WT synaptosomes. WT microglia fed with unstained synaptosomes are used as a negative control (grey-filled).*

(d) *NL4$^{-/-}$ hippocampal microglia show lower pHrodo^{TM}Red MFI compared to WT microglia when they both are fed with the same WT-derived synaptosomes (circle: WT microglia fed with WT synaptosomes; dot: NL4$^{-/-}$ microglia fed with WT synaptosomes; Unpaired t test with Welch's correction, n_{WT}=9; $n_{NL4-/-}$=9; p=0.009).*

(e) *WT hippocampal microglia show lower levels of pHrodo^{TM}Red^{+} MFI when fed with NL4$^{-/-}$ synaptosomes (circle: WT microglia fed with WT synaptosomes; dot: WT microglia fed with NL4$^{-/-}$ synaptosomes; Unpaired t test with Welch's correction, male: n=9, p=0.001)*

(f and g)*. Microglia isolated from NL4$^{-/-}$ hippocampus do not differ from WT when they both are fed with either NL4$^{-/-}$[f] or WT[g] synaptosomes (circle[f]: WT microglia fed with NL4$^{-/-}$ synaptosomes; dot[f] : NL4$^{-/-}$ microglia fed with NL4$^{-/-}$ synaptosomes; circle[g]: NL4$^{-/-}$ microglia fed with WT*

*synaptosomes; dot[g]: NL4$^{-/-}$ microglia fed with NL4$^{-/-}$ synaptosomes). pHrodo^{TM}Red^{+} MFI values from each sample are normalized to the MFI of microglia fed with unstained synaptosomes and presented as fold-change relative to WT microglia for all given datasets. Each dot indicates one mouse and data is presented as mean ± SEM on all plots (Unpaired t-test with Welch's correction, n_{WT}=9 $n_{NL4-/-}$=9, p^{f}=0,94, p^{g}=0.103, *P < 0.05; **P < 0.01; ***P < 0.001; NL4$^{-/-}$ indicates Nlgn4-KO on the presented plots).*

3A.3 *Nlgn4*-KO male shows major dysregulations in the TREM2 signaling pathway in the hippocampus

We reported two complementary observations so far to indicate less engulfment of both vGLUT1^{+} synapses and total synaptosomes by *Nlgn4*-KO microglia. These results clearly indicate an impaired state of synaptic engulfment in the hippocampus of *Nlgn4*-KO compared to WT. According to several studies, signaling via TREM2, CX3CR1, IL33R, SIRPα, and complement proteins are primarily implicated as the pathways that control microglia-mediated synaptic engulfment (Filipello et al., 2019; Paolicelli et al., 2011; Vainchtein et al., 2018; Stevens et al., 2007; Ding et al., 2021). To determine which pathways might be responsible for the observed microglial phenotype, we next examined the dynamics of these pathways in the *Nlgn4*-KO hippocampus. We checked the expression CD11b subunit of C3 receptor (CR3), IL33 receptor (IL33R), SIRPα, Fractalkine receptor (CX3CR1) and TREM2 on microglia in the WT and *Nlgn4*-KO hippocampus along with their interaction partners C3, C1QB, C4A, IL33, and CX3CL1 **(Figure 3A.3).** We found a significantly lower surface expression of TREM2 by *Nlgn4*-KO microglia compared to WT **(Figure 3A.4 b-c).** Amongst all investigated pathways, the lower expression of TREM2 might explain the pattern of the observed, lower synaptic engulfment-related phenotype of the *Nlgn4*-KO microglia **(Figure 3A.3, Figures 3A.4 c and 3A.4 d).** Therefore, we next examined the other key regulators in the TREM2 pathway that involve APOE, sTREM2, and TYROBP. We reported higher levels of soluble TREM2 **(Figure**

3A.4 e), lower levels of APOE **(Figure 3A.4 f)**, yet, found no difference in TYROBP **(Figure 3A.4 g)** in the *Nlgn4*-KO hippocampus. Together, these findings point to major dysregulations in the TREM2 signaling in the hippocampus of *Nlgn4*-KO males, which is consistent with the previously described impairments in the synaptic engulfment shown in the **Figure 3A.1**. Except for the TREM2 surface expression, the only significant difference was found in CD11b (C3R) expression, which shows higher expression on *Nlgn4*-KO microglia compared to the WT, (**Figure 3A.3 a and b)** and this was not reflected on the function of microglial engulfment of synapses.

Since sTREM2 can be generated via cleavage of surface TREM2 by the ADAM10 enzyme or via alternative splicing of the *Trem2* gene (Filipello et al., 2022), we next tested the ADAM10 enzyme and reported lower enzymatic activity in the *Nlgn4*-KO hippocampus in comparison to the WT **(Figure 3A.4 h)**. The concentration of ADAM10, on the other hand, did not show a significant difference in the WT and *Nlgn4*-KO hippocampus **(Figure 3A.4 k).** Thus, rather than processing of the surface TREM2 by ADAM10, our data support the alternative splicing route as the driving source of the elevated levels of sTREM2 in the *Nlgn4*-KO hippocampus.

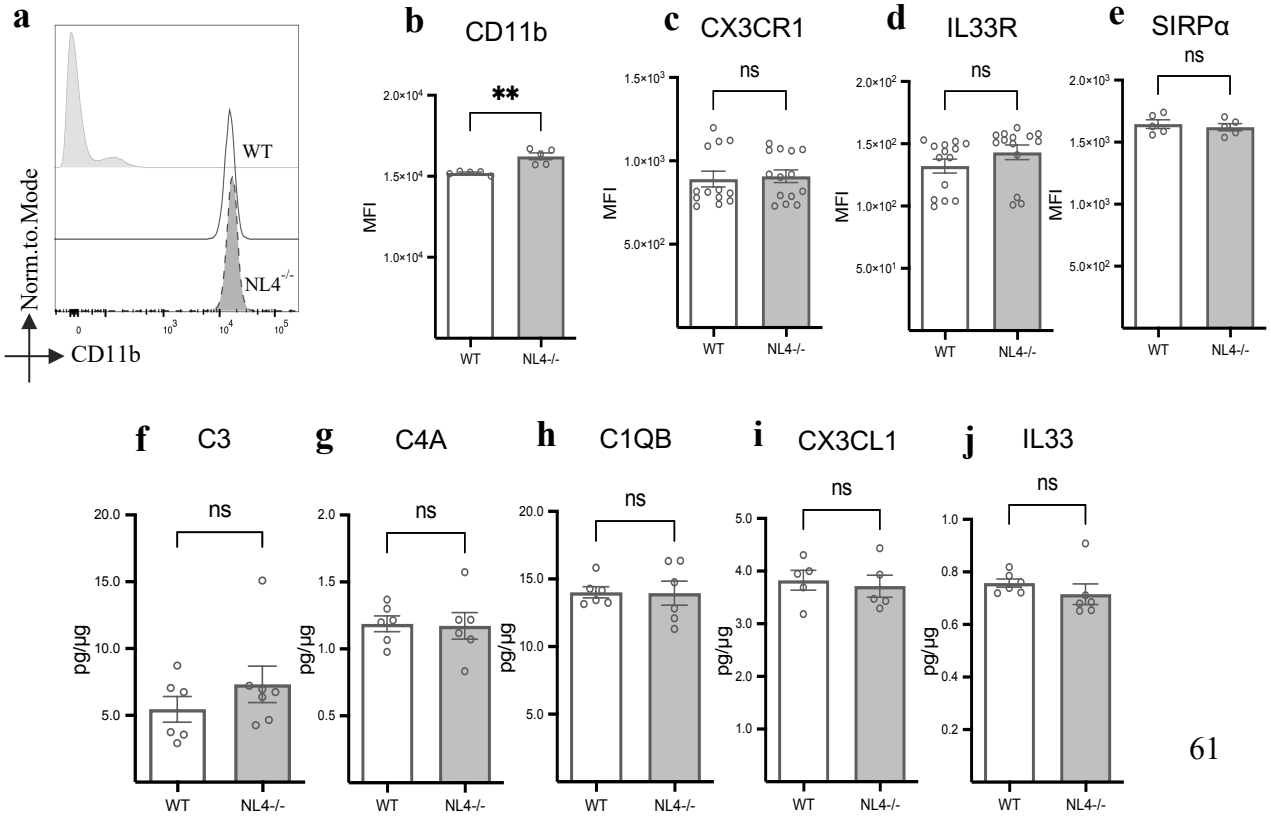

Figure 3A. 3 *Targets in the pathways driving microglia-mediated synaptic pruning do not show a significant difference between WT and NL4$^{-/-}$ hippocampus except for the higher expression of CD11b by the NL4$^{-/-}$ microglia.*

(a) *Representative overlayed histogram comparing fluorescence intensity of CD11b subunit of the CR3 from WT and NL4$^{-/-}$ microglia (Histograms: grey line: WT male, grey-filled dashes: NL4$^{-/-}$, light grey-filled: unstained control).*

(b) *Comparison of CD11b (CR3 subunit) MFI of freshly isolated microglia from the hippocampus of WT and NL4$^{-/-}$ mice. Bar plots indicate a significantly higher level of CD11b MFI in NL4$^{-/-}$microglia compared to the WT (Unpaired t test with Welch's correction, CR3: n_{WTmale}=5 $n_{NL4-/-male}$=5, p=0.007).*

(c) *Comparison of CX3CR1 MFI from freshly isolated hippocampal microglia indicates no significant difference comparing WT and NL4$^{-/-}$ (Unpaired t test with Welch's correction: n_{WTmale}=13, $n_{NL4-/-male}$=14, p=0.777).*

(d) *Comparison of IL33R MFI from freshly isolated hippocampal microglia of WT and NL4$^{-/-}$ mice. Bar plots indicate no significant difference comparing WT and NL4$^{-/-}$ (Unpaired t test with Welch's correction, n_{WTmale}=14, $n_{NL4-/-male}$=14, p=0.188).*

(e) *Comparison of SIRPα MFI from freshly isolated hippocampal microglia of WT and NL4$^{-/-}$ mice. Bar plots indicate no significant difference comparing WT and NL4$^{-/-}$(Unpaired t-test with Welch's correction; n_{WTmale}=5, $n_{NL4-/-male}$=5, p=0.606).*

(f/ g/ h/ I /j) *Bar plot showing no significant difference in the protein expression levels of C3, C4A, C1QB, CX3CL1, IL33 in the WT and NL4$^{-/-}$ hippocampus. Data is normalized to the total protein concentration per sample and represented as mean ± SEM. (Unpaired t test with Welch's correction, n_{WT}=6 $n_{NL4-/-}$=6, p^{C3}=0.292, p^{C4A}=0.896, p^{C1QB}=0.946, p^{CX3CL1}=0.688, p^{IL33}=0.357, *P < 0.05; **P < 0.01; ***P < 0.001; NL4$^{-/-}$ indicates Nlgn4-KO on the presented plots).*

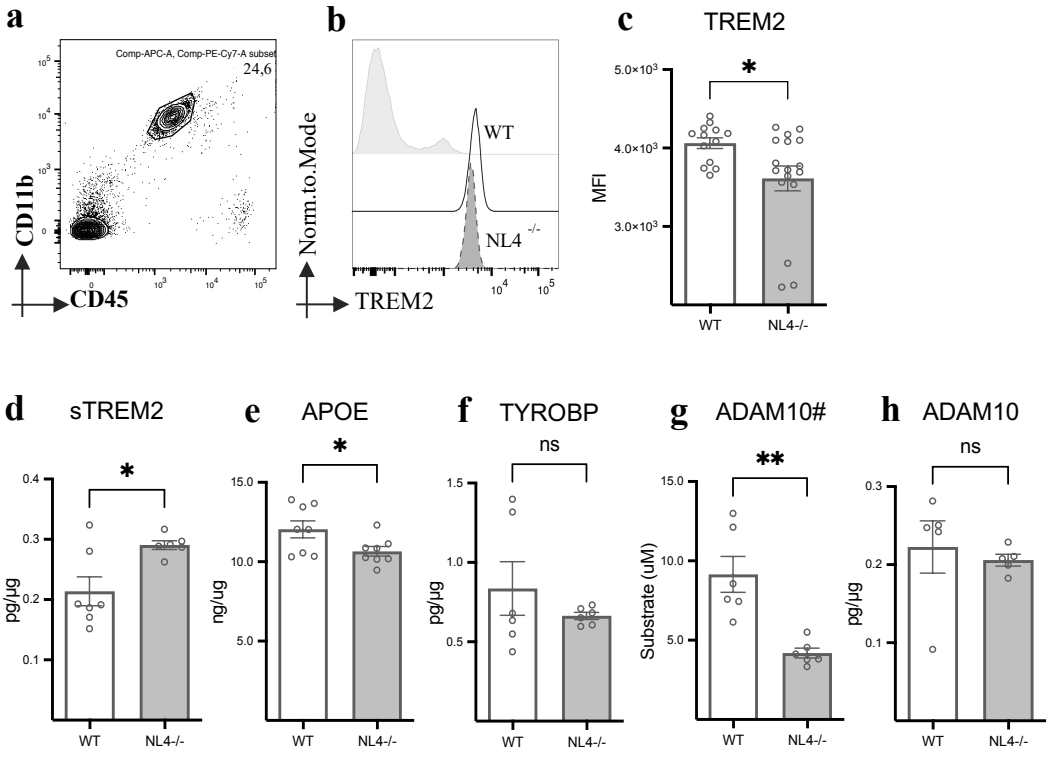

Figure 3A. 4 *NL4$^{-/-}$ males show major dysregulations in the TREM2 signaling pathway.*

(a) *Gating strategy to analyze TREM2 fluorescence intensity on CD11b^{++}/CD45^{+} microglia population.*

(b) *Representative overlayed histograms comparing fluorescence intensity of TREM2 from WT and NL4$^{-/-}$ microglia (grey line: WT male, grey-filled dashes: NL4$^{-/-}$ male, light grey-filled: unstained control).*

(c) *Comparison of TREM2 MFI from freshly isolated hippocampal microglia (CD11b^{++}/CD45^{+}) of WT and NL4$^{-/-}$ mice. Bar plots indicate a significant decrease of TREM2 MFI in NL4$^{-/-}$ male microglia. Each dot indicates one mouse and data is presented as mean ± SEM (Unpaired t-test with Welch's correction: n_{WT}=13 $n_{NL4-/-}$=17, p=0.016).*

(d) *Increase in sTREM2 levels is shown in the NL4$^{-/-}$ male hippocampus compared to the WT male. Data is normalized to the total protein concentration per sample and represented as mean ± SEM. (Unpaired t-test with Welch's correction: n_{WT}=7 $n_{NL4-/-}$=6, p=0.017).*

(e) *APOE protein level is significantly lower in the NL4$^{-/-}$ hippocampus. Data is normalized to the total protein concentration per sample and represented as mean ± SEM (Unpaired t-test with Welch's correction: n_{WT}=8 $n_{NL4-/-}$=8, p=0.04).*

(f) *No difference is detected in the expression levels of TYROBP (DAP12) in the hippocampus of NL4$^{-/-}$ compared to WT controls. Data is normalized to the total protein concentration per sample and represented as mean ± SEM. (Unpaired t-test with Welch's correction: n_{WT}=6 $n_{NL4-/-}$=6, p=0.35).*

(g) *ADAM10 enzyme activity in the hippocampus is lower in the NL4$^{-/-}$ compared to WT. Final cleaved substrate (5-FAM /QXL^{TM}520) concentration is quantified to assess enzymatic activity between WT and NL4$^{-/-}$ samples (Fluorescence signal originates from the cleaved substrate, processed by the ADAM10).* ***(h)*** *No difference is detected in the expression levels of ADAM10 in the hippocampus of NL4 $^{-/-}$ compared to WT controls. Data is normalized to the total protein concentration per sample and represented as mean ± SEM. (Unpaired t-test with Welch's correction: n_{WT}=5 $n_{NL4-/-}$=5, p=0.64). Data are shown as mean ± SEM and each dot indicates one mouse. (*P < 0.05; **P < 0.01; ***P < 0.001 taken for all datasets; NL4$^{-/-}$ indicates Nlgn4-KO on the plots).*

3A.4 Dysregulations in the ADAM10 activity start early in development without an impact on the TREM2 pathway and microglial engulfment of synapses

We reported major dysregulations in the TREM2 pathway in the *Nlgn4*-KO adult hippocampus, which we hypothesize to be connected to the lower microglial engulfment of synapses. Therefore, we next investigated whether dysregulations in the TREM2 pathway emerge early in development by checking the expression of surface TREM2, sTREM2, ADAM10, as well as enzymatic activity of ADAM10 in the *Nlgn4*-KO hippocampus at P15. We found no changes in the expression of surface TREM2 and sTREM2 in the NL4$^{-/-}$ hippocampus **(Figure 3A.5 a and b).** Yet**,** similar to the adult stage, our findings indicate a decrease in the ADAM10 activity, but not in concentration **(Figure 3A.5 c and d)**, suggesting that the dysregulation of enzyme activity starts early in development. In addition, we compared the microglial expression of CD11b, SIRPα, and IL33R between WT and *Nlgn4*-KO microglia at P15, and did not observe any significant differences **(Figure 3A.5 e, f and h)**. However, we detected a significantly lower expression of CX3CR1 in the *Nlgn4*-KO microglia, which may have a potential effect on microglial function at this earlier developmental time point (P15) **(Figure 3A.5 g)**.

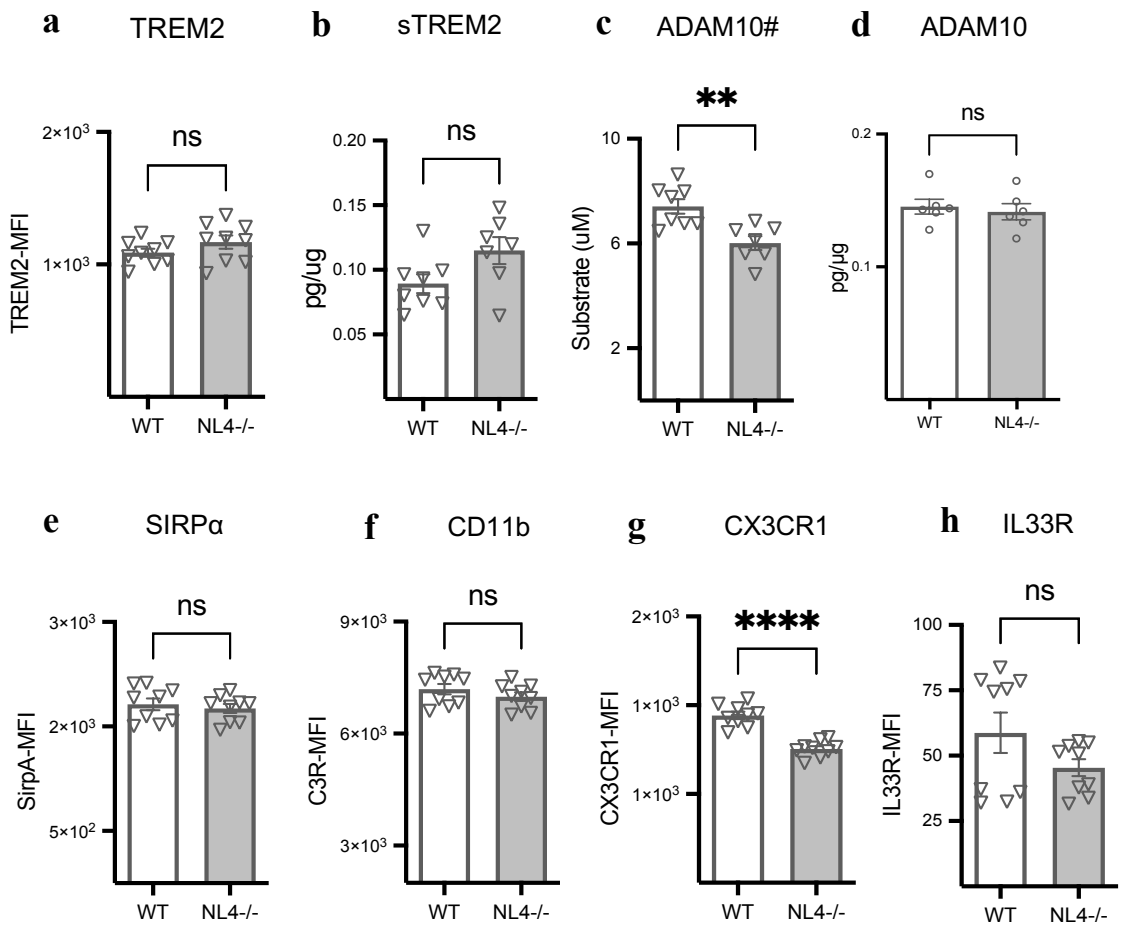

Figure 3A. 5 *Dysregulation in the ADAM10 enzymatic activity starts early in development at P15.*

(a) *Expression levels of surface TREM2 was analyzed by quantifying TREM2 MFI signal on freshly isolated microglia ($CD11b^{++}/CD45^{+}$) and no difference was found comparing WT and $NL4^{-/-}$ hippocampus (Unpaired t test with Welch's correction, TREM2: $n_{WT}=8$ $n_{NL4-/-}=8$ $p=0.19$).*

(b) *sTREM2 protein levels measured in the hippocampus indicate no difference in $NL4^{-/-}$ and WT. sTREM2 data is normalized to the total protein concentration per sample and presented as mean ± SEM on bar plots (Unpaired t-test with Welch's correction, sTREM2: $n_{WT}=8$ $n_{NL4-/-}=8$ $p=0.067$).*

(c) *ADAM10 enzyme in $NL4^{-/-}$ hippocampus shows a significantly lower activity compared to age-matching WT. Final cleaved substrate (5-FAM /QXL^{TM}520) concentration is quantified to compare enzymatic activity between WT and $NL4^{-/-}$ samples ($n_{WT}=8$ $n_{NL4-/-}=7$ $p=0.003$).*

(d) *Expression levels of the ADAM10 enzyme in $NL4^{-/-}$ hippocampus shows no significant difference compared to age-matching WT. Data is normalized to the total protein concentration per sample and presented as mean ± SEM on bar plots ($n_{WT}=6$ $n_{NL4-/-}=6$ $p=0.65$).*

(e) *Expression level of SIRPα is analyzed by quantifying SIRPα MFI signal from freshly isolated microglia. No difference was detected comparing WT and NL4$^{-/-}$ male hippocampus (Unpaired t-test with Welch's correction, SIRPα: n_{WT}=9 $n_{NL4-/-}$=9 p=0.584).*

(f) *Expression level of CR3 is analyzed by quantifying MFI signal of the CD11b subunit of CR3 on freshly isolated microglia. No significant difference was found comparing WT and NL4$^{-/-}$ male hippocampus (Unpaired t-test with Welch's correction, C3-R: n_{WT}=9 $n_{NL4-/-}$=9 p=0.273).*

(g) *Expression level of CX3CR1 is analyzed by quantifying CX3CR1 MFI signal on freshly isolated microglia and found lower in NL4$^{-/-}$ hippocampus compared to WT (Unpaired t test with Welch's correction, CX3CR1: n_{WT}=9 $n_{NL4-/-}$=9 p= <0.0001).*

(h) *Expression level of IL33R is analyzed by quantifying IL33R MFI signal on freshly isolated microglia. No difference was detected comparing WT and NL4$^{-/-}$ male hippocampus (Unpaired t-test with Welch's correction, IL33R: n_{WT}=9 $n_{NL4-/-}$=9 p=0.141; *P < 0.05; **P < 0.01; ***P < 0.001 for all datasets; NL4$^{-/-}$ indicates Nlgn4-KO on the presented plots).*

3A.5 Microglial engulfment of synapses is not affected in the *Nlgn4*-KO hippocampus at P15

Microglia from *Nlgn4*-KO hippocampus did not exhibit a difference in the expression of TREM2 and sTREM2, yet showed lower levels of CX3CR1 at P15. Therefore, we next investigated whether the synaptic engulfment by microglia at this stage was affected. First, we examined whether there was any difference in the engulfment of vGLUT1^{+} synapses in the hippocampus; and found that neither the percentage of vGLUT1^{+} microglia nor the engulfment of vGLUT1^{+} synapses by microglia in the *Nlgn4*-KO hippocampus were affected **(Figure 3A.6 a and b)**. We next checked the engulfment of total synaptosomes by microglia, which as well showed no difference in the *Nlgn4*-KO hippocampus compared to the WT **(Figure 3A.6 c)**. Therefore, we conclude that impaired engulfment of synapses by microglia develops gradually over time and becomes evident at P90, which coincides with significant dysregulations in the TREM2 pathway in the *Nlgn4*-KO hippocampus.

Interestingly, when WT microglia were fed either with WT or *Nlgn4*-KO derived synaptosomes, there was no significant difference in their engulfment, contrary to what was reported at P90 **(Figure 3A.6 d and 3A.2 e)**. When *Nlgn4*-KO synaptosomes were fed to microglia from either WT or *Nlgn4*-KO hippocampus, we similarly did not report any significant difference. Likewise, when synaptosomes from WT or *Nlgn4*-KO hippocampus were fed to *Nlgn4*-KO microglia, we also did not find any difference in the microglial engulfment of synaptosomes from both groups **(Figure 3A.6 e and f).**

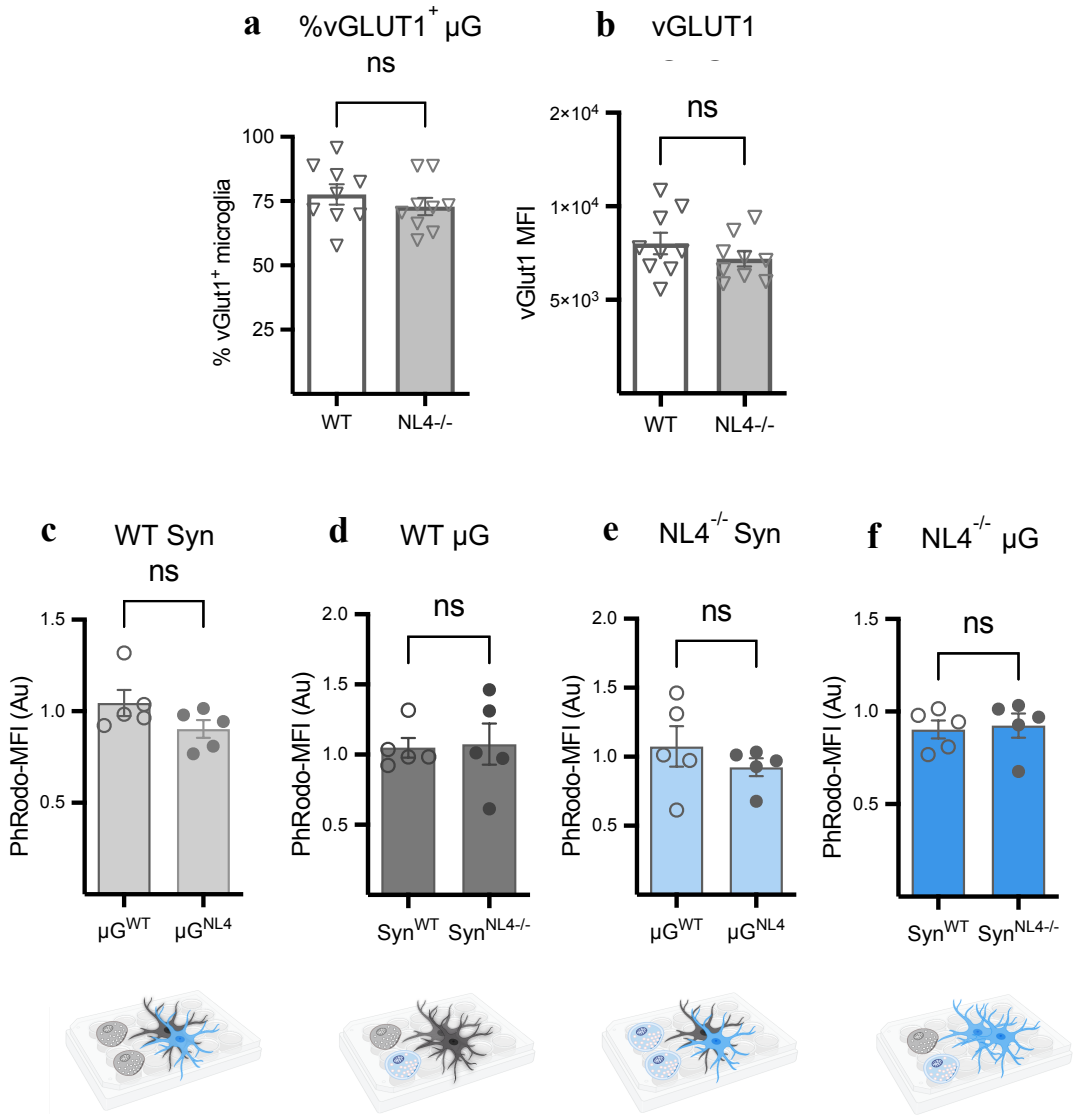

Figure 3A. 6 *Microglial engulfment of synapses is not affected in the NL4$^{-/-}$ hippocampus at P15.*

(a and b) *Bar plots show the percentage of vGLUT1^{+} microglia (CD11b^{++}/CD45^{+}/Viability^{-}) and vGLUT1-MFI comparing synaptic engulfment in the WT and NL4$^{-/-}$ hippocampus that show no significant difference. Each dot indicates one mouse and data is shown as mean ± SEM (Unpaired t test with Welch's correction, male: n_{WT}=9 $n_{NL4-/-}$=9, p=0.376).*

(c) *Freshly isolated microglia from WT and NL4$^{-/-}$ hippocampus were fed with the same WT synaptosomes, and no significant difference was detected in the pHrodo^{TM}Red MFI of microglial cells (circle: WT microglia fed with WT synaptosomes; dot: NL4$^{-/-}$ microglia fed with WT synaptosomes; Unpaired t test with Welch's correction, male: n=5, p=0.14).*

(d) *Freshly isolated microglia from WT hippocampus were fed either with WT or NL4$^{-/-}$ synaptosomes, and no significant difference was detected in the pHrodo^{TM}Red MFI of microglial cells (circle: WT microglia fed with WT synaptosomes; dot: WT microglia fed with NL4$^{-/-}$ synaptosomes, Unpaired t test with Welch's correction, male: n=5, p=0.87).*

(e) *Freshly isolated microglia from WT and NL4$^{-/-}$ hippocampus were fed with the same NL4$^{-/-}$ synaptosomes, and no significant difference was detected in the pHrodo^{TM}Red MFI analyzed from microglial cells (circle: WT microglia fed with NL4$^{-/-}$ synaptosomes; dot: NL4$^{-/-}$ microglia fed with NL4$^{-/-}$ synaptosomes, Unpaired t test with Welch's correction, male: n=5, p=0.38).*

(f) *Freshly isolated microglia from NL4$^{-/-}$ hippocampus were fed either with WT or NL4$^{-/-}$ synaptosomes, and no significant difference was detected in the pHrodo^{TM}Red MFI analyzed from microglial cells (circle: NL4$^{-/-}$ microglia fed with WT synaptosomes; dot: NL4$^{-/-}$ microglia fed with NL4$^{-/-}$ synaptosomes, Unpaired t test with Welch's correction, male: n=5, p=0.79). pHrodo^{TM}Red^{+} MFI values from each sample are normalized to the MFI of microglia fed with unstained synaptosomes and presented as relative to WT microglia for all given datasets. Each dot indicates one mouse and data is presented as mean ± SEM for all given datasets. (Statistical significance was shown as *P < 0.05; **P < 0.01; ***P < 0.001; NL4$^{-/-}$ indicates Nlgn4-KO on the presented plots).*

3A.6 ADAM10 enzymatic activity is not affected at P3 in the *Nlgn4*-KO hippocampus

Since we reported impaired enzymatic activity of ADAM10 at P15, where microglial engulfment of synapses and TREM2 signaling were not affected, we next traced back to other developmental stages to find out where does the dysregulation in ADAM10 enzymatic activity starts. Based on our findings, we hypothesized a potential direct effect of NL4 levels on the

ADAM10 enzymatic activity; therefore, we picked P3, where expression of NL4 protein in the WT hippocampus is the lowest compared to later developmental time points (Jamain et al., 2008). We investigated the enzymatic activity and expression levels of ADAM10 at P3, and found no significant difference between WT and *Nlgn4*-KO **(Figure 3A.7 a and b)**.

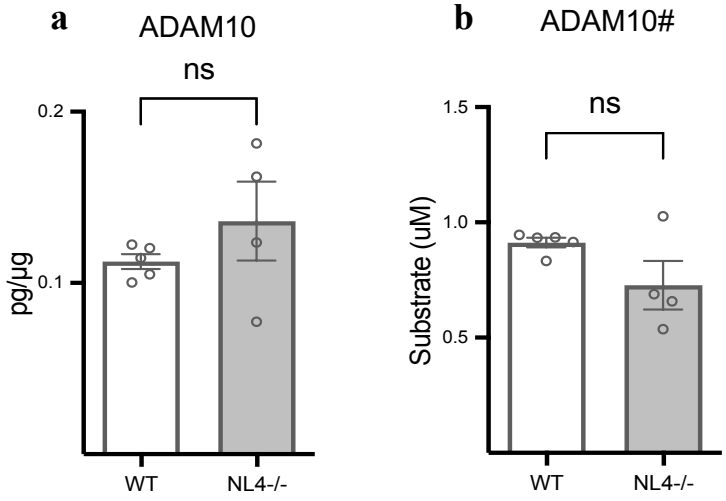

Figure 3A. 7 *ADAM10 enzymatic activity is not affected at P3 in the NL4$^{-/-}$ hippocampus.*

(a) *Expression levels of ADAM10 in the hippocampus indicated no significant difference between the NL4$^{-/-}$ and WT at P3. ADAM10 protein levels are normalized to the total protein concentration per sample and presented as mean ± SEM on bar plots (Unpaired t-test with Welch's correction, n_{WT}=5 $n_{NL4-/-}$=4 p=0.38)*

(b) *ADAM10 enzyme in NL4$^{-/-}$ hippocampus shows no significant difference in the activity compared to age-matching WT at P3. Final cleaved substrate (5-FAM /QXL^{TM}520) concentration was quantified to compare enzymatic activity between WT and NL4$^{-/-}$ samples (n_{WT}=5 $n_{NL4-/-}$=4 p=0.17). Each dot indicates one mouse and data is presented as mean ± SEM for all given datasets. (Statistical significance was shown as *P < 0.05; **P < 0.01; ***P < 0.001; NL4$^{-/-}$ indicates Nlgn4-KO on the presented plots).*

3A.7 NL4 deficiency does not have a major effect on the synaptosome proteome

We hypothesize two potential mechanisms explaining why WT microglia engulf significantly lower amounts of synaptosomes derived from the *Nlgn4*-KO hippocampus compared to WT

at P90 (**Figure 3A.2 e**). The absence of NL4 may either directly impair the cross-talk of microglia and synapses or affect the expression of other synaptic proteins that may signal microglia to phagocyte, resulting in an indirect effect of NL4 on microglia. To test the second hypothesis, we performed tandem mass tag (TMT) mass spectrometry by using hippocampal synaptosomes from the WT and *Nlgn4*-KO mice at P90, and analyzed relative protein abundances. Three proteins, one of which was NL4, were differentially regulated between WT and *Nlgn4*-KO hippocampus. Only NNT and WDFY1 proteins showed significantly lower expression in the *Nlgn4*-KO hippocampus compared to the WT, among 8214 proteins detected in total **(Figure 3A.8),** suggesting no major difference between the WT and *Nlgn4*-KO synaptosome proteomes.

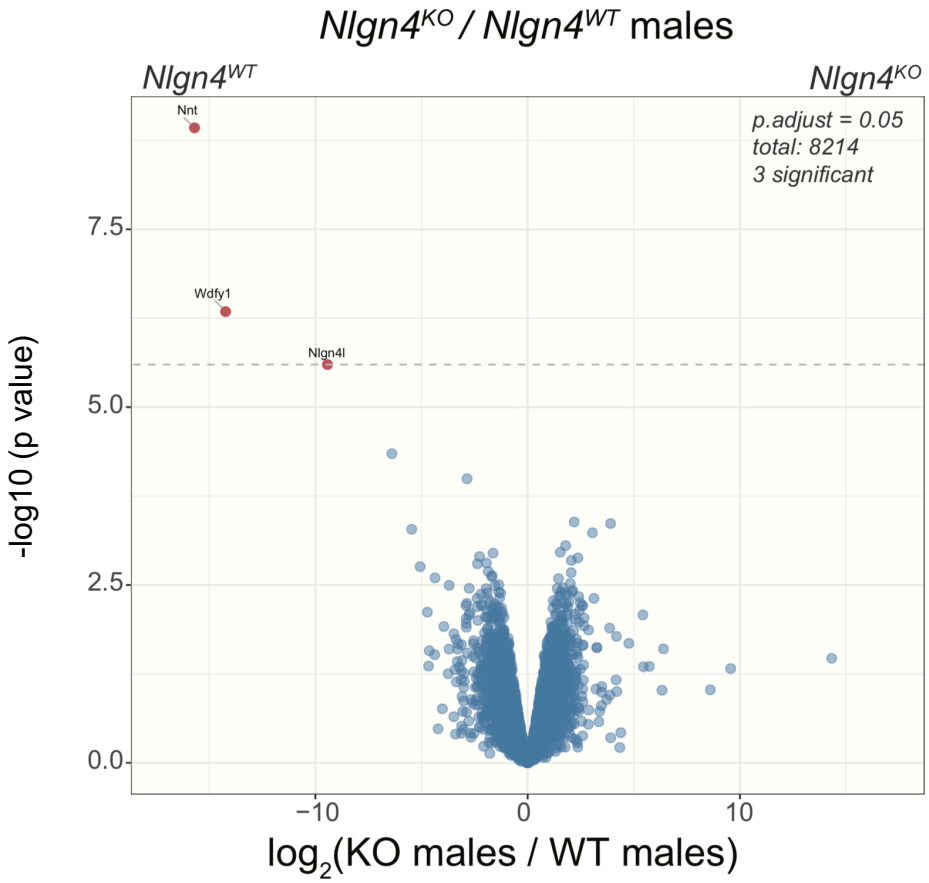

Figure 3A. 8 *NL4 absence does not have a major effect on the synaptosome proteome of the Nlgn4-KO hippocampus.*

Volcano plot indicates significantly lower expression of NNT (Log2-FC: 15.69; Adj.p value= 9.73E-06), WDFY1 (Log2-FC: 14.22; Adj.p value= 0.0018) and NLGN4l (Log2-FC: 9.43; Adj.p value= 0.006) proteins in the Nlgn4-KO hippocampal synaptosomes compared to the WT (n_{WT}=4 $n_{Nlgn4\text{-}KO}$=4, P90).

3A.8 *Nlgn4*-KO mice show impaired spatial memory and cognitive flexibility

We have, so far, provided proof of an impaired synaptic engulfment by microglia along with significant dysregulations in the TREM2 pathway in the *Nlgn4*-KO hippocampus (P90). We further reported lower enzymatic activity of ADAM10, which plays a key role in synaptic plasticity in the brain (Endres & Deller, 2017; Vezzoli et al., 2019). We, therefore, next tested whether these findings at the cellular level may have a potential behavioral translation. Given the critical role of the hippocampus in memory (Fortin, Agster & Eichenbaum, 2002), we employed the Morris Water Maze (MWM) test to assess spatial memory and cognitive flexibility of the *Nlgn4*-KO mice. Within the first three days of acquisition, the mice learned how to use spatial cues to find a submerged platform in an open swimming area **(Figure 3A.9 a)**. *Nlgn4*-KO mice performed relatively poorly throughout the acquisition phase compared to the WT, indicating impaired spatial learning **(Figure 3A.9 b, P1)**. When the platform position was reversed from P1 to P2, when the mice had to start looking for the new place of the platform and learn the P2 position in the same environment, *Nlgn4*-KO mice performed again significantly worse than the WT, indicating an impaired cognitive flexibility **(Figure 3A.9 b, P2)**. We, therefore, report also the behavioral phenotype of the *Nlgn4*-KO mice by focusing on learning and memory in parallel to our molecular and cellular findings focusing on microglial engulfment of synapses in the hippocampus.

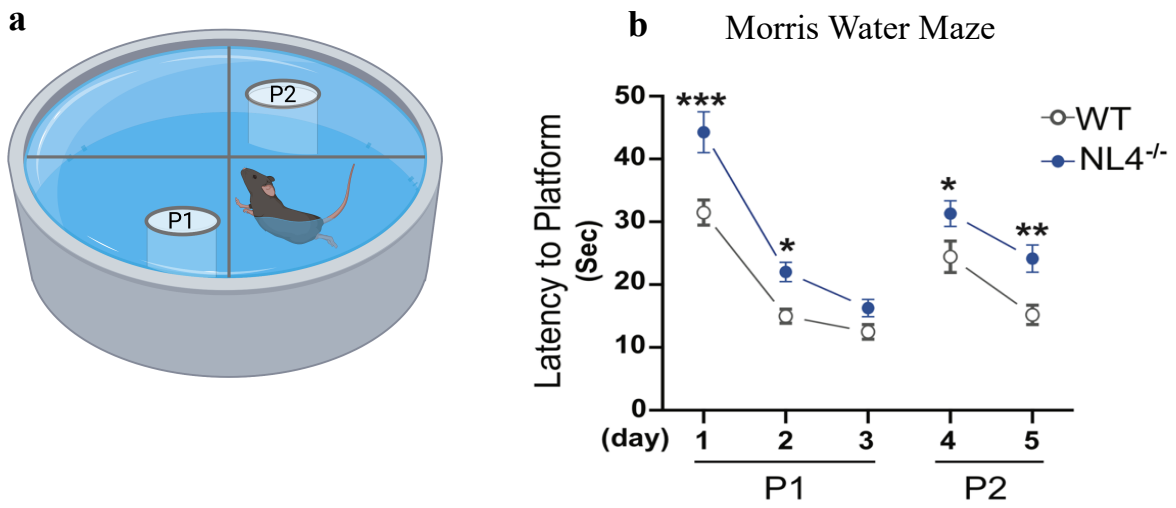

Figure 3A. 9 *NL4$^{-/-}$ mice show impaired spatial memory and cognitive flexibility.*

(a) *Schematic representation of the Morris water maze (MWM) setup (created by using biorender.com).*

(b) *Male NL4$^{-/-}$ mice (P90) used significantly longer time to find the submerged platform in the acquisition phase (P1), and showed an impaired performance during the reversal training (P2) (Repeated 2-way ANOVA individually for acquisition and reversal parts (n_{WT}=29 $n_{NL4-/-}$=30; day1 : p<0.001 t = 4.716, day2: p<0.05 t=2.592, day4: p<0.05 t=2.324, day5: p<0.01 t=3.014; NL4$^{-/-}$ indicates Nlgn4-KO on the presented plots).*

4A DISCUSSION

Over the years, numerous independent research groups have shown evidence of synaptic elements inside microglia in different brain regions, and highlighted the critical role of microglia in synaptic pruning (Stevens et al., 2007; Tremblay et al., 2010; Paolicelli et al., 2011; Schafer et al., 2012; Filipello et al., 2018; Weinhard et al., 2018). MRI and fMRl studies indicated synaptic overconnectivity in the brains of autistic subjects (Wass, 2011; Gao & Penzes, 2015), and we previously reported reduced microglia motility, ATP response, antigen presentation potential along with reduced gamma oscillation power specifically in males in the *Nlgn4*-KO hippocampus (Guneykaya et al., 2023). Based on these results, in the current study, we narrowed our attention to the microglial engulfment of synapses and found that it was significantly reduced in the hippocampus of male *Nlgn4*-KO compared to the WT. Given that autism is more prevalent in males compared to females (Hodges et al., 2020), it is notable that our earlier and present findings indicate a series of effects on the synaptic network and microglia that are more pronounced in males. Therefore, the remainder of our findings are exclusively focused on males and provide characterization of multiple pathways linked to microglial engulfment of synapses at different developmental stages.

We investigated five distinct signaling pathways, including the TREM2 (Filipello et al., 2018), fractalkine (Paolicelli et al., 2011), complement (Stevens et al., 2007), IL33R (Vainchtein et al., 2018), and SIRPα-mediated pathways (Ding et al., 2021; Lehrman et al., 2018), which have been extensively reported to regulate microglial engulfment of synapses. Our findings point to significant dysregulations in the TREM2 pathway (**Figure 3A.4**), which we hypothesized to be linked to the impairments in synaptic engulfment in the *Nlgn4*-KO hippocampus. Parallel to this, at P15, where we have no difference in the surface levels of TREM2 between the WT

and *Nlgn4*-KO microglia, we also did not observe any deficits in synaptic engulfment (**Figures 3A.6**). Therefore, we herein suggest a potential role of TREM2 signaling in the regulation of microglial engulfment of synapses in the *Nlgn4*-KO hippocampus. TREM2 signaling mediates several crucial microglial functions, such as survival, phagocytosis, cellular metabolism, actin remodeling & motility, and synaptic pruning (Brown & St. George-Hyslop, 2022; Filipello et al., 2022). Lower motility, disrupted energy metabolism, and lower phagocytosis towards apoptotic neurons that have been reported in the *Nlgn4*-KO hippocampus (Guneykaya et al., 2023) also relate to the dysregulations in the TREM2 signaling in addition to lower engulfment of synapses presented in this study. Filipello et al. (2018) reported that TREM2 is required for synaptic engulfment by microglia, and also revealed a series of alterations in *Trem2*-KO mice, such as lower microglia density, aberrant microglia morphology, and reduced microglial engulfment of synapses in the hippocampus in addition to impaired sociability. These findings show striking similarities to the *Nlgn4*-KO mice regarding both microglial and behavioral alterations (Filipello et al., 2018; Guneykaya et al., 2023). Reduced TREM2 levels in post-mortem analysis of autistic patients have also been reported, indicating an associating role of TREM2 levels with the disease pathophysiology (Filipello et al., 2018); which is in line with our findings in the *Nlgn4*-KO mouse model.

Interestingly, we also reported significantly reduced enzymatic activity of ADAM10 metalloproteinase in the *Nlgn4*-KO hippocampus (**Figure 3A.4 h**). ADAM10 can mediate synaptic formation, and its activity can be regulated by changes in synaptic network activity (Endres & Deller, 2017; Vezzoli et al., 2019). *Nlgn4*-KO mice exhibited reduced power of gamma oscillation (Hammer et al., 2015; Guneykaya et al., 2023), slightly increased E/I in the hippocampus, impaired GABAergic transmission in the hippocampal CA3 (Hammer et al.,

2015), a hypo-reactive network in the somatosensory cortex (Delattre et al., 2013), and impaired glutamatergic transmission in the barrel cortex (Unichenko et al., 2017). These findings together indicate that the overall network activity in the *Nlgn4*-KO brain, including the hippocampus, is dysregulated. Given that ADAM10 levels or function can be affected by such dysregulations (Endres & Deller, 2017; Vezzoli et al., 2019), we hypothesize that reduction in the ADAM10 enzymatic activity might be due to the alterations in the neural network activity. Changes in the ADAM10 function may also affect synaptic plasticity and cognitive flexibility (Endres & Deller, 2017; Vezzoli et al., 2019), and *Adam10* conditional knockout mice showed an impaired spatial learning and memory (Prox et al., 2013). We, therefore, hypothesized that the changes in ADAM10 activity may have similar potential behavioral translations, and that was indeed the case considering *Nlgn4*-KO mice exhibited impaired learning and cognitive flexibility (**Figure 3A.9**). Another hypothesis favors that this behavioral phenotype can be a direct result of a lack of NL4. Yet, we propose that both impaired ADAM10 function and loss of NL4 mediate this prominent behavioral phenotype in cooperation considering ADAM10 can target neuroligins (Suzuki et al., 2012; Venkatesh et al., 2017; Kuhn et al., 2016), including NL4, to mediate their surface levels and ectodomain shedding.

At P15, we did not find any significant difference in either the synaptic engulfment or surface levels of TREM2, whereas the dysregulations in both become evident at P90, suggesting a gradual worsening in the microglial function and TREM2 signaling. Contrary to microglia, dysregulations in the gamma oscillation already starts early in the development (P15) along with impaired ultrasonic vocalizations (Ju et al., 2014; Hammer et al., 2015). These data suggest that dysregulations in synaptic network oscillations as well as behavior already start early in development, but microglia seem to be affected only later on. Considering our

hypothesis that the dysregulations in the synaptic network affect ADAM10 function, we also checked ADAM10 activity at this earlier stage (P15) and reported reduced activity, which again supports our hypothesis regarding the potential reason behind the lower ADAM10 activity.

Interestingly, we also reported higher microglial surface levels of the CD11b subunit of CR3, with no significant change in C1Qb, C4A, and C3 in the hippocampus at P90. CR3 is among the major phagocytic receptors expressed by microglia and mainly involved in the phagocytosis of synaptic elements, Aβ plaques, and apoptotic cells (Czirr et al., 2017; Silvermann & Wong, 2018). Therefore, higher levels of surface CD11b may suggest higher phagocytosis of these targets, which have been tested to be opposite in the previous study (Guneykaya et al., 2023) for apoptotic neurons and in the current study for vGLUT1^{+} synapses and total synaptosomes. As indicated by this data, changes in the levels of a protein, which is related to a particular function, do not always translate to a functional change due to the interaction of various parameters in the dynamic microenvironment to which microglia are exposed (Paolicelli et al., 2022). Similarly, we reported lower surface expression of CX3CR1 by microglia in the *Nlgn4*-KO hippocampus at P15, suggesting a potential effect, which does not correspond to our functional findings regarding microglial engulfment of synapses at this developmental point. However, other possible functions mediated by fractalkine receptor signaling or CR3 signaling should be the focus of future studies to examine whether the reported changes in their expression translate to other functional alterations.

Apart from the microglia function, we reported that when *Nlgn4*-KO-derived synaptosomes were fed to WT microglia, they were not as efficiently engulfed compared to the WT synaptosomes (**Figure 3A.2 e**). This data suggests that *Nlgn4*-KO synaptosomes somehow cannot efficiently signal microglia to engulf, meaning that they might have an altered "eat

me" or "don't eat me" signals either on synaptosome surfaces or within their synaptic composition. There is also another intriguing possibility, where NL4 might be a ligand directly signaling microglia to phagocyte synaptic components, so that WT microglia cannot efficiently phagocytose synaptosomes in the absence of NL4. We investigated one of these possibilities by analyzing the protein composition of synaptosomes from the *Nlgn4*-KO hippocampus. Our mass spectrometry data showed that only three synaptic proteins have significantly lower expression levels in the *Nlgn4*-KO synaptosomes, one of which is the NL4 protein. The second one is nicotinamide nucleotide transhydrogenase (NNT), which is present in the mitochondrial inner membrane and catalyzes the reduction of NADP to NAPH (Francisco et al., 2018). Therefore, reduced expression of this protein might affect mitochondrial metabolism. However, we did not find any evidence in the literature suggesting that this protein could potentially signal microglial phagocytosis. The third significant hit was WD repeat and FYVE domain-containing protein-1 (WDFY1), which indeed is an interesting target given that it positively regulates Toll-like receptor 3 (TLR3) and TLR4-mediated signaling pathways and that it has been implicated in pathways associated with lysosomal function (Yun-Hong et al., 2015). Therefore, its lower expression can relate to changes in phagocytosis; however, it hasn't been implied in the context of microglial engulfment of synapses in the current literature, and only a few studies focus on its role in microglia (Babagana et al., 2020; Zheng et al., 2021). We, therefore, speculate that this protein might have a potential role in the lower engulfment of synapses, although this is not supported by the current data and the literature. The question of why a target of the TLR3/4 signaling pathway is downregulated in response to NL4 loss is not within the scope of the current study but remains to be answered in future studies. In sum, our data indicate only minor changes in the synaptic protein composition and do not point to a direct effect on the microglial engulfment of synapses. Yet,

such slight changes based just on the protein levels and synaptic protein composition may not always reflect the full extent of an effect. Post-translational modifications of synaptic proteins, such as phosphorylation and glycosylation, as well as changes in the enzymatic activity of some synaptic proteins that are heavily involved in synaptic function should also be considered. ADAM10 represents a valuable example, given that we did not report any changes in its levels based on the mass spectrometry and ELISA data, but reported a significant change in its enzymatic activity, which we hypothesize to impact the synaptic function and behavior. Therefore, we underline that minimal alterations in the synaptic protein levels do not always correspond to an overall minor effect.

What drives the interaction between NL4 and microglia is a key question raised by our findings. Considering that microglia do not express NL4 protein (Guneykaya et al., 2023), the interaction between NL4 and microglia could be indirect, since microglia sense changes in neural network activity (Umpierre & Wu, 2021) and gamma oscillation (Iaccarino et al., 2016). We speculate that the phenotype and function of microglia may be altered due to the disruption of gamma oscillation (Guneykaya et al., 2023), as well as due to the changes in synaptic network activity (Hammer et al., 2015) in the *Nlgn4*-KO hippocampus. We herein report dysregulated ADAM10 activity as an additional potential consequence of the dysregulations in the neural network activity in the *Nlgn4*-KO hippocampus. Since there is no significant difference in microglial engulfment of synapses at P15, our data point to a later effect on the microglia, which supports the hypothesis of an indirect interaction that negatively affects microglia over time. Nevertheless, synaptic engulfment may not be the first function to be compromised; thus, a normal synaptic engulfment function does not necessarily indicate that microglia are not affected at P15. We already found reduced surface

area and volume of microglia (De Marzo & Compagnion, 2023; unpublished data) along with lower microglial expression of CX3CR1 in the *Nlgn4*-KO hippocampus at P15, suggesting that microglial dysregulations already start at this early stage. Morphological changes in microglia, as well as lower expression of CX3CR1 may point to an altered microglial function, which will be the main focus of future studies.

Notably, we also showed that WT microglia could not efficiently engulf *Nlgn4*-KO-derived synaptosomes when compared to WT synaptosomes at P90. The absence of major alterations in synaptic protein composition in the *Nlgn4*-KO hippocampus is suggestive of a direct effect of NL4 on microglia, whose absence may directly affect the microglial phagocytosis. Our findings, therefore, support both the direct and indirect interaction hypotheses, and provide a fundamental basis and open questions for future studies to decipher the interaction between NL4 and microglia.

In the *Nlgn4*-KO hippocampus, ADAM10 activity is reduced at an early stage of development (P15) and continues to be so at P90. It is important to note that there is a lower expression of NL4 protein at P3, when compared to later developmental stages in the WT hippocampus (Jamain et al., 2008). P3 is also the only time point where we did not detect any dysregulation in the ADAM10 enzymatic activity between the WT and *Nlgn4*-KO hippocampus. The lower enzymatic activity in the *Nlgn4*-KO hippocampus emerged rather at later stages, P15 and P90, when compared to age-matched WT. Notably, the difference between WT and *Nlgn4*-KO hippocampus in terms of NL4 expression becomes more evident at these later developmental points (P15 and P90) since WTs have higher NL4 expression at P90 and P15 than at P3, and *Nlgn4*-KO has no expression at all (Jamain et al., 2008). This data, therefore, suggests that

ADAM10 activity might directly be regulated by changes in the NL4 levels. It has previously been reported that cleaved NL3 promotes ADAM10 expression to positively regulate its own cleavage (Dang et al., 2021). Similarly, we propose that lack of NL4 can contribute to the lower enzymatic activity of ADAM10, which in turn can cleave its NL targets less efficiently in the *Nlgn4*-KO hippocampus. Impaired ADAM10 can also affect the proteolytic processing of the microglial surface TREM2 (Endres & Deller, 2017). Yet, it is hard to detect if the shedding of surface TREM2 is affected by the changes in the ADAM10 activity, since both surface and sTREM2 levels can be regulated by different mechanisms apart from the ADAM10 activity, such as alternative splicing of the *Trem2* gene or action of the ADAM17 enzyme (Filipello at al., 2022).

Our findings suggest that microglia respond to the loss of NL4, either as a result of a direct or indirect mechanism, by suppressing the TREM2 signaling. They reduce the surface TREM2 levels, which can negatively affect the TREM2 signaling, and generate more sTREM2, which can act as a decoy receptor to competitively bind TREM2 ligands (Filipello et al., 2022). In addition, as a TREM2 ligand, lower levels of APOE may also negatively affect TREM2 signaling in the *Nlgn4*-KO hippocampus.

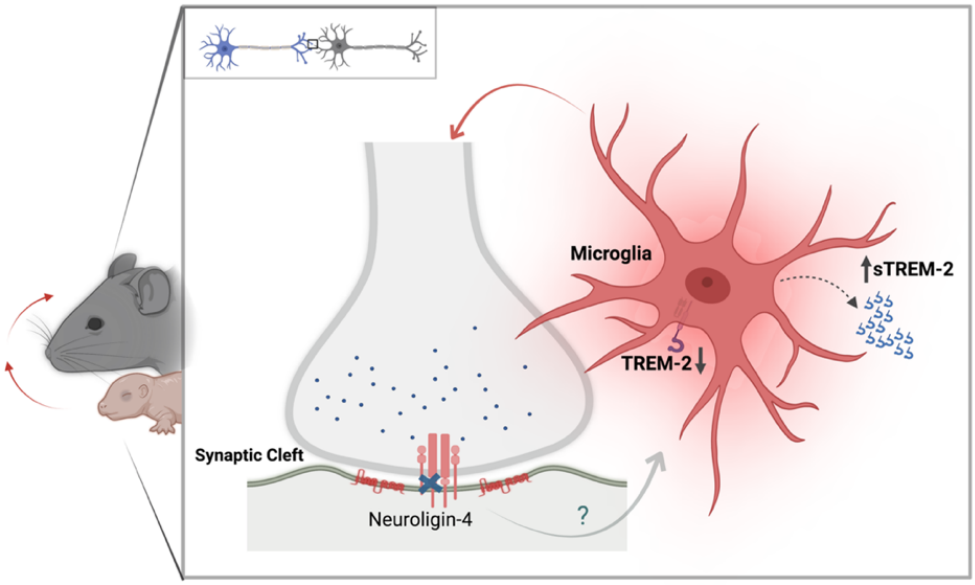

Figure 4A. 1 *A summary of the main findings affecting microglial function in the Nlgn4-KO mouse model of autism (created by using biorender.com).*

Therefore, our study presents strong evidence of dysregulated TREM2 signaling in the *Nlgn4*-KO hippocampus, which is in line with the functional data we have presented in the previous (Guneykaya et al., 2023) and present studies. The hypothetical mechanism behind lower surface TREM2 and higher sTREM2 expression might be a switch in the transcriptional program of microglia to generate sTREM2 via alternative splicing instead of generating surface TREM2. Our data is in line with this hypothesis, considering the higher levels of sTREM2 cannot be explained by the ectodomain shedding of surface TREM2, given the lower ADAM10 activity. It is also important to highlight that the TREM2 and sTREM2 levels are under the control of a complex regulatory mechanism as opposed to being dependent on the activity of a single enzyme such as ADAM10.

In conclusion, our study identifies the dysregulation of TREM2 signaling along with its effect on microglial engulfment of synapses as a potential target in the *Nlgn4*-KO model and establishes a foundation for future studies aiming to target this pathway to further investigate microglia-synapse interaction in the context of autism.

PROJECT (B)

Great majority of preclinical research on innate high anxiety so far has focused on male rodents, leaving females mostly uncharacterized and led to conclusions for both sexes based on the male-driven findings. This applies especially for the reported alterations in neural connectivity, transmission, and neuroinflammation (Dine et al., 2015; Salomé et al., 2004; Rooney et al., 2020). Due to the previous reports stating higher density of phagocytic microglia in the hippocampus of HAB male mice (Rooney et al., 2020), we hypothesized a potential consequence of such phenotype also on the engulfment of synapses by microglia. Since the role of microglial engulfment of synapses, as well as microglial heterogeneity and sex-linked differences remain unknown in the context of innate high anxiety, these aspects became the major focus of this project.

In the present study;

1- I reported the heterogeneity and sexual dimorphism of microglia at single-cell resolution in mice with innate high anxiety (HAB).

2- I characterized microglial engulfment of synapses in the HAB male and HAB female hippocampus using *in vitro* and *ex vivo* functional assays, both for vGLUT1^{+} excitatory synapses and for total synaptosomes.

3- I investigated potential targets driving aberrant engulfment of synapses by microglia in the HAB hippocampus.

4- I addressed the effect of minocycline treatment on microglial engulfment of synapses.

2B Material & Methods

2B.1 Animals

All mice of both sexes used for the present study were on a CD-1 genetic background and were handled according to the governmental and internal regulations. HAB and NAB mice were selectively inbred for their specific anxiety-related behavior at the Department of Pharmacology, Innsbruck Medical University, Innsbruck, Austria; and were kindly provided by Prof. Dr. Nicolas Singewald. The mice were group-housed in individually ventilated cages under standard laboratory conditions with 12:12 light/dark cycle at the animal core facility of the MDC. Food and water were provided ad libitum. All mice used in functional and single-cell RNA sequencing experiments were at post-natal day 84-91 (P84-91).

2B.2 Ethics Statement

All procedures involving handling of living animals were performed in strict accordance with the German Animal Protection Law and were approved by the Regional Office for Health and Social Services in Berlin (Landesamt für Gesundheit und Soziales, Berlin, Germany, G0061/21). Mice were sacrificed with an overdose intraperitoneal injection of pentobarbital (Narcoren, Merial GmbH, Hallbergmoos, Germany) followed by decapitation.

2B.3 Microglia Isolation for Single-cell RNA Sequencing

Enzymatic dissociation protocol was adapted from Marsh et al., 2022. Mice were deeply anesthetized and intracardially perfused with 15 ml ice-cold artificial cerebrospinal fluid (aCSF; 87 mM NaCl, 2.5 mM KCl, 1.25 mM NaH2PO4, 26 mM NaHCO3, 25 mM glucose, 1 mM CaCl2, 7 mM MgSO4, 20 mM HEPES in ddH_2O) supplemented with a transcriptional &

translational inhibitor cocktail including 10 µM Triptolide, 27.1 µg /ml Anisomycin and 5 µg/ml Actinomycin D (Saunders et al., 2018). Brains were removed and kept in ice cold Hibernate-A medium (ThermoFisher Scientific, catalog no. A1247501) supplemented with B27 (ThermoFisher Scientific, catalog no. 17504044, 1/50). They were quickly sliced into 8 even sections using surgical scissors and placed into Miltenyi's gentleMACS C Tubes (catalog no. 130-093-237) including papain solution (Worthington, catalog no. LK003150) supplemented with the inhibitor cocktail to start tissue dissociation at 37°C for 30 minutes. Purpose of using the inhibitor cocktail was to prevent *ex vivo* microglial activation in response to the isolation procedure at the 37°C (Marsh et al., 2022). **Figure 2B.1** shows the isolation procedure did not result in a cluster-specific artificial *ex vivo* activation signature in microglia, which do not show high expression levels of *ex vivo* activation-related genes such as *Fos, Jun, Egr-1, Junb* (Marsh et al., 2022). Samples were centrifuged for 5 min at 300g and filtered through a 70-µm filter. 1 ml aCSF was added to each tube, and cell were pelleted at 300g for 5 min (4°C). Cell suspension including 22 % Percoll (GE Healthcare, catalog no. 17-0891-01) in 2 ml final volume was gently overlaid with 2 ml DPBS (ThermoFisher Scientific, catalog no. J61196.AP). Samples were centrifuged at 3000g, 4°C for 10 min, and myelin cloud as well as rest of the supernatant were removed. Pellets were washed once with 1 ml aCSF, spun down at 400g for 8 min and re-suspended in 100 µl FACS buffer (DPBS with 0.2% BSA).

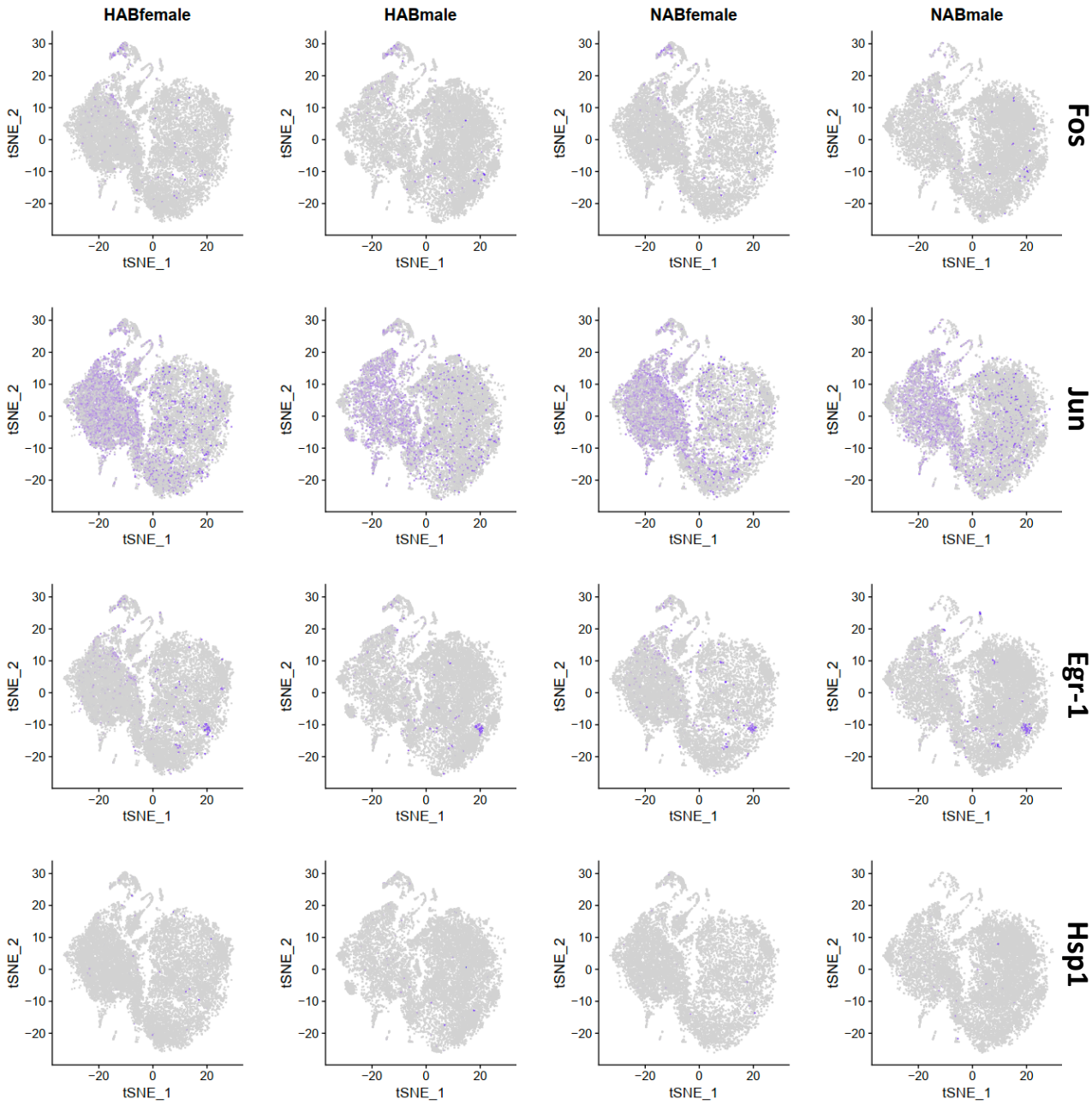

Figure 2B. 1 *Microglia isolated from HAB and NAB brains do not show a strong, cluster-specific ex vivo activation signature due to the isolation procedure.*

t-SNE plots indicate no cluster-specific high expression levels of Fos, Jun, Egr-1, Hsp1a and Junb genes in the single-cell RNA sequencing dataset from all biological subgroups analyzed.

2B.4 Fluorescence-Activated Cell Sorting (FACS)

All buffers and solutions were prechilled to 4°C before use. Cell suspensions were incubated with a fixable viability antibody (ThermoFisher, catalog no.L34969, 1/1000) for 30 minutes at 4°C. Upon washing with 1 ml ice cold PBS, cells were pelleted at 300g, 5min; and incubated with anti-CD16/CD32 for 10 min on ice (ThermoFisher Scientific, catalog no.14-0161-82; 1/200). Cells were followingly stained with an antibody master mix **(Table 2B.1)** for 25 min at 4°C, and spun down for 5 min at 300g. 250 ul FACS buffer was used per sample to resuspend the cells. Sterile 1.5 ml Eppendorf tubes were precoated with 50% BSA (Sigma Aldrich, catalog no. A3608) overnight at 4°C to collect the FACS-sorted microglia. The gating strategy to sort microglia is given in the **Figure 2B.2**. BD FACS Aria III with 100-µm nozzle and purity mode was used to sort the final population to be loaded in the 10X chromium controller.

Table 2B. 1 *FACS antibodies used to stain and sort microglia for the single-cell RNA sequencing.*

Antigen	Conct.	Fluorochrome	Company	Product #
CD45	1/50	APC	BD	559864
CD44	1/100	BV421	BioLegend	103040
CD11b	1/100	PECy7	BD	553311
Lineage				
Ly6C	1/100	PE	BioLegend	128026
Ly6G	1/100	PE	BioLegend	127606
B220	1/100	PE	BioLegend	103206
TCRb	1/100	PE	BD	553170
TCRgd	1/100	PE	BioLegend	118105
NK1.1	1/100	PE	BioLegend	108705
Ter119	1/100	PE	BD	557915

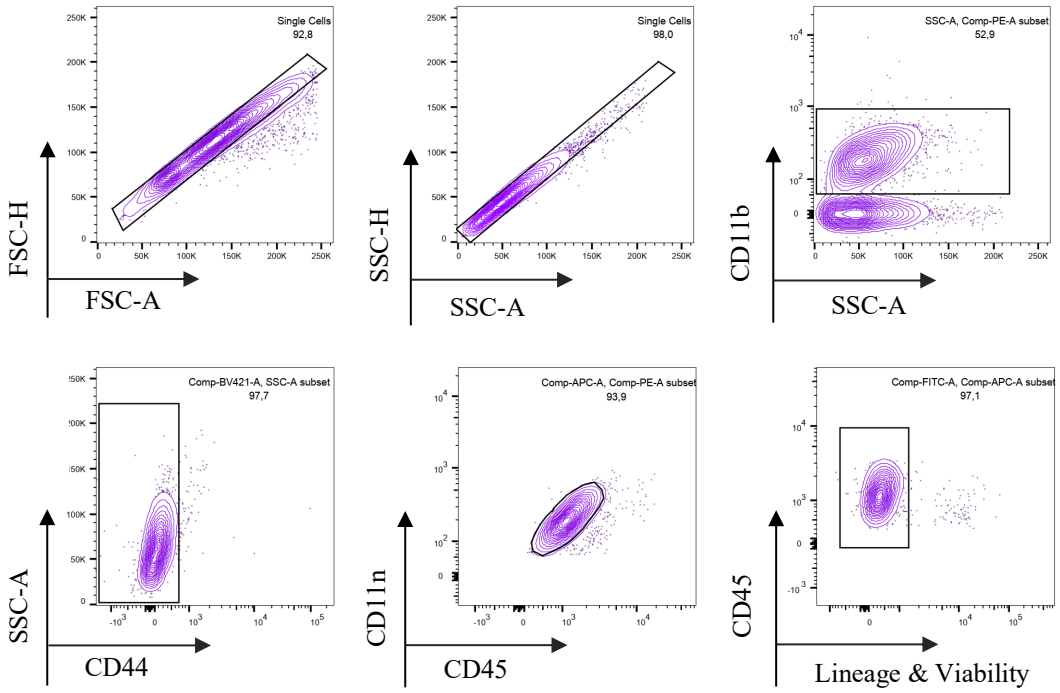

Figure 2B. 2 *Representative FACS plots indicating the gating strategy to sort microglia from HAB and NAB brains for the single-cell RNA sequencing.*

Antibodies listed on the Table 2.1 were used to stain microglia, specifically. Viable and single cells were gated as CD11b^{++}/ CD45^{+}/ CD44^{-}/ Lineage^{-} final population. (Lineage markers: Ly6C^{FITC}, Ly6G^{FITC}, Viability^{FITC}, B220^{FITC}, TCRb^{FITC}, TCRgd^{FITC}, NK1.1^{FITC}, Ter119^{FITC}).

2B.5 Single-cell RNA Sequencing (scRNA-seq) using 10X Genomics

16,500 cells per sample were loaded into the 10X Chromium controller (10X Genomics, Pleasanton, USA) and library preparation was conducted using 10X single-cell 3' v3 protocol according to manufacturer's instructions (paired-end reads, R1 = 28, i7 = 8, R2 = 91). All 8 libraries, each representing an individual animal, were submitted to Berlin Institute for Medical Systems Biology (BIMSB), Genomics Core Facility, and sequenced with an Illumina NovaSeq sequencer to a depth of around 70,000 reads per cell according to the 10X Genomics's recommendations. The gene-cell count matrix was constructed using cellranger

count version 2.0.2 using the Ensembl GRCm38.p5 (mm10) as the reference genome. The R Seurat package (Stuart et al., 2019) was used for the analysis of the single-cell RNA-Seq data. Only genes found in a minimum of 5 cells were included in the study. In addition, we eliminated from the analysis any cells with fewer than 200 identified genes, as well as any cells with a mitochondrial gene percentage greater than 25%. Data were log normalized and scaled using the standard Seurat preprocessing.

Default parameters were used for identifying anchor genes between the data sets. Dimensionality reduction was performed using t-SNE by using 24 principal components, which were decided by using JackStraw analysis and ElbowPlot. We used the standard Seurat workflow (Stuart et al., 2019) and scCustomize R package (Marsh, 2021) for clustering and visualization. The standard workflow consisted of data normalization/ scaling, PCA analysis, and t-SNE clustering. To compare clusters, marker genes were identified using the Wilcoxon Rank Sum test of the Seurat. Marker genes from previous single cell studies (Masuda et al., 2020; Zeisel et al., 2015; Hammond et al., 2019) were used for manual annotation of the microglia clusters. Differential expression analysis was carried out using DESeq2 (Love et al., 2014) and MAST test (Finak et al., 2015) of the Seurat R package. Gene set enrichment analysis on the gene ontology was carried out using the ShinyGO gene set enrichment tool (Ge et al., 2020). All quantified microglial genes ranked based on the log2FC values in descending order were used as the background, while significantly different genes (pAdj<0.001) ranked based on the log2FC values in descending order were used as the target set. Significantly up- and downregulated genes were analyzed separately using the same background genes, and adjusted p-value cut-off was set as < 0.05 for the enrichment analysis.

2B.6 Flow Cytometry Analysis of Microglial Surface Markers

Flow cytometry-based analysis of the microglial surface markers was carried out exactly as described in the materials and method section of the project A.

2B.7 Microglial Engulfment of vGLUT1 Synapses

Intracellular vGLUT1 staining was carried out exactly as described in the materials and method section of the project A. Gating strategy to analyze vGLUT1-MFI and the percentage of vGLUT1^{+} microglia is depicted on the **Figure 2B.3**.

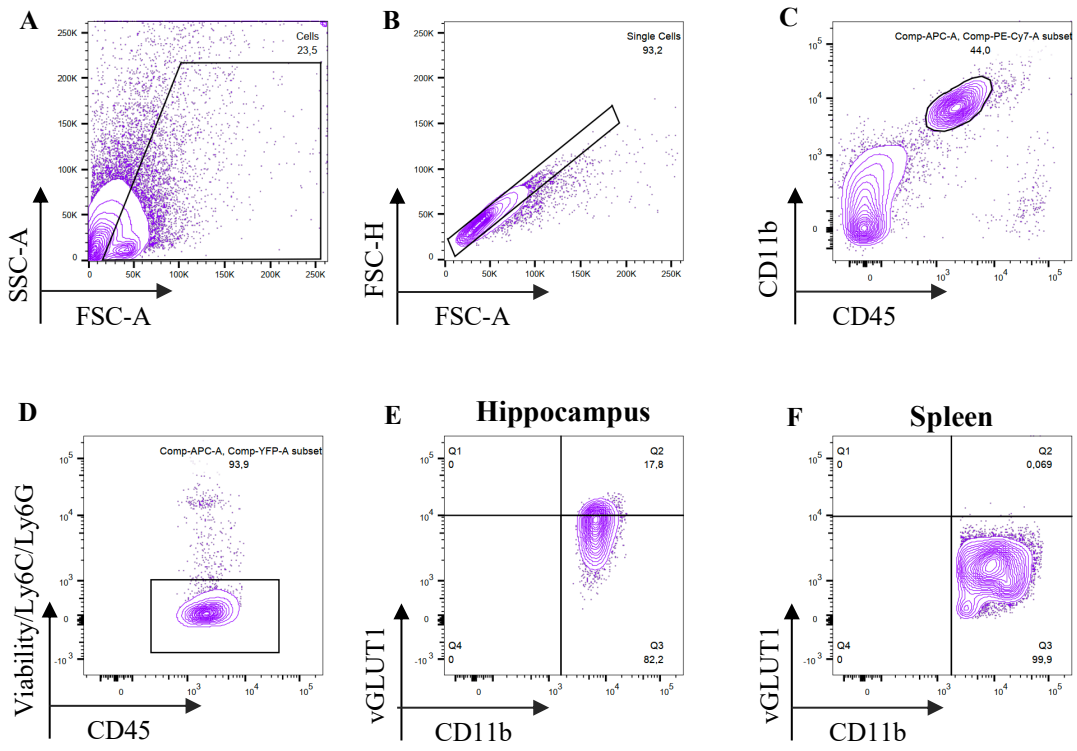

Figure 2B. 3 *Representative FACS plots indicating the gating strategy to analyze the percentage of vGLUT1^{+} microglia in the hippocampus.*

The gate was defined starting from the end-point of vGLUT1 signal (F) from the spleen macrophages, which were used as the negative control. A, B and C define CD11b^{+}/ CD45^{+} microglia population, which was also gated to analyze the engulfment of pHrodo^{TM}Red-labeled total synaptosomes by microglia in

addition to vGLUT1^{+} synapses. Detailed description of the gating strategy and the data analysis is provided in the materials and methods section of the project A.

2B.8 Total Synaptosome Isolation and pHrodo^{TM}Red Labeling

Total synaptosome isolation and pHrodo^{TM}Red labeling of synaptosomes was carried out exactly as described in the materials and method section of the project A.

2B.9 *In vitro* Minocycline Treatment and Synaptosome Engulfment Assay

Under deep anesthesia, 12 weeks old mice were transcardially perfused with DPBS. Microglia isolation was carried out exactly as described in the materials and method section of the project A. Microglia were seeded in 12-well culture plates at a density of 2.5 x 10^4 cells per well. After 1h at 37^{o}C, 20 µM minocycline (Sigma-Aldrich, catalog no. M9511) supplemented into each well apart from the control (untreated condition) wells, and cultivated for 24h or 48h. After the respective cultivation times, medium was gently taken out and cells were supplied with 500µl fresh DMEM per well, supplemented with 1/50 synaptosomes per well, and incubated for 2h at 37^{o}C. For analyses, cells were washed with DPBS 3 times, detached using trypsin solution (ThermoFisher Scientific, catalog no. R001100), and stained with fixable viability (ThermoFisher Scientific, catalog no. L34969, 1/1000) at 4^{o}C for 25 minutes. Afterwards, cells were resuspended in FACS buffer with CD16/CD32 (ThermoFisher Scientific, catalog no. 14-0161-82, 1/200) for 10 minutes on ice and followingly stained with 1/100 CD11b, 1/100 CD45 at 4^{o}C for 20 minutes. After the incubation, data were acquired using BD Aria II and analyzed using FlowJo v10 (BD Bioscience). **Figure 2B.3 (A-C)** shows how microglia are defined to quantify engulfment of PhRodo^{TM}Red-labeled total synaptosomes by microglia. Mean fluorescence intensity of PhRodo^{TM}Red was analyzed from the CD11b^{++}/ CD45^{+}/ Viable population to quantify the microglial engulfment of total synaptosomes.

2B.10 Minocycline Treatment

The dosages of minocycline administered systematically were determined according to previous studies demonstrating its impact on microglia and behavior (Kreisel et al., 2014; Rooney et al., 2020). Mice received 40 mg/kg/day of minocycline (Sigma-Aldrich, catalog no. M9511) administered via drinking water for a period of 28 days. The drug intake was adjusted by adapting the dosage based on the drinking volume and body weight per cage to ensure the proper intake dosage. Body weight and drinking volume were regularly monitored throughout the course of the treatment.

2B.11 17β-Estradiol ELISA

Blood samples were collected from the HAB and NAB female mice, which were used for the vGLUT1-specific synaptic pruning assay. They were centrifuged at 1000 rpm, 4^{o}C for 20 minutes. Serum was collected, and 50 μl per sample was used to quantify 17β-Estradiol concentration using 17β-Estradiol high sensitivity ELISA kit (Enzo, catalog no. ADI-900-174) according to manufacturer's instructions. Absorption values were detected using TECAN Infinite^{R}200 plate reader, and the data was analyzed using a standard curve constructed by the known concentrations and absorption values of the 17β-Estradiol.

2B.12 Statistical Analysis

Data analyses were performed with GraphPad Prism 8.0 software (GraphPad Software Inc., USA). The correlation was evaluated by Pearson's co-efficiency analysis. A 95% confidence interval was used for statistical evaluation, and $P < 0.05$ was considered as statistically significant in all sampled groups. Data are presented as means ± standard error of the mean (S.E.M.). The respective statistical tests are mentioned in the figure legends.

3B RESULTS

3B.1. Single-cell RNA sequencing reveals sexual dimorphism of microglia in mice with innate high anxiety

To address microglia heterogeneity in mice with high anxiety-related behavior (HAB) and normal anxiety-related behavior (NAB), we did single-cell RNA sequencing of HAB and NAB brains (whole brain excluding cerebellum) of both sexes. By using various genes related to a particular microglia function or state, we identified 10 clusters involving a cluster of border-associated macrophages (BAM), which we identified based on the expression of markers genes such as *Mrc-1, Ms4a7, and Pf4* (Hammond et al., 2019) **(Figures 3B.1, 3B.2 and 3B.3)**. The microglial identity of the remaining clusters was confirmed based on their expression levels of the canonical microglia marker genes such as *P2ry12, Tmem119, and Hexb* **(Figures 3B.1, 3B.2 and 3B.3).** Our data indicate a great degree of microglial heterogeneity based on their transcriptional state. The expression of genes, which were previously published to define different microglia clusters (Masuda et al., 2019; Hammond et al., 2019; Zeisel et al., 2015) indicates different transcriptional states, which also suggest potential differences in the microglial function. Apart from the potential functional differences, the gene expression profile of different microglia clusters also indicates their homeostatic or activated state, which was previously described as a decrease in the expression of microglial genes such as *P2ry12*, *Cx3cr1*, *Tmem119*, and *Hexb* (Masuda et al.,2020) **(Figures 3B.2 and 3B.3).** Different microglia clusters in our dataset shows varying levels of expression mainly for homeostasis, phagocytosis, interferon response, and proliferation-related genes **(Figures 3B.2 and 3B.3)**. Furthermore, the microglia heterogeneity reflected in our dataset is not only limited to their

gene expression profile, but also reflected in their percentages in the HAB and NAB brains, especially between different sexes **(Figure 3B.4)**.

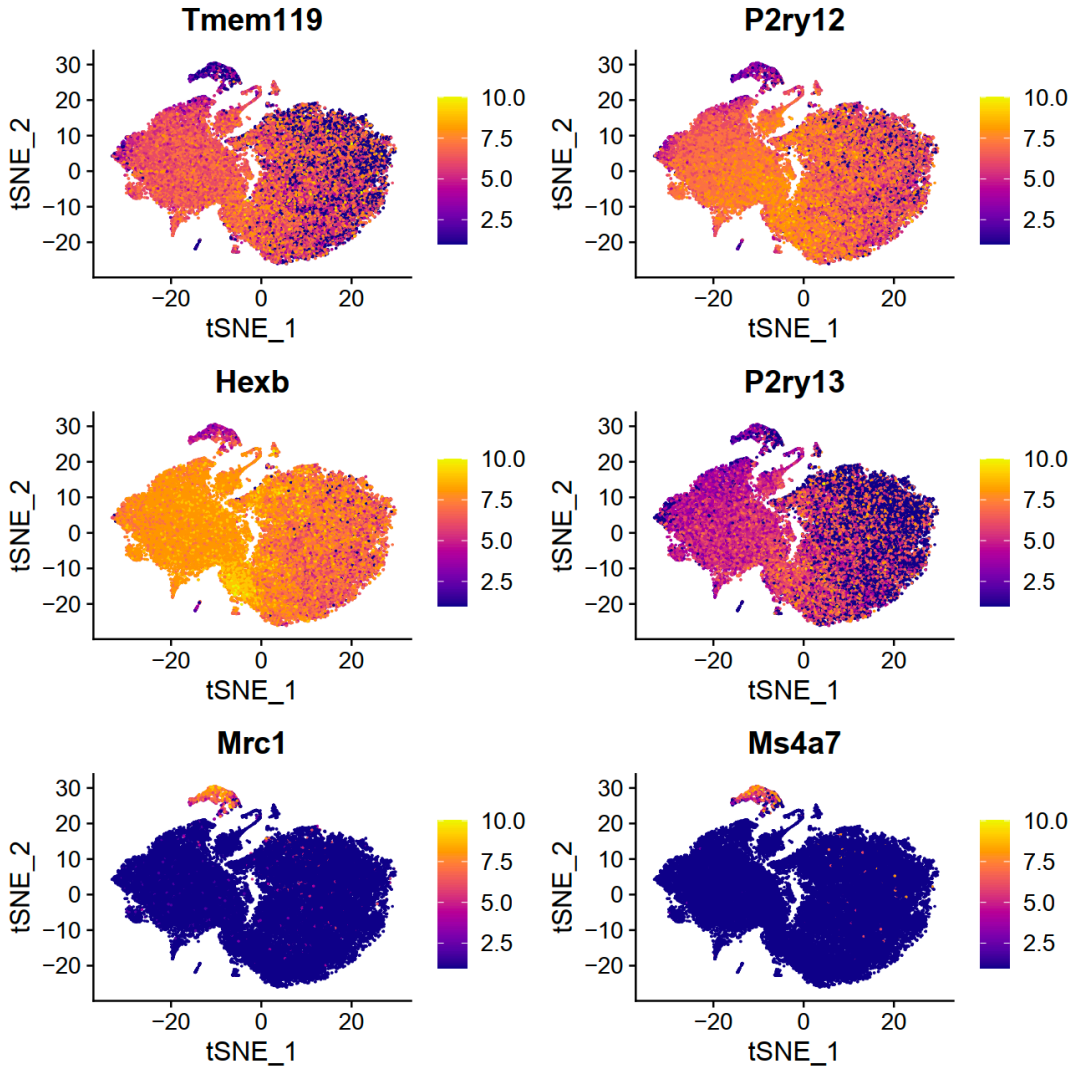

Figure 3B. 1 *High expression of microglial marker genes P2ry12, Tmem119 and Hexb shown by the t-distributed stochastic neighbor embedding (t-SNE) plots in all clusters.*

BAM cluster shows high expression of Mrc1 and Ms4a7, which are expressed at low levels in the microglia clusters.

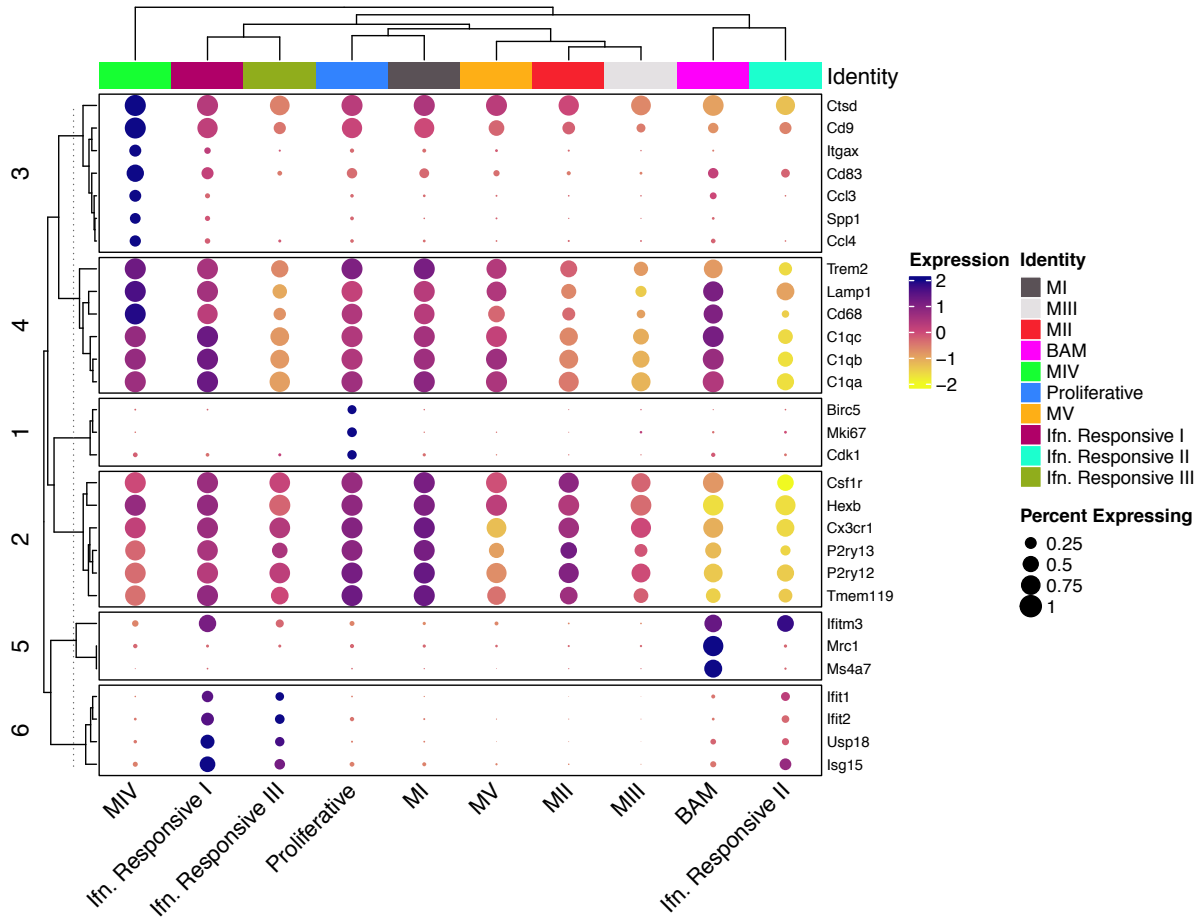

Figure 3B. 2 *Dot plot indicating the expression levels of genes that define distinct microglia clusters and the BAM cluster.*

Most microglia detected in the HAB and NAB brains belong to the MI, MII, and MIII clusters, constituting approximately 90% of the total microglia analyzed. These clusters express relatively different levels of canonical microglia signature genes such as *Tmem119, P2ry12, P2ry13* and *Hexb* **(Figure 3B.2 and 3B.3)**. In the HAB and NAB brains of both sexes, we found striking differences in the proportion and gene expression profile of each microglia clusters.

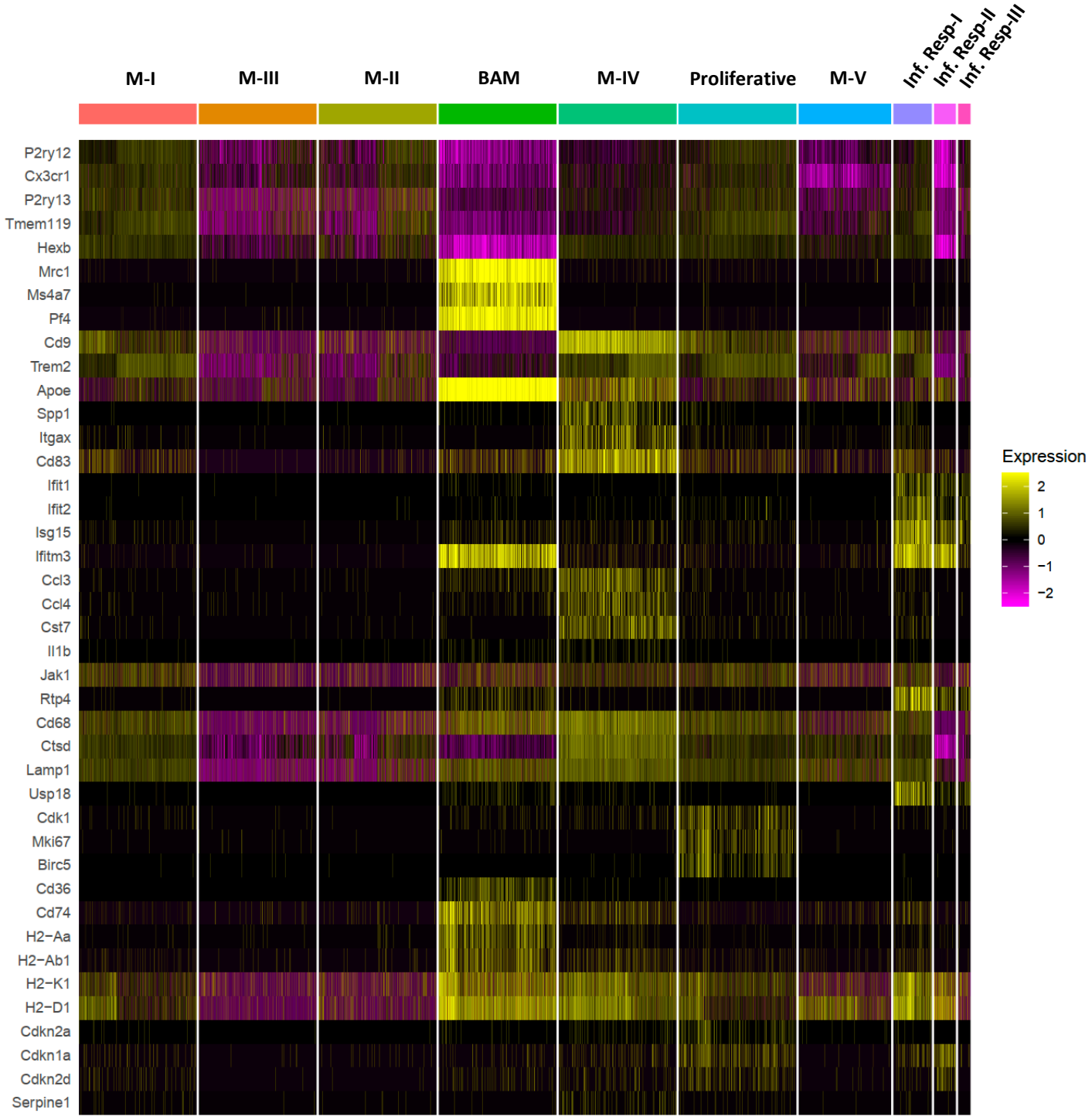

Figure 3B. 3 *Heatmap indicating the relative expression of genes that define different microglial states and clusters.*

MI cluster expresses high levels of microglial canonical marker genes (Hexb, P2ry12, Tmem119). It also shows high expression of phagocytosis-associated (Cd68, Trem2, Lamp1); interferon response-associated genes (Ifit2, Isg15, Ifitm3) (yellow: high expression; pink: low expression). MII and MIII clusters show lower expression of microglial canonical marker genes, and show low expression of

phagocytosis-related genes. MIV cluster indicates low levels of P2ry12, Tmem119, Hexb and high levels of Trem2, Cd9, Spp1. M-V cluster is similar to the MII and MIII in terms of the expression levels of canonical microglial marker genes but shows higher levels of phagocytosis-related genes compared to MII and MIII. Proliferative microglia cluster is characterized based on high expression of Mki67, Birc5 and Cdk1 genes. Interferon-responsive (Ifn. Resp I, II and III) clusters are characterized based on high expression of interferon-response genes (Ifit1,Ifit2,Isg15, Ifitm3). BAM cluster is characterized based on the exclusive high expression of Mrc1, Ms4a7 and Pf4 genes to distinguish them from the microglia clusters.

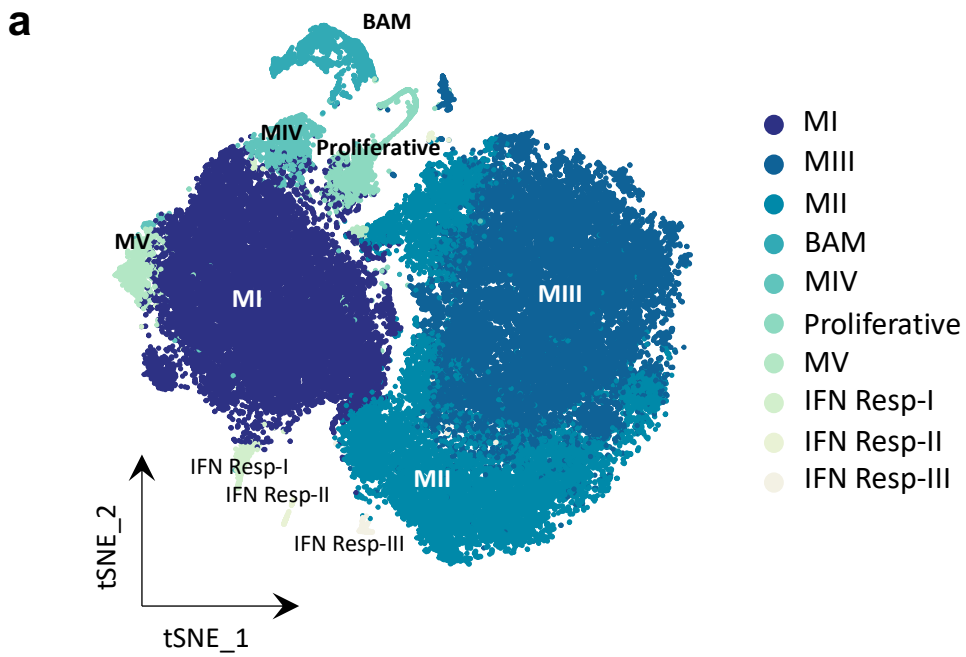

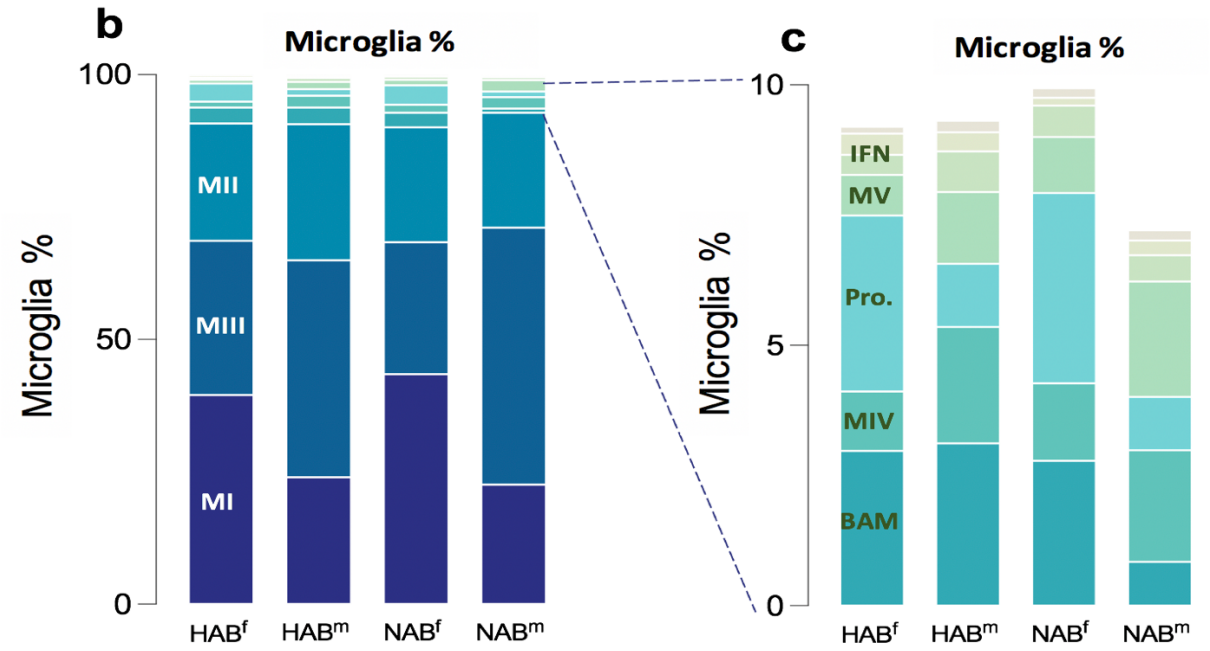

Figure 3B. 4 *Single-cell RNA sequencing reveals 9 microglia clusters diversified in their percentage and gene expression status in the HAB male and female brains.*

(a) *t-distributed stochastic neighbor embedding (t-SNE) reveals 10 different clusters (9 microglia and 1 BAM) in HAB and NAB brains of both sexes (n=8, 52.363 cells analyzed).*

(b and c) *Different microglia clusters show varying percentages in the HAB and NAB brains of both sexes. Percentage of MI, MIII, MII, BAM, MIV, Proliferative, MV, Interferon (IFN)-responsive I, IFN. Responsive II and IFN. Responsive III. in HAB male: 23.94%, 41.02%, 25.71%, 3.11%, 2.23%, 1.21%, 1.37%, 0.77%, 0.37%, 0.22%; HAB female: 39.47%, 29.16%, 22.15%, 2.97%, 1.14%, 3.37%, 0.77%, 0.38%, 0.41%, 0.12%; NAB male: 22.61%, 48.49%, 21.67%, 0.84%, 2.14%, 1.02%, 2.21%, 0.50%, 0.27%, 0.20%; NAB female: 43.42%, 24.95%, 21.67%, 2.78%, 1.49%, 3.65%, 1.07%, 0.59%, 0.15%, 0.18%, respectively. Major microglia clusters (MI, MII and MIII) are highlighted on the first bar plot (left) and represent ~90% of the total microglia analyzed. Rest of the microglia clusters and BAM are highlighted on the second bar plot (right) and represent ~10% of the total microglia analyzed.*

Table 3B. 1 *Percentages of different microglia clusters are indicated for each group.*

Cluster Name	HAB female %	HAB male %	NAB female %	NAB male %
MI	39,48	23,94	43,43	22,61
MIII	29,17	41,02	24,96	48,50
MII	22,16	25,72	21,68	21,67
BAM	2,97	3,11	2,78	0,84
MIV	1,14	2,24	1,49	2,14
Proliferative	3,38	1,21	3,65	1,03
MV	0,78	1,38	1,08	2,21
IFN. Responsive I	0,39	0,78	0,60	0,51
IFN. Responsive II	0,41	0,37	0,15	0,28
IFN. Responsive III	0,13	0,22	0,18	0,20

The MI cluster shows high expression levels of *Hexb, Tmem119, and P2ry12*, indicating a homeostatic state **(Figure 3B.3)**. The percentage of the MI cluster in the HAB female is ~39% whereas ~24% in the HAB male, indicating a sex difference in the proportion of this microglia cluster. NAB brains indicate a similar sexual dimorphism, where we found MI cluster as ~43% in female and ~22% in male **(Figure 3B.4 b and Table 3B.1)**. This data indicates higher percentage of MI cluster in females compared to males, for both HAB and NAB groups. When compared HAB and NABs with matching sexes, there is a slight decrease (4%) of this cluster in HAB female compared to the NAB female. In males, on the other hand, we found similar proportions of MI in HAB and NAB groups **(Figure 3B.4 b and Table 3B.1)**.

The MII cluster shows relatively lower expression levels of homeostatic genes compared to the MI cluster; indicating a transitionary phase between the homeostatic and activated states. It shows roughly similar percentages in HAB female, NAB female and NAB male, but a slight increase (3%) in the HAB male brain compared to the other groups **(Figure 3B.4 b and Table 3B.1)**.

The MIII cluster shows low expression levels of *Hexb, Tmem119, and P2ry12*, indicating an activated state **(Figure 3B.3)**. The percentage of the MIII cluster in HAB female is ~29%, whereas it is ~41% in the HAB male, indicating a sex-linked difference in the proportion of this microglia cluster. NAB brains indicate a similar sexual dimorphism, where the MIII cluster represents ~25% of the microglia in female and ~48% in male **(Figure 3B.4 b and Table 3B.1)**. This data indicates lower percentage of MIII cluster in females compared to males, for both HAB and NAB groups. When compared HAB and NAB brains with matching sexes, there is a slight increase (5%) of this cluster in the HAB female compared to the NAB female. In males, on the other hand, there is a decrease (7%) in the HAB male compared to the NAB male. **(Figure 3B.4 b and Table 3B.1)**.

Among these three major clusters, constituting the 90% of the microglia analyzed **(Figure 3B.4 b)**, MI and MIII represent the opposite states at transcriptional level and they both exhibit striking sexual dimorphism, as MI is almost 2 times higher in females; and MIII is almost 2 times higher in males for both groups of HAB and NABs. When matching sexes were compared between HAB and NAB groups only, there is a slightly lower percentage of MI in the HAB female. MIII on the other hand is more abundant in HAB female; whereas less in HAB male compared to their sex-matching NAB controls **(Figure 3B.4 b and Table 3B.1)**.

Apart from these major microglia clusters, the rest represent the 10% of the total microglia analyzed, and their percentages also suggest sexual dimorphism, especially for the microglia at the proliferative state, showing high expression of cell cycle-associated genes such as *Cdk1*, *Mki67* and *Birc5*. This cluster constitutes ~3% of the HAB female, 1.2% of the HAB male, 3.6% of the NAB female and 1% of the NAB male microglia **(Figure 3B.4 b and Table 3B.1)**. The BAM

cluster, identified by the high expression of *Ms4a7* and *Mrc1,* is almost 3 times enriched in the HAB male compared to the NAB male, which might suggest their contributing role, especially in the state of HAB male brain. The MIV cluster shows high expression of genes such as *Trem2, Cd9, Spp1, Itgax,* and *Cd83,* which defines the DAM state (Hammond et al., 2019; Masuda et al., 2020) **(Figure 3B.3)**. This cluster constitutes ~1.1% of the HAB female, %2.2 of HAB male, 1.4% of NAB female and 2.1% of the NAB male microglia **(Table 3B.1)**. The proportion of this cluster in different groups again suggests sexual dimorphism, and is lower in females compared to males in both HAB and NAB groups. MV cluster is closely related to the MIII cluster in terms of its activated state. However, it also shows higher expression of genes related to phagocytic function, such as *Cd68, Lamp1,* and *Ctsd*. **(Figure 3B.3)**. It constitutes ~0.8 % of the microglia detected in the HAB female, %1.3 in HAB male, 1% in NAB female and 2.2% in NAB male brains **(Table 3B.1)**. This cluster shows a slightly lower proportion in females compared to males, in both HAB and NAB groups.

Finally, interferon-responsive microglia clusters (IFN. resp-I, II, and III) were characterized based on a high expression of interferon response genes such as *Ifnar, Ifitm3, Ifit2* compared to the rest **(Figure 3B.3)**. Proportion of these clusters is ~0.4%, 0.4%, 0.13% in the HAB female, and ~0.8%, 0.4%, 0.2% in the HAB male, respectively **(Table 3B.1)**. NABs also show similar percentages of these clusters, which are ~0.5%, ~0.3%, ~0.2% in male, and ~0.6%, ~0.15%, ~0.2% in female, respectively **(Table 3B.1)**.

Altogether, the present dynamics of different microglia clusters in terms of their proportion and gene expression status suggest a notable sex difference in the HAB and NAB brains.

3B.2. Microglia with high potential of synaptic engulfment and phagocytosis are enriched in the female brain

Considering the sexual dimorphism reflected by the percentage dynamics of different microglia clusters, especially MI and MIII as the major clusters detected in our dataset, we next focused on their gene expression profile. Interestingly, in the MI cluster, we found a higher expression of genes related to phagocytosis and synaptic engulfment such as *Cd68*, *Trem2*, *C1qb*, *C1qc*, *Lamp1*, *Cx3cr1* compared to the MII and MIII **(Figure 3B.5)**. Furthermore, we also detected a high expression of genes related to interferon response such as *Ifngr1* and *Ifnar2* in the MI cluster **(Figure 3B.5)**. This cluster is almost doubled in percentage in the HAB female brain compared to the HAB male; moreover, a similar sexual dimorphism is also reflected in the NABs comparing male and female **(Figure 3B.4 b and Table 3.1)**. The MIII cluster shows a lower expression of the genes related to phagocytosis and synaptic engulfment **(Figure 3B.5)**, moreover they represent a lower percentage in females compared to males in both groups **(Figure 3B.4 b and Table 3B.1)**.

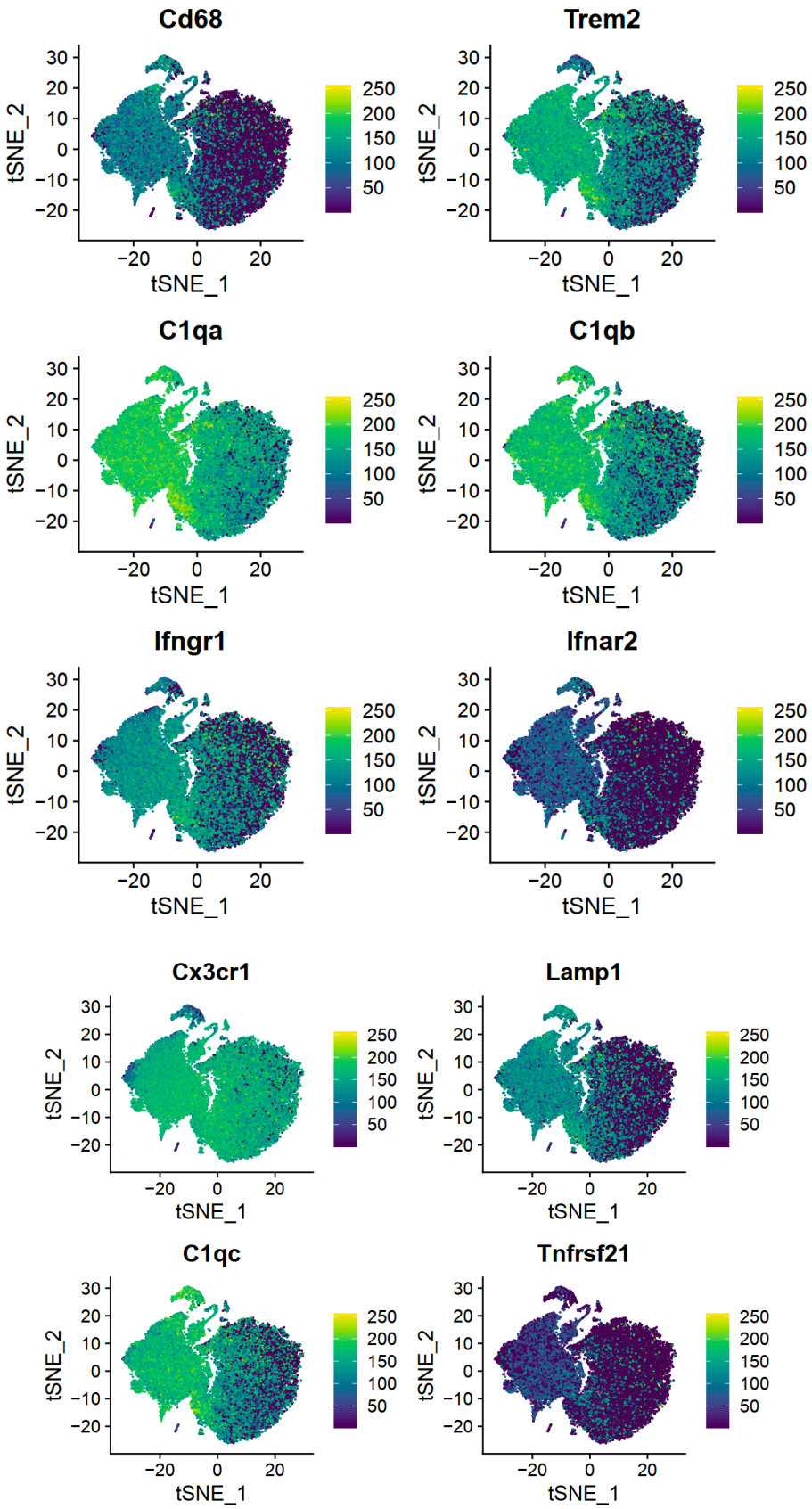

Figure 3B. 5 *MI cluster shows high expression of genes related to phagocytosis, synaptic pruning as well as interferon response.*

tSNE plots showing higher expression (lighter color) of genes associated to synaptic engulfment and phagocytosis such as CD68, Trem2, C1a, C1qb, C1qc, Cx3cr1, Lamp1 in the MI cluster. Genes associated to interferon response such as Ifngr1, Ifnar2 also show higher expression in the MI cluster.

The MII cluster similarly indicates a lower potential of phagocytosis; however, we did not observe such striking sex-linked differences in their percentages as opposed to the MI and MIII **(Figure 3B.4 b and Table 3B.1)**. Our data suggest that the female brain holds a greater proportion of microglia, which have a higher potential for synaptic engulfment and phagocytosis. Whereas, they hold a lower percentage of MIII, which has a lower potential for the respective functions **(Figures 3B.4 b and 3B.5)**. Notably, this data suggests a sexual dimorphism in microglial engulfment of synapses in the groups of HAB and NABs at the transcriptomics level, which might be relevant for the synaptic organization and regulation in male and female brains.

3B.3. HAB female microglia engulf more vGLUT1^{+} excitatory synapses in the hippocampus

Our single-cell RNA sequencing data points to an evident sex difference in the percentage dynamics and gene expression status of microglia, indicating an elevated potential for synaptic engulfment in the females compared to males in both HAB and NAB groups. We, therefore, next tested the engulfment of synapses by microglia, at postnatal day (P)90 in the hippocampus, which offers a promising microenvironment considering its dynamic nature in terms of synaptic re-organization and plasticity at the adult stage (Leuner & Gould, 2010). We showed that HAB female microglia engulf more vGLUT1^{+} synapses compared to the NAB female as well as to the HAB male **(Figures 3B.6 b and c)**. We also analyzed the percentage of

vGLUT1^{+} microglia in the hippocampus and showed a higher percentage only in HAB female compared to the NAB female **(Figure 3B.6 d)**. These findings suggest a sex-specific state of higher engulfment towards excitatory synapses by microglia in the hippocampus of HAB female compared to the other groups. The engulfment of vGLUT1^{+} synapses by NAB male and NAB female microglia did not indicate a sex difference **(Figures 3B.6 b and c)**. Due to this HAB female-specific state of microglia on the functional level, we next focused exclusively on the HAB female and HAB male microglia for the rest of the study, and analyzed differentially expressed markers, which may provide deeper insights into the basis of the sexually dimorphic microglia function.

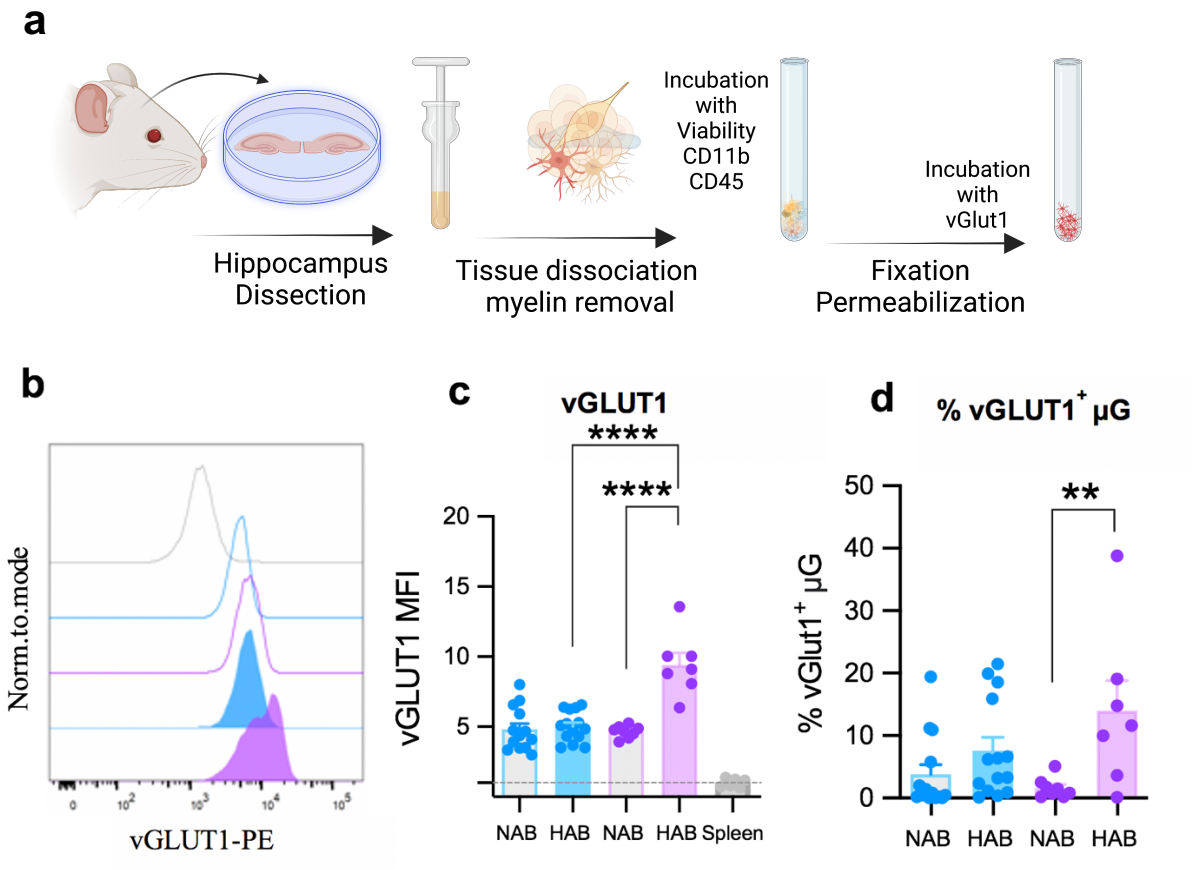

Figure 3B. 6 *Microglia engulf more vGLUT1^{+} synapses in the hippocampus of the HAB female compared to the HAB male.*

(a) *Schematic representation of the experimental workflow (created by using biorender.com).*

(b) *Representative overlayed histograms indicating the difference in vGLUT1-MFI for both sexes of HAB and NAB microglia.*

(c) *vGLUT1-MFI indicating the engulfment of vGLUT1^{+} synapses by CD11b^{++}/CD45^{+}/Ly6C^{-}/Ly6G^{-} hippocampal microglia is significantly higher in the HAB female microglia compared to the NAB female and HAB male. vGLUT1-MFI values are normalized to the spleen, which is used as a negative control. (2-way ANOVA with Šídák's multiple comparisons test, $n^{HABmale}$=14, $n^{NABmale}$=14, $n^{HABfemale}$=7, $n^{NABfemale}$=8; $p^{HABmale/NABmale}$ =0.999, $p^{HABfemale/NABfemale}$< 0.0001, $p^{HABmale/HABfemale}$ < 0.0001, $p^{NABmale/NABfemale}$>0.999, $p^{HABmale/NABfemale}$ =0.993, $p^{HABfemale/NABmale}$ < 0.0001).*

(d) *Percentage of vGLUT1^{+} microglia in hippocampus of HAB female (purple) is significantly higher compared to NAB female; whereas, no difference was detected between HAB male and NAB male (2-way ANOVA with Šídák's multiple comparisons test, $n^{HABmale}$=14, $n^{NABmale}$=14, $n^{HABfemale}$=7, $n^{NABfemale}$=8; $p^{HABmale/NABmale}$ =0.343, $p^{HABfemale/NABfemale}$= 0.010, $p^{HABmale/HABfemale}$=0.145, $p^{NABmale/NABfemale}$ =0.771, $p^{HABmale/NABfemale}$= 0.402, $p^{HABfemale/NABmale}$ =0.034). Data are represented as mean ± SEM, and each dot indicates 1 mouse. *P < 0.05; **P < 0.01; ***P < 0.001.*

3B.4. MI and MIII clusters express higher levels of genes associated with synaptic pruning and inflammatory response in the HAB female brain

We have so far shown that the MI and MIII clusters, which are the major microglia clusters detected in our dataset, indicate striking sex-linked differences in their percentage dynamics comparing male and female brains. These clusters represent a quite opposite states of microglia by which MI is more homeostatic and has a higher potential for synaptic engulfment; whereas, MIII indicates a lower potential of that while representing an activated state of microglia. When we compared the gene expression profiles of these two clusters in HAB male and HAB female brains **(Figure 3B.7)**, we found that the genes related to inflammatory response such as *Nfkb1*, *Il6ra*, and *Ifngr1* are upregulated in HAB female brain as compared with HAB male brain in the MI cluster **(Figure 3B.7c).** Interestingly, we also observed that in this cluster, which is highly phagocytic based on its gene expression profile,

the expression of genes related to phagocytosis as well as to synaptic engulfment such as *Cd68, Trem2*, *Itgam*, *Cx3cr1*, are higher in the HAB female compared to the HAB male **(Figure 3B.7c and Table 3B.2).** Therefore, we can conclude that this phagocytic cluster is even more prone to engulf synapses in the HAB female brain compared to the HAB male, based on its gene expression profile in addition to its higher percentage in the HAB female brain **(Figure 3B.7 and c)**. When we analyzed the MIII cluster, which has a low potential for phagocytosis; we similarly observed higher expression of genes related to inflammatory response in the HAB female **(Figure 3B.7d and Table 3B.4)**. Moreover, we showed that HAB female microglia express higher levels of *Trem2*, *C1qa*, *C1qb*, *Cx3cr1*, *Itgam*, and *Cd68* compared to HAB male, indicating that MIII cluster as well shows a higher potential to engulf synapses in the HAB female brain compared to the male **(Figure 3B.7d and Table 3B.4).** Overall, the analysis of these major clusters indicates potential markers that could drive the elevated engulfment of synapses in the HAB female brain compared to the HAB male; furthermore, reveals that the gene expression profile of these clusters indicates a state that is more prone to inflammation in the HAB female brain **(Figure 3B.7)**. Therefore; we overall show that MI and MIII clusters display significantly higher expression levels of synaptic engulfment-related genes such as *Trem2*, *Cx3cr1*, *Itgam, Cd68* in the HAB female brain compared to the HAB male. These markers serve as promising potential candidates to differentially modulate microglial engulfment of synapses in the HAB male and HAB female brain. Although the MII cluster does not indicate a major difference in its percentage comparing HAB male and HAB females, expression levels of *Trem2, C1qa, Cd68,* and *Ifngr1* are also higher in HAB female microglia compared to the HAB male **(Table 3B.3)**.

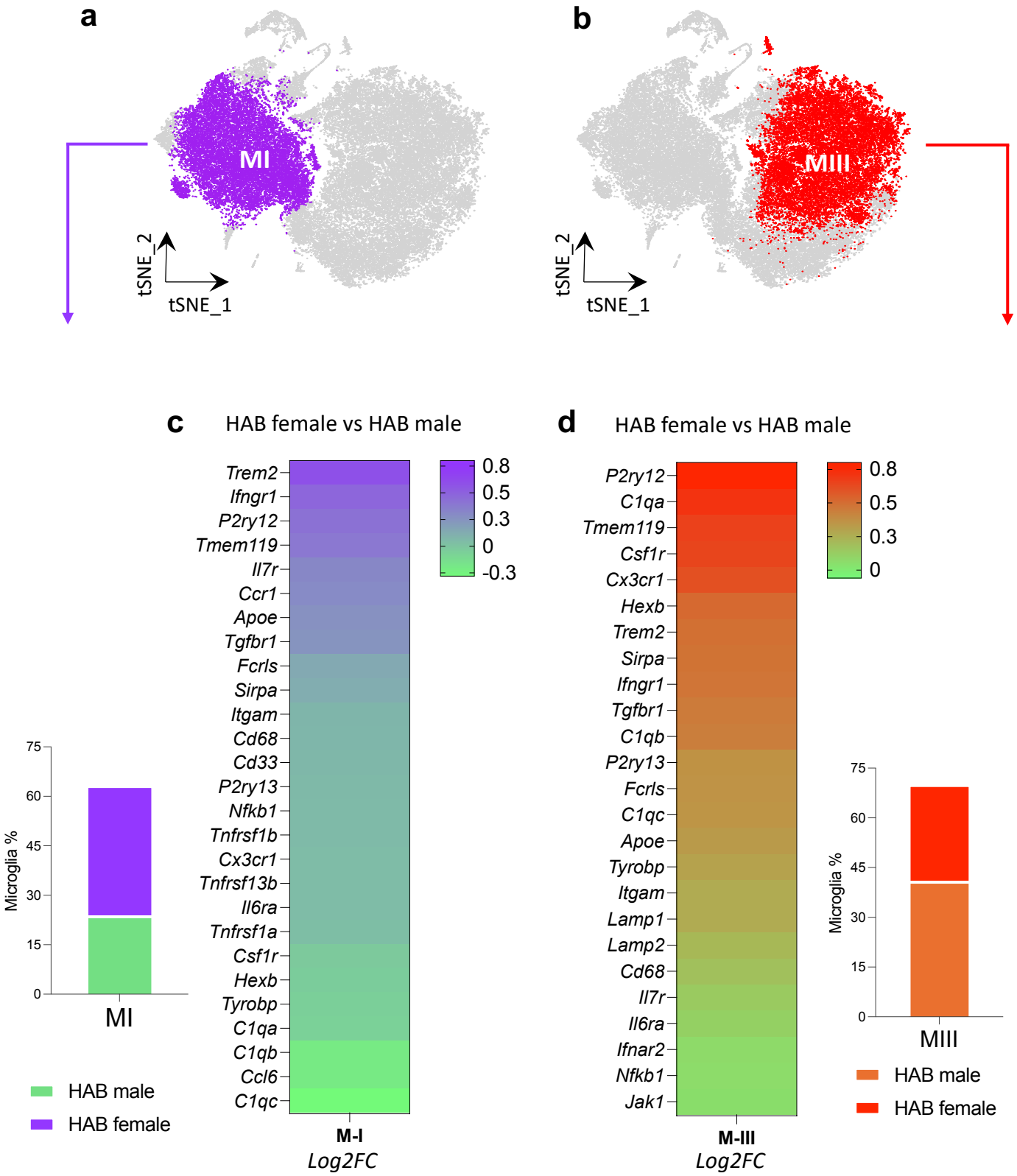
a
MI
tSNE_2
tSNE_1
b
MIII
tSNE_2
tSNE_1
c
HAB female vs HAB male
Trem2
Ifngr1
P2ry12
Tmem119
Il7r
Ccr1
Apoe
Tgfbr1
Fcrls
Sirpa
Itgam
Cd68
Cd33
P2ry13
Nfkb1
Tnfrsf1b
Cx3cr1
Tnfrsf13b
Il6ra
Tnfrsf1a
Csf1r
Hexb
Tyrobp
C1qa
C1qb
Ccl6
C1qc
0.8
0.5
0.3
0
-0.3
M-I
Log2FC
Microglia %
75
60
45
30
15
0
MI
HAB male
HAB female
d
HAB female vs HAB male
P2ry12
C1qa
Tmem119
Csf1r
Cx3cr1
Hexb
Trem2
Sirpa
Ifngr1
Tgfbr1
C1qb
P2ry13
Fcrls
C1qc
Apoe
Tyrobp
Itgam
Lamp1
Lamp2
Cd68
Il7r
Il6ra
Ifnar2
Nfkb1
Jak1
0.8
0.5
0.3
0
M-III
Log2FC
Microglia %
75
60
45
30
15
0
MIII
HAB male
HAB female

Figure 3B. 7 *Phagocytosis and inflammation-associated genes in MI and MIII clusters show higher expression levels in the HAB female compared to the HAB male.*

(a and b) *Feature plot highlighting the MI (purple) and MIII (red) clusters, respectively.*
(c) *Heatmap indicating a selected set of genes that are differentially regulated in the MI cluster of HAB female and HAB male brains. Bar plot indicates a higher percentage of MI cluster in the HAB female brain compared to the HAB male. Genes associated with synaptic pruning and phagocytosis (Trem2, Cx3cr1, Itgam, Cd68), inflammatory response (Nfkbi, Il6r, Ifngr1) show higher expression in HAB female compared to HAB male in the MI cluster. Heatmaps indicate log2 fold-change (Log2-FC) of the selected genes that are differentially regulated between HAB male and HAB female samples (DESeq2 test run via Seurat, pAdj <0.001).*
(d) *Heatmap indicating a selected set of genes that are differentially regulated in the MIII cluster of HAB female and HAB male brains. Bar plot indicates a lower percentage of MIII cluster in the HAB female brain compared to the HAB male. Genes associated with synaptic pruning and phagocytosis (Trem2, C1qa, C1qb, Cd68, Cx3cr1, Itgam), inflammatory response (Nfkbi, Il6r, Ifngr1, Jak1) show higher expression in the HAB female compared to the HAB male in the MIII cluster. Heatmaps indicate log2 fold-change (Log2-FC) of the selected genes that are differentially regulated between HAB male and HAB female samples (DESeq2 test run via Seurat, pAdj <0.001).*

Table 3B. 2 *Top 50 significantly regulated genes in the MI major cluster.*

The first table (a) indicates the top 50 upregulated genes in HAB male compared to the HAB female, ordered based on the log2FC values in descending order. The second table(b) indicates the top 50 downregulated genes in the HAB male compared to the HAB female, based on the absolute log2FC values in ascending order (DESeq2 test via Seurat, pAdj <0.001).

a

Genes	avg_log2FC	p_val_adj
Ly6e	1,913066922	0
Hpgd	1,424872461	0
Ccr6	1,361185316	0
Ctsb	1,100831496	0
H2-D1	0,947550716	0
BC004004	0,84021676	0
Oaf	0,686307956	8,2402E-286
Ubb	0,594398473	1,7692E-289
Sgk1	0,593185489	5,2299E-153
Chst12	0,591630889	1,111E-173
Rnaset2a	0,585464257	0
mt-Nd3	0,563427594	1,3723E-149
Klk8	0,545904782	3,5597E-143
Nrp1	0,530793052	1,0882E-22
mt-Nd5	0,511875837	1,8514E-115
mt-Nd4l	0,496642264	3,5355E-111
Siglece	0,478629986	1,57481E-13
Tspan13	0,464131034	2,1104E-119
Rps28	0,46178212	3,0761E-106
Ly86	0,456530454	9,0646E-184
Cacna1a	0,437995144	9,40407E-30
Ramp1	0,433911131	6,51062E-86
Cd9	0,427558686	4,34862E-82
Rpl35	0,424780593	1,49061E-84
Rps27	0,421183737	1,44287E-91
Trim12c	0,417000765	1,34576E-10
mt-Nd1	0,409283764	3,5238E-88
H2-K1	0,404535796	1,31056E-56
Tpp1	0,402661346	7,11991E-80
Glrp1	0,397812969	2,27782E-25
Cd63	0,390096974	6,14702E-46
Cd300c2	0,381544834	8,22004E-77
Tmem181a	0,375899133	2,41199E-14
Gm11808	0,375520038	4,38684E-82
Cadm1	0,358044794	9,27151E-58
Rpl29	0,357244896	5,15304E-57
Rpl37	0,352479085	1,86448E-59
Stambpl1	0,349301408	1,32988E-71
Rpl38	0,348915538	3,944E-54
mt-Atp8	0,34809799	5,91621E-57
Rps21	0,345961073	1,28549E-60
Lyz2	0,343097084	6,19989E-26

b

Genes	avg_log2FC	p_val_adj
Trim5	-0,26198589	3,80102E-14
Ttc28	-0,26295213	3,32182E-50
Apoe	-0,26343759	3,01252E-08
Rnase4	-0,26373871	7,0192E-169
Olfml3	-0,26689685	3,2799E-103
Smap2	-0,26795772	6,5621E-109
Peli2	-0,27146927	1,17711E-61
Slc9a9	-0,27380898	1,99619E-65
Cd164	-0,27895169	1,5105E-99
Bhlhe41	-0,27945672	6,96062E-70
Actn1	-0,28265899	4,02534E-27
Cap1	-0,29136693	5,10383E-92
Lhfpl2	-0,29426482	2,84391E-65
Armc3	-0,29839461	3,84192E-65
Ccr1	-0,29914612	1,75369E-05
Dock4	-0,30128422	1,98828E-89
Hs6st1	-0,3041212	3,73411E-81
Ccdc12	-0,30849385	3,1738E-103
Pla2g4a	-0,31049515	1,3757E-77
Ccr5	-0,31079714	1,3497E-102
Il7r	-0,31827566	2,98871E-69
Slc37a2	-0,32309154	2,23816E-72
Fchsd2	-0,32423748	6,78654E-83
Glul	-0,33023737	2,0483E-145
Pag1	-0,34278027	4,2898E-119
Nrip1	-0,34418586	1,4469E-117
Ltc4s	-0,34611691	9,1688E-131
C5ar2	-0,35378023	6,08899E-72
Itgav	-0,35428913	1,4822E-101
Cbl	-0,3583296	3,3212E-102
Mxra8	-0,3599969	1,17415E-69
Cd34	-0,36476379	9,44705E-65
Grap	-0,36607411	2,4586E-118
Nmt1	-0,37115582	2,6154E-151
Trim30d	-0,3764082	5,52638E-66
Tmem119	-0,39231147	3,0536E-294
Tns1	-0,39337558	3,8911E-107
P2ry12	-0,42162453	0
Man2a2	-0,45310712	2,1011E-155
Ecscr	-0,4625516	5,9817E-152
Jam2	-0,47430282	5,6983E-197
Ifngr1	-0,4769563	0

mt-Nd2	0,340820346	5,92409E-58
mt-Co2	0,339080523	3,16018E-63
Gm26917	0,326348667	3,58534E-28
mt-Nd4	0,323032057	6,17124E-50
Ctsc	0,320889449	9,17775E-42
Rpl39	0,313618531	1,09287E-34
Fth1	0,311588101	5,2003E-35

Fam111a	-0,49401651	2,6258E-147
Bank1	-0,54979181	6,2386E-201
Trem2	-0,58883749	0
Xist	-0,61928659	1,4973E-38
Npl	-0,73993883	0
Colec12	-0,83977847	0
Cwc22	-1,15452251	0

Table 3B. 3 *Top 50 significantly regulated genes in the MII major cluster.*

The first table (a) indicates the top 50 upregulated genes in HAB male compared to the HAB female, ordered based on the log2FC values in descending order. The second table(b) indicates the top 50 downregulated genes in the HAB male compared to the HAB female, based on the absolute log2FC values in ascending order (DESeq2 test via Seurat, pAdj <0.001).

a

Genes	avg_log2FC	p_val_adj
Cacna1a	1,46912294	2,1849E-146
Ly6e	1,367542816	5,939E-147
Ccr6	1,360613986	1,6883E-160
Gm26917	1,296413	1,8222E-155
mt-Nd3	1,239165908	2,2761E-192
mt-Nd5	1,054990524	4,6827E-133
mt-Nd4l	1,020850542	6,7815E-105
mt-Nd1	0,990169977	5,2414E-135
Fam193b	0,940273011	6,07688E-64
mt-Atp8	0,938052457	2,62333E-76
Tmem181a	0,930431098	1,72351E-81
Chd7	0,903020764	1,38831E-75
mt-Nd2	0,899037786	4,6596E-126
Gm42418	0,897771834	0
mt-Co2	0,879566692	2,6319E-113
Glrp1	0,869613078	2,5804E-55
mt-Nd4	0,845874223	7,2822E-102
Itpr2	0,779446301	6,25697E-59
mt-Cytb	0,762447288	1,20258E-78
mt-Co3	0,762319538	1,17575E-87
mt-Co1	0,75355477	3,50846E-91
Ankrd11	0,732387094	1,98104E-54

b

Genes	avg_log2FC	p_val_adj
Itgav	-0,59482078	2,5168E-67
Rnase4	-0,59681413	2,89E-103
Itm2c	-0,59711556	1,2618E-81
Olfml3	-0,60006971	2,7715E-94
Trim30d	-0,60012342	9,1736E-54
Lpcat2	-0,60205867	7,5732E-98
Bank1	-0,60528855	4,7451E-56
Csf1r	-0,60870592	4,811E-197
Slc3a2	-0,61786687	2,7941E-57
Slc9a9	-0,62181061	6,2311E-62
Rplp1	-0,62471541	3,297E-124
Lamp1	-0,62537712	1,052E-117
Ccr5	-0,62791313	1,622E-109
Psap	-0,62981309	1,382E-175
Lpcat3	-0,63116033	3,9729E-56
Scamp2	-0,63519069	7,258E-103
Ltc4s	-0,64328971	3,738E-88
Gm43221	-0,64354909	7,7089E-41
Bhlhe41	-0,6494875	2,7025E-66
Sirpa	-0,65097215	8,983E-136
C1qa	-0,6516001	1,354E-222
Alox5ap	-0,65236583	4,8641E-91

Hpgd	0,722810249	6,74026E-39
Tcirg1	0,71741692	7,92573E-64
Rgl2	0,697819859	8,71937E-43
Macf1	0,692875346	2,93206E-91
mt-Atp6	0,686940914	1,05792E-71
Prkcd	0,673153494	5,58301E-69
Safb2	0,665663969	1,49545E-48
Gm47283	0,659108957	1,3506E-53
Ash1l	0,658522309	1,538E-57
Pnisr	0,630083993	7,74619E-88
Plcb2	0,624727892	1,49276E-34
Pde1b	0,621219046	1,33859E-27
Rbm25	0,619270905	1,91436E-83
Cfap74	0,600354163	7,3295E-25
Senp2	0,593623917	2,25283E-42
Stard9	0,582862481	1,81488E-34
Srrm2	0,581109892	7,60573E-60
Pou2f2	0,5799622	4,35629E-53
Golga4	0,573977533	1,16991E-24
Hnrnpl	0,567204622	1,24178E-37
Adap2	0,560517355	3,13625E-63
Col6a3	0,558438827	6,39776E-20
Trip11	0,555126518	8,88791E-35
Golgb1	0,549125318	1,04476E-30
Stambpl1	0,544616267	6,43471E-24
Zc3h13	0,542127021	3,03459E-18
Tbc1d16	0,541908389	7,07785E-25
Bdp1	0,53970276	4,31449E-21

Cd68	-0,66529392	2,775E-89
Cd34	-0,67501658	1,3565E-65
Serinc3	-0,67989428	2,898E-195
Ctsd	-0,6890018	2,55E-259
Hspa5	-0,69119574	2,177E-99
Tmem173	-0,69390768	3,2705E-83
Jam2	-0,70212166	3,5664E-67
Tmbim6	-0,72138413	6,702E-127
Selplg	-0,74876963	3,988E-218
Itm2b	-0,76791135	2,602E-240
Pla2g15	-0,78537132	2,441E-113
Laptm5	-0,80348907	4,265E-244
P2ry13	-0,80893085	6,388E-149
Arsb	-0,82063153	8,553E-108
Adgrg1	-0,83595424	1,052E-145
Cd164	-0,8484976	4,642E-163
Sparc	-0,85754436	2,8E-306
Cmtm6	-0,8597549	9,865E-177
Cd81	-0,87414699	3,181E-234
Trem2	-0,89840936	4,823E-212
Ifngr1	-0,94914734	4,853E-202
Gpr34	-0,94956559	7,351E-239
Slc2a5	-0,98705604	5,347E-177
P2ry12	-0,98850025	0
Tmem119	-1,00703819	3,268E-289
Tsix	-1,10715139	7,915E-194
Colec12	-1,69940087	0
Cwc22	-1,89193015	0

Table 3B. 4 *Top 50 significantly regulated genes in the MIII major cluster.*

The first table (a) indicates the top 50 upregulated genes in HAB male compared to the HAB female, ordered based on the log2FC values in descending order. The second table (b) indicates the top 50 downregulated genes in the HAB male compared to the HAB female, based on the absolute log2FC values in ascending order (DESeq2 test via Seurat, pAdj <0.001).

a

Genes	avg_log2FC	p_val_adj
mt-Nd1	0,54396455	1,32109E-09
mt-Nd3	0,523467571	8,83019E-24
Gm26917	0,418037464	1,17344E-06
mt-Nd5	0,401356799	5,19791E-15
mt-Nd4l	0,363605693	8,17339E-22
Srrm2	0,148148899	0,000116235
Son	0,113225023	1,82291E-35
Macf1	0,087034744	2,03472E-31
Srrm1	0,085187161	2,9193E-05
Ankrd11	0,073112591	2,12681E-05
Atrx	0,070812203	7,13153E-11
Trip11	0,064386199	0,000224967
Golgb1	0,06306558	0,00025179
Srek1	0,062615561	0,000388818
Ctsb	0,055834181	0,000129987
Bod1l	0,055435143	4,4062E-06
Prpf38b	0,055377517	1,09779E-05
Pou2f2	0,053501258	1,61434E-12
Ighm	0,051026548	0,000984436
Rbm25	0,048370943	1,06962E-18
Safb2	0,047365251	1,25634E-06
Aim2	0,04714052	9,11258E-05
Stard9	0,046546311	3,29086E-06
Golga4	0,046385728	6,38123E-06
Nipbl	0,045915387	1,97425E-08
Mef2a	0,044841465	1,07204E-17
Plcb2	0,044389531	6,21558E-06
Huwe1	0,044085344	4,59187E-07
Pnisr	0,042563979	5,023E-21
Dock10	0,040646025	1,00337E-10
Ddx39b	0,04046824	1,47814E-07
Col27a1	0,039803385	1,39038E-08
Ash1l	0,039584281	1,85139E-10
Nav3	0,038834237	8,29054E-20
Rbm5	0,038436594	4,82959E-12
Gm28187	0,03504255	0,00056552
Sltm	0,033896027	5,9378E-06
Usp8	0,032176184	5,23062E-08
Ppcdc	0,030318629	1,95962E-05
Zfp638	0,029769276	1,1818E-10
Numa1	0,028423916	1,88353E-08
Gramd1a	0,027966037	9,78776E-05

b

Genes	avg_log2FC	p_val_adj
Tmbim6	-0,32504515	8,5065E-146
Olfml3	-0,33164916	1,3535E-146
Apoe	-0,33238969	1,6961E-173
Adgrg1	-0,34103068	1,6151E-139
Fcer1g	-0,34543775	1,5718E-188
Pag1	-0,34570159	4,1823E-162
B2m	-0,34645872	2,0577E-198
C1qc	-0,35631212	7,0375E-189
Colec12	-0,35765083	2,15268E-55
Fcrls	-0,36423951	1,444E-203
Marcks	-0,36487425	2,8548E-236
P2ry13	-0,37119275	5,9166E-185
Kctd12	-0,38534161	3,6203E-189
Cd164	-0,39172843	1,1669E-189
Ddx5	-0,40517002	1,0776E-218
Rplp1	-0,41497004	3,3636E-246
Itgb5	-0,41598078	7,1964E-226
Mpeg1	-0,43506317	1,2677E-222
C1qb	-0,43973059	5,0976E-265
Vsir	-0,44097887	1,2062E-239
Tgfbr1	-0,44999299	4,9286E-230
Ccr5	-0,45622334	9,3173E-212
Actb	-0,4575251	0
Lgmn	-0,46153322	1,0813E-280
Ifngr1	-0,47634007	5,5042E-286
Malat1	-0,48357406	3,3507E-202
Psap	-0,48487609	1,0008E-272
Cmtm6	-0,4851608	7,5276E-248
Sirpa	-0,48641432	1,0155E-259
Trem2	-0,4927889	0
Tmsb4x	-0,50783335	0
Hexb	-0,51812884	0
Serinc3	-0,5616526	0
Laptm5	-0,59589161	0
Cx3cr1	-0,60433403	0
Gpr34	-0,61010419	0
Selplg	-0,62805798	0
Ctss	-0,63619584	0
Cd81	-0,63809017	0
Csf1r	-0,64915483	0
Tmem119	-0,66382041	0
Cst3	-0,69029679	0

Srrt	0,026616227	0,000142059
Baz1b	0,026437456	2,38869E-08
Usp48	0,023695252	0,000617337
Baz2b	0,022396416	2,9807E-07
Srsf11	0,022247516	2,50672E-14
Setd2	0,021764977	8,06041E-13
Resf1	0,021367498	6,36038E-08

C1qa	-0,715885	0
Ctsd	-0,72625159	0
Itm2b	-0,73309678	0
Sparc	-0,74159054	0
P2ry12	-0,78917937	0
Cwc22	-0,93862341	0
Xist	-1,0597814	1,8641E-120

The pathways differentially regulated between HAB male and HAB female brains in these clusters also indicated major differences between them. For instance, 'regulation of cell migration', 'cell motility', 'homeostatic process' as well as 'synapse pruning', 'regulation of inflammatory response', and 'microglial cell activation' were among the top pathways differentially regulated between HAB male and HAB female brains in the MI and MIII clusters, respectively **(Figure 3B.8)**. This data suggests that apart from the regulation of synaptic pruning, there are many other pathways regulated differently between the HAB male and HAB female brains.

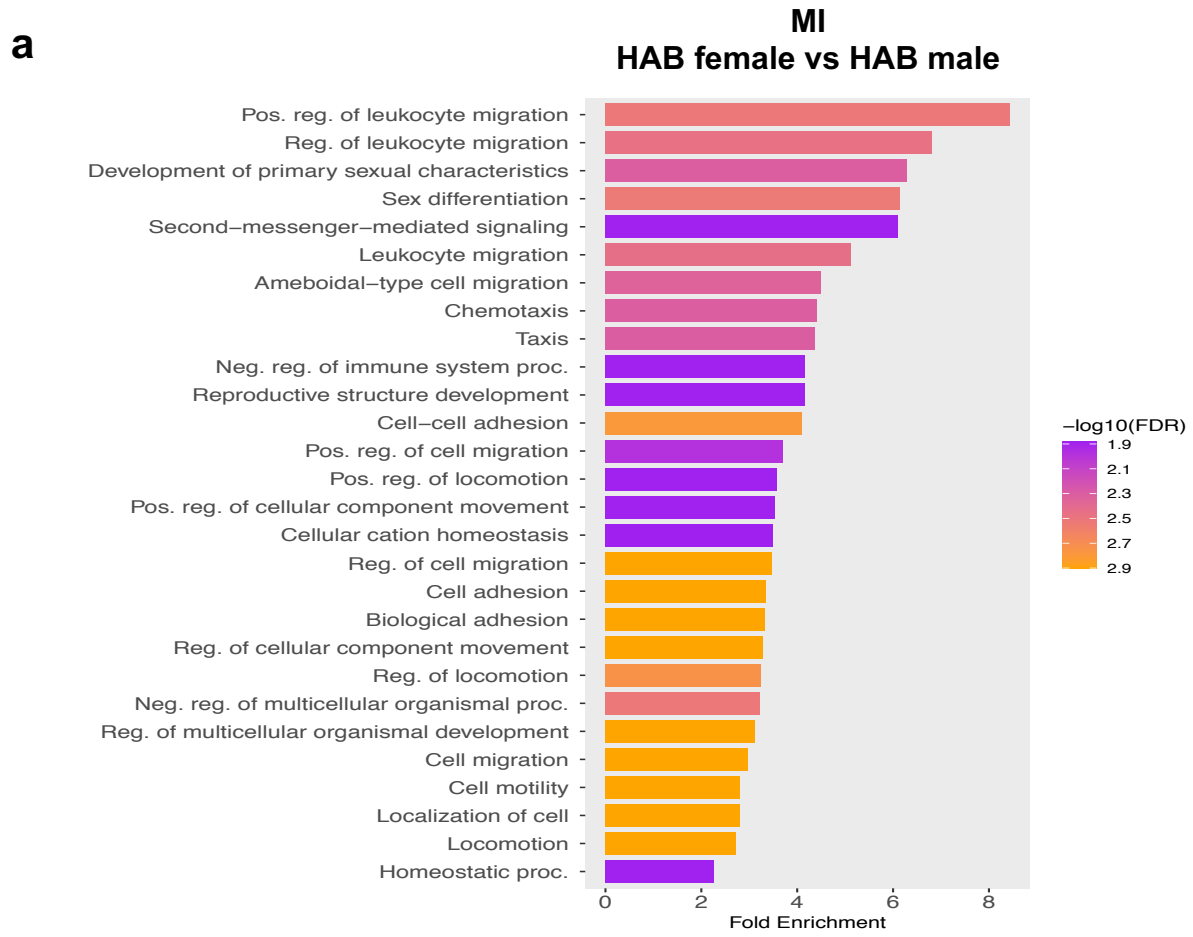

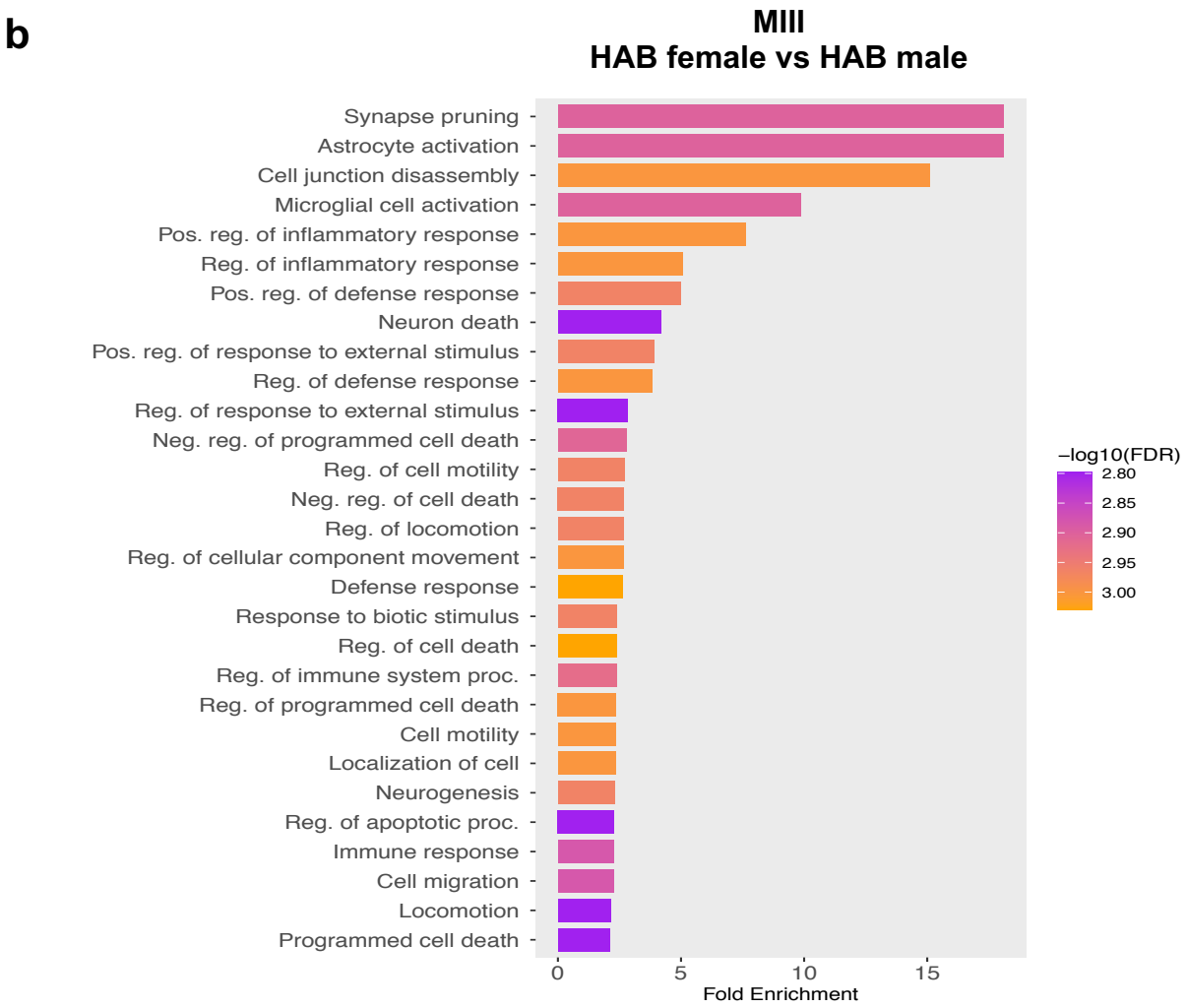

Figure 3B. 8 *Gene set enrichment analysis on the gene ontology indicates differential regulation of diverse pathways in the HAB female brain compared to the HAB male.*

Gene set enrichment analysis indicating significantly enriched expression modules with genes related to various pathways such as cell locomotion and homeostasis in the MI cluster and synaptic pruning, regulation of immune response in the MIII cluster based on the differentially regulated genes in HAB female microglia compared to the HAB male (pAdj <0.05).

3B.5. HAB female microglia express higher levels of synaptic engulfment-related markers in the hippocampus

Since we investigated the differential gene expression profile of the HAB male and HAB female, by focusing on the MI and MIII major microglia clusters, and identified the candidate genes in the whole brain; we next validated these findings in the hippocampus by checking surface levels of CX3CR1 (encoded by *Cx3cr1*), TREM2 (encoded by *Trem2*), and CR3 (encoded by *Itgam*), which have previously been shown to modulate synaptic engulfment by microglia (Paolicelli et al., 2011; Filipello et al., 2018; Stevens et al., 2007). Our data reveals elevated expression levels of these three markers in the HAB female microglia compared to the HAB male in the hippocampus and at the protein level **(Figure 3B.9)**.

Taken together, we showed higher expression of synaptic engulfment-related genes in the HAB female microglia compared to the HAB male **(Figure 3B.8)**. These findings suggest an elevated potential for microglial engulfment of synapses in the HAB female, which was validated on a functional level by showing higher levels of vGLUT1^{+} synaptic engulfment in the female HAB hippocampus compared to the other groups including HAB male **(Figure 3B.7)**. We also validated higher expression of the pruning-associated markers such as TREM2 by HAB female microglia compared to the HAB male in the hippocampus **(Figure 3B.9)**.

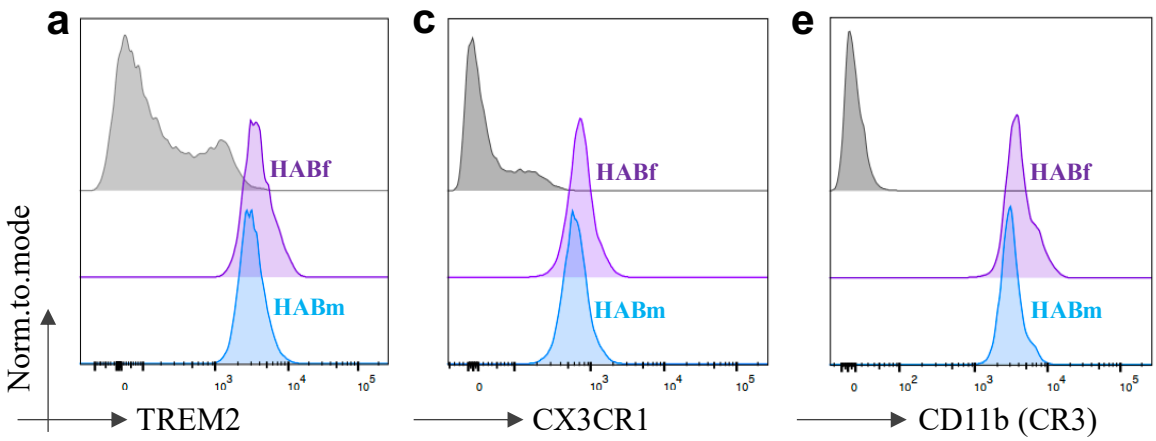

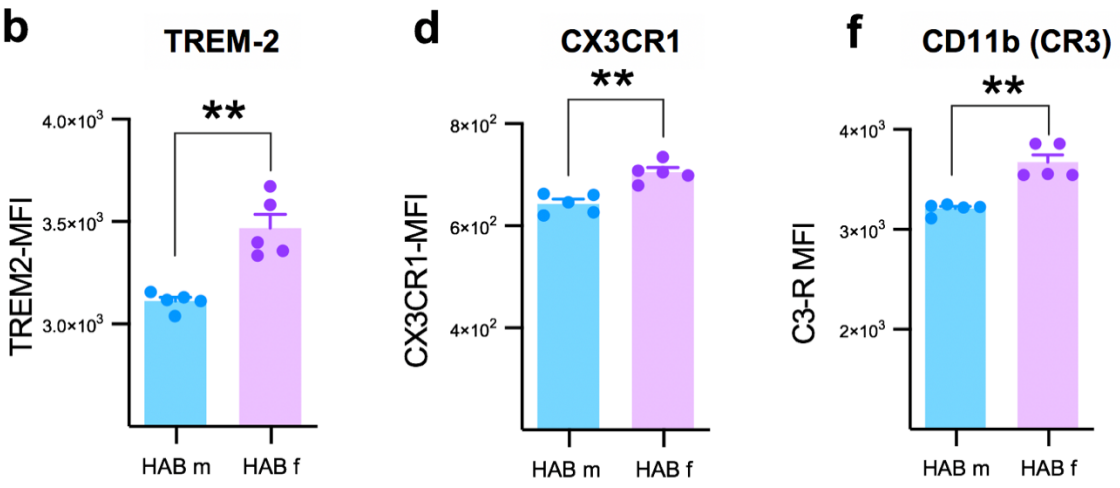

Figure 3B. 9 *HAB female microglia show higher levels of TREM2, CX3CR1, CR3 in the hippocampus.*

(a-c-e) *Representative overlayed histograms indicating MFI signal of TREM2, CX3CR1 and CD11b subunit of CR3 from hippocampal microglia of HAB male and HAB female (male: blue; female: magenta).*

(b-d-f) *Surface expression levels of microglia-specific TREM2, CX3CR1, and CD11b subunit of CR3 are higher in the HAB female hippocampus compared to the HAB male (Student's t test with Welch's correction,* p^{TREM2}*=0.004;* p^{CX3CR1}*=0.001,* p^{C3R}*=0.002;* n^{male}*=5;* n^{female}*=5; Data are represented as mean ± SEM, and each dot indicates 1 mouse.*P < 0.05; **P < 0.01; ***P < 0.001.)*

3B.6. Minocycline alleviates higher engulfment of synapses by HAB female microglia

It was previously reported that minocycline alleviates high anxiety-related behavioral symptoms in the HAB mice and influences microglia in both innate anxiety (Rooney et al., 2020) and other models of psychiatric disorders (Mattei et al., 2017). We, therefore, next tested the *in vivo* effect of minocycline on microglia of HAB male and HAB female mice by supplying it in the drinking water for 4 weeks **(Figure 3B.10 a).** We checked the engulfment of vGLUT1^{+} synapses by microglia in response to the treatment, and reported a significant reduction of synaptic over-engulfment by the HAB female microglia to the level of HAB male **(Figure 3B.10 b)**.

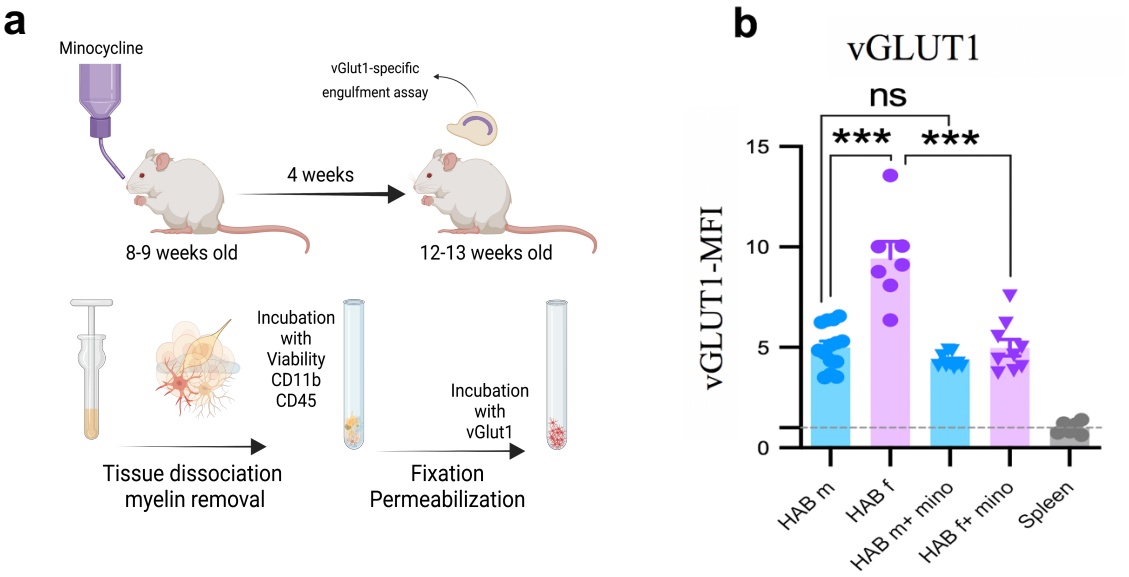

Figure 3B. 10 *Systemic minocycline administration alleviates microglial over-engulfment of vGLUT1⁺ synapses in the HAB female hippocampus.*

(a) *Schematic overview of the minocycline treatment and vGLUT1-specific synaptic engulfment assay (created by using Biorender.com)*

(b) *Significant reduction in the engulfment of vGLUT1⁺ synapses by HAB female microglia in response to minocycline treatment is shown. Data indicates no difference between HAB female and HAB male after 4 weeks of minocycline treatment (2-way ANOVA with Šídák's multiple comparisons test,* $n^{HABmale}$*=14,* $n^{HABfemale}$*=7,* $n_{mino}{}^{HABmale}$ *=9,* $n_{mino}{}^{HABfemale}$*=9,* $pAdj^{HABm/HABf}$*< 0.001,* $pAdj^{HABm/HABm\text{-}mino}$*= 0.996,* $pAdj^{HABf/HABf\text{-}mino}$*< 0.001, pAdj* $^{HABm\text{-}mino/HABf\text{-}mino}$*=0.848; Data are represented as mean ± SEM, and each dot indicates 1 mouse *P < 0.05; **P < 0.01; ***P < 0.001).*

Minocycline acts also on other cells and organ systems when supplied *in vivo* (Möller et al., 2016). Therefore, we next explored the direct effect of minocycline on microglial engulfment of synapses. We used pHrodo™Red-labeled synaptosomes and supplemented them to freshly MACS- isolated microglia (CD11b- enriched cells) from the hippocampus of HAB male and HAB female at P90 **(Figure 3B.11 a)**. We then analyzed the engulfment of pHrodo™Red-labeled synaptosomes by MACS-isolated microglia and found higher engulfment by HAB female microglia both after 24h and 48h in culture compared to the HAB male **(Figures 3B.11 b and**

c). After 24h of *in vitro* minocycline treatment, we found no difference in the synaptosome engulfment comparing HAB male and HAB female microglia to the untreated controls **(Figure 3B.11 b).** However, after 48h of treatment, we detected a significant decrease in the engulfment of total synaptosomes specifically by the HAB female microglia compared to the untreated control **(Figure 3B.11 c)**.

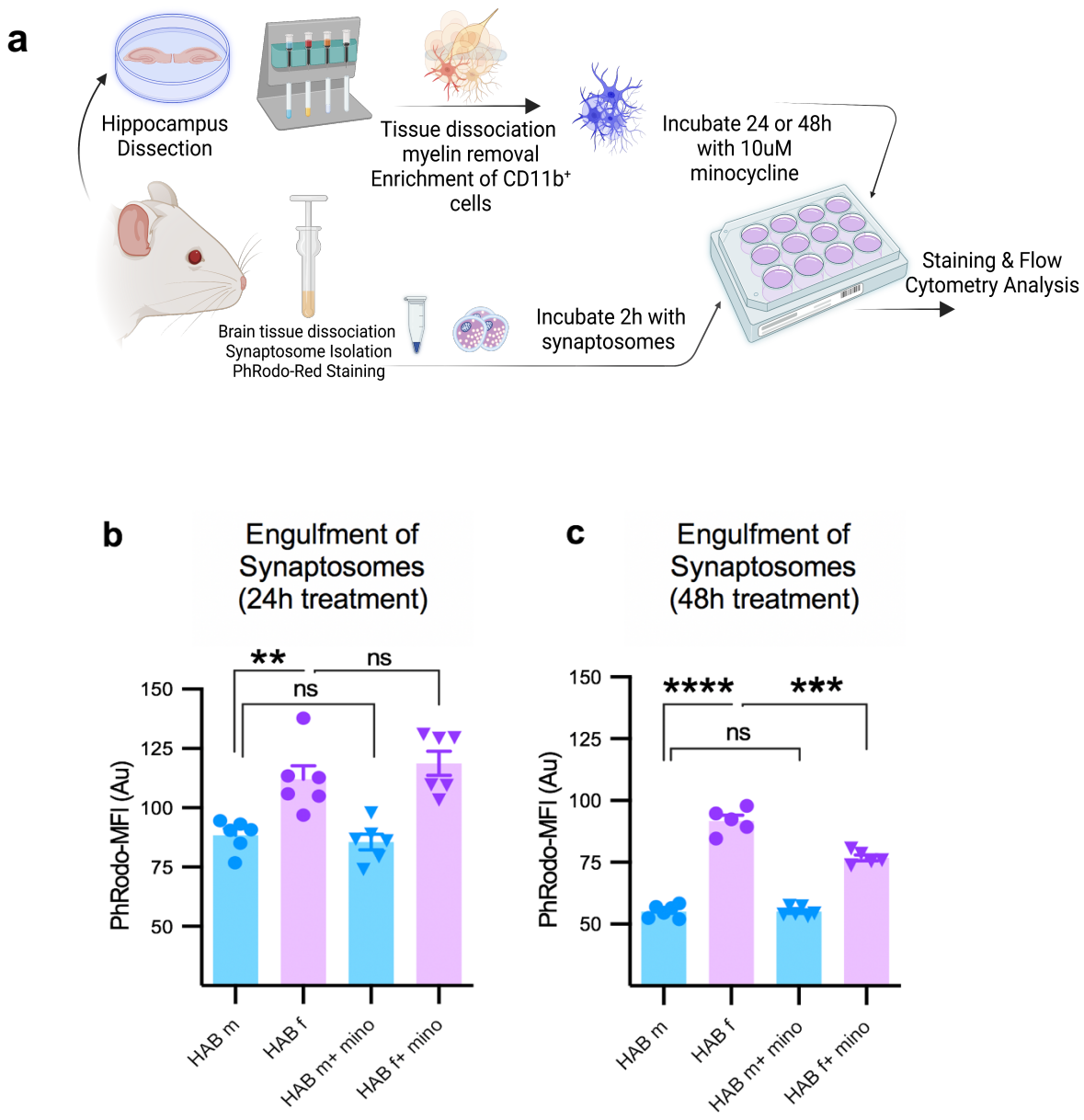

Figure 3B. 11 *In vitro minocycline treatment alleviates microglial over-engulfment of synaptosomes in the HAB female.*

(a) *Schematic representation of the experimental steps depicting in vitro minocycline treatment and the synaptosome engulfment assay (created by using biorender.com).*
(b) *HAB female microglia engulf more pHRodo^{TM} Red-labeled synaptosomes compared to HAB male after 24h in culture. In vitro minocycline treatment do not have any effect on total synaptosome engulfment by microglia. Engulfment ability of HAB male and female microglia was calculated by the pHRodo^{TM} Red -MFI signal of CD11b^{++}/CD45^{+}/Viable cells from the treated and untreated conditions (2-way ANOVA with Šídák's multiple comparisons test, $n^{HABmale}$=6, $n^{HABfemale}$=6, , $pAdj^{HABm/HABf}$= 0.007, $pAdj^{HABm/HABm\text{-}mino}$= 0.997, $pAdj^{HABf/HABf\text{-}mino}$= 0.852, $pAdj^{HABm\text{-}mino/HABf\text{-}mino}$=0.0003). Details of the experimental procedure are explained in the materials and methods section of the project A.*
(c) *HAB female microglia engulf more pHRodo^{TM}Red-labeled synaptosomes compared to HAB male after 48h in culture. In vitro minocycline treatment shows an effect on total synaptosome engulfment only on the HAB female microglia. Engulfment ability of the HAB male and female microglia was calculated by the pHRodo^{TM}Red-MFI signal of CD11b^{++}/CD45^{+}/Viable cells from the treated and untreated conditions (2-way ANOVA with Šídák's multiple comparisons test, $n^{HABmale}$=6, $n^{HABfemale}$=5, $pAdj^{HABm/HABf}$< 0.0001, $pAdj^{HABm/HABm\text{-}mino}$> 0.999, $pAdj^{HABf/HABf\text{-}mino}$< 0.0001, $pAdj^{HABm\text{-}mino/HABf\text{-}mino}$<0.0001. Data are represented as mean ± SEM, and each dot indicates one mouse; *P < 0.05; **P < 0.01; ***P < 0.001).*

Together, these findings indicate that HAB female microglia hold a higher potential to engulf vGLUT1^{+} excitatory synapses -*ex vivo*- and total synaptosomes -*in vitro*- compared to the HAB male microglia. We also provided evidence that both *in vitro* and *in vivo* minocycline treatments significantly alleviate this intrinsic state of higher engulfment of synapses by the HAB female microglia **(Figures 3B.10 and 3B.11)**.

3B.7. Serum 17β-Estradiol levels do not indicate a correlation with synaptic engulfment in the HAB and NAB females

We finally investigated the 17β -Estradiol (E2) levels in the serum samples of HAB and NAB females, whose brains were used in the vGLUT1-specific synaptic engulfment assay. Our data indicate no significant correlation between serum 17β -Estradiol levels and the microglial engulfment of vGLUT1^{+} synapses neither in NAB or in HAB females **(Figure 3B.12 a and b).** We also did not find any significant difference in the 17β-Estradiol levels in the HAB and NAB female serums. Therefore, we can also clarify that the HAB female-specific differences in synaptic engulfment reported in this study are not due to a possible effect of the Estrus cycle (**Figure 3B.12 c).**

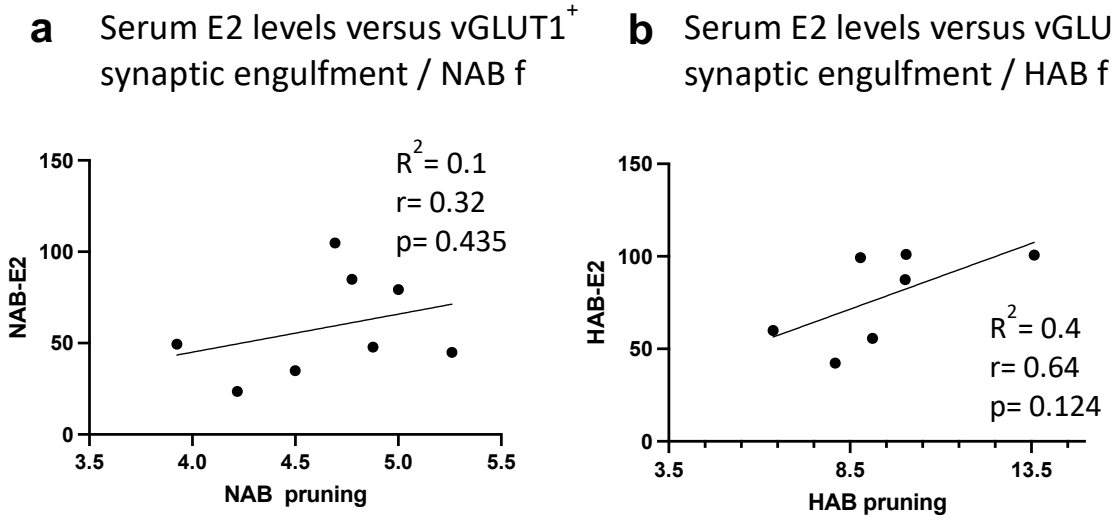

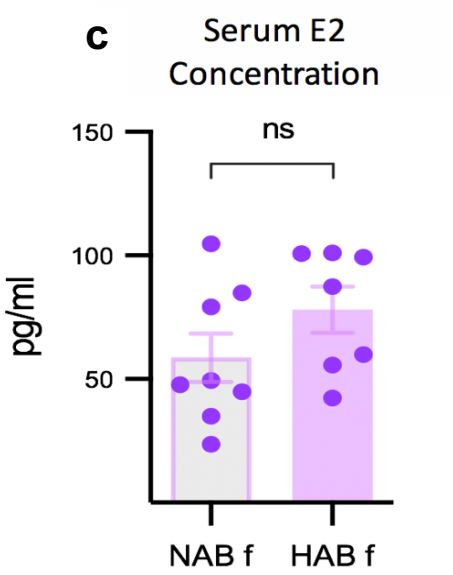

Figure 3B. 12 *HAB and NAB females do not show a difference in their levels of serum 17β -Estradiol..*

(a and b) *There is no significant correlation between microglial engulfment of vGLUT1⁺ synapses and serum 17β -Estradiol levels of the HAB and NAB females (Pearson correlation analysis; NAB female: R^2=0.1, r=0.32, p=0.435 ; n^{NABf} =8; HAB female: R^2=0.4, r=0.64, p=0.124, n^{HABf}=7).*

(c) *No significant difference was detected in the serum 17β -Estradiol levels of the HAB female and NAB female mice, whose brains were used for the vGLUT1-specific synaptic engulfment assay (Student's t test with Welch's correction, p=0.177, n^{HABf} =7, n^{NABf} =8. Data are represented as mean ± SEM, and each dot indicates one mouse; *P < 0.05; **P < 0.01; ***P < 0.001).*

4B DISCUSSION

Many psychiatric disorders, including anxiety and comorbid depression, exhibit sex-linked differences in their prevalence, clinical manifestation as well as at the cellular level (Bangasser & Valentino, 2014). Moreover, these differences are often associated with immune dysregulation and neural circuit alterations (Tubbs et al., 2020; Gasperzs et al., 2017; Ressler & Mayberg, 2007). Considering the critical role of microglia in immune response (Kettenmann et al., 2011) and synaptic refinement (Paolicelli et al., 2011; Schafer et al., 2012; Ji et al., 2013; Miyamato et al., 2016; Vainchtein & Molofsky, 2020); it is surprising that very few studies addressed sex-linked differences in microglial cells in the context of anxiety. To address this gap, this study presents three pertinent findings: 1) we report heterogeneity and sexual dimorphism of microglia at single-cell resolution in a context of innate high anxiety and comorbid depression. Microglia clusters bearing a prominent signature of synaptic engulfment and phagocytosis are enriched in the HAB female brain compared to the HAB male. We moreover found that genes related to synaptic engulfment such as *Trem2, C1qa, Cd68* show higher expression in HAB female in major microglia clusters compared to the HAB male. 2) We functionally supported these findings by demonstrating that the hippocampal microglia of HAB females engulf more vGLUT1^{+} excitatory synapses and total synaptosomes than those of HAB males. Our findings revealing altered synaptic engulfment by microglia are in line with other studies that found a link between altered brain connectivity and anxiety-like behavior (Kalin et al., 2017). Since alterations in the microglial pruning of excitatory synapses in the paraventricular nucleus of the hypothalamus (Bolton et al., 2022) and prefrontal cortex (Socodato et al., 2020) have been reported to be associated with anxiety-

related behavior; we focused on vGLUT1^{+} excitatory synapses at the outset of the study. Moreover, we showed that our findings are not specific to excitatory synapses but also valid for the engulfment of total synaptosomes by microglia. 3) We report that *in vitro* and *in vivo* minocycline treatment modulates synaptic engulfment by microglia, and in particular that the treatment significantly lowers the high engulfment of synapses by HAB female microglia.

Our data indicate that the MI cluster, in particular, holds a great capacity to modulate synapses and, therefore, could represent a promising cellular subset to target anxiety-associated alterations in the HAB female brain. The MII and MIII clusters, on the other hand, represent a state quite opposite to that of MI by showing lower expression of genes related to synaptic engulfment (*Trem2, C1qb, C1qc, Cd68*), as well as homeostasis (*Hexb, Tmem119, P2ry12*). The higher expression of *Trem2, Tyrobp, Cd9, Spp1, Ccl3,* and *Ccl4* in the MIV cluster indicates similarities to the previously reported disease-associated microglia (DAM) signature, which originally is associated with Alzheimer's disease (AD) models (Keren-Shaul et al.2017). However, such signatures should be cautiously assessed since the definitions of different microglial states or clusters are highly context-dependent. Microglia display diverse states and responses based on the signals they receive from their microenvironment (Hanisch & Kettenmann, 2007). These states can be represented by a variety of transcriptional changes that do not always correspond to a function (Paolicelli et al., 2022). For instance, downregulation of *P2ry12, Tmem119*, *Hexb* as shown in the MIII cluster, has been linked to a particular microglia state called white matter-associated microglia (WAM) in the Alzheimer context as well as regarded as an activated state of microglia (Safaiyan et al., 2021; Masuda et al., 2020). However, these core microglia marker genes are also under regulation of various signals, and do not show a steady expression (Paolicelli et al., 2022). Therefore, changes in

their expression levels are not always sufficient for defining a similar microglial state in the context of anxiety, unless it is functionally validated. Their lower expression in one context may suggest myelin debris clearance (Safaiyan et al., 2021), while in another, it may indicate a physiological state based on the cues received from the microenvironment. For this reason, we refrain from relating these clusters to those observed in earlier publications in the context of different diseases.

We found many genes upregulated in the HAB female compared to the HAB male, particularly in the MIII cluster, and they point to regulation of critical pathways, including '*regulation of immune response'*, '*synaptic pruning'*, '*microglial activation', and 'neurogenesis'*. Among these pathways, the current study particularly focused on the synaptic engulfment by microglia, since it holds a strong potential to modulate synapses. According to autopsy reports (Zhao et al., 2012; Duric et al., 2013) and functional magnetic resonance imaging (fMRI) studies (Zeng et al., 2012), patients with depression and comorbid anxiety showed altered brain connectivity, particularly synapse loss. Additionally, preclinical research has also indicated synapse loss in depression and anxiety context due to high microglial engulfment of synapses (Han et al., 2022). The high microglial engulfment of synapses presented here could as well potentially drive the loss of synapses, which remains to be investigated.

Although females have been repeatedly reported to have a higher prevalence of anxiety-related disorders (McLean et al., 2011; Kessler et al., 2012; Moser et al., 2016; Strand et al., 2021), pre-clinical research mostly relies on data from males. Sex-linked differences in microglia have been reported by several groups, in contexts of both health (Hanamsagar et al., 2017; Guneykaya et al., 2018; Villa et al., 2018) and disease (Kalm et al., 2013; Acaz-

Fonseca et al., 2015; Bodhankar et al., 2015; Kodama & Gan, 2019). Such differences in the context of innate high anxiety have largely remained unexplored, but studies have shown that chronic stress exerts different effects on male and female microglia (Wohleb et al., 2018; Bollinger, 2021). The significance of these findings lies in the fact that chronic stress has been implicated as a profound risk factor for anxiety- and depression-related behavior (Conrad et al., 2011; Bouter et al., 2020). It also alters the microglia morphology and the expression of immunoregulatory factors by microglia differently in males and females (Bollinger, 2021). Furthermore, Wohleb et al. (2018) reported enhanced microglial engulfment of synapses in the medial prefrontal cortex of male mice, but not female, in response to chronic high stress. As sentinels of the CNS, microglia are overly sensitive to signals from their surroundings (Kettenmann et al., 2011; Kettenmann, Kirchhoff & Verkhratsky, 2013). Chronic stress is also known to alter neural activity (Wilber et al., 2011), which can be detected by microglia and could drive potential pruning-associated consequences in the stress-induced anxiety models. Similarly, it has been shown that HAB mice display changes in basal neurotransmission at the ventral CA3-CA1 synapses of the hippocampus (Dine et al., 2015), which could have a potential impact on microglia-mediated synaptic pruning. Yet, that particular study investigated only male mice and we were unable to detect a functional phenotype in the HAB male microglia in terms of the engulfment of synapses. HAB females, on the other hand, show an evident phenotype of synaptic over-engulfment compared to HAB male and NAB female. Another study that exclusively focused on HAB female mice found that high innate anxiety with comorbid depression and anhedonia was accompanied by a lower rate of neurogenesis and impairments in the functional integration of newly generated neurons in the hippocampus (Sah et al., 2012). We add to these observations by reporting elevated engulfment of synapses by HAB female microglia, and hypothesize that microglia with an over-reactive state of

synaptic engulfment could have an impact on integration of newly born neurons in the HAB female hippocampus. These findings are also in parallel with clinical data reporting decreased hippocampal connectivity and volume in patients with depression (Campbell et al., 2004; Ge et al., 2019).

Given that our findings on synaptic engulfment are female-specific, what would be the ground for explaining these sex differences? Gonadal hormones appear to have a role to drive some of these sex differences (Bollinger et al.,2019; 2021). Receptors for glucocorticoid (GC), estrogen, and androgen are expressed on microglia, which makes them responsive to variations and fluctuations in these hormonal signals (Sierra et al.,2008; Carrillo-de Sauvage et al.,2013; Horchar & Wohleb, 2019). Hormones have a crucial role in mediating sex-specific neural (Garrett et al.,2009; Shansky et al.,2010) and microglial responses (Bollinger et al.,2019). In a very intriguing study, Caetano et al. (2017) used prenatal exposure to GC to induce high anxiety behavior in male and female rats, and they found that microglia in the mPFC exhibit sexually dimorphic morphology, with females having less complex morphology and males having hyper-ramified morphology. When an experimental anxiolytic adenosine A2AR agonist was administered to these rats, the males showed a drop in anxiety, and the hyper-ramified morphology of male microglia was also restored, while there was no effect on either behavior or microglial morphology in females (Caetano et al.,2017). This study reports striking sex differences in morphology of microglia and their response to stimuli, even though there were no sex-linked differences detected in the high anxiety behavior of males and females, which both exhibited elevated anxiety compared to normal controls (Caetano et al.,2017). Likewise, no behavioral differences were detected between HAB males and females using classical behavioral tests to assess anxiety-like behavior, such as the elevated plus maze

(EPM) and light-dark test (LD) (Sartori & Ugursu, 2022; unpublished data). These classical tests demonstrate certain limitations, which include introducing a novel environment and inducing a stress response (Bailey et al., 2009; Börchers et al., 2022). Several studies have revealed some sex-linked differences with varying results amongst tests and shown deviations from human findings, indicating that these classical tests have poor predictive power for both detecting rodent sex differences and for reflecting human findings (Börchers et al., 2022; Lee et al., 2022). Such tests may also understate sex-related differences, particularly in females, because most of them were validated only in males (Donner& Lowry, 2013; Börchers et al., 2022). This means that our findings at the cellular and molecular level might have numerous different behavioral manifestations, whose detection calls for more comprehensive behavioral tests such as 3D spontaneous behavior mapping (Huang et al., 2021). However, such in depth behavioral characterization was not within the scope of the current study.

Microglia are critical players in the organization of neural circuits through phagocytosis of synapses mainly via fractalkine receptor (CX3CR1), complement receptor 3 (CR3), and the triggering receptor expressed on myeloid cells 2 (TREM2) (Paolicelli et al., 2011; Filipello et al., 2018; Furusawa & Emoto, 2020; Qin et al., 2022). These three signaling pathways have been widely reported to modulate microglial engulfment of synapses in different brain regions. Liu et al. (2020) reported that CX3CR1-CX3CL1 signaling is associated with depressive-like behavior, anxiety and anhedonia. It has also been shown that TREM2 signaling is necessary for a functional synapse elimination by microglia (Filipello et al., 2018). Similarly, C3-deficient mice display an excessive number of synapses and resilience to anxiety, confirming the role of C1q-C3-CR3 axis in synaptic pruning (Stevens et al.,2007; Furusawa & Emoto, 2020) and depressive-like behavior (Crider et al., 2018). While these observations are

not specifically focused on the context of innate high anxiety, they support our functional findings indicating the higher engulfment of synapses by female HAB microglia, which express higher surface levels of TREM2, CR3 and CX3CR1 than HAB male microglia. We therefore hypothesize that these signaling pathways might contribute to driving the reported functional differences in microglia in the hippocampus of HAB mice.

Several studies have shown that minocycline, a lipophilic broad-spectrum antibiotic, ameliorates stress-induced anxiety in rodent models (Molina-Hernández et al., 2008; Levkovitz et al., 2015; Liu et al., 2018; Wang et al., 2018; Zhang, Kalueff & Song, 2019). Moreover, it has been shown that minocycline exerts unspecific, complex effects on microglia, resulting in changes in cellular density, morphology, and reactivity in a context-dependent manner (Yrjänheikki et al., 1998; Strahan et al., 2017; Mattei et al., 2017; Wang et al., 2017; 2018). It crosses the blood-brain barrier (Garrido-Mesa, Zarzuelo, & Gálvez, 2013), and has been clinically tested on patients with major depressive disorder and anxiety with promising results (Dean et al.,2017; Zazula et al., 2021). Rooney et al. (2020) reported the anxiolytic effects of minocycline on HAB male mice after 28 days of systemic administration. They also reported that the treatment reduced the density of $CD68^{+}$ microglia in the dentate gyrus of the hippocampus, and concluded that minocycline modulates the phagocytic potential of microglia. In addition to these findings, we herein provide functional data showing that hippocampal HAB female microglia engulf more synapses compared to the HAB male and NABs, which was reduced in response to the minocycline treatment. On the other hand, HAB male microglia neither exhibited differences in phagocytosis compared to NABs, nor responded to the minocycline treatment. We underline that phagocytic potential does not only concern the synaptic engulfment, but also the engulfment of apoptotic and necrotic

cells (Green, Oguin & Martinez, 2016), bacteria and viruses (Nau et al., 2014), neural precursors (Sierra et al.,2010), and amyloid plaques (Huang et al.,2021). Therefore; phagocytosis of other targets cannot be ruled out, even though a significant difference in the microglial engulfment of synapses was not observed in the HAB male. Given that a higher percentage of $CD68^{+}$ microglia was detected in the HAB male hippocampus (Rooney et al.2020), future studies should test the phagocytosis of other potential targets by HAB microglia.

Interestingly, Han et al. (2022) recently reported higher engulfment of synapses by microglia in the hippocampus of a chronic social defeat stress (CSDS)-induced mouse model of depression. They further showed that minocycline suppressed the higher microglial engulfment of synapses (Han et al., 2022), which is strikingly parallel to our findings. In a different study using the poly(I:C) model for schizophrenia, the effect of minocycline treatment was again demonstrated to functionally restore microglial phagocytosis to the normal levels in the hippocampus (Mattei et al., 2017). These results, albeit in different contexts, point to a potential impact of minocycline on microglial phagocytosis, which we also reported in the present study.

In the absence of a stressor, genetic modification or immune challenge; our mouse model allowed us to obtain a thorough understanding of the microglial heterogeneity in the context of innate high anxiety and comorbid depression. We herein provide an overview of the microglia phenotype in a sexually dimorphic manner and present evidence of higher synaptic engulfment by microglia in the HAB female brain. These findings suggest microglial

engulfment of synapses as a critical potential target, which can be addressed by minocycline treatment. We further underline the necessity of including both sexes in the anxiety research given the known differences in terms of risk and prevalence, as well as the sex-linked differences we have reported in microglia phenotype and function. Our findings establish a foundation for future studies that will focus on sexual dimorphism regarding the interplay of microglia and synapses as well as the modulatory effects of minocycline.

5 CONCLUSIONS

5.1 The Role of Microglial Engulfment of Synapses and TREM2 in Murine Models of Psychiatric Symptoms

Using a range of technical approaches in two independent projects employing different mouse models, I herein report two convergent findings in the contexts of innate high anxiety & depression and autism. The first is the dysregulated microglial engulfment of synapses in both mouse models. It is impaired in the *Nlgn4*-KO, only in males; while it is excessive in the HAB model, only in females. These findings point to a sex-specific difference, which interestingly is in parallel with the prevalence of anxiety and autism (Hodges et al., 2020; Strand et al., 2021). Both impaired and excessive engulfment of synapses by microglia hold a great potential to alter synaptic networks, and impact behavior (Tay et al., 2017). Clinical studies already indicate altered brain connectivity in autism (Wass 2011; Gao & Penzes, 2015) as well as in anxiety and depression (Kalin et al., 2017), which are in line with our findings. Therefore, the reported microglial dysregulations in both models can serve as promising targets in future studies to investigate and modulate interaction of microglia with synapses.

The second convergent finding is the regulation of TREM2 expression by microglial cells. Interestingly, I reported lower surface expression of TREM2 in the *Nlgn4*-KO hippocampus compared to the WT, whereas higher expression of it in the HAB female compared to the HAB male, as well as NAB female. Moreover, changes in the TREM2 levels also reflect the functional changes regarding the altered engulfment of synapses by microglia in both mouse models. Therefore, I propose that microglial surface TREM2 levels can be a useful biomarker to monitor potential changes in microglial engulfment of synapses in these mouse models,

and that TREM2 signaling represents a promising target for different murine models of psychiatric disorders due to its high potential to affect synaptic networks, as well as behavior.

With the knowledge and awareness that synaptic engulfment by microglia is not the only microglial dysregulation in these psychiatric models, I report a striking association between this microglial function and clinical findings, as well as the prevalence studies. This dissertation provides a foundation for future research focusing more on the interplay of microglia and synapses, especially the role of TREM2 signaling, in the context of psychiatric diseases. I moreover highlight the sexual dimorphism at the cellular level, in both models, thus emphasizing the importance of including both sexes in studies given that female-oriented studies are largely neglected in preclinical psychiatric research.

To summarize,

1. I propose TREM2 as a potential mediator, among others, to modulate microglial engulfment of synapses in the hippocampus of both HAB and *Nlgn4*-KO mouse models.
2. I add to existing literature another form of microglial dysregulation in the preclinical models of psychiatric disorders (Steiner et al., 2008; Morgan et al., 2010; Sominsky et al., 2012; Torres-Platas et al., 2014; Wohleb et al., 2017; Mattei et al., 2017; Tay et al., 2017; Ozaki et al., 2020; Hayes et al., 2021; Guneykaya et al., 2023). I suggest that dysregulated synaptic engulfment by microglia represents a promising target in psychiatric disorders, since it has a potential to affect synaptic connectivity and behavior.

3. I report striking sex differences in both models at the cellular level, and emphasize importance of including both sexes in studies, at least before focusing further on a certain dysregulation only in the affected sex.
4. In this dissertation; expression of many different genes and proteins were elaborately studied to obtain a hint for a dysregulated microglial function. Our results support that differences in the expression of certain genes as well as proteins are not always reflected on the respective functions. Considering the amount of research in the field relying solely on changes in the expression levels of certain markers to state functional effects, our findings highlight the importance of their functional validation.

5.2 Limitations of the Study and Future Prospects

In the first project (**A**), in which I studied the context of autism; I have reported lower engulfment of vGLUT1^{+} excitatory synapses and total synaptosomes by microglia. However, I was not able to report the engulfment of GABAergic inhibitory synapses due to technical limitations. Considering the decreased GABAergic synaptic transmission in the *Nlgn4*-KO hippocampus (Hammer et al., 2015); it would have been neat to report as well the engulfment of GABAergic synapses, since microglial engulfment of synapses is indeed affected by changes in the neural transmission (Trembley et al., 2010; Schafer et al., 2012; Wu et al., 2015). However, the commercial flow cytometry antibodies I have tested for this purpose did not work to detect inhibitory synaptic markers inside microglia. We will focus on this part in future studies by using other technical approaches such as immunohistochemistry and imaging.

The second limitation of this study is that I did not reveal the consequence of the dysregulated microglial engulfment of synapses on overall synaptic connectivity in the *Nlgn4-KO* model due to technical limitations. The gold standard would be to perform a synaptic spine density analysis to examine such potential consequences in the *Nlgn4*-KO brain. We will focus on this aspect in future studies to complement our findings more comprehensively. In addition to these future prospects, we will also manipulate NL4 levels by lentiviral transduction of shRNA targeting *Nlgn4* in WT hippocampal organotypic brain slices to test the direct effect of NL4 levels on the enzymatic activity of ADAM10. Overall, these experiments will broaden our understanding of the interplay of microglia and synapses by focusing on the role of ADAM10, NL4, and TREM2 in the *Nlgn4*-KO brain.

Astrocytes also play a key role in synaptic refinement, and more importantly, they express neuroligins and neurexins at high levels (Tan & Eroglu, 2021). Therefore, in depth characterization of astrocytes is also another future research prospect, which will be highly complementary to understand the direct effect of NL4 loss on astrocyte function as well as on the crosstalk of microglia and astrocytes at synaptic junctions.

In the second project (**B**), in which I studied the context of high anxiety and comorbid depression, I reported striking sex-linked differences in microglial heterogeneity and synaptic engulfment. However, I did not report the behavioral consequences of these differences at the cellular level due to technical limitations. HAB male and HAB female mice already show higher levels of anxiety compared to the sex-matching NABs (Sah et al., 2012; Rooney et al., 2020). Detecting sex-specific differences between HAB male and HAB female mice, considering their existing high levels of innate anxiety, requires more sophisticated behavioral

tests rather than the classical approaches such as EPM. Investigating the behavioral translation of our cellular findings will be the focus of future studies. Similar to the autism project (**A**), I also aim to report the consequence of dysregulated microglial engulfment of synapses on overall synaptic connectivity in the HAB brains in future studies. Another limitation concerns the effect of minocycline on microglia, which I reported both *in vivo* and *in vitro*. However, I did not outline the mechanism of action through which minocycline modulates the synaptic engulfment by microglia. In future studies, I will focus on this aspect to specifically report the effects of minocycline on different signaling pathways that regulate synaptic engulfment by microglia to better understand its specific targets and the mechanism of action.

6 REFERENCES

Aarum, J., Sandberg, K., Haeberlein, S. L., & Persson, M. A. (2003). Migration and differentiation of neural precursor cells can be directed by microglia. *Proceedings of the National Academy of Sciences of the United States of America*, *100*(26), 15983–15988. https://doi.org/10.1073/pnas.2237050100

Acaz-Fonseca, E., Duran-Carabali, L. E., & Delevatti, R. S. (2015). Sex differences in glia reactivity after cortical brain injury. Glia, 63(11), 1966–1981. https://doi.org/10.1002/glia.22867.

Agid, O., Shapira, B., Zislin, J., Ritsner, M., Hanin, B., Murad, H., Troudart, T., Bloch, M., Heresco-Levy, U., & Lerer, B. (1999). Environment and vulnerability to major psychiatric illness: a case control study of early parental loss in major depression, bipolar disorder and schizophrenia. *Molecular psychiatry*, *4*(2), 163–172. https://doi.org/10.1038/sj.mp.4000473

Amaral, D. G., Schumann, C. M., & Nordahl, C. W. (2008). Neuroanatomy of autism. *Trends in neurosciences*, *31*(3), 137–145. https://doi.org/10.1016/j.tins.2007.12.005

American Psychiatric Association. (2013). Diagnostic and Statistical Manual of Mental Disorders. 5th Ed. American Psychiatric Association. https://doi.org/10.1176/appi.books.9780890425596

Anderson, G.R., Aoto, J., Tabuchi, K., Fo¨ ldy, C., Covy, J., Yee, A.X., Wu, D., Lee, S.J., Chen, L., Malenka, R.C., and Su¨dhof, T.C. (2015). b-Neurexins Control Neural Circuits by Regulating Synaptic Endocannabinoid Signaling. *Cell*, 162, 593–606. DOI: 10.1016/j.cell.2015.06.056.

Aoto, J., Martinelli, D.C., Malenka, R.C., Tabuchi, K., and Südhof, T.C. (2013). Presynaptic neurexin-3 alternative splicing trans-synaptically controls post-synaptic AMPA receptor trafficking. *Cell*, 154, 75–88. DOI: 10.1016/j.cell.2013.05.060.

Asperger H. (1944) Asperger: Die Autistischen Psychopaten in Kindesalter.

Atladóttir, H. O., Thorsen, P., Østergaard, L., Schendel, D. E., Lemcke, S., Abdallah, M., & Parner, E. T. (2010). Maternal infection requiring hospitalization during pregnancy and autism spectrum disorders. *Journal of autism and developmental disorders*, *40*(12), 1423–1430. https://doi.org/10.1007/s10803-010-1006-y

Babagana, M., Oh, K. S., Chakraborty, S., Pacholewska, A., Aqdas, M., & Sung, M. H. (2021). Hedgehog dysregulation contributes to tissue-specific inflammaging of resident macrophages. *Aging*, *13*(15), 19207–19229. https://doi.org/10.18632/aging.203422

Bailey, K. R., & Crawley, J. N. (2009). Anxiety-Related Behaviors in Mice. In J. J. Buccafusco (Ed.), *Methods of Behavior Analysis in Neuroscience*. (2nd ed.). CRC Press/Taylor & Francis.

Bangasser, D. A., & Valentino, R. J. (2014). Sex differences in stress-related psychiatric disorders: Neurobiological perspectives. Frontiers in Neuroendocrinology, 35(3), 303–319. https://doi.org/10.1016/j.yfrne.2014.03.008.

Bayer, T. A., Buslei, R., Havas, L., & Falkai, P. (1999). Evidence for activation of microglia in patients with psychiatric illnesses. *Neuroscience letters*, *271*(2), 126–128. https://doi.org/10.1016/s0304-3940(99)00545-5

Bemben, M. A., Shipman, S. L., Nicoll, R. A., & Roche, K. W. (2015). The cellular and molecular landscape of neuroligins. *Trends in neurosciences*, *38*(8), 496–505. https://doi.org/10.1016/j.tins.2015.06.004

Blinzinger, K., & Kreutzberg, G. (1968). Displacement of synaptic terminals from regenerating motoneurons by microglial cells. *Zeitschrift fur Zellforschung und mikroskopische Anatomie (Vienna, Austria : 1948)*, *85*(2), 145–157. https://doi.org/10.1007/BF00325030

Blundell, J., Blaiss, C. A., Etherton, M. R., Espinosa, F., Tabuchi, K., Walz, C., Bolliger, M. F., Südhof, T. C., & Powell, C. M. (2010). Neuroligin-1 deletion results in impaired spatial memory and increased repetitive behavior. *The Journal of neuroscience : the official journal of the Society for Neuroscience*, *30*(6), 2115–2129. https://doi.org/10.1523/JNEUROSCI.4517-09.2010

Bodhankar, S., Chen, Y., Vandenbark, A. A., & Murphy, S. J. (2015). Role for microglia in sex differences after ischemic stroke: Importance of M2. Metabolic Brain Disease, 30(6), 1515–1529. https://doi.org/10.1007/s11011-015-9714-9.

Boksa P. (2010). Effects of prenatal infection on brain development and behavior: a review of findings from animal models. *Brain, behavior, and immunity*, *24*(6), 881–897. https://doi.org/10.1016/j.bbi.2010.03.005

Bolliger, M. F., Pei, J., Maxeiner, S., Boucard, A. A., Grishin, N. V., & Südhof, T. C. (2008). Unusually rapid evolution of Neuroligin-4 in mice. *Proceedings of the National Academy of Sciences of the United States of America*, *105*(17), 6421–6426. https://doi.org/10.1073/pnas.0801383105

Bollinger, J. L. (2021). Uncovering microglial pathways driving sex-specific neurobiological effects in stress and depression. Brain, Behavior, & Immunity - Health, 16, 100320. https://doi.org/10.1016/j.bbih.2021.100320.

Bollinger, J. L., Salinas, I., Fender, E., Sengelaub, D. R., & Wellman, C. L. (2019). Gonadal hormones differentially regulate sex-specific stress effects on glia in the medial prefrontal cortex. *Journal of neuroendocrinology*, *31*(8), e12762. https://doi.org/10.1111/jne.12762

Bolton, J. L., Short, A. K., Othy, S., Kooiker, C. L., Shao, M., Gunn, B. G., Beck, J., Bai, X., Law, S. M., Savage, J. C., Lambert, J. J., Belelli, D., Tremblay, M. È., Cahalan, M. D., & Baram, T. Z. (2022). Early stress-induced impaired microglial pruning of excitatory synapses on immature CRH-expressing neurons provokes aberrant adult stress responses. *Cell reports*, *38*(13), 110600. https://doi.org/10.1016/j.celrep.2022.110600

Borcel, E., Palczynska, M., Krzisch, M., Dimitrov, M., Ulrich, G., Toni, N., & Fraering, P. C. (2016). Shedding of neurexin 3β ectodomain by ADAM10 releases a soluble fragment that affects the development of newborn neurons. *Scientific reports*, *6*, 39310. https://doi.org/10.1038/srep39310

Börchers, S., Krieger, J. P., Asker, M., Maric, I., & Skibicka, K. P. (2022). Commonly-used rodent tests of anxiety-like behavior lack predictive validity for human sex differences. *Psychoneuroendocrinology*, *141*, 105733. https://doi.org/10.1016/j.psyneuen.2022.105733

Bourgeois, J. P., & Rakic, P. (1993). Changes of synaptic density in the primary visual cortex of the macaque monkey from fetal to adult stage. The Journal of Neuroscience, 13, 2801-2820. https://doi.org/10.1523/JNEUROSCI.13-07-02801.1993

Bourne, J. N., & Harris, K. M. (2008). Balancing structure and function at hippocampal dendritic spines. *Annual Review of Neuroscience, 31*, 47-67. doi: 10.1146/annurev.neuro.31.060407.125646

Bouter, Y., Lopez-Canul, M., Coenen, A. M. L., & Mansouri, F. A. (2020). Chronic psychosocial stress causes increased anxiety-like behavior and alters endocannabinoid levels in the brain of C57Bl/6J mice. Cannabis and Cannabinoid Research, 5(1), 51–61. https://doi.org/10.1089/can.2019.0041.

Brioschi, S., d'Errico, P., Amann, L. S., Janova, H., Wojcik, S. M., Meyer-Luehmann, M., Rajendran, L., Wieghofer, P., Paolicelli, R. C., & Biber, K. (2020). Detection of Synaptic Proteins in Microglia by Flow Cytometry. *Frontiers in molecular neuroscience*, *13*, 149. https://doi.org/10.3389/fnmol.2020.00149

Brown A. S. (2012). Epidemiologic studies of exposure to prenatal infection and risk of schizophrenia and autism. *Developmental neurobiology*, *72*(10), 1272–1276. https://doi.org/10.1002/dneu.22024

Brown, A. S., Begg, M. D., Gravenstein, S., Schaefer, C. A., Wyatt, R. J., Bresnahan, M., Babulas, V. P., & Susser, E. S. (2004). Serologic evidence of prenatal influenza in the etiology of schizophrenia. *Archives of general psychiatry*, *61*(8), 774–780. https://doi.org/10.1001/archpsyc.61.8.774

Brown, G. C., & Neher, J. J. (2014). Microglial phagocytosis of live neurons. *Nature reviews. Neuroscience*, *15*(4), 209–216. https://doi.org/10.1038/nrn3710

Brown, G. C., & St George-Hyslop, P. (2022). Does Soluble TREM2 Protect Against Alzheimer's Disease?. *Frontiers in aging neuroscience*, *13*, 834697. https://doi.org/10.3389/fnagi.2021.834697

Bruttger, J., Karram, K., Wörtge, S., Regen, T., Marini, F., Hoppmann, N., Klein, M., Blank, T., Yona, S., Wolf, Y., Mack, M., Pinteaux, E., Müller, W., Zipp, F., Binder, H., Bopp, T., Prinz, M., Jung, S., & Waisman, A. (2015). Genetic Cell Ablation Reveals Clusters of Local Self-Renewing Microglia in the Mammalian Central Nervous System. *Immunity*, *43*(1), 92–106. https://doi.org/10.1016/j.immuni.2015.06.012

Budreck, E. C., & Scheiffele, P. (2007). Neuroligin-3 is a neuronal adhesion protein at GABAergic and glutamatergic synapses. *The European journal of neuroscience*, *26*(7), 1738–1748. https://doi.org/10.1111/j.1460-9568.2007.05842.x

Budreck, E. C., Kwon, O. B., Jung, J. H., Baudouin, S., Thommen, A., Kim, H. S., Fukazawa, Y., Harada, H., Tabuchi, K., Shigemoto, R., Scheiffele, P., & Kim, J. H. (2013). Neuroligin-1 controls synaptic abundance of NMDA-type glutamate receptors through extracellular coupling. *Proceedings of the National Academy of Sciences of the United States of America*, *110*(2), 725–730. https://doi.org/10.1073/pnas.1214718110

Burton, S. D., Johnson, J. W., Zeringue, H. C., & Meriney, S. D. (2012). Distinct roles of neuroligin-1 and SynCAM1 in synapse formation and function in primary hippocampal neuronal cultures. *Neuroscience*, *215*, 1–16. https://doi.org/10.1016/j.neuroscience.2012.04.047

Butovsky, O., Jedrychowski, M. P., Cialic, R., Krasemann, S., Murugaiyan, G., Fanek, Z., Greco, D. J., Wu, P. M., Doykan, C. E., Kiner, O., Lawson, R. J., Frosch, M. P., Pochet, N., Fatimy, R. E., Krichevsky, A. M., Gygi, S. P., Lassmann, H., Berry, J., Cudkowicz, M. E., & Weiner, H. L. (2015). Targeting miR-155 restores abnormal microglia and attenuates disease in SOD1 mice. *Annals of neurology*, *77*(1), 75–99. https://doi.org/10.1002/ana.24304

Butz, S., Okamoto, M., & Südhof, T. C. (1998). A tripartite protein complex with the potential to couple synaptic vesicle exocytosis to cell adhesion in brain. *Cell*, *94*(6), 773–782. https://doi.org/10.1016/s0092-8674(00)81736-5

Yuen, R. K., Merico, D., Bookman, M., L Howe, J., Thiruvahindrapuram, B., Patel, R. V., Whitney, J., Deflaux, N., Bingham, J., Wang, Z., Pellecchia, G., Buchanan, J. A., Walker, S., Marshall, C. R., Uddin, M., Zarrei, M., Deneault, E., D'Abate, L., Chan, A. J., Koyanagi, S., … Scherer, S. W. (2017). Whole genome sequencing resource identifies 18 new candidate genes for autism spectrum disorder. *Nature neuroscience*, *20*(4), 602–611. https://doi.org/10.1038/nn.4524

Caetano, L., Pinheiro, H., Patrício, P., Mateus-Pinheiro, A., Alves, N. D., Coimbra, B., Baptista, F. I., Henriques, S. N., Cunha, C., Santos, A. R., Ferreira, S. G., Sardinha, V. M., Oliveira, J. F., Ambrósio, A. F., Sousa, N., Cunha, R. A., Rodrigues, A. J., Pinto, L., & Gomes, C. A. (2017). Adenosine A_{2A} receptor regulation of microglia morphological remodeling-gender bias in

physiology and in a model of chronic anxiety. *Molecular psychiatry*, *22*(7), 1035–1043. https://doi.org/10.1038/mp.2016.173

Cajal S. (1913). Un nuevo proceder para la impregnación de la neuroglía. *Bol. Soc. Esp. Bio.* 2, 104–108

Campbell, S., Marriott, M., Nahmias, C., & MacQueen, G. M. (2004). Lower hippocampal volume in patients suffering from depression: a meta-analysis. *The American journal of psychiatry*, *161*(4), 598–607. https://doi.org/10.1176/appi.ajp.161.4.598

Careaga, M., Van de Water, J., & Ashwood, P. (2010). Immune dysfunction in autism: a pathway to treatment. *Neurotherapeutics : the journal of the American Society for Experimental NeuroTherapeutics*, *7*(3), 283–292. https://doi.org/10.1016/j.nurt.2010.05.003

Carrillo-de Sauvage, M. Á., Maatouk, L., Arnoux, I., Pasco, M., Sanz Diez, A., Delahaye, M., Herrero, M. T., Newman, T. A., Calvo, C. F., Audinat, E., Tronche, F., & Vyas, S. (2013). Potent and multiple regulatory actions of microglial glucocorticoid receptors during CNS inflammation. *Cell death and differentiation*, *20*(11), 1546–1557. https://doi.org/10.1038/cdd.2013.108

Casanova, M. F., Buxhoeveden, D. P., Switala, A. E., & Roy, E. (2002). Minicolumnar pathology in autism. *Neurology*, 58(3), 428-432. https://doi.org/10.1212/WNL.58.3.428

Casanova, M. F., van Kooten, I. A., Switala, A. E., van Engeland, H., Heinsen, H., Steinbusch, H. W., Hof, P. R., Trippe, J., Stone, J., & Schmitz, C. (2006). Minicolumnar abnormalities in autism. *Acta neuropathologica*, *112*(3), 287–303. https://doi.org/10.1007/s00401-006-0085-5

Chanda, S., Hale, W. D., Zhang, B., Wernig, M., & Südhof, T. C. (2017). Unique versus Redundant Functions of Neuroligin Genes in Shaping Excitatory and Inhibitory Synapse Properties. *The Journal of neuroscience : the official journal of the Society for Neuroscience*, *37*(29), 6816–6836. https://doi.org/10.1523/JNEUROSCI.0125-17.2017

Chaudhry, I. B., Hallak, J., Husain, N., Minhas, F., Stirling, J., Richardson, P., Dursun, S., Dunn, G., & Deakin, B. (2012). Minocycline benefits negative symptoms in early schizophrenia: a randomised double-blind placebo-controlled clinical trial in patients on standard treatment. *Journal of psychopharmacology (Oxford, England)*, *26*(9), 1185–1193. https://doi.org/10.1177/0269881112444941

Chen, L. Y., Jiang, M., Zhang, B., Gokce, O., & Südhof, T. C. (2017). Conditional Deletion of All Neurexins Defines Diversity of Essential Synaptic Organizer Functions for Neurexins. *Neuron*, *94*(3), 611–625.e4. https://doi.org/10.1016/j.neuron.2017.04.011

Chen, S. K., Tvrdik, P., Peden, E., Cho, S., Wu, S., Spangrude, G., & Capecchi, M. R. (2010). Hematopoietic origin of pathological grooming in Hoxb8 mutant mice. *Cell*, *141*(5), 775–785. https://doi.org/10.1016/j.cell.2010.03.055

Chih, B., Afridi, S. K., Clark, L., & Scheiffele, P. (2004). Disorder-associated mutations lead to functional inactivation of neuroligins. *Human molecular genetics*, *13*(14), 1471–1477. https://doi.org/10.1093/hmg/ddh158

Chih, B., Engelman, H., & Scheiffele, P. (2005). Control of excitatory and inhibitory synapse formation by neuroligins. *Science, 307*, 1324-1328. doi: 10.1126/science.1107470

Chocholska, S., Rossier, E., Barbi, G., & Kehrer-Sawatzki, H. (2006). Molecular cytogenetic analysis of a familial interstitial deletion Xp22.2-22.3 with a highly variable phenotype in female carriers. *American journal of medical genetics. Part A*, *140*(6), 604–610. https://doi.org/10.1002/ajmg.a.31145

Chubykin, A. A., Atasoy, D., Etherton, M. R., Brose, N., Kavalali, E. T., Gibson, J. R., & Südhof, T. C. (2007). Activity-dependent validation of excitatory versus inhibitory synapses by neuroligin-1 versus neuroligin-2. *Neuron*, *54*(6), 919–931. https://doi.org/10.1016/j.neuron.2007.05.029

Chung, W. S., Allen, N. J., & Eroglu, C. (2015). Astrocytes Control Synapse Formation, Function, and Elimination. *Cold Spring Harbor perspectives in biology*, *7*(9), a020370. https://doi.org/10.1101/cshperspect.a020370

Chung, W. S., Welsh, C. A., Barres, B. A., & Stevens, B. (2015). Do glia drive synaptic and cognitive impairment in disease?. *Nature neuroscience*, *18*(11), 1539–1545. https://doi.org/10.1038/nn.4142

Cline H. (2005). Synaptogenesis: a balancing act between excitation and inhibition. *Current biology : CB*, *15*(6), R203–R205. https://doi.org/10.1016/j.cub.2005.03.010

Comoletti, D., Flynn, R. E., Boucard, A. A., Demeler, B., Schirf, V., Shi, J., Jennings, L. L., Newlin, H. R., Südhof, T. C., & Taylor, P. (2006). Gene selection, alternative splicing, and post-translational processing regulate neuroligin selectivity for beta-neurexins. *Biochemistry*, *45*(42), 12816–12827. https://doi.org/10.1021/bi0614131

Connor, S. A., Ammendrup-Johnsen, I., Chan, A. W., Kishimoto, Y., Murayama, C., Kurihara, N., Tada, A., Ge, Y., Lu, H., Yan, R., LeDue, J. M., Matsumoto, H., Kiyonari, H., Kirino, Y., Matsuzaki, F., Suzuki, T., Murphy, T. H., Wang, Y. T., Yamamoto, T., & Craig, A. M. (2016). Altered Cortical Dynamics and Cognitive Function upon Haploinsufficiency of the Autism-Linked Excitatory Synaptic Suppressor MDGA2. *Neuron*, *91*(5), 1052–1068. https://doi.org/10.1016/j.neuron.2016.08.016

Conrad, K. L., Louderback, K. M., Gessner, C. P., & Winder, D. G. (2011). Stress-induced alterations in anxiety-like behavior and adaptations in plasticity in the bed nucleus of the stria terminalis. *Physiology & behavior*, *104*(2), 248–256. https://doi.org/10.1016/j.physbeh.2011.03.001

Cox, J., & Mann, M. (2008). MaxQuant enables high peptide identification rates, individualized p.p.b.-range mass accuracies and proteome-wide protein quantification. *Nature biotechnology*, *26*(12), 1367–1372. https://doi.org/10.1038/nbt.1511

Crider, A., Feng, T., Pandya, C. D., Davis, T., Nair, A., Ahmed, A. O., Baban, B., Turecki, G., & Pillai, A. (2018). Complement component 3a receptor deficiency attenuates chronic stress-induced monocyte infiltration and depressive-like behavior. *Brain, behavior, and immunity*, *70*, 246–256. https://doi.org/10.1016/j.bbi.2018.03.004

Crocq M. A. (2015). A history of anxiety: from Hippocrates to DSM. *Dialogues in clinical neuroscience*, *17*(3), 319–325. https://doi.org/10.31887/DCNS.2015.17.3/macrocq

Cross-Disorder Group of the Psychiatric Genomics Consortium (2013). Genetic relationship between five psychiatric disorders estimated from genome-wide SNPs. Nature Genetics, 45, 984-994. https://doi.org/10.1038/ng.2711

Czirr, E., Castello, N. A., Mosher, K. I., Castellano, J. M., Hinkson, I. V., Lucin, K. M., Baeza-Raja, B., Ryu, J. K., Li, L., Farina, S. N., Belichenko, N. P., Longo, F. M., Akassoglou, K., Britschgi, M., Cirrito, J. R., & Wyss-Coray, T. (2017). Microglial complement receptor 3 regulates brain Aβ levels through secreted proteolytic activity. *The Journal of experimental medicine*, *214*(4), 1081–1092. https://doi.org/10.1084/jem.20162011

Dahlhaus, R., Hines, R. M., Eadie, B. D., Kannangara, T. S., Hines, D. J., Brown, C. E., Christie, B. R., & El-Husseini, A. (2010). Overexpression of the cell adhesion protein neuroligin-1 induces learning deficits and impairs synaptic plasticity by altering the ratio of excitation to inhibition in the hippocampus. *Hippocampus*, *20*(2), 305–322. https://doi.org/10.1002/hipo.20630

Dalva, M. B., McClelland, A. C., & Kayser, M. S. (2007). Cell adhesion molecules: signalling functions at the synapse. *Nature reviews. Neuroscience*, *8*(3), 206–220. https://doi.org/10.1038/nrn2075

Dang, N. N., Pang, Z. P., Chen, X. F., Huang, B. Y., Ye, W. J., Chen, X. L., & Zhang, X. (2021). NLGN3 Upregulates Expression of ADAM10 to Promote the Cleavage of NLGN3 via Activating the LYN Pathway in Human Gliomas. Frontiers in Cell and Developmental Biology, 9, 662763. https://doi.org/10.3389/fcell.2021.662763

Dantzer, R., O'Connor, J. C., Freund, G. G., Johnson, R. W., & Kelley, K. W. (2008). From inflammation to sickness and depression: when the immune system subjugates the brain. *Nature reviews. Neuroscience*, *9*(1), 46–56. https://doi.org/10.1038/nrn2297

Davalos, D., Grutzendler, J., Yang, G., Kim, J. V., Zuo, Y., Jung, S., Littman, D. R., Dustin, M. L., & Gan, W. B. (2005). ATP mediates rapid microglial response to local brain injury in vivo. *Nature neuroscience*, *8*(6), 752–758. https://doi.org/10.1038/nn1472

Dean, B., Gibbons, A. S., Tawadros, N., Brooks, L., Everall, I. P., & Scarr, E. (2013). Different changes in cortical tumor necrosis factor-α-related pathways in schizophrenia and mood disorders. *Molecular psychiatry*, *18*(7), 767–773. https://doi.org/10.1038/mp.2012.95

Dean, C., Scholl, F. G., Choih, J., DeMaria, S., Berger, J., Isacoff, E., & Scheiffele, P. (2003). Neurexin mediates the assembly of presynaptic terminals. *Nature neuroscience*, *6*(7), 708–716. https://doi.org/10.1038/nn1074

Dean, O. M., Kanchanatawan, B., Ashton, M., Mohebbi, M., Ng, C. H., Maes, M., Berk, L., Sughondhabirom, A., Tangwongchai, S., Singh, A. B., McKenzie, H., Smith, D. J., Malhi, G. S., Dowling, N., & Berk, M. (2017). Adjunctive minocycline treatment for major depressive disorder: A proof of concept trial. *The Australian and New Zealand journal of psychiatry*, *51*(8), 829–840. https://doi.org/10.1177/0004867417709357

del Río-Hortega, P. (1919a). El tercer elemento de los centros nerviosos. I. La microglia en estado normal. *Boll Socieded Esp Biol.* 9, 69–120.

del Río-Hortega, P. (1919b). El "tercer elemento" de Los Centros Nerviosos. II. Intervencion de la microglia en los procesos patologicos (Cellulas en bastocito y cuerpos granulo-adiposos). *Bol. Soc. Esp Biol.* 9, 91–103.

del Río-Hortega, P. (1919c). El "tercer elemento" de los centros nerviosos. III. Naturaleza probable de la microglía. *Bol. Soc. Esp Biol.* 8, 108–115.

del Río-Hortega, P. (1919d). El "tercer elemento de los centros nerviosos". IV. Poder fagocitario y movilidad de la microglía. *Bol. Soc. Esp Biol.* 8, 155–166.

Del-Aguila, J. L., Benitez, B. A., Li, Z., Dube, U., Mihindukulasuriya, K. A., Budde, J. P., Farias, F. H. G., Fernández, M. V., Ibanez, L., Jiang, S., Perrin, R. J., Cairns, N. J., Morris, J. C., Harari, O., & Cruchaga, C. (2019). TREM2 brain transcript-specific studies in AD and TREM2 mutation carriers. *Molecular neurodegeneration*, *14*(1), 18. https://doi.org/10.1186/s13024-019-0319-3

Delattre, V., La Mendola, D., Meystre, J., Markram, H., & Markram, K. (2013). Nlgn4 knockout induces network hypo-excitability in juvenile mouse somatosensory cortex in vitro. *Scientific reports*, *3*, 2897. https://doi.org/10.1038/srep02897

Derecki, N. C., Cronk, J. C., Lu, Z., Xu, E., Abbott, S. B., Guyenet, P. G., & Kipnis, J. (2012). Wild-type microglia arrest pathology in a mouse model of Rett syndrome. *Nature*, *484*(7392), 105–109. https://doi.org/10.1038/nature10907

Di Marco, B., Bonaccorso, C. M., Aloisi, E., D'Antoni, S., & Catania, M. V. (2016). Neuro-Inflammatory Mechanisms in Developmental Disorders Associated with Intellectual Disability and Autism Spectrum Disorder: A Neuro- Immune Perspective. *CNS & neurological disorders drug targets*, *15*(4), 448–463. https://doi.org/10.2174/1871527315666160321105039

Dieleman, G. C., Huizink, A. C., Tulen, J. H., Utens, E. M., & Tiemeier, H. (2016). Stress reactivity predicts symptom improvement in children with anxiety disorders. *Journal of affective disorders*, *196*, 190–199. https://doi.org/10.1016/j.jad.2016.02.022

Dine, J., Ionescu, I. A., Avrabos, C., Yen, Y. C., Holsboer, F., Landgraf, R., Schmidt, U., & Eder, M. (2015). Intranasally applied neuropeptide S shifts a high-anxiety electrophysiological endophenotype in the ventral hippocampus towards a "normal"-anxiety one. *PloS one*, *10*(4), e0120272. https://doi.org/10.1371/journal.pone.0120272

Ding, X., Wang, J., Huang, M., Chen, Z., Liu, J., Zhang, Q., Zhang, C., Xiang, Y., Zen, K., & Li, L. (2021). Loss of microglial SIRPα promotes synaptic pruning in preclinical models of neurodegeneration. *Nature communications*, *12*(1), 2030. https://doi.org/10.1038/s41467-021-22301-1

DiSabato, D. J., Quan, N., & Godbout, J. P. (2016). Neuroinflammation: the devil is in the details. *Journal of neurochemistry*, *139 Suppl 2*(Suppl 2), 136–153. https://doi.org/10.1111/jnc.13607

Donner, N. C. and Lowry, C. A. (2013) 'Sex differences in anxiety and emotional behavior.', *Pflugers Archiv : European journal of physiology*. Germany, 465(5), pp. 601–626. doi: 10.1007/s00424-013-1271-7.

Doshi-Velez, F., Ge, Y., & Kohane, I. (2014). Comorbidity clusters in autism spectrum disorders: an electronic health record time-series analysis. Pediatrics, 133(1), e54-e63. https://doi.org/10.1542/peds.2013-0819

Dowlati, Y., Herrmann, N., Swardfager, W., Liu, H., Sham, L., Reim, E. K., & Lanctôt, K. L. (2010). A meta-analysis of cytokines in major depression. *Biological psychiatry*, *67*(5), 446–457. https://doi.org/10.1016/j.biopsych.2009.09.033

Duric, V., Banasr, M., Stockmeier, C. A., Simen, A. A., Newton, S. S., Overholser, J. C., Jurjus, G. J., Dieter, L., & Duman, R. S. (2013). Altered expression of synapse and glutamate related genes in post-mortem hippocampus of depressed subjects. *The international journal of neuropsychopharmacology*, *16*(1), 69–82. https://doi.org/10.1017/S1461145712000016

El-Kordi, A., Winkler, D., Hammerschmidt, K., Kästner, A., Krueger, D., Ronnenberg, A., Ritter, C., Jatho, J., Radyushkin, K., Bourgeron, T., Fischer, J., Brose, N., & Ehrenreich, H. (2013). Development of an autism severity score for mice using Nlgn4 null mutants as a construct-valid model of heritable monogenic autism. *Behavioural brain research*, *251*, 41–49. https://doi.org/10.1016/j.bbr.2012.11.016

Endres, K., & Deller, T. (2017). Regulation of Alpha-Secretase ADAM10 *In vitro* and *In vivo*: Genetic, Epigenetic, and Protein-Based Mechanisms. *Frontiers in molecular neuroscience*, *10*, 56. https://doi.org/10.3389/fnmol.2017.00056

Erblich, B., Zhu, L., Etgen, A. M., Dobrenis, K., & Pollard, J. W. (2011). Absence of colony stimulation factor-1 receptor results in loss of microglia, disrupted brain development and olfactory deficits. *PloS one*, *6*(10), e26317. https://doi.org/10.1371/journal.pone.0026317

Etherton, M., Földy, C., Sharma, M., Tabuchi, K., Liu, X., Shamloo, M., Malenka, R.C., and Südhof, T.C. (2011a). Autism-linked neuroligin-3 R451C mutation differentially alters hippocampal and cortical synaptic function. Proc. Natl. Acad. Sci. USA 108, 13764–13769. https://doi.org/10.1073/pnas.1111093108

Etkin, A., & Schatzberg, A. F. (2011). Common abnormalities and disorder-specific compensation during implicit regulation of emotional processing in generalized anxiety and major depressive disorders. *The American journal of psychiatry*, *168*(9), 968–978. https://doi.org/10.1176/appi.ajp.2011.10091290

Färber, K., & Kettenmann, H. (2005). Physiology of microglial cells. *Brain research. Brain research reviews*, *48*(2), 133–143. https://doi.org/10.1016/j.brainresrev.2004.12.003

Feinberg I. (1982). Schizophrenia: caused by a fault in programmed synaptic elimination during adolescence?. *Journal of psychiatric research*, *17*(4), 319–334. https://doi.org/10.1016/0022-3956(82)90038-3

Feuerbach, D., Schindler, P., Barske, C., Joller, S., Beng-Louka, E., Worringer, K. A., Kommineni, S., Kaykas, A., Ho, D. J., Ye, C., Welzenbach, K., Elain, G., Klein, L., Brzak, I., Mir, A. K., Farady, C. J., Aichholz, R., Popp, S., George, N., & Neumann, U. (2017). ADAM17 is the main sheddase for the generation of human triggering receptor expressed in myeloid cells (hTREM2) ectodomain and cleaves TREM2 after Histidine 157. *Neuroscience letters*, *660*, 109–114. https://doi.org/10.1016/j.neulet.2017.09.034

Filipello, F., Morini, R., Corradini, I., Zerbi, V., Canzi, A., Michalski, B., Erreni, M., Markicevic, M., Starvaggi-Cucuzza, C., Otero, K., Piccio, L., Cignarella, F., Perrucci, F., Tamborini, M., Genua, M., Rajendran, L., Menna, E., Vetrano, S., Fahnestock, M., Paolicelli, R. C., … Matteoli, M. (2018). The Microglial Innate Immune Receptor TREM2 Is Required for Synapse Elimination and Normal Brain Connectivity. *Immunity*, *48*(5), 979–991.e8. https://doi.org/10.1016/j.immuni.2018.04.016

Filipello, F., Goldsbury, C., You, S. F., Locca, A., Karch, C. M., & Piccio, L. (2022). Soluble TREM2: Innocent bystander or active player in neurological diseases?. *Neurobiology of disease*, *165*, 105630. https://doi.org/10.1016/j.nbd.2022.105630

Fillman, S. G., Cloonan, N., Catts, V. S., Miller, L. C., Wong, J., McCrossin, T., Cairns, M., & Weickert, C. S. (2013). Increased inflammatory markers identified in the dorsolateral prefrontal cortex of individuals with schizophrenia. *Molecular psychiatry*, *18*(2), 206–214. https://doi.org/10.1038/mp.2012.110

Finak, G., McDavid, A., Yajima, M., Deng, J., Gersuk, V., Shalek, A. K., Slichter, C. K., Miller, H. W., McElrath, M. J., Prlic, M., Linsley, P. S., & Gottardo, R. (2015). MAST: a flexible statistical

framework for assessing transcriptional changes and characterizing heterogeneity in single-cell RNA sequencing data. *Genome biology*, *16*, 278. https://doi.org/10.1186/s13059-015-0844-5

Földy, C., Malenka, R.C., and Südhof, T.C. (2013). Autism-associated neuroligin-3 mutations commonly disrupt tonic endocannabinoid signaling. Neuron 78, 498–509. https://doi.org/10.1016/j.neuron.2013.02.036

Fontenelle, L. F., Barbosa, I. G., Luna, J. V., de Sousa, L. P., Abreu, M. N., & Teixeira, A. L. (2012). A cytokine study of adult patients with obsessive-compulsive disorder. *Comprehensive psychiatry*, *53*(6), 797–804. https://doi.org/10.1016/j.comppsych.2011.12.007

Fortin, N. J., Agster, K. L., & Eichenbaum, H. B. (2002). Critical role of the hippocampus in memory for sequences of events. Nature Neuroscience, 5(5), 458-462. https://doi.org/10.1038/nn834

Francisco, A., Ronchi, J. A., Navarro, C. D. C., Figueira, T. R., & Castilho, R. F. (2018). Nicotinamide nucleotide transhydrogenase is required for brain mitochondrial redox balance under hampered energy substrate metabolism and high-fat diet. *Journal of neurochemistry*, *147*(5), 663–677. https://doi.org/10.1111/jnc.14602

Frick, L. R., Williams, K., & Pittenger, C. (2013). Microglial dysregulation in psychiatric disease. *Clinical & developmental immunology*, *2013*, 608654. https://doi.org/10.1155/2013/608654

Friedman, H. V., Bresler, T., Garner, C. C., & Ziv, N. E. (2000). Assembly of new individual excitatory synapses: time course and temporal order of synaptic molecule recruitment. *Neuron*, *27*(1), 57–69. https://doi.org/10.1016/s0896-6273(00)00009-x

Furusawa, K., & Emoto, K. (2020). Scrap and Build for Functional Neural Circuits: Spatiotemporal Regulation of Dendrite Degeneration and Regeneration in Neural Development and Disease. *Frontiers in cellular neuroscience*, 14, 613320. doi: https://doi.org/10.3389/fncel.2020.613320

Gangwar, S. P., Zhong, X., Seshadrinathan, S., Chen, H., Machius, M., & Rudenko, G. (2017). Molecular Mechanism of MDGA1: Regulation of Neuroligin 2:Neurexin Trans-synaptic Bridges. *Neuron*, *94*(6), 1132–1141.e4. https://doi.org/10.1016/j.neuron.2017.06.009

Gao, R., & Penzes, P. (2015). Common mechanisms of excitatory and inhibitory imbalance in schizophrenia and autism spectrum disorders. *Current molecular medicine*, *15*(2), 146–167. https://doi.org/10.2174/1566524015666150303003028

Garrett, J. E. and Wellman, C. L. (2009) 'Chronic stress effects on dendritic morphology in medial prefrontal cortex: sex differences and estrogen dependence.', *Neuroscience*. United States, 162(1), pp. 195–207. doi: 10.1016/j.neuroscience.2009.04.057.

Garrido-Mesa, N., Zarzuelo, A. and Gálvez, J. (2013) 'Minocycline: far beyond an antibiotic.', *British journal of pharmacology*. England, 169(2), pp. 337–352. doi: 10.1111/bph.12139.

Gaspersz, R., Lamers, F., Wittenberg, G., Beekman, A. T. F., van Hemert, A. M., Schoevers, R. A., & Penninx, B. W. J. H. (2017). The role of anxious distress in immune dysregulation in patients with major depressive disorder. *Translational psychiatry*, *7*(12), 1268. https://doi.org/10.1038/s41398-017-0016-3

Gattermann, R., Fritzsche, P., Neumann, K., Al-Hussein, I., Kayser, A., Abiad, M., & Yakti, R. (2001). Notes on the current distribution and the ecology of wild golden hamsters (Mesocricetus auratus). Journal of Zoology, 254(1), 1-4. https://doi.org/10.1017/S0952836901000851

Gaugler, T., Klei, L., Sanders, S. J., Bodea, C. A., Goldberg, A. P., Lee, A. B., ... & Buxbaum, J. D. (2014). Most genetic risk for autism resides with common variation. Nature Genetics, 46, 881-885. https://doi.org/10.1038/ng.3039

Ge, R., Torres, I., Brown, J. J., Gregory, E., McLellan, E., Downar, J. H., Blumberger, D. M., Daskalakis, Z. J., Lam, R. W., & Vila-Rodriguez, F. (2019). Functional disconnectivity of the hippocampal network and neural correlates of memory impairment in treatment-resistant depression. *Journal of affective disorders*, *253*, 248–256. https://doi.org/10.1016/j.jad.2019.04.096

Ge, S. X., Jung, D. and Yao, R. (2020) 'ShinyGO: a graphical gene-set enrichment tool for animals and plants', *Bioinformatics*, 36(8), pp. 2628–2629. doi: 10.1093/bioinformatics/btz931.

Geloso, M. C., & D'Ambrosi, N. (2021). Microglial Pruning: Relevance for Synaptic Dysfunction in Multiple Sclerosis and Related Experimental Models. *Cells*, *10*(3), 686. https://doi.org/10.3390/cells10030686

Gerrow, K., Romorini, S., Nabi, S. M., Colicos, M. A., Sala, C., & El-Husseini, A. (2006). A preformed complex of postsynaptic proteins is involved in excitatory synapse development. *Neuron*, *49*(4), 547–562. https://doi.org/10.1016/j.neuron.2006.01.015

Gibson, J. R., Huber, K. M., & Südhof, T. C. (2009). Neuroligin-2 deletion selectively decreases inhibitory synaptic transmission originating from fast-spiking but not from somatostatin-positive interneurons. *The Journal of neuroscience : the official journal of the Society for Neuroscience*, *29*(44), 13883–13897. https://doi.org/10.1523/JNEUROSCI.2457-09.2009

Gilbert, J., & Man, H. Y. (2017). Fundamental elements in autism: from neurogenesis and neurite growth to synaptic plasticity. Frontiers in Cellular Neuroscience, 11, 359. https://doi.org/10.3389/fncel.2017.00359

Ginhoux, F., Greter, M., Leboeuf, M., Nandi, S., See, P., Gokhan, S., Mehler, M. F., Conway, S. J., Ng, L. G., Stanley, E. R., Samokhvalov, I. M., & Merad, M. (2010). Fate mapping analysis reveals that adult microglia derive from primitive macrophages. *Science (New York, N.Y.)*, *330*(6005), 841–845. https://doi.org/10.1126/science.1194637

Ginhoux, F., Lim, S., Hoeffel, G., Low, D., & Huber, T. (2013). Origin and differentiation of microglia. *Frontiers in cellular neuroscience*, *7*, 45. https://doi.org/10.3389/fncel.2013.00045

Gogolla, N., Leblanc, J. J., Quast, K. B., Südhof, T. C., Fagiolini, M., & Hensch, T. K. (2009). Common circuit defect of excitatory-inhibitory balance in mouse models of autism. *Journal of neurodevelopmental disorders*, *1*(2), 172–181. https://doi.org/10.1007/s11689-009-9023-x

Gokce, O., Stanley, G.M., Treutlein, B., Neff, N.F., Camp, J.G., Malenka, R.C., Rothwell, P.E., Fuccillo, M.V., Su¨dhof, T.C., and Quake, S.R. (2016). Cellular Taxonomy of the Mouse Striatum as Revealed by Single-Cell RNA-Seq. *Cell Rep.*, 16, 1126–1137. DOI: 10.1016/j.celrep.2016.06.059.

Goldmann, T., Wieghofer, P., Jordão, M. J., Prutek, F., Hagemeyer, N., Frenzel, K., Amann, L., Staszewski, O., Kierdorf, K., Krueger, M., Locatelli, G., Hochgerner, H., Zeiser, R., Epelman, S., Geissmann, F., Priller, J., Rossi, F. M., Bechmann, I., Kerschensteiner, M., Linnarsson, S., … Prinz, M. (2016). Origin, fate and dynamics of macrophages at central nervous system interfaces. *Nature immunology*, *17*(7), 797–805. https://doi.org/10.1038/ni.3423

Gomez-Arboledas, A., Acharya, M. M. and Tenner, A. J. (2021) 'The Role of Complement in Synaptic Pruning and Neurodegeneration'. *ImmunoTargets and Therapy*, Volume 10, pp. 373–386. doi: 10.2147/itt.s305420

Gray E. G. (1959). Axo-somatic and axo-dendritic synapses of the cerebral cortex: an electron microscope study. *Journal of anatomy*, *93*(Pt 4), 420–433.

Green, D. R., Oguin, T. H. and Martinez, J. (2016) 'The clearance of dying cells: table for two.', *Cell death and differentiation*. England, 23(6), pp. 915–926. doi: 10.1038/cdd.2015.172.

Grove, J., Ripke, S., Als, T. D., Mattheisen, M., Walters, R. K., Won, H., ... & Børglum, A. D. (2019). Identification of common genetic risk variants for autism spectrum disorder. Nature Genetics, 51, 431-444. https://doi.org/10.1038/s41588-019-0344-8

Guang, S., Pang, N., Deng, X., Yang, L., He, F., Wu, L., Chen, C., Yin, F., & Peng, J. (2018). Synaptopathology Involved in Autism Spectrum Disorder. *Frontiers in cellular neuroscience*, *12*, 470. https://doi.org/10.3389/fncel.2018.00470

Guneykaya, D., Ivanov, A., Hernandez, D. P., Haage, V., Wojtas, B., Meyer, N., ... & Kettenmann, H. (2018). Transcriptional and translational differences of microglia from male and female brains. Cell Reports, 24(10), 2773-2783.e6. https://doi.org/10.1016/j.celrep.2018.08.001.

Guneykaya, D., Ugursu, B., Logiacco, F., Popp, O., Feiks, M. A., Meyer, N., Wendt, S., Semtner, M., Cherif, F., Gauthier, C., Madore, C., Yin, Z., Çınar, Ö., Arslan, T., Gerevich, Z., Mertins, P., Butovsky, O., Kettenmann, H., & Wolf, S. A. (2023). Sex-specific microglia state in the Neuroligin-4 knock-out mouse model of autism spectrum disorder. *Brain, behavior, and immunity*, *111*, 61–75. Advance online publication. https://doi.org/10.1016/j.bbi.2023.03.023

Gupta, S., Ellis, S. E., Ashar, F. N., Moes, A., Bader, J. S., Zhan, J., West, A. B., & Arking, D. E. (2014). Transcriptome analysis reveals dysregulation of innate immune response genes and neuronal activity-dependent genes in autism. *Nature communications*, *5*, 5748. https://doi.org/10.1038/ncomms6748

Haar, S., Berman, S., Behrmann, M., & Dinstein, I. (2016). Anatomical abnormalities in autism? Cerebral Cortex, 26(4), 1440–1452. https://doi.org/10.1093/cercor/bhu24240.

Hammer, M. (2012). *Characterization of Neuroligin 4, a Protein Involved in Autism Spectrum Disorders* [Doctoral Thesis: Charakterisierung von Neuroligin 4, einem an Autismus-Spektrum-Störungen beteiligten Protein. Retrieved from: https://ediss.uni-goettingen.de/handle/11858/00-1735-0000-000D-F0C6-F

Hammer, M., Krueger-Burg, D., Tuffy, L. P., Cooper, B. H., Taschenberger, H., Goswami, S. P., Ehrenreich, H., Jonas, P., Varoqueaux, F., Rhee, J. S., & Brose, N. (2015). Perturbed Hippocampal Synaptic Inhibition and γ-Oscillations in a Neuroligin-4 Knockout Mouse Model of Autism. *Cell reports*, *13*(3), 516–523. https://doi.org/10.1016/j.celrep.2015.09.011

Hammond, T. R., Dufort, C., Dissing-Olesen, L., Giera, S., Young, A., Wysoker, A., Walker, A. J., Gergits, F., Segel, M., Nemesh, J., Marsh, S. E., Saunders, A., Macosko, E., Ginhoux, F., Chen, J., Franklin, R. J. M., Piao, X., McCarroll, S. A., & Stevens, B. (2019). Single-Cell RNA Sequencing of Microglia throughout the Mouse Lifespan and in the Injured Brain Reveals Complex Cell-State Changes. *Immunity*, *50*(1), 253–271.e6. https://doi.org/10.1016/j.immuni.2018.11.004

Han, Q. Q., Shen, S. Y., Chen, X. R., Pilot, A., Liang, L. F., Zhang, J. R., Li, W. H., Fu, Y., Le, J. M., Chen, P. Q., & Yu, J. (2022). Minocycline alleviates abnormal microglial phagocytosis of synapses in a mouse model of depression. *Neuropharmacology*, *220*, 109249. https://doi.org/10.1016/j.neuropharm.2022.109249

Hanamsagar, R., Bilbo, S. D., & Mcgill, B. E. (2017). Generation of a microglial developmental index in mice and in humans reveals a sex difference in maturation and immune reactivity. Glia, 65(9), 1504–1520. https://doi.org/10.1002/glia.23176.

Hanisch, U.-K. and Kettenmann, H. (2007) 'Microglia: active sensor and versatile effector cells in the normal and pathologic brain', *Nature Neuroscience*. Nature Publishing Group, 10, p. 1387. https://doi.org/10.1038/nn1997.

Harrison, N. A., Brydon, L., Walker, C., Gray, M. A., Steptoe, A., Dolan, R. J., & Critchley, H. D. (2009). Neural origins of human sickness in interoceptive responses to

inflammation. *Biological psychiatry*, *66*(5), 415–422. https://doi.org/10.1016/j.biopsych.2009.03.007

Hartmann, D., de Strooper, B., Serneels, L., Craessaerts, K., Herreman, A., Annaert, W., Umans, L., Lübke, T., Lena Illert, A., von Figura, K., & Saftig, P. (2002). The disintegrin/metalloprotease ADAM 10 is essential for Notch signalling but not for alpha-secretase activity in fibroblasts. *Human molecular genetics*, *11*(21), 2615–2624. https://doi.org/10.1093/hmg/11.21.2615

Hashimoto, D., Chow, A., Noizat, C., Teo, P., Beasley, M. B., Leboeuf, M., Becker, C. D., See, P., Price, J., Lucas, D., Greter, M., Mortha, A., Boyer, S. W., Forsberg, E. C., Tanaka, M., van Rooijen, N., García-Sastre, A., Stanley, E. R., Ginhoux, F., Frenette, P. S., … Merad, M. (2013). Tissue-resident macrophages self-maintain locally throughout adult life with minimal contribution from circulating monocytes. *Immunity*, *38*(4), 792–804. https://doi.org/10.1016/j.immuni.2013.04.004

Hata, Y., Butz, S., & Sudhof, T. C. (1996). CASK: a novel dlg/PSD95 homolog with an N-terminal calmodulin-dependent protein kinase domain identified by interaction with neurexins. The Journal of Neuroscience, 16, 2488-2494. https://doi.org/10.1523/JNEUROSCI.16-08-02488.1996

Hayashi, M. K., Tang, C., Verpelli, C., Narayanan, R., Stearns, M. H., Xu, R. M., Li, H., Sala, C., & Hayashi, Y. (2009). The postsynaptic density proteins Homer and Shank form a polymeric network structure. *Cell*, *137*(1), 159–171. https://doi.org/10.1016/j.cell.2009.01.050

Hayes, L. N. , Ang, K., Carloni, E., Li, F., Vincent, E., Paranjpe, M., Dolen, G., Goff, L.A., Ramos, A., Kano, S., Sawa, A. (2021) 'Prenatal immune stress induces a prolonged blunting of microglia activation that impacts striatal connectivity', *bioRxiv*, p. 2021.12.27.473694. doi: 10.1101/2021.12.27.473694.

Heine, M., Thoumine, O., Mondin, M., Tessier, B., Giannone, G., & Choquet, D. (2008). Activity-independent and subunit-specific recruitment of functional AMPA receptors at neurexin/neuroligin contacts. *Proceedings of the National Academy of Sciences of the United States of America*, *105*(52), 20947–20952. https://doi.org/10.1073/pnas.0804007106

Hines, R. M., Wu, L., Hines, D. J., Steenland, H., Mansour, S., Dahlhaus, R., Singaraja, R. R., Cao, X., Sammler, E., Hormuzdi, S. G., Zhuo, M., & El-Husseini, A. (2008). Synaptic imbalance, stereotypies, and impaired social interactions in mice with altered neuroligin 2 expression. *The Journal of neuroscience : the official journal of the Society for Neuroscience*, *28*(24), 6055–6067. https://doi.org/10.1523/JNEUROSCI.0032-08.2008

Hodges, H., Fealko, C., Soares, N., & Autism Treatment Network Behavioral Health Committee. (2020). A review of regression in autism spectrum disorder: what we know and what we need to learn. *Journal of Autism and Developmental Disorders, 50*(4), 1401-1418. https://doi.org/10.1007/s10803-019-04258-2

Hoon, M., Soykan, T., Falkenburger, B., Hammer, M., Patrizi, A., Schmidt, K. F., Sassoè-Pognetto, M., Löwel, S., Moser, T., Taschenberger, H., Brose, N., & Varoqueaux, F. (2011). Neuroligin-4 is localized to glycinergic postsynapses and regulates inhibition in the retina. *Proceedings of the National Academy of Sciences of the United States of America*, *108*(7), 3053–3058. https://doi.org/10.1073/pnas.1006946108

Horchar, M. J. and Wohleb, E. S. (2019) 'Glucocorticoid receptor antagonism prevents microglia-mediated neuronal remodeling and behavioral despair following chronic unpredictable stress.', *Brain, behavior, and immunity*. Netherlands, 81, pp. 329–340. doi: 10.1016/j.bbi.2019.06.030.

Hoshiko, M., Arnoux, I., Avignone, E., Yamamoto, N., & Audinat, E. (2012). Deficiency of the microglial receptor CX3CR1 impairs postnatal functional development of thalamocortical synapses in the barrel cortex. *The Journal of neuroscience : the official journal of the Society for Neuroscience*, *32*(43), 15106–15111. https://doi.org/10.1523/JNEUROSCI.1167-12.2012

Hou, R., Garner, M., Holmes, C., Osmond, C., Teeling, J., Lau, L., & Baldwin, D. S. (2017). Peripheral inflammatory cytokines and immune balance in Generalised Anxiety Disorder: Case-controlled study. *Brain, behavior, and immunity*, *62*, 212–218. https://doi.org/10.1016/j.bbi.2017.01.021

Hu, X., Luo, J. H., & Xu, J. (2015). The interplay between synaptic activity and neuroligin function in the CNS. *BioMed research international*, *2015*, 498957. https://doi.org/10.1155/2015/498957

Hu, Y. H., Zhang, Y., Jiang, L. Q., Wang, S., Lei, C. Q., Sun, M. S., Shu, H. B., & Liu, Y. (2015). WDFY1 mediates TLR3/4 signaling by recruiting TRIF. *EMBO reports*, *16*(4), 447–455. https://doi.org/10.15252/embr.201439637

Huang, K., Han, Y., Chen, K., Pan, H., Zhao, G., Yi, W., Li, X., Liu, S., Wei, P., & Wang, L. (2021). A hierarchical 3D-motion learning framework for animal spontaneous behavior mapping. *Nature communications*, *12*(1), 2784. https://doi.org/10.1038/s41467-021-22970-y

Huang, Y., Happonen, K. E., Burrola, P. G., O'Connor, C., Hah, N., Huang, L., Nimmerjahn, A., & Lemke, G. (2021). Microglia use TAM receptors to detect and engulf amyloid β plaques. *Nature immunology*, *22*(5), 586–594. https://doi.org/10.1038/s41590-021-00913-5

Hughes, C. S., Foehr, S., Garfield, D. A., Furlong, E. E., Steinmetz, L. M., & Krijgsveld, J. (2014). Ultrasensitive proteome analysis using paramagnetic bead technology. *Molecular systems biology*, *10*(10), 757. https://doi.org/10.15252/msb.20145625

Hundhausen, C., Misztela, D., Berkhout, T. A., Broadway, N., Saftig, P., Reiss, K., Hartmann, D., Fahrenholz, F., Postina, R., Matthews, V., Kallen, K. J., Rose-John, S., & Ludwig, A. (2003). The disintegrin-like metalloproteinase ADAM10 is involved in constitutive cleavage of CX3CL1

(fractalkine) and regulates CX3CL1-mediated cell-cell adhesion. *Blood*, *102*(4), 1186–1195. https://doi.org/10.1182/blood-2002-12-3775
Huttenlocher, PR. Synaptic density in human frontal cortex—developmental changes and effects of aging. *Brain Res* **163**, 195–205 (1979).

Iaccarino H.F., Singer AC, Martorell AJ, Rudenko A, Gao F, Gillingham TZ, Mathys H, Seo J, Kritskiy O, Abdurrob F, Adaikkan C, Canter RG, Rueda R, Brown EN, Boyden ES, Tsai LH (2016) Gamma frequency entrainment attenuates amyloid load and modifies microglia. *Nature*. doi: 10.1038/nature20587

Ichtchenko, K., Hata, Y., Nguyen, T., Ullrich, B., Missler, M., Moomaw, C., and Südhof, T.C. (1995). Neuroligin 1: a splice site-specific ligand for β-neurexins. Cell 81, 435–443. https://doi.org/10.1016/0092-8674(95)90396-8

Ichtchenko, K., Nguyen, T., and Südhof, T.C. (1996). Structures, alternative splicing, and neurexin binding of multiple neuroligins. J. Biol. Chem. 271, 2676–2682. https://doi.org/10.1074/jbc.271.5.2676

Jamain, S., Quach, H., Betancur, C., Råstam, M., Colineaux, C., Gillberg, I. C., Soderstrom, H., Giros, B., Leboyer, M., Gillberg, C., Bourgeron, T., & Paris Autism Research International Sibpair Study (2003). Mutations of the X-linked genes encoding neuroligins NLGN3 and NLGN4 are associated with autism. *Nature genetics*, *34*(1), 27–29. https://doi.org/10.1038/ng1136

Jamain, S., Radyushkin, K., Hammerschmidt, K., Granon, S., Boretius, S., Varoqueaux, F., Ramanantsoa, N., Gallego, J., Ronnenberg, A., Winter, D., Frahm, J., Fischer, J., Bourgeron, T., Ehrenreich, H., & Brose, N. (2008). Reduced social interaction and ultrasonic communication in a mouse model of monogenic heritable autism. *Proceedings of the National Academy of Sciences of the United States of America*, *105*(5), 1710–1715. https://doi.org/10.1073/pnas.0711555105

Ji, K., Akgul, G., Wollmuth, L. P., & Tsirka, S. E. (2013). Microglia actively regulate the number of functional synapses. *PloS one*, *8*(2), e56293. https://doi.org/10.1371/journal.pone.0056293

Jiang, M., Polepalli, J., Chen, L. Y., Zhang, B., Südhof, T. C., & Malenka, R. C. (2017). Conditional ablation of neuroligin-1 in CA1 pyramidal neurons blocks LTP by a cell-autonomous NMDA receptor-independent mechanism. *Molecular psychiatry*, *22*(3), 375–383. https://doi.org/10.1038/mp.2016.80

Johnson, C. P., & Myers, S. M. (2007). Identification and evaluation of children with autism spectrum disorders. Pediatrics, 120, 1183-1215. https://doi.org/10.1542/peds.2007-2361

Jonsson, T., Stefansson, H., Steinberg, S., Jonsdottir, I., Jonsson, P. V., Snaedal, J., Bjornsson, S., Huttenlocher, J., Levey, A. I., Lah, J. J., Rujescu, D., Hampel, H., Giegling, I., Andreassen, O. A., Engedal, K., Ulstein, I., Djurovic, S., Ibrahim-Verbaas, C., Hofman, A., Ikram, M. A., … Stefansson, K. (2013). Variant of TREM2 associated with the risk of Alzheimer's disease. *The New England journal of medicine*, *368*(2), 107–116. https://doi.org/10.1056/NEJMoa1211103

Ju, A., Hammerschmidt, K., Tantra, M., Krueger, D., Brose, N., & Ehrenreich, H. (2014). Juvenile manifestation of ultrasound communication deficits in the neuroligin-4 null mutant mouse model of autism. *Behavioural brain research*, *270*, 159–164. https://doi.org/10.1016/j.bbr.2014.05.019

Kalin N. H. (2020). The Critical Relationship Between Anxiety and Depression. *The American journal of psychiatry*, *177*(5), 365–367. https://doi.org/10.1176/appi.ajp.2020.20030305

Kalin, N. H. (2017). Mechanisms underlying the early risk to develop anxiety and depression: A translational approach. *European neuropsychopharmacology : the journal of the European College of Neuropsychopharmacology*, 27(6), 543–553. doi: https://doi.org/10.1016/j.euroneuro.2017.03.004

Kalm, M., Roughton, K., & Blomgren, K. (2013). Lipopolysaccharide sensitized male and female juvenile brains to ionizing radiation. Cell Death & Disease, 4(12), e962. https://doi.org/10.1038/cddis.2013.482.

Kanner, L. (1943). Child psychiatry - Mental deficiency. American Journal of Psychiatry, 99, 608-610.

Keith D, **El-Husseini A**. Excitation Control: Balancing PSD-95 Function at the Synapse. *Front Mol Neurosci*. 2008;1:4. Published 2008 Mar 28. doi:10.3389/neuro.02.004.2008

Kempuraj, D., Selvakumar, G. P., Ahmed, M. E., Raikwar, S. P., Thangavel, R., Khan, A., Zaheer, S. A., Iyer, S. S., Burton, C., James, D., & Zaheer, A. (2020). COVID-19, Mast Cells, Cytokine Storm, Psychological Stress, and Neuroinflammation. *The Neuroscientist : a review journal bringing neurobiology, neurology and psychiatry*, *26*(5-6), 402–414. https://doi.org/10.1177/1073858420941476

Keren-Shaul, H., Spinrad, A., Weiner, A., Matcovitch-Natan, O., Dvir-Szternfeld, R., Ulland, T. K., David, E., Baruch, K., Lara-Astaiso, D., Toth, B., Itzkovitz, S., Colonna, M., Schwartz, M., & Amit, I. (2017). A Unique Microglia Type Associated with Restricting Development of Alzheimer's Disease. *Cell*, *169*(7), 1276–1290.e17. https://doi.org/10.1016/j.cell.2017.05.018

Kessler, R. C., Petukhova, M., Sampson, N. A., Zaslavsky, A. M., & Wittchen, H.-U. (2012). Twelve-month and lifetime prevalence and lifetime morbid risk of anxiety and mood disorders in the United States. *International journal of methods in psychiatric research*, *21*(3), 169–184. https://doi.org/10.1002/mpr.1359

Kessler, R. C., Sampson, N. A., Berglund, P., Gruber, M. J., Al-Hamzawi, A., Andrade, L., Bunting, B., Demyttenaere, K., Florescu, S., de Girolamo, G., Gureje, O., He, Y., Hu, C., Huang, Y., Karam, E., Kovess-Masfety, V., Lee, S., Levinson, D., Medina Mora, M. E., Moskalewicz, J., … Wilcox, M. A. (2015). Anxious and non-anxious major depressive disorder in the World Health Organization World Mental Health Surveys. *Epidemiology and psychiatric sciences*, *24*(3), 210–226. https://doi.org/10.1017/S2045796015000189

Kettenmann, H., Hanisch, U. K., Noda, M., & Verkhratsky, A. (2011). Physiology of microglia. *Physiological reviews*, *91*(2), 461–553. https://doi.org/10.1152/physrev.00011.2010

Kettenmann, H., Kirchhoff, F., & Verkhratsky, A. (2013). Microglia: new roles for the synaptic stripper. *Neuron*, 77(1), 10–18. doi: https://doi.org/10.1016/j.neuron.2012.12.023

Kierdorf, K., & Prinz, M. (2017). Microglia in steady state. *The Journal of clinical investigation*, *127*(9), 3201–3209. https://doi.org/10.1172/JCI90602

Kierdorf, K., Erny, D., Goldmann, T., Sander, V., Schulz, C., Perdiguero, E. G., Wieghofer, P., Heinrich, A., Riemke, P., Hölscher, C., Müller, D. N., Luckow, B., Brocker, T., Debowski, K., Fritz, G., Opdenakker, G., Diefenbach, A., Biber, K., Heikenwalder, M., Geissmann, F., … Prinz, M. (2013). Microglia emerge from erythromyeloid precursors via Pu.1- and Irf8-dependent pathways. *Nature neuroscience*, *16*(3), 273–280. https://doi.org/10.1038/nn.3318

Kim, H. J., Cho, M. H., Shim, W. H., Kim, J. K., Jeon, E. Y., Kim, D. H., & Yoon, S. Y. (2017). Deficient autophagy in microglia impairs synaptic pruning and causes social behavioral defects. *Molecular psychiatry*, *22*(11), 1576–1584. https://doi.org/10.1038/mp.2016.103

Kim, J. A., Kim, D., Won, S. Y., Han, K. A., Park, D., Cho, E., Yun, N., An, H. J., Um, J. W., Kim, E., Lee, J. O., Ko, J., & Kim, H. M. (2017). Structural Insights into Modulation of Neurexin-Neuroligin Trans-synaptic Adhesion by MDGA1/Neuroligin-2 Complex. *Neuron*, *94*(6), 1121–1131.e6. https://doi.org/10.1016/j.neuron.2017.05.034

Kinney, D. K., Munir, K. M., Crowley, D. J., & Miller, A. M. (2008). Prenatal stress and risk for autism. *Neuroscience and biobehavioral reviews*, *32*(8), 1519–1532. https://doi.org/10.1016/j.neubiorev.2008.06.004

Kleijer, K. T., Schmeisser, M. J., Krueger, D. D., Boeckers, T. M., Scheiffele, P., Bourgeron, T., Brose, N., & Burbach, J. P. (2014). Neurobiology of autism gene products: towards pathogenesis and drug targets. *Psychopharmacology*, *231*(6), 1037–1062. https://doi.org/10.1007/s00213-013-3403-3

Klenk, M. M., Strauman, T. J., & Higgins, E. T. (2011). Regulatory focus and anxiety: A self-regulatory model of GAD-depression comorbidity. *Personality and Individual Differences*, 50(7), 935–943. doi: https://doi.org/10.1016/j.paid.2010.12.003

Kneussel, M., Brandstätter, J. H., Gasnier, B., Feng, G., Sanes, J. R., & Betz, H. (2001). Gephyrin-independent clustering of postsynaptic GABA(A) receptor subtypes. *Molecular and cellular neurosciences*, *17*(6), 973–982. https://doi.org/10.1006/mcne.2001.0983

Kodama, L., & Gan, L. (2019). Do Microglial Sex Differences Contribute to Sex Differences in Neurodegenerative Diseases? Trends in Molecular Medicine, 25(9), 741–749. https://doi.org/10.1016/j.molmed.2019.05.001.

Köhler, O., Benros, M. E., Nordentoft, M., Farkouh, M. E., Iyengar, R. L., Mors, O., & Krogh, J. (2014). Effect of anti-inflammatory treatment on depression, depressive symptoms, and adverse effects: a systematic review and meta-analysis of randomized clinical trials. *JAMA psychiatry*, *71*(12), 1381–1391. https://doi.org/10.1001/jamapsychiatry.2014.1611

Koizumi, S., Shigemoto-Mogami, Y., Nasu-Tada, K., Shinozaki, Y., Ohsawa, K., Tsuda, M., Joshi, B. V., Jacobson, K. A., Kohsaka, S., & Inoue, K. (2007). UDP acting at P2Y6 receptors is a mediator of microglial phagocytosis. *Nature*, *446*(7139), 1091–1095. https://doi.org/10.1038/nature05704

Kreisel, T., Frank, M. G., Licht, T., Reshef, R., Ben-Menachem-Zidon, O., Baratta, M. V., Maier, S. F., & Yirmiya, R. (2014). Dynamic microglial alterations underlie stress-induced depressive-like behavior and suppressed neurogenesis. *Molecular psychiatry*, *19*(6), 699–709. https://doi.org/10.1038/mp.2013.155

Krueger-Burg, D., Papadopoulos, T., & Brose, N. (2017). Organizers of inhibitory synapses come of age. *Current opinion in neurobiology*, *45*, 66–77. https://doi.org/10.1016/j.conb.2017.04.003

Krueger, D. D., Tuffy, L. P., Papadopoulos, T., & Brose, N. (2012). The role of neurexins and neuroligins in the formation, maturation, and function of vertebrate synapses. *Current opinion in neurobiology*, *22*(3), 412–422. https://doi.org/10.1016/j.conb.2012.02.012

Kuhn, P. H., Colombo, A. V., Schusser, B., Dreymueller, D., Wetzel, S., Schepers, U., Herber, J., Ludwig, A., Kremmer, E., Montag, D., Müller, U., Schweizer, M., Saftig, P., Bräse, S., & Lichtenthaler, S. F. (2016). Systematic substrate identification indicates a central role for the metalloprotease ADAM10 in axon targeting and synapse function. *eLife*, *5*, e12748. https://doi.org/10.7554/eLife.12748

Kumar, S., Reynolds, K., Ji, Y., Gu, R., Rai, S., & Zhou, C. J. (2019). Impaired neurodevelopmental pathways in autism spectrum disorder: a review of signaling mechanisms and crosstalk. Journal of Neurodevelopmental Disorders, 11, 10. https://doi.org/10.1186/s11689-019-9268-y

Laumonnier, F., Bonnet-Brilhault, F., Gomot, M., Blanc, R., David, A., Moizard, M. P., Raynaud, M., Ronce, N., Lemonnier, E., Calvas, P., Laudier, B., Chelly, J., Fryns, J. P., Ropers, H. H., Hamel, B. C., Andres, C., Barthélémy, C., Moraine, C., & Briault, S. (2004). X-linked mental retardation and autism are associated with a mutation in the NLGN4 gene, a member of the neuroligin family. *American journal of human genetics*, *74*(3), 552–557. https://doi.org/10.1086/382137

Lawson-Yuen, A., Saldivar, J. S., Sommer, S., & Picker, J. (2008). Familial deletion within NLGN4 associated with autism and Tourette syndrome. *European journal of human genetics : EJHG*, *16*(5), 614–618. https://doi.org/10.1038/sj.ejhg.5202006

Lawson, L. J., Perry, V. H., Dri, P., & Gordon, S. (1990). Heterogeneity in the distribution and morphology of microglia in the normal adult mouse brain. *Neuroscience*, *39*(1), 151–170. https://doi.org/10.1016/0306-4522(90)90229-w

Lee, K., Kim, Y., Lee, S. J., Qiang, Y., Lee, D., Lee, H. W., Kim, H., Je, H. S., Südhof, T. C., & Ko, J. (2013). MDGAs interact selectively with neuroligin-2 but not other neuroligins to regulate inhibitory synapse development. *Proceedings of the National Academy of Sciences of the United States of America*, *110*(1), 336–341. https://doi.org/10.1073/pnas.1219987110

Lee, S. E., Greenough, E.K., Oancea, P., Fonken, L.K., Gaudet, A.D. (2022) 'Anxiety-like behaviors in mice unmasked: Revealing sex differences in anxiety using a novel light-heat conflict test', *bioRxiv*, p. 2022.09.02.506410. doi: 10.1101/2022.09.02.506410.

Lehrman, E. K., Wilton, D. K., Litvina, E. Y., Welsh, C. A., Chang, S. T., Frouin, A., Walker, A. J., Heller, M. D., Umemori, H., Chen, C., & Stevens, B. (2018). CD47 Protects Synapses from Excess Microglia-Mediated Pruning during Development. *Neuron*, *100*(1), 120–134.e6. https://doi.org/10.1016/j.neuron.2018.09.017

Lenz, K. M., Nugent, B. M., Haliyur, R., & McCarthy, M. M. (2013). Microglia are essential to masculinization of brain and behavior. *The Journal of neuroscience : the official journal of the Society for Neuroscience*, *33*(7), 2761–2772. https://doi.org/10.1523/JNEUROSCI.1268-12.2013

Leuner, B., & Gould, E. (2010). Structural plasticity and hippocampal function. *Annual review of psychology*, *61*, 111–C3. https://doi.org/10.1146/annurev.psych.093008.100359

Lévi, S., Logan, S. M., Tovar, K. R., & Craig, A. M. (2004). Gephyrin is critical for glycine receptor clustering but not for the formation of functional GABAergic synapses in hippocampal neurons. *The Journal of neuroscience : the official journal of the Society for Neuroscience*, *24*(1), 207–217. https://doi.org/10.1523/JNEUROSCI.1661-03.2004

Levinson, J. N., & El-Husseini, A. (2005). Building excitatory and inhibitory synapses: balancing neuroligin partnerships. *Neuron*, *48*(2), 171–174. https://doi.org/10.1016/j.neuron.2005.09.017

Levinson, J. N., Chéry, N., Huang, K., Wong, T. P., Gerrow, K., Kang, R., Prange, O., Wang, Y. T., & El-Husseini, A. (2005). Neuroligins mediate excitatory and inhibitory synapse formation: involvement of PSD-95 and neurexin-1beta in neuroligin-induced synaptic specificity. *The Journal of biological chemistry*, *280*(17), 17312–17319. https://doi.org/10.1074/jbc.M413812200

Levkovitz, Y., Fenchel, D., Kaplan, Z., Zohar, J., & Cohen, H. (2015). Early post-stressor intervention with minocycline, a second-generation tetracycline, attenuates post-traumatic stress response in an animal model of PTSD. *European neuropsychopharmacology : the journal of the European College of Neuropsychopharmacology*, *25*(1), 124–132. https://doi.org/10.1016/j.euroneuro.2014.11.012

Li, Z., Ma, L., Kulesskaya, N., Võikar, V., & Tian, L. (2014). Microglia are polarized to M1 type in high-anxiety inbred mice in response to lipopolysaccharide challenge. *Brain, behavior, and immunity*, *38*, 237–248. https://doi.org/10.1016/j.bbi.2014.02.008

Li, Z., & Sheng, M. (2003). Some assembly required: the development of neuronal synapses. *Nature Reviews Molecular Cell Biology, 4*, 833-841. doi: 10.1038/nrm1242

Lim, H. K., Yoon, J. H., & Song, M. (2022). Autism Spectrum Disorder Genes: Disease-Related Networks and Compensatory Strategies. *Frontiers in molecular neuroscience*, *15*, 922840. https://doi.org/10.3389/fnmol.2022.922840

Lipkin, W. I., Bresnahan, M. and Susser, E. (2023) 'Cohort-guided insights into gene–environment interactions in autism spectrum disorders', *Nature Reviews Neurology*, 19(2), pp. 118–125. doi: 10.1038/s41582-022-00764-0.

Liu, H. Y., Yue, J., Hu, L. N., Cheng, L. F., Wang, X. S., Wang, X. J., & Feng, B. (2018). Chronic minocycline treatment reduces the anxiety-like behaviors induced by repeated restraint stress through modulating neuroinflammation. *Brain research bulletin*, *143*, 19–26. https://doi.org/10.1016/j.brainresbull.2018.08.015

Liu, X., Hua, F., Yang, D., Lin, Y., Zhang, L., Ying, J., Sheng, H., & Wang, X. (2022). Roles of neuroligins in central nervous system development: focus on glial neuroligins and neuron neuroligins. *Journal of translational medicine*, *20*(1), 418. https://doi.org/10.1186/s12967-022-03625-y

Liu, Y., Zhang, T., Meng, D., Sun, L., Yang, G., He, Y., & Zhang, C. (2020). Involvement of CX3CL1/CX3CR1 in depression and cognitive impairment induced by chronic unpredictable stress and relevant underlying mechanism. *Behavioural brain research*, *381*, 112371. https://doi.org/10.1016/j.bbr.2019.112371

Love, M. I., Huber, W., & Anders, S. (2014). Moderated estimation of fold change and dispersion for RNA-seq data with DESeq2. *Genome biology*, 15(12), 550. doi: 10.1186/s13059-014-0550-8.

Macarov, M., Zeigler, M., Newman, J. P., Strich, D., Sury, V., Tennenbaum, A., & Meiner, V. (2007). Deletions of VCX-A and NLGN4: a variable phenotype including normal intellect. *Journal of intellectual disability research : JIDR*, *51*(Pt 5), 329–333. https://doi.org/10.1111/j.1365-2788.2006.00880.x

MacMillan, H. L., Fleming, J. E., Streiner, D. L., Lin, E., Boyle, M. H., Jamieson, E., Duku, E. K., Walsh, C. A., Wong, M. Y., & Beardslee, W. R. (2001). Childhood abuse and lifetime psychopathology in a community sample. *The American journal of psychiatry*, *158*(11), 1878–1883. https://doi.org/10.1176/appi.ajp.158.11.1878

Maenner, M. J., Shaw, K. A., Bakian, A. V., Bilder, D. A., Durkin, M. S., Esler, A., Furnier, S. M., Hallas, L., Hall-Lande, J., Hudson, A., Hughes, M. M., Patrick, M., Pierce, K., Poynter, J. N., Salinas, A., Shenouda, J., Vehorn, A., Warren, Z., Constantino, J. N., DiRienzo, M., … Cogswell, M. E. (2021). Prevalence and Characteristics of Autism Spectrum Disorder Among Children Aged 8 Years - Autism and Developmental Disabilities Monitoring Network, 11 Sites, United States, 2018. *Morbidity and mortality weekly report. Surveillance summaries (Washington, D.C. : 2002)*, *70*(11), 1–16. https://doi.org/10.15585/mmwr.ss7011a1

Maes M. (1993). A review on the acute phase response in major depression. *Reviews in the neurosciences*, *4*(4), 407–416. https://doi.org/10.1515/revneuro.1993.4.4.407

Maes, M., Berk, M., Goehler, L., Song, C., Anderson, G., Gałecki, P., & Leonard, B. (2012). Depression and sickness behavior are Janus-faced responses to shared inflammatory pathways. *BMC medicine*, *10*, 66. https://doi.org/10.1186/1741-7015-10-66

Maes, M., Meltzer, H. Y., Scharpe, S., Cooreman, W., Uyttenbroeck, W., Suy, E., Vandervorst, C., Calabrese, J., Raus, J., & Cosyns, P. (1993). Psychomotor retardation, anorexia, weight loss, sleep disturbances, and loss of energy: psychopathological correlates of hyperhaptoglobinemia during major depression. Psychiatry Res, 47, 229-241. https://doi.org/10.1016/0165-1781(93)90081-Q

Marcinkiewicz, M., & Seidah, N. G. (2000). Coordinated expression of beta-amyloid precursor protein and the putative beta-secretase BACE and alpha-secretase ADAM10 in mouse and human brain. *Journal of neurochemistry*, *75*(5), 2133–2143. https://doi.org/10.1046/j.1471-4159.2000.0752133.x

Markus, E. J., Petit, T. L.(1987). Synaptic structural changes during development and aging. *Brain research*, *432*(2), 239–248. https://doi.org/10.1016/0165-3806(87)90048-4

Marro, S. G., Chanda, S., Yang, N., Janas, J. A., Valperga, G., Trotter, J., Zhou, B., Merrill, S., Yousif, I., Shelby, H., Vogel, H., Kalani, M. Y. S., Südhof, T. C., & Wernig, M. (2019). Neuroligin-4 Regulates Excitatory Synaptic Transmission in Human Neurons. *Neuron*, *103*(4), 617–626.e6. https://doi.org/10.1016/j.neuron.2019.05.043

Marsh S.E. (2021). scCustomize: Custom Visualizations & Functions for Streamlined Analyses of Single Cell Sequencing. doi: 10.5281/zenodo.5706430.

Marsh, S. E., Walker, A. J., Kamath, T., Dissing-Olesen, L., Hammond, T. R., de Soysa, T. Y., Young, A. M. H., Murphy, S., Abdulraouf, A., Nadaf, N., Dufort, C., Walker, A. C., Lucca, L. E., Kozareva, V., Vanderburg, C., Hong, S., Bulstrode, H., Hutchinson, P. J., Gaffney, D. J., Hafler, D. A., … Stevens, B. (2022). Dissection of artifactual and confounding glial signatures by single-cell sequencing of mouse and human brain. *Nature neuroscience*, *25*(3), 306–316. https://doi.org/10.1038/s41593-022-01022-8

Marshall, C. R., Noor, A., Vincent, J. B., Lionel, A. C., Feuk, L., Skaug, J., Shago, M., Moessner, R., Pinto, D., Ren, Y., Thiruvahindrapduram, B., Fiebig, A., Schreiber, S., Friedman, J., Ketelaars, C. E., Vos, Y. J., Ficicioglu, C., Kirkpatrick, S., Nicolson, R., Sloman, L., … Scherer, S. W. (2008).

Structural variation of chromosomes in autism spectrum disorder. *American journal of human genetics*, *82*(2), 477–488. https://doi.org/10.1016/j.ajhg.2007.12.009

Masi, A., DeMayo, M. M., Glozier, N., & Guastella, A. J. (2017). An Overview of Autism Spectrum Disorder, Heterogeneity and Treatment Options. *Neuroscience bulletin*, *33*(2), 183–193. https://doi.org/10.1007/s12264-017-0100-y

Masuda, T., Sankowski, R., Staszewski, O., & Prinz, M. (2020). Microglia Heterogeneity in the Single-Cell Era. *Cell reports*, *30*(5), 1271–1281. https://doi.org/10.1016/j.celrep.2020.01.010

Masuda, T., Sankowski, R., Staszewski, O., Böttcher, C., Amann, L., Sagar, Scheiwe, C., Nessler, S., Kunz, P., van Loo, G., Coenen, V. A., Reinacher, P. C., Michel, A., Sure, U., Gold, R., Grün, D., Priller, J., Stadelmann, C., & Prinz, M. (2019). Spatial and temporal heterogeneity of mouse and human microglia at single-cell resolution. *Nature*, *566*(7744), 388–392. https://doi.org/10.1038/s41586-019-0924-x

Matcovitch-Natan, O., Winter, D. R., Giladi, A., Vargas Aguilar, S., Spinrad, A., Sarrazin, S., Ben-Yehuda, H., David, E., Zelada González, F., Perrin, P., Keren-Shaul, H., Gury, M., Lara-Astaiso, D., Thaiss, C. A., Cohen, M., Bahar Halpern, K., Baruch, K., Deczkowska, A., Lorenzo-Vivas, E., Itzkovitz, S., … Amit, I. (2016). Microglia development follows a stepwise program to regulate brain homeostasis. *Science (New York, N.Y.)*, *353*(6301), aad8670. https://doi.org/10.1126/science.aad8670

Mattei, D., Ivanov, A., Ferrai, C., Jordan, P., Guneykaya, D., Buonfiglioli, A., Schaafsma, W., Przanowski, P., Deuther-Conrad, W., Brust, P., Hesse, S., Patt, M., Sabri, O., Ross, T. L., Eggen, B. J. L., Boddeke, E. W. G. M., Kaminska, B., Beule, D., Pombo, A., Kettenmann, H., … Wolf, S. A. (2017). Maternal immune activation results in complex microglial transcriptome signature in the adult offspring that is reversed by minocycline treatment. *Translational psychiatry*, *7*(5), e1120. https://doi.org/10.1038/tp.2017.80

Mattei, D., Ivanov, A., van Oostrum, M., Pantelyushin, S., Richetto, J., Mueller, F., Beffinger, M., Schellhammer, L., Vom Berg, J., Wollscheid, B., Beule, D., Paolicelli, R. C., & Meyer, U. (2020). Enzymatic Dissociation Induces Transcriptional and Proteotype Bias in Brain Cell Populations. *International journal of molecular sciences*, *21*(21), 7944. https://doi.org/10.3390/ijms21217944

Maxeiner, S., Benseler, F., Krasteva-Christ, G., Brose, N., & Südhof, T. C. (2020). Evolution of the Autism-Associated Neuroligin-4 Gene Reveals Broad Erosion of Pseudoautosomal Regions in Rodents. *Molecular biology and evolution*, *37*(5), 1243–1258. https://doi.org/10.1093/molbev/msaa014

McLean, C. P., Asnaani, A., Litz, B. T., & Hofmann, S. G. (2011). Gender differences in anxiety disorders: Prevalence, course of illness, comorbidity and burden of illness. Journal of Psychiatric Research, 45(8), 1027–1035. https://doi.org/10.1016/j.jpsychires.2011.03.006.

Merlot, E., Couret, D., & Otten, W. (2008). Prenatal stress, fetal imprinting and immunity. *Brain, behavior, and immunity*, *22*(1), 42–51. https://doi.org/10.1016/j.bbi.2007.05.007

Mertins, P., Tang, L. C., Krug, K., Clark, D. J., Gritsenko, M. A., Chen, L., Clauser, K. R., Clauss, T. R., Shah, P., Gillette, M. A., Petyuk, V. A., Thomas, S. N., Mani, D. R., Mundt, F., Moore, R. J., Hu, Y., Zhao, R., Schnaubelt, M., Keshishian, H., Monroe, M. E., … Carr, S. A. (2018). Reproducible workflow for multiplexed deep-scale proteome and phosphoproteome analysis of tumor tissues by liquid chromatography-mass spectrometry. *Nature protocols*, *13*(7), 1632–1661. https://doi.org/10.1038/s41596-018-0006-9

Mildner, A., Schmidt, H., Nitsche, M., Merkler, D., Hanisch, U. K., Mack, M., Heikenwalder, M., Brück, W., Priller, J., & Prinz, M. (2007). Microglia in the adult brain arise from Ly-6ChiCCR2+ monocytes only under defined host conditions. *Nature neuroscience*, *10*(12), 1544–1553. https://doi.org/10.1038/nn2015

Missler, M., & Südhof, T. C. (1998). Neurexins: three genes and 1001 products. *Trends in genetics : TIG*, *14*(1), 20–26. https://doi.org/10.1016/S0168-9525(97)01324-3

Miyamoto, A., Wake, H., Ishikawa, A. W., Eto, K., Shibata, K., Murakoshi, H., Koizumi, S., Moorhouse, A. J., Yoshimura, Y., & Nabekura, J. (2016). Microglia contact induces synapse formation in developing somatosensory cortex. *Nature communications*, *7*, 12540. https://doi.org/10.1038/ncomms12540

Molina-Hernández, M., Téllez-Alcántara, N. P., Pérez-García, J., Olivera-Lopez, J. I., & Jaramillo-Jaimes, M. T. (2008). Desipramine or glutamate antagonists synergized the antidepressant-like actions of intra-nucleus accumbens infusions of minocycline in male Wistar rats. *Progress in neuro-psychopharmacology & biological psychiatry*, *32*(7), 1660–1666. https://doi.org/10.1016/j.pnpbp.2008.06.010

Möller, T., Bard, F., Bhattacharya, A., Biber, K., Campbell, B., Dale, E., Eder, C., Gan, L., Garden, G. A., Hughes, Z. A., Pearse, D. D., Staal, R. G., Sayed, F. A., Wes, P. D., & Boddeke, H. W. (2016). Critical data-based re-evaluation of minocycline as a putative specific microglia inhibitor. *Glia*, *64*(10), 1788–1794. https://doi.org/10.1002/glia.23007

Mordelt A, de Witte LD. (2023) Microglia-mediated synaptic pruning as a key deficit in neurodevelopmental disorders: Hype or hope?. *Curr Opin Neurobiol*.;79:102674. doi:10.1016/j.conb.2022.102674

Morgan, J. T., Chana, G., Pardo, C. A., Achim, C., Semendeferi, K., Buckwalter, J., Courchesne, E., & Everall, I. P. (2010). Microglial activation and increased microglial density observed in the dorsolateral prefrontal cortex in autism. *Biological psychiatry*, *68*(4), 368–376. https://doi.org/10.1016/j.biopsych.2010.05.024

Moser, J. S., Moran, T. P., Schroder, H. S., Donnellan, M. B., & Yeung, N. (2016). Sex moderates the association between symptoms of anxiety, but not obsessive-compulsive disorder, and

error-monitoring brain activity: A meta-analytic review. Psychophysiology, 53(1), 21–29. https://doi.org/10.1111/psyp.12509.

Nakanishi M., Nomura J, Ji X, Tamada K, Arai T, Takahashi E, Bu□can M, Takumi T. (2017). Functional significance of rare neuroligin 1 variants found in autism. *PLoS Genet.*, 13, e1006940. DOI: 10.1371/journal.pgen.1006940.

Yanguas-Casás, N. (2020) 'Physiological sex differences in microglia and their relevance in neurological disorders', pp. 13–22. doi: 10.20517/2347-8659.2019.31.

Nau, R., Ribes, S., Djukic, M., & Eiffert, H. (2014). Strategies to increase the activity of microglia as efficient protectors of the brain against infections. *Frontiers in cellular neuroscience*, *8*, 138. https://doi.org/10.3389/fncel.2014.00138

Navlakha, S., Barth, A. L., & Bar-Joseph, Z. (2015). Decreasing-Rate Pruning Optimizes the Construction of Efficient and Robust Distributed Networks. *PLoS computational biology*, *11*(7), e1004347. https://doi.org/10.1371/journal.pcbi.1004347

Nettis, M. A., Lombardo, G., Hastings, C., Zajkowska, Z., Mariani, N., Nikkheslat, N., Worrell, C., Enache, D., McLaughlin, A., Kose, M., Sforzini, L., Bogdanova, A., Cleare, A., Young, A. H., Pariante, C. M., & Mondelli, V. (2021). Augmentation therapy with minocycline in treatment-resistant depression patients with low-grade peripheral inflammation: results from a double-blind randomised clinical trial. *Neuropsychopharmacology : official publication of the American College of Neuropsychopharmacology*, *46*(5), 939–948. https://doi.org/10.1038/s41386-020-00948-6

Network and Pathway Analysis Subgroup of Psychiatric Genomics Consortium (2015). Psychiatric genome-wide association study analyses implicate neuronal, immune and histone pathways. *Nature neuroscience*, *18*(2), 199–209. https://doi.org/10.1038/nn.3922

Nguyen, P. T., Dorman, L. C., Pan, S., Vainchtein, I. D., Han, R. T., Nakao-Inoue, H., Taloma, S. E., Barron, J. J., Molofsky, A. B., Kheirbek, M. A., & Molofsky, A. V. (2020). Microglial Remodeling of the Extracellular Matrix Promotes Synapse Plasticity. *Cell*, *182*(2), 388–403.e15. https://doi.org/10.1016/j.cell.2020.05.050

Nichols, M. J. and Newsome, W. T. (1999) 'The neurobiology of cognition', *Nature*, 402(6761), pp. C35–C38. doi: 10.1038/35011531.

Nickl-Jockschat, T., Habel, U., Michel, T. M., Manning, J., Laird, A. R., Fox, P. T., Schneider, F., & Eickhoff, S. B. (2012). Brain structure anomalies in autism spectrum disorder--a meta-analysis of VBM studies using anatomic likelihood estimation. *Human brain mapping*, *33*(6), 1470–1489. https://doi.org/10.1002/hbm.21299

Nicolson, R., DeVito, T. J., Vidal, C. N., Sui, Y., Hayashi, K. M., Drost, D. J., Williamson, P. C., Rajakumar, N., Toga, A. W., & Thompson, P. M. (2006). Detection and mapping of hippocampal abnormalities in autism. *Psychiatry research*, *148*(1), 11–21. https://doi.org/10.1016/j.pscychresns.2006.02.005

Nimmerjahn, A., Kirchhoff, F., & Helmchen, F. (2005). Resting microglial cells are highly dynamic surveillants of brain parenchyma in vivo. *Science (New York, N.Y.)*, *308*(5726), 1314–1318. https://doi.org/10.1126/science.1110647

Okawa, S., Saltó, C., Ravichandran, S., Yang, S., Toledo, E. M., Arenas, E., & Del Sol, A. (2018). Transcriptional synergy as an emergent property defining cell subpopulation identity enables population shift. *Nature communications*, *9*(1), 2595. https://doi.org/10.1038/s41467-018-05016-8

Ozaki, K., Kato, D., Ikegami, A., Hashimoto, A., Sugio, S., Guo, Z., Shibushita, M., Tatematsu, T., Haruwaka, K., Moorhouse, A. J., Yamada, H., & Wake, H. (2020). Maternal immune activation induces sustained changes in fetal microglia motility. *Scientific reports*, *10*(1), 21378. https://doi.org/10.1038/s41598-020-78294-2

Paolicelli RC, Ferretti MT. (2017) Function and Dysfunction of Microglia during Brain Development: Consequences for Synapses and Neural Circuits. *Front Synaptic Neurosci*. 2017;9:9. Published 2017 May 10. doi:10.3389/fnsyn.2017.00009

Paolicelli, R. C., Bolasco, G., Pagani, F., Maggi, L., Scianni, M., Panzanelli, P., Giustetto, M., Ferreira, T. A., Guiducci, E., Dumas, L., Ragozzino, D., & Gross, C. T. (2011). Synaptic pruning by microglia is necessary for normal brain development. *Science (New York, N.Y.)*, *333*(6048), 1456–1458. https://doi.org/10.1126/science.1202529

Paolicelli, R. C., & Gross, C. T. (2011). Microglia in development: linking brain wiring to brain environment. *Neuron glia biology*, *7*(1), 77–83. https://doi.org/10.1017/S1740925X12000105

Paolicelli, R. C., Sierra, A., Stevens, B., Tremblay, M. E., Aguzzi, A., Ajami, B., Amit, I., Audinat, E., Bechmann, I., Bennett, M., Bennett, F., Bessis, A., Biber, K., Bilbo, S., Blurton-Jones, M., Boddeke, E., Brites, D., Brône, B., Brown, G. C., Butovsky, O., … Wyss-Coray, T. (2022). Microglia states and nomenclature: A field at its crossroads. *Neuron*, *110*(21), 3458–3483. https://doi.org/10.1016/j.neuron.2022.10.020

Parkhurst, C. N., Yang, G., Ninan, I., Savas, J. N., Yates, J. R., 3rd, Lafaille, J. J., Hempstead, B. L., Littman, D. R., & Gan, W. B. (2013). Microglia promote learning-dependent synapse formation through brain-derived neurotrophic factor. *Cell*, *155*(7), 1596–1609. https://doi.org/10.1016/j.cell.2013.11.030

Passos, I. C., Vasconcelos-Moreno, M. P., Costa, L. G., Kunz, M., Brietzke, E., Quevedo, J., Salum, G., Magalhães, P. V., Kapczinski, F., & Kauer-Sant'Anna, M. (2015). Inflammatory markers in post-traumatic stress disorder: a systematic review, meta-analysis, and meta-regression. *The lancet. Psychiatry*, *2*(11), 1002–1012. https://doi.org/10.1016/S2215-0366(15)00309-0

Peixoto, R. T., Kunz, P. A., Kwon, H., Mabb, A. M., Sabatini, B. L., Philpot, B. D., & Ehlers, M. D. (2012). Transsynaptic signaling by activity-dependent cleavage of neuroligin-1. *Neuron*, *76*(2), 396–409. https://doi.org/10.1016/j.neuron.2012.07.006

Perry V. H. (1998). A revised view of the central nervous system microenvironment and major histocompatibility complex class II antigen presentation. *Journal of neuroimmunology*, *90*(2), 113–121. https://doi.org/10.1016/s0165-5728(98)00145-3

Petanjek, Z., Judas, M., Šimic, G., Rasin, M. R., Uylings, H. B., Rakic, P., & Kostovic, I. (2011). Extraordinary neoteny of synaptic spines in the human prefrontal cortex. Proceedings of the National Academy of Sciences of the United States of America, 108, 13281-13286. https://doi.org/10.1073/pnas.1105108108

Peters, A. (2006). The energy request of inflammation. Endocrinology, 147, 4550-4552. https://doi.org/10.1210/en.2006-0815

Pettem, K. L., Yokomaku, D., Luo, L., Linhoff, M. W., Prasad, T., Connor, S. A., Siddiqui, T. J., Kawabe, H., Chen, F., Zhang, L., Rudenko, G., Wang, Y. T., Brose, N., & Craig, A. M. (2013). The specific α-neurexin interactor calsyntenin-3 promotes excitatory and inhibitory synapse development. *Neuron*, *80*(1), 113–128. https://doi.org/10.1016/j.neuron.2013.07.016

Piccio, L., Buonsanti, C., Cella, M., Tassi, I., Schmidt, R. E., Fenoglio, C., Rinker, J., 2nd, Naismith, R. T., Panina-Bordignon, P., Passini, N., Galimberti, D., Scarpini, E., Colonna, M., & Cross, A. H. (2008). Identification of soluble TREM-2 in the cerebrospinal fluid and its association with multiple sclerosis and CNS inflammation. *Brain : a journal of neurology*, *131*(Pt 11), 3081–3091. https://doi.org/10.1093/brain/awn217

Pinto, D., Delaby, E., Merico, D., Barbosa, M., Merikangas, A., Klei, L., Thiruvahindrapuram, B., Xu, X., Ziman, R., Wang, Z., Vorstman, J. A., Thompson, A., Regan, R., Pilorge, M., Pellecchia, G., Pagnamenta, A. T., Oliveira, B., Marshall, C. R., Magalhaes, T. R., Lowe, J. K., … Scherer, S. W. (2014). Convergence of genes and cellular pathways dysregulated in autism spectrum disorders. *American journal of human genetics*, *94*(5), 677–694. https://doi.org/10.1016/j.ajhg.2014.03.018

Pocock, J. M., & Kettenmann, H. (2007). Neurotransmitter receptors on microglia. *Trends in neurosciences*, *30*(10), 527–535. https://doi.org/10.1016/j.tins.2007.07.007

Prange, O., Wong, T. P., Gerrow, K., Wang, Y. T., & El-Husseini, A. (2004). A balance between excitatory and inhibitory synapses is controlled by PSD-95 and neuroligin. *Proceedings of the National Academy of Sciences of the United States of America*, *101*(38), 13915–13920. https://doi.org/10.1073/pnas.0405939101

Prevalence of autism spectrum disorder among children aged 8 years - autism and developmental disabilities monitoring network, 11 sites, United States, 2016. *Morbidity and Mortality Weekly Report,* *69*(4), 1-12. https://www.cdc.gov/mmwr/volumes/69/ss/ss6904a1.htm?s_cid=ss6904a1_w

Priller, J., Flügel, A., Wehner, T., Boentert, M., Haas, C. A., Prinz, M., Fernández-Klett, F., Prass, K., Bechmann, I., de Boer, B. A., Frotscher, M., Kreutzberg, G. W., Persons, D. A., & Dirnagl, U. (2001). Targeting gene-modified hematopoietic cells to the central nervous system: use of green fluorescent protein uncovers microglial engraftment. *Nature medicine*, *7*(12), 1356–1361. https://doi.org/10.1038/nm1201-1356

Prinz, M., & Priller, J. (2014). Microglia and brain macrophages in the molecular age: from origin to neuropsychiatric disease. *Nature reviews. Neuroscience*, *15*(5), 300–312. https://doi.org/10.1038/nrn3722

Prox, J., Bernreuther, C., Altmeppen, H., Grendel, J., Glatzel, M., D'Hooge, R., Stroobants, S., Ahmed, T., Balschun, D., Willem, M., Lammich, S., Isbrandt, D., Schweizer, M., Horré, K., De Strooper, B., & Saftig, P. (2013). Postnatal disruption of the disintegrin/metalloproteinase ADAM10 in brain causes epileptic seizures, learning deficits, altered spine morphology, and defective synaptic functions. *The Journal of neuroscience : the official journal of the Society for Neuroscience*, *33*(32), 12915–12928a. https://doi.org/10.1523/JNEUROSCI.5910-12.2013

Purves D., Augustine G.J., Fitzpatrick D., Katz, L.C., LaMantia, A-S., McNamara, J.O., Williams, S.M. (2001) Neuroscience. 2nd edition. Sunderland: Sinauer Associates. Excitatory and Inhibitory Postsynaptic Potentials. Available from: https://www.ncbi.nlm.nih.gov/books/NBK11117/

Qiao, Q., Ma, L., Li, W., Tsai, J. W., Yang, G., & Gan, W. B. (2016). Long-term stability of axonal boutons in the mouse barrel cortex. *Developmental neurobiology*, *76*(3), 252–261. https://doi.org/10.1002/dneu.22311

Qin, Q., Wang, M., Yin, Y., & Tang, Y. (2022). The Specific Mechanism of TREM2 Regulation of Synaptic Clearance in Alzheimer's Disease. *Frontiers in immunology*, *13*, 845897. https://doi.org/10.3389/fimmu.2022.845897

Qu, W. and Li, L. (2020) 'Loss of TREM2 Confers Resilience to Synaptic and Cognitive Impairment in Aged Mice.', *The Journal of neuroscience : the official journal of the Society for Neuroscience*. United States, 40(50), pp. 9552–9563. doi: 10.1523/JNEUROSCI.2193-20.2020.

Racine, N., McArthur, B. A., Cooke, J. E., Eirich, R., Zhu, J., & Madigan, S. (2021). Global Prevalence of Depressive and Anxiety Symptoms in Children and Adolescents During COVID-19: A Meta-analysis. *JAMA pediatrics*, *175*(11), 1142–1150. https://doi.org/10.1001/jamapediatrics.2021.2482

Rao, N. P., Venkatasubramanian, G., Ravi, V., Kalmady, S., Cherian, A., & Yc, J. R. (2015). Plasma cytokine abnormalities in drug-naïve, comorbidity-free obsessive-compulsive disorder. *Psychiatry research*, *229*(3), 949–952. https://doi.org/10.1016/j.psychres.2015.07.009

Ressler, K. J., & Mayberg, H. S. (2007). Targeting abnormal neural circuits in mood and anxiety disorders: from the laboratory to the clinic. *Nature neuroscience*, *10*(9), 1116–1124. https://doi.org/10.1038/nn1944

Réu, P., Khosravi, A., Bernard, S., Mold, J. E., Salehpour, M., Alkass, K., Perl, S., Tisdale, J., Possnert, G., Druid, H., & Frisén, J. (2017). The Lifespan and Turnover of Microglia in the Human Brain. *Cell reports*, *20*(4), 779–784. https://doi.org/10.1016/j.celrep.2017.07.004

Richards, E. M., Zanotti-Fregonara, P., Fujita, M., Newman, L., Farmer, C., Ballard, E. D., Machado-Vieira, R., Yuan, P., Niciu, M. J., Lyoo, C. H., Henter, I. D., Salvadore, G., Drevets, W. C., Kolb, H., Innis, R. B., & Zarate, C. A., Jr (2018). PET radioligand binding to translocator protein (TSPO) is increased in unmedicated depressed subjects. *EJNMMI research*, *8*(1), 57. https://doi.org/10.1186/s13550-018-0401-9

Richards, R., Greimel, E., Kliemann, D., Koerte, I. K., Schulte-Körne, G., Reuter, M., & Wachinger, C. (2020). Increased hippocampal shape asymmetry and volumetric ventricular asymmetry in autism spectrum disorder. *NeuroImage. Clinical*, *26*, 102207. https://doi.org/10.1016/j.nicl.2020.102207

Ritchie, M. E., Phipson, B., Wu, D., Hu, Y., Law, C. W., Shi, W., & Smyth, G. K. (2015). Limma Powers Differential Expression Analyses for RNA-Sequencing and Microarray Studies. *Nucleic Acids Research*, 43(7), e47. https://doi.org/10.1093/nar/gkv007

Rogers, J. P., Chesney, E., Oliver, D., Pollak, T. A., McGuire, P., Fusar-Poli, P., Zandi, M. S., Lewis, G., & David, A. S. (2020). Psychiatric and neuropsychiatric presentations associated with severe coronavirus infections: a systematic review and meta-analysis with comparison to the COVID-19 pandemic. *The lancet. Psychiatry*, *7*(7), 611–627. https://doi.org/10.1016/S2215-0366(20)30203-0

Rooney, S., Sah, A., Unger, M. S., Kharitonova, M., Sartori, S. B., Schwarzer, C., Aigner, L., Kettenmann, H., Wolf, S. A., & Singewald, N. (2020). Neuroinflammatory alterations in trait anxiety: modulatory effects of minocycline. *Translational psychiatry*, *10*(1), 256. https://doi.org/10.1038/s41398-020-00942-y

Rosenblat, J. D., Cha, D. S., Mansur, R. B., & McIntyre, R. S. (2014). Inflamed moods: a review of the interactions between inflammation and mood disorders. *Progress in neuro-psychopharmacology & biological psychiatry*, *53*, 23–34. https://doi.org/10.1016/j.pnpbp.2014.01.013

Rothwell, P.E., Fuccillo, M.V., Maxeiner, S., Hayton, S.J., Gokce, O., Lim, B.K., Fowler, S.C., Malenka, R.C., and Südhof, T.C. (2014). Autism-associated neuroligin-3 mutations commonly impair striatal circuits to boost repetitive behaviors. Cell 158, 198–212. https://doi.org/10.1016/j.cell.2014.04.045

Rubenstein, J. L., **& Merzenich, M. M.** (2003). Model of autism: increased ratio of excitation/inhibition in key neural systems. *Genes, brain, and behavior*, *2*(5), 255–267. https://doi.org/10.1034/j.1601-183x.2003.00037.x

Sah, A., Schmuckermair, C., Sartori, S. B., Gaburro, S., Kandasamy, M., Irschick, R., Klimaschewski, L., Landgraf, R., Aigner, L., & Singewald, N. (2012). Anxiety- rather than depression-like behavior is associated with adult neurogenesis in a female mouse model of higher trait anxiety- and comorbid depression-like behavior. *Translational psychiatry*, *2*(10), e171. https://doi.org/10.1038/tp.2012.94

Sakers, K., & Eroglu, C. (2019). Control of neural development and function by glial neuroligins. Current Opinion in Neurobiology, 57, 163-170. https://doi.org/10.1016/j.conb.2019.03.007

Salomé, N., Salchner, P., Viltart, O., Sequeira, H., Wigger, A., Landgraf, R., & Singewald, N. (2004). Neurobiological correlates of high (HAB) versus low anxiety-related behavior (LAB): differential Fos expression in HAB and LAB rats. *Biological psychiatry*, *55*(7), 715–723. https://doi.org/10.1016/j.biopsych.2003.10.021

Salter, M. W., & Stevens, B. (2017). Microglia emerge as central players in brain disease. *Nature medicine*, *23*(9), 1018–1027. https://doi.org/10.1038/nm.4397

Sato, W., Kochiyama, T., Uono, S., Yoshimura, S., Kubota, Y., Sawada, R., Sakihama, M., & Toichi, M. (2017). Reduced Gray Matter Volume in the Social Brain Network in Adults with Autism Spectrum Disorder. *Frontiers in human neuroscience*, *11*, 395. https://doi.org/10.3389/fnhum.2017.00395

Saunders, A., Macosko, E. Z., Wysoker, A., Goldman, M., Krienen, F. M., de Rivera, H., Bien, E., Baum, M., Bortolin, L., Wang, S., Goeva, A., Nemesh, J., Kamitaki, N., Brumbaugh, S., Kulp, D., & McCarroll, S. A. (2018). Molecular Diversity and Specializations among the Cells of the Adult Mouse Brain. *Cell*, *174*(4), 1015–1030.e16. https://doi.org/10.1016/j.cell.2018.07.028

Schafer, D. P., Lehrman, E. K., & Stevens, B. (2013). The "quad-partite" synapse: microglia-synapse interactions in the developing and mature CNS. *Glia*, *61*(1), 24–36. https://doi.org/10.1002/glia.22389

Schafer, D. P., Lehrman, E. K., Kautzman, A. G., Koyama, R., Mardinly, A. R., Yamasaki, R., Ransohoff, R. M., Greenberg, M. E., Barres, B. A., & Stevens, B. (2012). Microglia sculpt postnatal neural circuits in an activity and complement-dependent manner. *Neuron*, *74*(4), 691–705. https://doi.org/10.1016/j.neuron.2012.03.026

Schapitz, I. U., Behrend, B., Pechmann, Y., Lappe-Siefke, C., Kneussel, S. J., Wallace, K. E., Stempel, A. V., Buck, F., Grant, S. G., Schweizer, M., Schmitz, D., Schwarz, J. R., Holzbaur, E. L., & Kneussel, M. (2010). Neuroligin 1 is dynamically exchanged at postsynaptic sites. *The Journal of neuroscience : the official journal of the Society for Neuroscience*, *30*(38), 12733–12744. https://doi.org/10.1523/JNEUROSCI.0896-10.2010

Scheefhals, N. and MacGillavry, H. D. (2018) 'Functional organization of postsynaptic glutamate receptors.', *Molecular and cellular neurosciences*. United States, 91, pp. 82–94. doi: 10.1016/j.mcn.2018.05.002.

Schlepckow, K., Kleinberger, G., Fukumori, A., Feederle, R., Lichtenthaler, S. F., Steiner, H., & Haass, C. (2017). An Alzheimer-associated TREM2 variant occurs at the ADAM cleavage site and affects shedding and phagocytic function. *EMBO molecular medicine*, *9*(10), 1356–1365. https://doi.org/10.15252/emmm.201707672

Schreiner, D., Nguyen, T.M., Russo, G., Heber, S., Patrignani, A., Ahrne´ , E., and Scheiffele, P. (2014). Targeted combinatorial alternative splicing generates brain region-specific repertoires of neurexins. *Neuron*, 84, 386–398. DOI: 10.1016/j.neuron.2014.09.011.

Scott-Hewitt, N., Perrucci, F., Morini, R., Erreni, M., Mahoney, M., Witkowska, A., Carey, A., Faggiani, E., Schuetz, L. T., Mason, S., Tamborini, M., Bizzotto, M., Passoni, L., Filipello, F., Jahn, R., Stevens, B., & Matteoli, M. (2020). Local externalization of phosphatidylserine mediates developmental synaptic pruning by microglia. *The EMBO journal*, *39*(16), e105380. https://doi.org/10.15252/embj.2020105380

Sellgren, C. M., Gracias, J., Watmuff, B., Biag, J. D., Thanos, J. M., Whittredge, P. B., Fu, T., Worringer, K., Brown, H. E., Wang, J., Kaykas, A., Karmacharya, R., Goold, C. P., Sheridan, S. D., & Perlis, R. H. (2019). Increased synapse elimination by microglia in schizophrenia patient-derived models of synaptic pruning. *Nature neuroscience*, *22*(3), 374–385. https://doi.org/10.1038/s41593-018-0334-7

Shansky, R. M., Hamo, C., Hof, P. R., Lou, W., McEwen, B. S., & Morrison, J. H. (2010). Estrogen promotes stress sensitivity in a prefrontal cortex-amygdala pathway. *Cerebral cortex (New York, N.Y. : 1991)*, *20*(11), 2560–2567. https://doi.org/10.1093/cercor/bhq003

Sheng, J., Ruedl, C., & Karjalainen, K. (2015). Most Tissue-Resident Macrophages Except Microglia Are Derived from Fetal Hematopoietic Stem Cells. *Immunity*, *43*(2), 382–393. https://doi.org/10.1016/j.immuni.2015.07.016

Sheng, M., & Kim, E. (2011). The postsynaptic organization of synapses. *Cold Spring Harbor perspectives in biology*, *3*(12), a005678. https://doi.org/10.1101/cshperspect.a005678

Sheng, X., Yao, Y., Huang, R., Xu, Y., Zhu, Y., Chen, L., Zhang, L., Wang, W., Zhuo, R., Can, D., Chang, C. F., Zhang, Y. W., Xu, H., Bu, G., Zhong, L., & Chen, X. F. (2021). Identification of the minimal active soluble TREM2 sequence for modulating microglial phenotypes and amyloid pathology. *Journal of neuroinflammation*, *18*(1), 286. https://doi.org/10.1186/s12974-021-02340-7

Shinoda, Y., Sadakata, T., & Furuichi, T. (2013). Animal models of autism spectrum disorder (ASD): a synaptic-level approach to autistic-like behavior in mice. *Experimental animals*, *62*(2), 71–78. https://doi.org/10.1538/expanim.62.71

Shipman, S. L., Schnell, E., Hirai, T., Chen, B. S., Roche, K. W., & Nicoll, R. A. (2011). Functional dependence of neuroligin on a new non-PDZ intracellular domain. *Nature neuroscience*, *14*(6), 718–726. https://doi.org/10.1038/nn.2825

Shultz, S. R., Bao, F., Omana, V., Chiu, C., Brown, A., & Cain, D. P. (2012). Repeated mild lateral fluid percussion brain injury in the rat causes cumulative long-term behavioral impairments, neuroinflammation, and cortical loss in an animal model of repeated concussion. *Journal of neurotrauma*, *29*(2), 281–294. https://doi.org/10.1089/neu.2011.2123

Sierra, A., Gottfried-Blackmore, A., Milner, T. A., McEwen, B. S., & Bulloch, K. (2008). Steroid hormone receptor expression and function in microglia. *Glia*, *56*(6), 659–674. https://doi.org/10.1002/glia.20644

Sierra, A., Encinas, J. M., Deudero, J. J., Chancey, J. H., Enikolopov, G., Overstreet-Wadiche, L. S., Tsirka, S. E., & Maletic-Savatic, M. (2010). Microglia shape adult hippocampal neurogenesis through apoptosis-coupled phagocytosis. *Cell stem cell*, *7*(4), 483–495. https://doi.org/10.1016/j.stem.2010.08.014

Sierra, A., de Castro, F., Del Río-Hortega, J., Rafael Iglesias-Rozas, J., Garrosa, M., & Kettenmann, H. (2016). The "Big-Bang" for modern glial biology: Translation and comments on Pío del Río-Hortega 1919 series of papers on microglia. *Glia*, *64*(11), 1801–1840. https://doi.org/10.1002/glia.23046

Silverman, S. M., & Wong, W. T. (2018). Microglia in the Retina: Roles in Development, Maturity, and Disease. *Annual review of vision science*, *4*, 45–77. https://doi.org/10.1146/annurev-vision-091517-034425

Simantov, E., Dahan, M., & Biran, G. (2022). The effect of the COVID-19 pandemic on the diagnosis of children with Autism Spectrum Disorder. *Autism, 26*(2), 226-234. https://doi.org/10.1177/13623613211022091

Simard, A. R., Soulet, D., Gowing, G., Julien, J. P., & Rivest, S. (2006). Bone marrow-derived microglia play a critical role in restricting senile plaque formation in Alzheimer's disease. *Neuron*, *49*(4), 489–502. https://doi.org/10.1016/j.neuron.2006.01.022

Socodato, R., Henriques, J. F., Portugal, C. C., Almeida, T. O., Tedim-Moreira, J., Alves, R. L., Canedo, T., Silva, C., Magalhães, A., Summavielle, T., & Relvas, J. B. (2020). Daily alcohol intake triggers aberrant synaptic pruning leading to synapse loss and anxiety-like behavior. *Science signaling*, *13*(650), eaba5754. https://doi.org/10.1126/scisignal.aba5754

Soczynska, J. K., Kennedy, S. H., Alsuwaidan, M., Mansur, R. B., Li, M., McAndrews, M. P., Brietzke, E., Woldeyohannes, H. O., Taylor, V. H., & McIntyre, R. S. (2017). A pilot, open-label, 8-week study evaluating the efficacy, safety and tolerability of adjunctive minocycline for the treatment of bipolar I/II depression. *Bipolar disorders*, *19*(3), 198–213. https://doi.org/10.1111/bdi.12496

Sominsky, L., Walker, A. K., Ong, L. K., Tynan, R. J., Walker, F. R., & Hodgson, D. M. (2012). Increased microglial activation in the rat brain following neonatal exposure to a bacterial mimetic. *Behavioural brain research*, *226*(1), 351–356. https://doi.org/10.1016/j.bbr.2011.08.038

Song, J.Y., Ichtchenko, K., Südhof, T.C., and Brose, N. (1999). Neuroligin 1 is a postsynaptic cell-adhesion molecule of excitatory synapses. Proc. Natl. Acad. Sci. USA 96, 1100–1105. https://doi.org/10.1073/pnas.96.3.1100

Squarzoni, P., Oller, G., Hoeffel, G., Pont-Lezica, L., Rostaing, P., Low, D., Bessis, A., Ginhoux, F., & Garel, S. (2014). Microglia modulate wiring of the embryonic forebrain. *Cell reports*, *8*(5), 1271–1279. https://doi.org/10.1016/j.celrep.2014.07.042

St Clair, M. C., Croudace, T., Dunn, V. J., Jones, P. B., Herbert, J., & Goodyer, I. M. (2015). Childhood adversity subtypes and depressive symptoms in early and late adolescence. *Development and psychopathology*, *27*(3), 885–899. https://doi.org/10.1017/S0954579414000625

Steiner, J., Bielau, H., Brisch, R., Danos, P., Ullrich, O., Mawrin, C., Bernstein, H. G., & Bogerts, B. (2008). Immunological aspects in the neurobiology of suicide: elevated microglial density in schizophrenia and depression is associated with suicide. *Journal of psychiatric research*, *42*(2), 151–157. https://doi.org/10.1016/j.jpsychires.2006.10.013

Stephan AH, Barres BA, Stevens B. (2012) 'The complement system: an unexpected role in synaptic pruning during development and disease'. *Annu Rev Neurosci*. 35:369-389. doi:10.1146/annurev-neuro-061010-113810

Stessman, H. A., Xiong, B., Coe, B. P., Wang, T., Hoekzema, K., Fenckova, M., Kvarnung, M., Gerdts, J., Trinh, S., Cosemans, N., Vives, L., Lin, J., Turner, T. N., Santen, G., Ruivenkamp, C., Kriek, M., van Haeringen, A., Aten, E., Friend, K., Liebelt, J., … Eichler, E. E. (2017). Targeted sequencing identifies 91 neurodevelopmental-disorder risk genes with autism and developmental-disability biases. *Nature genetics*, *49*(4), 515–526. https://doi.org/10.1038/ng.3792

Stevens, B., Allen, N. J., Vazquez, L. E., Howell, G. R., Christopherson, K. S., Nouri, N., Micheva, K. D., Mehalow, A. K., Huberman, A. D., Stafford, B., Sher, A., Litke, A. M., Lambris, J. D., Smith, S. J., John, S. W., & Barres, B. A. (2007). The classical complement cascade mediates CNS synapse elimination. *Cell*, *131*(6), 1164–1178. https://doi.org/10.1016/j.cell.2007.10.036

Stoodley, C. J., D'Mello, A. M., Ellegood, J., Jakkamsetti, V., Liu, P., Nebel, M. B., Gibson, J. M., Kelly, E., Meng, F., Cano, C. A., Pascual, J. M., Mostofsky, S. H., Lerch, J. P., & Tsai, P. T. (2017). Altered cerebellar connectivity in autism and cerebellar-mediated rescue of autism-related behaviors in mice. *Nature neuroscience*, *20*(12), 1744–1751. https://doi.org/10.1038/s41593-017-0004-1

Strahan, J. A., Walker, W. H., 2nd, Montgomery, T. R., & Forger, N. G. (2017). Minocycline causes widespread cell death and increases microglial labeling in the neonatal mouse brain. *Developmental neurobiology*, *77*(6), 753–766. https://doi.org/10.1002/dneu.22457

Strand, N., Fang, L., & Carlson, J. M. (2021). Sex Differences in Anxiety: An Investigation of the Moderating Role of Sex in Performance Monitoring and Attentional Bias to Threat in High Trait Anxious Individuals. Frontiers in Human Neuroscience, 15, 627589. https://doi.org/10.3389/fnhum.2021.627589.

Stratoulias, V., Venero, J. L., Tremblay, M. È., & Joseph, B. (2019). Microglial subtypes: diversity within the microglial community. *The EMBO journal*, *38*(17), e101997. https://doi.org/10.15252/embj.2019101997

Stuart, T., Butler, A., Hoffman, P., Hafemeister, C., Papalexi, E., Mauck, W. M., 3rd, Hao, Y., Stoeckius, M., Smibert, P., & Satija, R. (2019). Comprehensive Integration of Single-Cell Data. *Cell*, *177*(7), 1888–1902.e21. https://doi.org/10.1016/j.cell.2019.05.031

Südhof T. C. (2012). The presynaptic active zone. *Neuron*, *75*(1), 11–25. https://doi.org/10.1016/j.neuron.2012.06.012

Südhof T. C. (2013). Neurotransmitter release: the last millisecond in the life of a synaptic vesicle. *Neuron*, *80*(3), 675–690. https://doi.org/10.1016/j.neuron.2013.10.022

Südhof T. C. (2018). Towards an Understanding of Synapse Formation. *Neuron*, *100*(2), 276–293. https://doi.org/10.1016/j.neuron.2018.09.040

Südhof T. C. (2021). The cell biology of synapse formation. *The Journal of cell biology*, *220*(7), e202103052. https://doi.org/10.1083/jcb.202103052

Südhof T. C. (2008). Neuroligins and neurexins link synaptic function to cognitive disease. *Nature*, 455, 903–911. DOI: 10.1038/nature07456.

Südhof, T. C. (2017). Synaptic Neurexin Complexes: A Molecular Code for the Logic of Neural Circuits. Cell, 171, 745-769. https://doi.org/10.1016/j.cell.2017.10.024

Suzuki, K., Hayashi, Y., Nakahara, S., Kumazaki, H., Prox, J., Horiuchi, K., Zeng, M., Tanimura, S., Nishiyama, Y., Osawa, S., Sehara-Fujisawa, A., Saftig, P., Yokoshima, S., Fukuyama, T., Matsuki, N., Koyama, R., Tomita, T., & Iwatsubo, T. (2012). Activity-dependent proteolytic cleavage of neuroligin-1. *Neuron*, *76*(2), 410–422. https://doi.org/10.1016/j.neuron.2012.10.003

Suzuki, K., Sugihara, G., Ouchi, Y., Nakamura, K., Futatsubashi, M., Takebayashi, K., Yoshihara, Y., Omata, K., Matsumoto, K., Tsuchiya, K. J., Iwata, Y., Tsujii, M., Sugiyama, T., & Mori, N. (2013). Microglial activation in young adults with autism spectrum disorder. *JAMA psychiatry*, *70*(1), 49–58. https://doi.org/10.1001/jamapsychiatry.2013.272

Tan, C. X. and Eroglu, C. (2021) 'Cell adhesion molecules regulating astrocyte-neuron interactions.', *Current opinion in neurobiology*. England, 69, pp. 170–177. doi: 10.1016/j.conb.2021.03.015.

Tang, G., Gudsnuk, K., Kuo, S. H., Cotrina, M. L., Rosoklija, G., Sosunov, A., Sonders, M. S., Kanter, E., Castagna, C., Yamamoto, A., Yue, Z., Arancio, O., Peterson, B. S., Champagne, F., Dwork, A. J., Goldman, J., & Sulzer, D. (2014). Loss of mTOR-dependent macroautophagy causes autistic-like synaptic pruning deficits. *Neuron*, *83*(5), 1131–1143. https://doi.org/10.1016/j.neuron.2014.07.040

Tay, T. L., Béchade, C., D'Andrea, I., St-Pierre, M. K., Henry, M. S., Roumier, A., & Tremblay, M. E. (2018). Microglia Gone Rogue: Impacts on Psychiatric Disorders across the Lifespan. *Frontiers in molecular neuroscience*, *10*, 421. https://doi.org/10.3389/fnmol.2017.00421

Tay, T. L., Savage, J. C., Hui, C. W., Bisht, K., & Tremblay, M. È. (2017). Microglia across the lifespan: from origin to function in brain development, plasticity and cognition. *The Journal of physiology*, *595*(6), 1929–1945. https://doi.org/10.1113/JP272134

Thornton, P., Sevalle, J., Deery, M. J., Fraser, G., Zhou, Y., Ståhl, S., Franssen, E. H., Dodd, R. B., Qamar, S., Gomez Perez-Nievas, B., Nicol, L. S., Eketjäll, S., Revell, J., Jones, C., Billinton, A., St George-Hyslop, P. H., Chessell, I., & Crowther, D. C. (2017). TREM2 shedding by cleavage at the H157-S158 bond is accelerated for the Alzheimer's disease-associated H157Y variant. *EMBO molecular medicine*, *9*(10), 1366–1378. https://doi.org/10.15252/emmm.201707673

Torres-Platas, S. G., Cruceanu, C., Chen, G. G., Turecki, G., & Mechawar, N. (2014). Evidence for increased microglial priming and macrophage recruitment in the dorsal anterior cingulate white matter of depressed suicides. *Brain, behavior, and immunity*, *42*, 50–59. https://doi.org/10.1016/j.bbi.2014.05.007

Tremblay, M. È., Lowery, R. L., & Majewska, A. K. (2010). Microglial interactions with synapses are modulated by visual experience. *PLoS biology*, *8*(11), e1000527. https://doi.org/10.1371/journal.pbio.1000527

Trotter, J. H., Hao, J., Maxeiner, S., Tsetsenis, T., Liu, Z., Zhuang, X., & Südhof, T. C. (2019). Synaptic neurexin-1 assembles into dynamically regulated active zone nanoclusters. *The Journal of cell biology*, *218*(8), 2677–2698. https://doi.org/10.1083/jcb.201812076

Tubbs, J. D., Ding, J., Baum, L., & Sham, P. C. (2020). Immune dysregulation in depression: Evidence from genome-wide association. *Brain, behavior, & immunity - health*, *7*, 100108. https://doi.org/10.1016/j.bbih.2020.100108

Tynan, R. J., Naicker, S., Hinwood, M., Nalivaiko, E., Buller, K. M., Pow, D. V., Day, T. A., & Walker, F. R. (2010). Chronic stress alters the density and morphology of microglia in a subset

of stress-responsive brain regions. *Brain, behavior, and immunity*, *24*(7), 1058–1068. https://doi.org/10.1016/j.bbi.2010.02.001

Udina, M., Castellví, P., Moreno-España, J., Navinés, R., Valdés, M., Forns, X., Langohr, K., Solà, R., Vieta, E., & Martín-Santos, R. (2012). Interferon-induced depression in chronic hepatitis C: a systematic review and meta-analysis. *The Journal of clinical psychiatry*, *73*(8), 1128–1138. https://doi.org/10.4088/JCP.12r07694

Ueno, M., Fujita, Y., Tanaka, T., Nakamura, Y., Kikuta, J., Ishii, M., & Yamashita, T. (2013). Layer V cortical neurons require microglial support for survival during postnatal development. *Nature neuroscience*, *16*(5), 543–551. https://doi.org/10.1038/nn.3358

Ullrich, B., Ushkaryov, Y. A., & Südhof, T. C. (1995). Cartography of neurexins: more than 1000 isoforms generated by alternative splicing and expressed in distinct subsets of neurons. *Neuron*, *14*(3), 497–507. https://doi.org/10.1016/0896-6273(95)90306-2

Umpierre, A. D. and Wu, L.-J. (2021) 'How microglia sense and regulate neuronal activity.', *Glia*. United States, 69(7), pp. 1637–1653. doi: 10.1002/glia.23961.

Unichenko, P., Yang, J. W., Kirischuk, S., Kolbaev, S., Kilb, W., Hammer, M., Krueger-Burg, D., Brose, N., & Luhmann, H. J. (2018). Autism Related Neuroligin-4 Knockout Impairs Intracortical Processing but not Sensory Inputs in Mouse Barrel Cortex. *Cerebral cortex (New York, N.Y. : 1991)*, *28*(8), 2873–2886. https://doi.org/10.1093/cercor/bhx165

Uranova, N. A., Zimina, I. S., Vikhreva, O. V., Krukov, N. O., Rachmanova, V. I., & Orlovskaya, D. D. (2010). Ultrastructural damage of capillaries in the neocortex in schizophrenia. *The world journal of biological psychiatry : the official journal of the World Federation of Societies of Biological Psychiatry*, *11*(3), 567–578. https://doi.org/10.3109/15622970903414188

Ushkaryov, Y. A., & Sudhof, T. C. (1993). Neurexin III alpha: extensive alternative splicing generates membrane-bound and soluble forms. Proceedings of the National Academy of Sciences of the United States of America, 90, 6410-6414. https://doi.org/10.1073/pnas.90.14.6410

Ushkaryov, Y. A., Petrenko, A. G., Geppert, M., & Südhof, T. C. (1992). Neurexins: synaptic cell surface proteins related to the alpha-latrotoxin receptor and laminin. *Science (New York, N.Y.)*, *257*(5066), 50–56. https://doi.org/10.1126/science.1621094

Vainchtein, I. D., & Molofsky, A. V. (2020). Astrocytes and Microglia: In Sickness and in Health. *Trends in neurosciences*, 43(3), 144–154. doi: https://doi.org/10.1016/j.tins.2020.01.003

Vainchtein, I. D., Chin, G., Cho, F. S., Kelley, K. W., Miller, J. G., Chien, E. C., Liddelow, S. A., Nguyen, P. T., Nakao-Inoue, H., Dorman, L. C., Akil, O., Joshita, S., Barres, B. A., Paz, J. T., Molofsky, A. B., & Molofsky, A. V. (2018). Astrocyte-derived interleukin-33 promotes microglial synapse engulfment and neural circuit development. *Science (New York, N.Y.)*, *359*(6381), 1269–1273. https://doi.org/10.1126/science.aal3589

Vargas, D. L., Nascimbene, C., Krishnan, C., Zimmerman, A. W., & Pardo, C. A. (2005). Neuroglial activation and neuroinflammation in the brain of patients with autism. *Annals of neurology*, *57*(1), 67–81. https://doi.org/10.1002/ana.20315

Varoqueaux, F., Aramuni, G., Rawson, R. L., Mohrmann, R., Missler, M., Gottmann, K., Zhang, W., Südhof, T. C., & Brose, N. (2006). Neuroligins determine synapse maturation and function. *Neuron*, *51*(6), 741–754. https://doi.org/10.1016/j.neuron.2006.09.003

Varoqueaux, F., Jamain, S., & Brose, N. (2004). Neuroligin 2 is exclusively localized to inhibitory synapses. *European journal of cell biology*, *83*(9), 449–456. https://doi.org/10.1078/0171-9335-00410

Venkatesh, H. S., Johung, T. B., Caretti, V., Noll, A., Tang, Y., Nagaraja, S., Gibson, E. M., Mount, C. W., Polepalli, J., Mitra, S. S., Woo, P. J., Malenka, R. C., Vogel, H., Bredel, M., Mallick, P., Monje, M., & Rich, J. N. (2017). Targeting neuronal activity-regulated neuroligin-3 dependency in high-grade glioma. Nature, 549(7673), 533-537. https://doi.org/10.1038/nature24014

Vezzoli, E., Caron, I., Talpo, F., Besusso, D., Conforti, P., Battaglia, E., Sogne, E., Falqui, A., Petricca, L., Verani, M., Martufi, P., Caricasole, A., Bresciani, A., Cecchetti, O., Rivetti di Val Cervo, P., Sancini, G., Riess, O., Nguyen, H., Seipold, L., Saftig, P., … Zuccato, C. (2019). Inhibiting pathologically active ADAM10 rescues synaptic and cognitive decline in Huntington's disease. *The Journal of clinical investigation*, *129*(6), 2390–2403. https://doi.org/10.1172/JCI120616

Villa, K. L., Berry, K. P., Subramanian, J., Cha, J. W., Chan Oh, W., Kwon, H. B., Kubota, Y., So, P. T., & Nedivi, E. (2016). Inhibitory Synapses Are Repeatedly Assembled and Removed at Persistent Sites In Vivo. *Neuron*, *90*(3), 662–664. https://doi.org/10.1016/j.neuron.2016.03.035

Villa, A., Gelosa, P., Castiglioni, L., Cimino, M., Rizzi, N., Pepe, G., ... & Tremoli, E. (2018). Sex-specific features of microglia from adult mice. Cell Reports, 23(12), 3501–3511. https://doi.org/10.1016/j.celrep.2018.05.048.

Virchow R. (1858) Die Cellularpathologie in ihrer Begründung auf physiologische und pathologische Gewebelehre. Berlin, Germany(20): August Hirschwald.

Voineagu, I., Wang, X., Johnston, P., Lowe, J. K., Tian, Y., Horvath, S., Mill, J., Cantor, R. M., Blencowe, B. J., & Geschwind, D. H. (2011). Transcriptomic analysis of autistic brain reveals convergent molecular pathology. *Nature*, *474*(7351), 380–384. https://doi.org/10.1038/nature10110

Waites, C. L., Craig, A. M., & Garner, C. C. (2005). Mechanisms of vertebrate synaptogenesis. *Annual review of neuroscience*, *28*, 251–274. https://doi.org/10.1146/annurev.neuro.27.070203.144336

Wang, H. T., Huang, F. L., Hu, Z. L., Zhang, W. J., Qiao, X. Q., Huang, Y. Q., Dai, R. P., Li, F., & Li, C. Q. (2017). Early-Life Social Isolation-Induced Depressive-Like Behavior in Rats Results in Microglial Activation and Neuronal Histone Methylation that Are Mitigated by Minocycline. *Neurotoxicity research*, *31*(4), 505–520. https://doi.org/10.1007/s12640-016-9696-3

Wang, T., Guo, H., Xiong, B., Stessman, H. A., Wu, H., Coe, B. P., Turner, T. N., Liu, Y., Zhao, W., Hoekzema, K., Vives, L., Xia, L., Tang, M., Ou, J., Chen, B., Shen, Y., Xun, G., Long, M., Lin, J., Kronenberg, Z. N., … Eichler, E. E. (2016). De novo genic mutations among a Chinese autism spectrum disorder cohort. *Nature communications*, *7*, 13316. https://doi.org/10.1038/ncomms13316

Wang, W., Wang, R., Xu, J., Qin, X., Jiang, H., Khalid, A., Liu, D., Pan, F., Ho, C. S. H., & Ho, R. C. M. (2018). Minocycline Attenuates Stress-Induced Behavioral Changes via Its Anti-inflammatory Effects in an Animal Model of Post-traumatic Stress Disorder. *Frontiers in psychiatry*, *9*, 558. https://doi.org/10.3389/fpsyt.2018.00558

Wang, Y. L., Han, Q. Q., Gong, W. Q., Pan, D. H., Wang, L. Z., Hu, W., Yang, M., Li, B., Yu, J., & Liu, Q. (2018). Microglial activation mediates chronic mild stress-induced depressive- and anxiety-like behavior in adult rats. *Journal of neuroinflammation*, *15*(1), 21. https://doi.org/10.1186/s12974-018-1054-3

Warren, K. M., Reeves, T. M., & Phillips, L. L. (2012). MT5-MMP, ADAM-10, and N-cadherin act in concert to facilitate synapse reorganization after traumatic brain injury. *Journal of neurotrauma*, *29*(10), 1922–1940. https://doi.org/10.1089/neu.2012.2383

Wass S. (2011). Distortions and disconnections: disrupted brain connectivity in autism. *Brain and cognition*, *75*(1), 18–28. https://doi.org/10.1016/j.bandc.2010.10.005

Weger, M. and Sandi, C. (2018) 'High anxiety trait: A vulnerable phenotype for stress-induced depression.', *Neuroscience and biobehavioral reviews*. United States, 87, pp. 27–37. doi: 10.1016/j.neubiorev.2018.01.012.

Wegiel, J., Kuchna, I., Nowicki, K., Imaki, H., Wegiel, J., Marchi, E., Ma, S. Y., Chauhan, A., Chauhan, V., Bobrowicz, T. W., de Leon, M., Louis, L. A., Cohen, I. L., London, E., Brown, W. T., & Wisniewski, T. (2010). The neuropathology of autism: defects of neurogenesis and neuronal migration, and dysplastic changes. *Acta neuropathologica*, *119*(6), 755–770. https://doi.org/10.1007/s00401-010-0655-4

Weinhard, L., di Bartolomei, G., Bolasco, G., Machado, P., Schieber, N. L., Neniskyte, U., Exiga, M., Vadisiute, A., Raggioli, A., Schertel, A., Schwab, Y., & Gross, C. T. (2018). Microglia remodel synapses by presynaptic trogocytosis and spine head filopodia induction. *Nature communications*, *9*(1), 1228. https://doi.org/10.1038/s41467-018-03566-5

Wilber, A. A., Walker, A. G., Southwood, C. J., Farrell, M. R., Lin, G. L., & Rebec, G. V. (2011). Chronic stress alters neural activity in medial prefrontal cortex during retrieval of extinction. Neuroscience, 174, 115–131. https://doi.org/10.1016/j.neuroscience.2010.10.070.

Wohleb, E. S., Hanke, M. L., Corona, A. W., Powell, N. D., Stiner, L. M., Bailey, M. T., ... & Sheridan, J. F. (2018). Stress-induced neuronal colony stimulating factor 1 provokes microglia-mediated neuronal remodeling and depressive-like behavior. Biological Psychiatry, 83(1), 38–49. https://doi.org/10.1016/j.biopsych.2017.05.026.

Wolf, S. A., Boddeke, H. W., & Kettenmann, H. (2017). Microglia in Physiology and Disease. *Annual review of physiology*, *79*, 619–643. https://doi.org/10.1146/annurev-physiol-022516-034406

Wolfer, D. P., Müller, U., Stagliar, M., & Lipp, H. P. (1997). Assessing the effects of the 129/Sv genetic background on swimming navigation learning in transgenic mutants: a study using mice with a modified beta-amyloid precursor protein gene. *Brain research*, *771*(1), 1–13. https://doi.org/10.1016/s0006-8993(97)00673-2

Wu, Y., Dissing-Olesen, L., MacVicar, B. A., & Stevens, B. (2015). Microglia: Dynamic Mediators of Synapse Development and Plasticity. *Trends in immunology*, *36*(10), 605–613. https://doi.org/10.1016/j.it.2015.08.008

Wunderlich, P., Glebov, K., Kemmerling, N., Tien, N. T., Neumann, H., & Walter, J. (2013). Sequential proteolytic processing of the triggering receptor expressed on myeloid cells-2 (TREM2) protein by ectodomain shedding and γ-secretase-dependent intramembranous cleavage. *The Journal of biological chemistry*, *288*(46), 33027–33036. https://doi.org/10.1074/jbc.M113.517540

Xiong, J., Lipsitz, O., Nasri, F., Lui, L. M. W., Gill, H., Phan, L., Chen-Li, D., Iacobucci, M., Ho, R., Majeed, A., & McIntyre, R. S. (2020). Impact of COVID-19 pandemic on mental health in the general population: A systematic review. *Journal of affective disorders*, *277*, 55–64. https://doi.org/10.1016/j.jad.2020.08.001

Yan, J., Oliveira, G., Coutinho, A., Yang, C., Feng, J., Katz, C., Sram, J., Bockholt, A., Jones, I. R., Craddock, N., Cook, E. H., Jr, Vicente, A., & Sommer, S. S. (2005). Analysis of the neuroligin 3 and 4 genes in autism and other neuropsychiatric patients. *Molecular psychiatry*, *10*(4), 329–332. https://doi.org/10.1038/sj.mp.4001629

Yrjänheikki, J., Keinänen, R., Pellikka, M., Hökfelt, T., & Koistinaho, J. (1998). Tetracyclines inhibit microglial activation and are neuroprotective in global brain ischemia. *Proceedings of the National Academy of Sciences of the United States of America*, *95*(26), 15769–15774. https://doi.org/10.1073/pnas.95.26.15769

Yumoto, T., Kato, A., Kakizaki, T., Shibuki, K., & Yanagawa, Y. (2020). Autism-associated variants of neuroligin 4X impair synaptogenic activity by various molecular mechanisms. Molecular Autism, 11(1), 68. https://doi.org/10.1186/s13229-020-00373-y

Yuzaki M. (2018). Two Classes of Secreted Synaptic Organizers in the Central Nervous System. *Annual review of physiology*, *80*, 243–262. https://doi.org/10.1146/annurev-physiol-021317-121322

Zazula, R., Husain, M. I., Mohebbi, M., Walker, A. J., Chaudhry, I. B., Khoso, A. B., Ashton, M. M., Agustini, B., Husain, N., Deakin, J., Young, A. H., Berk, M., Kanchanatawan, B., Ng, C. H., Maes, M., Berk, L., Singh, A. B., Malhi, G. S., & Dean, O. M. (2021). Minocycline as adjunctive treatment for major depressive disorder: Pooled data from two randomized controlled trials. *The Australian and New Zealand journal of psychiatry*, *55*(8), 784–798. https://doi.org/10.1177/0004867420965697

Zeisel, A., Muñoz-Manchado, A. B., Codeluppi, S., Lönnerberg, P., La Manno, G., Juréus, A., Marques, S., Munguba, H., He, L., Betsholtz, C., Rolny, C., Castelo-Branco, G., Hjerling-Leffler, J., & Linnarsson, S. (2015). Brain structure. Cell types in the mouse cortex and hippocampus revealed by single-cell RNA-seq. *Science (New York, N.Y.)*, *347*(6226), 1138–1142. https://doi.org/10.1126/science.aaa1934

Zeng, L. L., Shen, H., Liu, L., Wang, L., Li, B., Fang, P., Zhou, Z., Li, Y., & Hu, D. (2012). Identifying major depression using whole-brain functional connectivity: a multivariate pattern analysis. *Brain : a journal of neurology*, *135*(Pt 5), 1498–1507. https://doi.org/10.1093/brain/aws059

Zhan, Y., Paolicelli, R. C., Sforazzini, F., Weinhard, L., Bolasco, G., Pagani, F., Vyssotski, A. L., Bifone, A., Gozzi, A., Ragozzino, D., & Gross, C. T. (2014). Deficient neuron-microglia signaling results in impaired functional brain connectivity and social behavior. *Nature neuroscience*, *17*(3), 400–406. https://doi.org/10.1038/nn.3641

Zhang, B., Chen, L. Y., Liu, X., Maxeiner, S., Lee, S. J., Gokce, O., & Südhof, T. C. (2015). Neuroligins Sculpt Cerebellar Purkinje-Cell Circuits by Differential Control of Distinct Classes of Synapses. *Neuron*, *87*(4), 781–796. https://doi.org/10.1016/j.neuron.2015.07.020

Zhang, B., Gokce, O., Hale, W. D., Brose, N., & Südhof, T. C. (2018). Autism-associated neuroligin-4 mutation selectively impairs glycinergic synaptic transmission in mouse brainstem synapses. *The Journal of experimental medicine*, *215*(6), 1543–1553. https://doi.org/10.1084/jem.20172162

Zhang, C., Kalueff, A. V., & Song, C. (2019). Minocycline ameliorates anxiety-related self-grooming behaviors and alters hippocampal neuroinflammation, GABA and serum cholesterol levels in female Sprague-Dawley rats subjected to chronic unpredictable mild stress. *Behavioural brain research*, 363, 109–117. doi: https://doi.org/10.1016/j.bbr.2019.01.045

Zhang, C., Milunsky, J. M., Newton, S., Ko, J., Zhao, G., Maher, T. A., Tager-Flusberg, H., Bolliger, M. F., Carter, A. S., Boucard, A. A., Powell, C. M., & Südhof, T. C. (2009). A neuroligin-4 missense mutation associated with autism impairs neuroligin-4 folding and endoplasmic reticulum export. *The Journal of neuroscience : the official journal of the Society for Neuroscience*, *29*(35), 10843–10854. https://doi.org/10.1523/JNEUROSCI.1248-09.2009

Zhang, Y., Chen, K., Sloan, S. A., Bennett, M. L., Scholze, A. R., O'Keeffe, S., Phatnani, H. P., Guarnieri, P., Caneda, C., Ruderisch, N., Deng, S., Liddelow, S. A., Zhang, C., Daneman, R., Maniatis, T., Barres, B. A., & Wu, J. Q. (2014). An RNA-sequencing transcriptome and splicing database of glia, neurons, and vascular cells of the cerebral cortex. *The Journal of*

neuroscience : the official journal of the Society for Neuroscience, *34*(36), 11929–11947. https://doi.org/10.1523/JNEUROSCI.1860-14.2014

Zhao, J., Bao, A. M., Qi, X. R., Kamphuis, W., Luchetti, S., Lou, J. S., & Swaab, D. F. (2012). Gene expression of GABA and glutamate pathway markers in the prefrontal cortex of non-suicidal elderly depressed patients. *Journal of affective disorders*, *138*(3), 494–502. https://doi.org/10.1016/j.jad.2012.01.013

Zheng, Q., Li, G., Wang, S., Zhou, Y., Liu, K., Gao, Y., Zhou, Y., Zheng, L., Zhu, L., Deng, Q., Wu, M., Di, A., Zhang, L., Zhao, Y., Zhang, H., Sun, H., Dong, C., Xu, H., & Wang, X. (2021). Trisomy 21-induced dysregulation of microglial homeostasis in Alzheimer's brains is mediated by USP25. *Science advances*, *7*(1), eabe1340. https://doi.org/10.1126/sciadv.abe1340

Zheng, Z. H., Tu, J. L., Li, X. H., Hua, Q., Liu, W. Z., Liu, Y., Pan, B. X., Hu, P., & Zhang, W. H. (2021). Neuroinflammation induces anxiety- and depressive-like behavior by modulating neuronal plasticity in the basolateral amygdala. *Brain, behavior, and immunity*, *91*, 505–518. https://doi.org/10.1016/j.bbi.2020.11.007

Zhong, L., & Chen, X. F. (2019). The Emerging Roles and Therapeutic Potential of Soluble TREM2 in Alzheimer's Disease. *Frontiers in aging neuroscience*, *11*, 328. https://doi.org/10.3389/fnagi.2019.00328

Zhong, L., Chen, X. F., Wang, T., Wang, Z., Liao, C., Wang, Z., Huang, R., Wang, D., Li, X., Wu, L., Jia, L., Zheng, H., Painter, M., Atagi, Y., Liu, C. C., Zhang, Y. W., Fryer, J. D., Xu, H., & Bu, G. (2017). Soluble TREM2 induces inflammatory responses and enhances microglial survival. *The Journal of experimental medicine*, *214*(3), 597–607. https://doi.org/10.1084/jem.20160844

I. Affidavit

Statutory Declaration

"I, Bilge, Ugursu, by personally signing this document in lieu of an oath, hereby affirm that I prepared the submitted dissertation on the topic THE ROLE OF MICROGLIAL SYNAPTIC PRUNING IN MURINE MODELS OF PSYCHIATRIC SYMPTOMS, DIE ROLLE VON SYNAPTIC PRUNING DURCH MIKROGLIA IN EXPERIMENTELLEN MODELLEN VON PSYCHIATRISCHEN SYMPTOMEN, independently and without the support of third parties, and that I used no other sources and aids than those stated.

All parts which are based on the publications or presentations of other authors, either in letter or in spirit, are specified as such in accordance with the citing guidelines. The sections on methodology (in particular regarding practical work, laboratory regulations, statistical processing) and results (in particular regarding figures, charts and tables) are exclusively my responsibility.

Furthermore, I declare that I have correctly marked all of the data, the analyses, and the conclusions generated from data obtained in collaboration with other persons, and that I have correctly marked my own contribution and the contributions of other persons (cf. declaration of contribution). I have correctly marked all texts or parts of texts that were generated in collaboration with other persons.

My contributions to any publications to this dissertation correspond to those stated in the below joint declaration made together with the supervisor. All publications created within the scope of the dissertation comply with the guidelines of the ICMJE (International Committee of Medical Journal Editors; www.icmje.org) on authorship. In addition, I declare that I shall comply with the regulations of Charité – Universitätsmedizin Berlin on ensuring good scientific practice.

I declare that I have not yet submitted this dissertation in identical or similar form to another Faculty.

The significance of this statutory declaration and the consequences of a false statutory declaration under criminal law (Sections 156, 161 of the German Criminal Code) are known to me."

_____ _____

Date Signature

II. Curriculum Vitae

“My curriculum vitae does not appear in the electronic version of my paper for reasons of data protection.”

“My curriculum vitae does not appear in the electronic version of my paper for reasons of data protection.”

“My curriculum vitae does not appear in the electronic version of my paper for reasons of data protection.”

III. List of Publications

1. Guneykaya, D., **Ugursu, B.**, Logiacco, F., Popp, O., Feiks, M. A., Meyer, N., Wendt, S., Semtner, M., Cherif, F., Gauthier, C., Madore, C., Yin, Z., Çınar, Ö., Arslan, T., Gerevich, Z., Mertins, P., Butovsky, O., Kettenmann, H., & Wolf, S. A. (2023). Sex-specific microglia state in the Neuroligin-4 knock-out mouse model of autism spectrum disorder. *Brain, behavior, and immunity*, *111*, 61–75. https://doi.org/10.1016/j.bbi.2023.03.023

2. Hernández, D. C., Juelke, K., Müller, N. C., Durek, P., **Ugursu, B.**, Mashreghi, M. F., Rückert, T., & Romagnani, C. (2021). An in vitro platform supports generation of human innate lymphoid cells from $CD34^+$ hematopoietic progenitors that recapitulate ex vivo identity. *Immunity*, *54*(10), 2417–2432.e5. https://doi.org/10.1016/j.immuni.2021.07.019

3. Logiacco, F., Xia, P., Georgiev, S. V., Franconi, C., Chang, Y. J., **Ugursu, B.**, Sporbert, A., Kühn, R., Kettenmann, H., & Semtner, M. (2021). Microglia sense neuronal activity via GABA in the early postnatal hippocampus. *Cell reports*, *37*(13), 110128. https://doi.org/10.1016/j.celrep.2021.110128

4. Costa, A., Haage, V., Yang, S., Wegner, S., Ersoy, B., **Ugursu, B.**, Rex, A., Kronenberg, G., Gertz, K., Endres, M., Wolf, S. A., & Kettenmann, H. (2021). Deletion of muscarinic acetylcholine receptor 3 in microglia impacts brain ischemic injury. *Brain, behavior, and immunity*, *91*, 89–104. https://doi.org/10.1016/j.bbi.2020.09.008

IV. ACKNOWLEDGEMENT

Although I still cannot believe that I am composing this section, which represents a major milestone in my professional and personal life, I am endlessly grateful to everyone who supported me during such an extraordinary and challenging period of my life. I have grown tremendously as a person over the past four years, and learned a lot. It is still hard to believe that I survived a Ph.D. combined with a global pandemic with no family around.

I would like to express my greatest gratitude to my supervisor, Dr. Susanne Wolf, who believed in my potential, encouraged me to pursue a Ph.D. in the first place, and gave me the opportunity to work on two amazing projects. Susanne, I have learned a lot from you ! Thank you for your unwavering support through all these years, I owe you so much.

I would to like to thank Professor Helmut Kettenmann for allowing me to pursue my Ph.D. in his laboratory and for his incredibly constructive criticism. I would like to thank Professor Olaf Strauß for substantially improving my thesis, and for sharing a great deal of academic writing tips with me.

I am so grateful to Dr. Dilansu Guneykaya for always believing in me and supporting me, for teaching me so much, and for answering all of my questions at any time! Dilansu, you are such an incredible human being, thank you for always checking up on me over all these years and for making sure that I am not breaking down. Thank you for guiding me through difficult personal decisions for hours on your free weekends, which I know you don't get very often. I can’t believe I was lucky enough to be your student! I am also grateful to Dr. Ozcan Cinar for not getting irritated when I repeatedly stole his precious wife :)

I am extremely grateful to Regina Piske for all of her technical assistance, remarkable organizational skills, and constant support. You have no idea how much I appreciate you, Regina. Thank you for being so incredible and for never leaving me alone. I learned so much from you!

I would like to thank my dear Nine Kompier for being my "Ninechen" and the most lovely psychologist around! I would like to thank Inga Pompoes for her continuous help and support, especially with my German, for feeding me pizza always at the right time, for encouraging me to paint more, for always being by my side in the best and worst times and for her wisdom. You have a beautiful heart, Inga, I appreciate everything you've shared with me. I would like to thank Hannah Weidling and Edyta Motta for being amazing friends, colleagues, emergency shoulders, anything! Love you two guys, thank you so much for everything. I was really lucky to be around you. I would like to thank Fatma Cherif, Chufan Yan and Yuxuan Jiang for being so amazing and making me ask myself too many times how human beings can be so pure! Thank you guys, for being always so nice and positive. I will miss your energy in my life! I'd like to thank my wonderful colleagues Dr. Marcus Semtner, Mostafa Ghazy and Niccolò De Marzo for their support! I'd also like to acknowledge all the former Kettenmann lab members and current Wolf lab members for their support and company.

I would like to thank Birgit Jarchow for saving me from all the stress and bureaucracy, but especially for regularly checking up on me during the pandemic, when I was far away from my family and loved ones, and left out with a massive fear. I will never forget how caring you were to me Birgit, thank you so much for being an amazing human being. It was such a privilege having you around!

I am extremely grateful to Michaela Herzig and Annette Schledz, the coordinators of the MDC PhD program, for their constant support and help throughout my PhD journey. I don't know how I could have survived without their amazing guidance and help at every possible step. It will never be enough to express how much I appreciate them. Michaela and Annette, you both are so amazing and we are extremely lucky to have you by our side during such a challenging period of our careers!

I would like to thank my chosen sister, Esra Guben, for enduring me for ten years without a moment of doubt, and for her unlimited support during the darkest periods of my life. I adore you, 'Çipil gözlüm'. I cannot even dare to think of what I would do without you.

I would like to thank my beloved family; my sister, my mother, my brother, and my husband for their support in all my decisions and for basically being the ‘oxygen’ of my life. A special chapter comes here for my sister, Belgin Ugursu, and for my husband, Baris Isyar.

I am so grateful to my sister for being my little mama and papa while growing up, for making me who I am, for teaching me far more than a sister could do in a hundred years, for giving me a personality that I am proud of, for constantly providing me everything I have ever needed without even considering herself in the first place, for listening to me when I cry without passing any judgement, for cheering my every little tiny success that no one else would even care, for tolerating all of my mistakes and instabilities, and for always making me feel her endless love in this world. I'm not sure if I could survive a single minute without her warmth and sweet voice.

Finally, I would like to thank my heart, Baris Isyar, who has always been there for me through thick and thin. I wish there were enough words in this world to express my love for you, Baris. You made all my sufferings in this life bearable. You made all of my endless late-night working hours enjoyable and memorable. You became the breath I needed and cared for me always with a big smile on your beautiful face. How you have managed to do all these things for me with such grace and ease will forever be the mystery of you. You are my best friend, you are all my answers. “You found the light in me that I couldn’t find”, and I could not have done this without you.

I am eternally grateful to each and every one of you.

Bilge

V. Certificate of the accredited statistician

CHARITÉ

CharitéCentrum für Human- und Gesundheitswissenschaften

Charité | Campus Charité Mitte | 10117 Berlin

Institut für Biometrie und klinische Epidemiologie (iBikE)

Direktor: Prof. Dr. Frank Konietschke

Postanschrift:
Charitéplatz 1 | 10117 Berlin
Besucheranschrift:
Reinhardtstr. 58 | 10117 Berlin

Tel. +49 (0)30 450 562171
frank.konietschke@charite.de
https://biometrie.charite.de/

Name, Vorname: Ugursu, Bilge
Emailadresse: bilge.ugursu@charite.de
Matrikelnummer: 224045
PromotionsbetreuerIn: PD. Dr. Susanne Wolf,
Prof. Dr. Helmut Kettenmann, Prof. Dr. Olaf Strauß
Promotionsinstitution / Klinik: Experimental Ophthalmology & MDC Berlin-Psychoneuroimmunology

Bescheinigung

Hiermit bescheinige ich, dass Frau *Bilge Ugursu* innerhalb der Service Unit Biometrie des Instituts für Biometrie und klinische Epidemiologie (iBikE) bei mir eine statistische Beratung zu einem Promotionsvorhaben wahrgenommen hat. Folgende Beratungstermine wurden wahrgenommen:

- Termin 1: 14.04.2023

Folgende wesentliche Ratschläge hinsichtlich einer sinnvollen Auswertung und Interpretation der Daten wurden während der Beratung erteilt:

- 2-way ANOVA with multiple comparison
- 2-way repeated ANOVA
- Unpaired t-test
- Wilcoxon rank sum test
- Seurat Single Cell RNA sequencing analysis R package

Diese Bescheinigung garantiert nicht die richtige Umsetzung der in der Beratung gemachten Vorschläge, die korrekte Durchführung der empfohlenen statistischen Verfahren und die richtige Darstellung und Interpretation der Ergebnisse. Die Verantwortung hierfür obliegt allein dem Promovierenden. Das Institut für Biometrie und klinische Epidemiologie übernimmt hierfür keine Haftung.

Datum: 17.04.2023 Name der Beraterin: Dr.Pimrapat Gebert

Pimrapat Gebert Digital unterschrieben von Pimrapat Gebert Datum: 2023.04.17 10:13:33 +02'00'

Unterschrift BeraterIn, Institutsstempel

CHARITÉ UNIVERSITÄTSMEDIZIN BERLIN
Institut für Biometrie und Klinische Epidemiologie
Campus Charité Mitte
Charitéplatz 1 | D-10117 Berlin
Sitz: Reinhardtstr. 58